Schriftenreihe der Reiner Lemoine-Stiftung

Shivenes Shammugam

Raw materials and energy transformation process

Analysis of supply bottlenecks and implications on metal markets

Raw materials and energy transformation process - Analysis of supply bottlenecks and implications on metal markets

Dissertation

zur Erlangung des akademischen Grades

Dr.-Ing.

eingereicht an der

Mathematisch-Naturwissenschaftlich-Technischen Fakultät

der Universität Augsburg

von

Shivenes Shammugam

Augsburg, Mai 2019

Erstgutachter: Prof. Dr. Andreas Rathgeber

Zweitgutachter: Prof. Dr. Hans-Martin Henning

Tag der mündlichen Prüfung: 31. Oktober 2019

Schriftenreihe der Reiner Lemoine-Stiftung

Shivenes Shammugam

Raw materials and energy transformation process

Analysis of supply bottlenecks and implications on metal markets

Shaker Verlag
Düren 2019

Bibliographic information published by the Deutsche Nationalbibliothek
The Deutsche Nationalbibliothek lists this publication in the Deutsche Nationalbibliografie; detailed bibliographic data are available in the Internet at http://dnb.d-nb.de.

Zugl.: Augsburg, Univ., Diss., 2019

Printed in Germany.

ISBN 978-3-8440-7092-7
ISSN 2193-7575

Shaker Verlag GmbH • Am Langen Graben 15a • 52353 Düren
Phone: 0049/2421/99011-0 • Telefax: 0049/2421/99011-9
Internet: www.shaker.de • e-mail: info@shaker.de

List of scientific publications

Some parts of this thesis have been developed as part of scientific papers in collaboration with co-authors. These papers serve as a basis for some chapters, but were also revised and expanded in terms of content and editorially amended as part of the thesis. Chapters containing longer text passages or result representations are marked accordingly. In each case, the author had a significant share of all essays in this thesis.

- Shammugam, S.; Gervais, E.; Schlegl, T.; Rathgeber, A. (2019a): Raw metal needs and supply risks for the development of wind energy in Germany until 2050. In *Journal of Cleaner Production* 221, pp. 738-752.
  DOI: 10.1016/j.jclepro.2019.02.223
  Chapter: 2.3.1, 6, 10.1

- Shammugam, S; Rathgeber, A; Schlegl, T (2019b): Causality between metal prices. Is joint consumption a more important determinant than joint production of main and by-product metals? In *Resources Policy* 61, pp. 49–66.
  DOI: 10.1016/j.resourpol.2019.01.010
  Chapter: 3, 5.2.3, 10.2, 10.3

Acknowledgements

First and foremost, I would like to express my gratitude to Prof. Dr. Andreas Rathgeber for providing technical supervision as well as enormous motivation and support in successfully completing the thesis. I truly appreciate the positive working environment that you have created between us which led to fruitful discussions and constantly took away a large part of my concerns during the completion of the thesis.

Besides that, I would like to thank Prof. Dr. Hans-Martin Henning for his willingness to be the second supervisor and for the constructive discussions.

I am also grateful to my technical supervisor in Fraunhofer ISE, Dr. Thomas Schlegl for taking a leap of faith with me in starting a new subject area and for accepting nothing less than excellence from me.

Furthermore, I am indebted to the Reiner Lemoine Stiftung for providing me a PhD scholarship and made the work possible. I truly appreciate the discussions during the annual meetings and am glad to be part of an institution that shares my personal values.

Special thanks to my friends and colleagues in Fraunhofer ISE and at the University of Augsburg for playing a huge part in making my working environment extremely fun. Appreciation is also due to the constant discussions and feedback which led to improvements in the thesis. I am particularly indebted to Estelle Gervais for the enormous support in completion of this thesis.

Nobody has been more important to me in the pursuit of a PhD than my mother and brother, whose love and guidance are with me in whatever I pursue. Thank you for supporting me spiritually throughout the completion of this thesis and my life in general.

Contents

I. List of metal abbreviations

Ag	Silver
Al	Aluminium
Au	Gold
Cd	Cadmium
Co	Cobalt
Cr	Chromium
Cu	Copper
Dy	Dysprosium
Ga	Gallium
In	Indium
Li	Lithium
Mg	Magnesium
Mn	Manganese
Mo	Molybdenum
Na	Sodium
Nd	Neodymium
Ni	Nickel
Pb	Lead
Pd	Palladium
Pt	Platinum
Sb	Antimony
Si	Silicon
Se	Selenium
Sn	Tin
St	Steel
Ta	Tantalum
Te	Tellurium
Ti	Titanium
V	Vanadium
Zn	Zinc

II. List of general abbreviations

ADF	Augmented Dickey-Fuller
ARCH	Autoregressive conditional heteroscedasticity
BEV	Battery electric vehicles
BG	Breusch and Godfrey
BIC	Bayesian Information Criteria
BIPV	Building integrated photovoltaics
BMS	Battery management system
BOS	Balance of system
BSF	Back surface field
CdTe	Cadmium Telluride
CIGS	Copper-Indium-Gallium-Selenium
Con	Consumption
CPI	Consumer price index
CUSUM	Cumulative sum
CZTS	Copper-Zinc-Tin-Selenium
c-Si	Crystalline silicon
DFIG	Doubly-Fed Induction Generator
D/P ratio	Demand-to-production ratio
D/R ratio	Demand-to-reserve ratio
D/R_{base} ratio	Demand-to-reserve base ratio
EEG	Renewable energy act
EESG-DD	Electrically-Excited Synchronous Generator-Direct-Drive
EV	Electric vehicles
FedFund	Federal Fund Rates
FEVD	Forecast error variance decomposition
GDP	Gross domestic product
GHG	Greenhouse gasses
GW	Gigawatt
GWh	Gigawatt hours
H_0	Null-hypothesis
HEV	Hybrid electric vehicles
IRF	Impulse response function

KPSS	Kwiatkowski-Phillips-Schmidt-
kWh	Kilowatt hours
LCA	Life cycle analysis
Li-Air	Lithium-Air
Li-Ion	Lithium-Ion
Li-S	Lithium-Sulphur
LM	Lagrange Multiplier
LME	London Metal Exchange
MENA	Middle East & North Africa
MW	Megawatt
Na-S	Sodium-sulphur
NiMH	Nickel-metal hydride
OLS	Ordinary least squares
PGE	Platinum group elements
PHEV	Plug-in hybrid electric vehicle
PM	Permanent magnet
PMSG-DD	Permanent Magnet Synchronous Generator-Direct-Drive
PMSG-HS	Permanent Magnet Synchronous Generator – High Speed
PMSG-MS	Permanent Magnet Synchronous Generator-Middle Speed
Prod	Production
PV	Photovoltaic
REE	Rare earth elements
SCIG	Squirrel Cage Induction Generator Variable Speed
SLI	Starting, lighting, ignition
TCO	Transparent conducting oxides
TLB	Tension leg-buoy
TWh	Terawatt hours
VAR	Vector auto regression
VECM	Vector error correction model
VRF	Vanadium redox flow

1 Introduction

1.1 Background and motivation

The Kyoto Protocol was first concluded in 1997, which commits involved nations, including Germany, to reduce their greenhouse gas (GHG) emissions. On top of that, the EU defined the "2020 climate and energy package" in 2007, which targets a 20 % reduction on GHG emissions, 20 % improvement in energy efficiency and 20 % of the total energy consumption to be covered by renewable energy by 2020. In order to address these commitments as well as to create a climate-friendly and sustainable energy system in Germany, the so-called energy transformation process, also known as the "Energiewende", was initiated and several climate goals were defined. As an example, by 2050, the share of total electricity supply from renewable energy sources is to be successively increased to 80 % whereas the primary energy consumption is to be reduced by 50 % compared to the reference year of 2008. In conjunction with these goals, the Renewable Energy Sources Act was formed in Germany in order to grant priority to renewable energy sources and to facilitate sustainable development of energy supply. Based on the development of the GHG-emission in Germany as illustrated in Figure 1-1, it can be seen that Germany has successfully managed to reduce the emissions with respect to 1990. However, it can also be seen that a much stronger reduction of GHG-emission is required if the long terms climate goals are to be achieved in 2050.

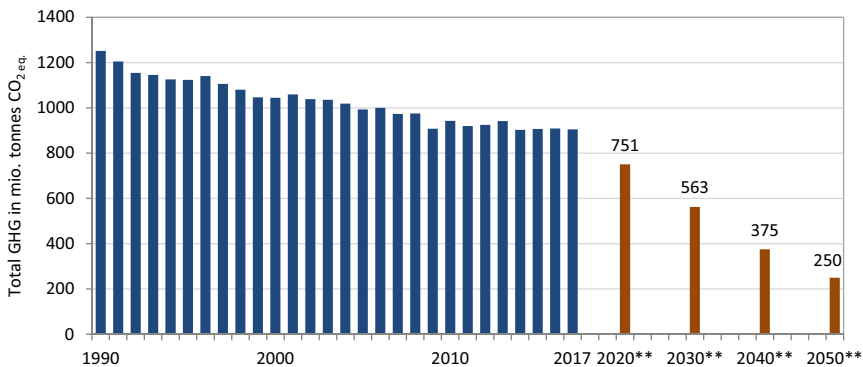

Figure 1-1: Emission of greenhouse gases in Germany as reported by the German Environment Agency in the National Inventory Reports for the German Greenhouse Gas Inventory 1990 to 2016 (as of 1/2018). The emissions in 2020 until 2050 refers to the targets defined in the Climate Protection Plan 2050 of the Federal Government. The emission target in 2050 refers to the minimum reduction goal of 80 % compared to the reference values in 1990.

In 2016, the GHG-emissions due to fuel combustion in sectors such as the energy generation, transport and in the manufacturing and construction industry contributed to 84 % of the total GHG-emissions in Germany. This means that the transformation of the energy sector plays a vital role in achieving the long term climate goals in Germany. Due to this reason, the development of the German energy system has been actively researched in the past years. Studies such as Henning and Palzer (2015), Achner et al. (2015) and BMWi (2017b) have investigated the technical viability of a future energy system with a high share of renewables. Although there are many ways of achieving it, these studies share the common fact that photovoltaic (PV) and wind energy will have the largest share in the German electricity production in the future. Apart from that, the transport sector is also set to undergo massive electrification, which would increase the deployment of batteries.

However, the development and production of innovative new products, such as renewable energy technologies, are expected to increase the utilization of new metals. Zepf et al. (2014) showed that the number of intensively used metals in energy pathways has massively increased under the influence of technological development, as specific material properties are essential for a large number of innovative technologies. Technologies such as PV and batteries, which have been predominantly based on silicon and lead historically, are currently utilizing new metals such as gallium and cobalt respectively. Similarly, wind turbines are relying on neodymium and dysprosium in order to increase reliability when the turbines get larger and are built at extreme distances from the shore. In fact, companies are already facing the challenge of ensuring the criticality of materials used in the development and production of energy technologies. For example, the wind turbine manufacturer, Vestas, decided to overhaul their product portfolio to manufacture wind turbines without permanent magnets (PMs) since China decided to limit the export of rare earth elements (REEs) in 2012. If the increasing use of scarce metals is left unchecked, it could lead to inevitable problems such as supply bottlenecks. This could then cripple the implementation of the proposed energy transformation process in Germany.

In the field of economics, various studies show that additional demand for a commodity will generally lead to higher prices (Borensztein and Reinhart 1994; Hamilton 2008). In some cases, an increase in commodity demand of a single considerably large industrial consumer can lead to higher prices of all related commodities (Rodrigo Cerda 2005; Klotz et al. 2014). With Germany being one of the leading actors of renewable energy systems globally, the economic effects of the increase in metal demand due to the deployment of renewable energies cannot be neglected. On a different note, increasing metal prices and volatility has been a constant motivation to analyse the behaviour of metal prices, especially for the economic planning of manufacturers and asset investments for financial investors. The impact of the price fluctuations of metals related to renewable energy technologies was apparent when the price of REEs hiked due to the export restriction by China (Pavel et al. 2017). In terms of the use of strategic metals in batteries in EV, automobile manufacturers are already trying to secure long-term metal supplies due to fear of increasing prices and supply restrictions (Simon 2018). One of the ways of how industries could protect themselves

from the economic risks and uncertainties related to metal prices is to have a well-diversified metal portfolio which can provide a stabilizing effect on price fluctuations. While this is relatively easy to be achieved by investors or mine operators who have the opportunity to utilize the by-products of a mine, the manufacturing industry requires a variety of metals that can substitute any critical metals in the products. However, portfolio diversification only effectively works if the related metals in either production or consumption do not react similarly to market information (CPA Australia 2012). These examples emphasize the need for knowledge on the price dependencies and relationship between various metals to be able to anticipate and be better prepared against price fluctuations and sudden change in the metal market.

1.2 Objectives and research questions

The aim of this thesis is therefore twofold. Firstly, the thesis aims at determining if the expected increase in metal demand due to the energy transformation process in Germany will lead to supply bottlenecks. In order to quantitatively address this question, several development pathways proposed by existing energy scenarios are evaluated. The total metallic raw material demand for the development of PV, wind turbines and batteries for stationary storage applications and electric vehicles in Germany until 2050 is determined. Additional demand due to maintenance and repair works during the lifespan of a technology as well as premature decommissioning is considered, in order to realistically estimate the total material requirements. In doing so, possible technological and market developments, such as material efficiency measures and breakthroughs of new technology concepts, are discussed. In order to account for the uncertainties in the market, the future technology mix is assessed for several technological roadmaps. The total demand is then compared to the global production and reserve levels of each metal in order to identify any possible bottlenecks in the future. Last but not least, the total recyclable metal demand that can be obtained from decommissioned technologies are identified, which can, in turn, lower any bottleneck risks by reducing the virgin metal demand. Overall, the analyses in this thesis provide an opportunity to ensure that severe bottlenecks in the supply of raw materials can be identified at an early stage and required measures can be taken beforehand in order to steer the energy transformation process in a cost-efficient way.

Secondly, this thesis aims at investigating the implications of the increasing metal demand due to the energy transformation process on the metal market. To this matter, a hypothesis is defined based on the findings in the literature, which is the basis of constructing the test set-ups. In the first part, the causality between the metal prices is investigated in terms of their nature of joint production and joint consumption. Additionally, a cross-technology analysis of the price dependencies among all relevant metals in PV, wind turbines and batteries is conducted, which, to the best knowledge to the author, has not been done before in existing literature. In the second part, a vector-autoregressive (VAR) structural analysis is conducted to analyse the market dynamics of selected critical metals. In

doing so, specific implications on metal prices can be investigated, such as a sudden surge in demand due to a technological breakthrough in renewable energy technologies. The main contribution of this thesis to the existing literature regarding this discipline is the metal-specific analyses which are relatively scarce in the literature.

More precisely, this thesis aims at answering the following research questions:

- Does the increasing metal demand due to the energy transformation process in Germany lead to supply bottlenecks?
- What are the economic implications of the increasing demand due to the energy transformation process in Germany on the metal market?

1.3 Structure of the thesis

The rest of this thesis is structured as follows. In chapter 2, the energy scenarios that are selected to be investigated in this thesis are compared and contrasted. Since these scenarios serve as the core of the subsequent analyses, their differences in terms of methodologies, key assumption and their proposed pathways are addressed in detail. At the end of this chapter, an overview of the technologies to be investigated, namely PV, wind turbines and batteries, are provided. The third chapter provides the theoretical basis of metal prices to provide insights in approaching the second research question. In particular, the relationships between jointly-produced and jointly-consumed metals are explained.

A thorough literature review regarding both research questions is provided in chapter 4. Three streams of literature are reviewed in detail for this purpose. Firstly, studies that have investigated the material demand for the relevant technologies and the supply bottlenecks are reviewed. This is followed by studies that investigated the causality between metal prices and lastly, the general market dynamics of metals. In doing so, research gaps in the literature are identified. Based on the findings in chapter 4, suitable methodologies and applied data are chosen and detailed in chapter 5.

The next three chapters are combinations of technology-specific methodologies and pre-results required in obtaining the material demand for PV, wind turbines and batteries, respectively. These include the material compositions, market shares and material efficiency measures, which are predominantly obtained from the literature. Using this information, the further development of the technologies is proposed at the end of each chapter. Chapter 9 presents the main results of this thesis, which are then discussed in detail in the following chapter. Finally, the thesis is concluded in chapter 11, in which the critical appraisal and prospects of further works are also provided.

2 Energy transformation pathways

Energy transformation pathways assist, among others, political discussions and provide guidance in making energy and climate policy decisions. While the pathways are not a prediction of how the future energy system will be structured, they propose possible scenarios for the evolution of the energy system in achieving certain climate goals based on fundamental assumptions and current knowledge. Currently, there are numerous studies proposing energy pathways in Germany commissioned from various parties including the government, industry associations and non-governmental organisations. Examples of some of the more recent pathways, but not limited to, are IRENA (2015), Gerhardt et al. (2015) and Ausfelder et al. (2017). The majority of the energy pathways share the common fact of proposing ways to reduce the CO_2 emissions in Germany to at least 80 % in 2050 compared to the reference emission values in 1990, which aligns with the national targets. Despite similar goal, the solutions in achieving this differ massively. This can be owed to two main factors, namely the methodology and key assumptions applied in the models and calculations. This proves that there are various possibilities in achieving climate goals, given that the framework conditions are favourable and carefully structured to steer the development in the proper path. Therefore, it is important to consider a variety of pathways while planning environmental policies which will shape the framework of the future energy system. Several meta-studies such as (Behn and Byfield 2016; Hillebrandt et al. 2015; Jülch et al. 2018; Burck et al. 2010) have compared and contrasted energy pathways to analyse the framework conditions under which the proposed energy system can be achieved. Although the numbers might vary, the key message is that the renewable energy technologies and the related infrastructures such as the power grid and storage systems have to be expanded while energy efficiency should be improved in all energy sectors.

Consequently, three pathways are selected to be investigated in terms of the raw material requirement in this thesis. The pathways are selected based on criteria such as the topicality, geographical relevance, target year, goal of reducing CO_2 emission and lastly the consideration of sector coupling. The interaction between the electricity, heating and transport sector is widely known as sector coupling, which plays an important role in coping with high shares of fluctuating renewable energies. The key idea of such an energy system is the elevated use of electricity from renewable energy sources in all sectors, thus reducing the need for fossil fuel for space heating, process heat, and transportation. As this would lead to an increase in electricity demand, and consequently of the renewable energy technologies, the consideration of sector coupling is therefore seen as a pivotal criterion in selecting the energy pathways. Upon consideration of these criteria, the following energy pathways, designated by the abbreviation that will be used henceforth, are selected to be analysed:

- **Long-term**: "Long-term scenarios for the transformation of energy System in Germany", conducted by Fraunhofer ISI, Consentec GmbH and ifeu (BMWi 2017a)
- **Climate protection**: "Climate Protection Scenario 2050", conducted by Öko Institut e.V. and Fraunhofer ISI (Repenning et al. 2016)
- **Transformation**: "Pathways for Transforming the German Energy System by 2050", conducted by Fraunhofer ISE (Henning and Palzer 2015)

The long-term and climate protection pathways, commissioned by the Federal Ministry for Economic Affairs and Energy (BMWi) and the Federal Ministry for the Environment, Nature Conservation and Nuclear Safety (BMUB) respectively, are often used as references in political discussions regarding energy and climate policies. The transformation pathway from the Fraunhofer Institute for Solar Energy Systems ISE is based on the cross-sectoral energy system model REMod (Palzer 2016). The differences between the pathways regarding the methodologies, key assumptions and core results are detailed in the following sections, with the focus on electricity generation.

2.1 Methodologies

Being structured - to a certain extent - upon previously published energy studies, the long-term pathway partly analyses and validates certain aspects of preceding studies. The main focus is not to present a single possible development of the energy system, but a solution space for the future energy system. A total of 12 scenarios are planned, in which the cost-optimal transformation path under different conditions will be derived, such as a decentralized system scenario or the low biomass potential scenario. Until the first quarter of 2019, 5 scenarios have been published, with the rest are planned to be released latest by the end of 2019. The central scenario of this study is the base scenario, which aspires after a cost-minimal pathway, in which the climate policy goals of reducing the greenhouse gasses (GHG) by 80 % in 2050 compared to the emission in 1990 are achieved. This scenario is chosen to be applied and investigated further in this dissertation. The modelling of this scenario was conducted in various sub-models that were optimized iteratively. One of the main strengths of this study is that not only is Germany modelled, but 42 other countries from Europe and the MENA region are also modelled and optimized together. This ensures a more realistic representation of the interaction between Germany and its neighbouring countries, especially in terms of the electricity exchange. Regarding the power plant expansion, several limits were pre-specified according to the German Renewable Energies Act (EEG). For example, a cumulatively installed PV capacity of 52 GW is set to be achieved in 2020 and to remain as the minimum level until 2050. In terms of wind turbines, at least 91 TWh of energy generation should be supplied by onshore turbines while offshore, 6.5 GW and 15 GW cumulatively installed capacity should be reached by 2020 and 2030, respectively. Expansions beyond these limits can be undertaken by the model if it sees fit. The feasibility of the expansions is then ensured by simulating the unit commitment of the power plants and by conducting a load flow analysis of the power grid.

The main goal of the climate protection pathway is to identify the achievable reduction in the GHG emissions if the current energy policy is carried forward into the future. Furthermore, it serves the purpose of identifying the required measures and strategies for meeting the climate goals and to analyse the cost-benefit relationship of achieving these goals for the consumer and ultimately, for the national economy. Three scenarios were analysed in this study, namely the current-measures-scenarios, where the current environmental policies are assumed unchanged in the future, and the KS80 and KS95, each representing the CO_2 reduction of 80 % and 95 % respectively compared to the emissions in 1990. In this thesis, the KS80 is chosen to be analysed further as this represents the minimum requirement in achieving the environmental goals in Germany, and is comparable in terms of the CO_2 reduction with the other selected scenarios. The modelling of the KS80 scenario was also carried out using several sub-models, such as the FORECAST (Fleiter 2018) and INVERT (Stadler et al. 2007) models. The investment in new power plants was set exogenously according to current market situations, planned projects and projections from the available literature. The operations of the power plants in meeting the hourly demand were optimized in the PowerFlex model (Hacker et al. 2011), with the total operational cost as the target function. The electricity import and export from Germany was obtained by modelling the electricity exchange between EU-27 countries and was provided as an input into the PowerFlex model.

In terms of the transformation pathway by Fraunhofer ISE derived from the REMod model, several scenarios have been published and discussed before. In this thesis, the "85/amb/Mix/beschl" scenario published by Henning and Palzer (2015) is chosen to be analysed as it was interpreted as the most promising scenario due to the results that were described to be more socially acceptable. The goal of this scenario is to derive a cost minimal target system, where the CO_2 emissions are 85 % lower compared to the reference emission values in 1990. The target function of the optimization is the minimization of the total cumulative cost from 2014 until 2050, which includes, among others, the investment costs, operational costs of power plants and fuel costs for conventional power plants. The CO_2 reduction is achieved by setting a constraint in the model so that the annual emission does not exceed the maximum limit. The merit order of the power plants in the hourly operations is set exogenously to reduce the optimization time. This means that the unit commitment of the power plants is not optimized in this pathway. Nevertheless, the model ensures that enough capacity is available for the demand to be adequately met in every hour. Unlike both aforementioned pathways, REMod does not consider the spatial distribution of the power plants as the energy activities are assumed to occur in a single node, i.e. that the energy produced by a technology at any time would simultaneously be available for the entire region without the need for electricity transmission in the power grid. Correspondingly, the power plants are aggregated according to their own type, which completely eliminates the requirements for a detailed power grid. The overview of some of the important methodologies applied by the studies is listed in Table 2-1.

Table 2-1: Overview of the methodologies applied by the energy pathways

	Long-term	Climate protection	Transformation
CO_2 reduction goals	80 %	80 %	85 %
Power plant expansion	Optimized expansion in ENERTILE, with minimum limits for PV and wind to be fulfilled in a given time period	Predefined exogenous to the model	Optimized expansion in REMod
Unit commitment	Optimised power plant deployment in OptEK	Optimised power plant deployment in PowerFlex	Predefined deployment sequence of power plants
Optimization target function	Minimal total cost	Minimal total cost	Minimal total cost
Spatial resolution of modelling	Germany is modelled in 6 regions. Europe and MENA region are modelled and optimized together.	Only the electricity sector of EU-27 countries are modelled and optimized to obtain import flows into Germany.	Germany as a single node, no neighbouring countries included in the model.
Power grid modelling	DC and AC power grids are modelled.	No power grid modelling, only the electricity losses in the grid is considered	No power grid modelling, only the electricity losses in the grid is considered
Non-energetic sectors	Not considered	Partially considered	Not considered
Potential analysis for expansion	GIS-based analysis for PV and wind potentials	GIS-based analysis for PV and wind potentials	Based on literature

2.2 Key assumptions

The CO_2 emission certificate prices are an important instrument to ensure the reduction of CO_2 emissions by imposing a high price on it, which ensures that renewable energies become more competitive than the conventional power plants in the future. While the long-term pathway expects the emission certificates to be priced at 100 €/t_{CO_2} in 2050, the climate protection pathway predicts a slightly higher price at 130 €/t_{CO_2}. In contrast to both pathways, which assume a linearly increasing price until 2050, the transformation pathway assumes that the maximum price of 100 €/t_{CO_2} has to be reached in 2030 and maintained at that level from then onwards.

Besides that, the projection of fossil fuel prices greatly influences the investment decisions and operating strategies of power plants. High fuel prices indirectly promote the expansion of renewable energy technologies as the costs of operating a conventional power plant would increase. Furthermore, this would also promote the implementation of energy efficiency measures in buildings in order to reduce the energy demand, such as refurbishments or even a technology switch towards the more cost-efficient renewable technologies. In the long-term pathway, the projections by the EU are mostly used in setting the prices of fossil fuel. As an example, the oil price in 2050 is projected to be around 68 €/MWh while the natural gas is slightly lower than 40 €/MWh. In the climate protection pathway, several studies such as the IEA (2013) and Matthes (2010) are used in order to obtain the projections of fuel prices. This leads to slightly higher prices than the long-term

pathway, with oil prices in 2050 about 90 €/MWh and the natural gas price at around 45 €/MWh. As for the transformation pathway, an annual increase of 2 % is assumed for all types of fossil fuel.

Another key assumption that significantly affects the results of the pathways is the projection of the energy demand. Two main factors that are essential in determining the development of energy demand is the demographic and economic growth. In the long-term and the climate protection pathways, these are modelled precisely for each sector. The transformation pathway uses available literature and assumptions in order to obtain the demand to feed into the model. In doing so, the electricity load used in REMod is based on the data from the European transmission system operators. Additional demand for room heating and hot water demand was calculated exogenously and included in the electricity load. Besides that, key assumptions regarding energy efficiency are also made with the goal of reducing the end and the primary energy demand. For example, several measures such as the reduction of room temperature or the increase of the refurbishment rate are undertaken to reduce the heating demand in the climate protection scenario. The refurbishment rate is differentiated in the transformation pathway between two levels of refurbishments; namely a complete refurbishment according to standards defined in Bürger et al. (2017) and an efficient refurbishment according to Feist (2011).

Assumptions regarding the electricity exchange between Germany and neighbouring countries can affect the outcome significantly, especially in terms of power plant capacities and electricity generation. In the long-term pathway, the share of renewable energy in the imported electricity is assumed to be identical to the average share of renewable energy in the European electricity system. On top of that, 10 % of the renewable energy share in Germany in 2050 can be provided by imported electricity. The assumptions differ slightly in the climate protection pathway, where 15 % of the electricity demand in Germany in 2050 can be fulfilled by imported electricity, which can consist of electricity from both renewables and conventional power plants. In contrast, the transformation pathway assumes a limited import and export capacity at 5 GW_{el}. This significantly small limit is intentionally selected to analyse the energy system of Germany with minimum balancing capacity from the neighbouring countries.

Table 2-2: Brief overview of selected key assumptions in the energy pathways

	Long-term	Climate protection	Transformation
CO_2 certificate prices	Continuous increment of the price, 100 €/ kt_{CO_2} in 2050	Continuous increment of the price, 130 €/kt_{CO_2} in 2050	Price increases to 100 €/kt_{CO_2} in 2030 and remains constant until 2050
Fossil fuel prices	Moderate increase, e.g. 68 €/MWh oil price in 2050	Strong increase, e.g. 90 €/MWh oil price in 2050	2% increment per annum of all fossil fuel prices
Demographic growth	-0.2 % in average between 2015-2050	-0.2 % in average between 2015-2050	-
Economic growth	0.8 % in average between 2015-2050	0.8 % in average between 2015-2050	-
Refurbishment rate of households	Depending on the building type, between 1.6 and 3 %	Depending on the year, between 1.3 and 2.2 %	600,000 refurbishments yearly

2.3 Proposed future energy pathways

In this subchapter, selected results from the energy pathways are presented in two segments. Firstly, the achieved GHG emission and energy reductions are compared to the national energy and climate policy targets. This provides an insight on how the methodology and key assumptions from the pathways affect the results with regards to the national goals. This is followed by the electricity generation and the expansion of generation capacity, which is used as an input for in determining the total material requirements.

To begin with, the minimum reduction of GHG emissions of at least 80 % in 2050 compared to 1990 is achieved in all pathways. The share of renewable energies in the electricity generation is successfully increased to more than 80 % whereas the reduction of the electricity demand for classical applications is reduced by 25 % in all scenarios. While the long-term and the climate protection pathways met the target of reducing the primary energy consumption by at least 50 %, the transformation pathway barely missed this by 1 %. On the one hand, these reductions are largely owed to the reduction of heating demand in the building sector and of the energy demand in the industry due to refurbishment and energy efficiency measures. On the other hand, the replacement of conventional power plants by renewable energies reduces energy losses due to the high efficiencies of renewable energy technologies.

Furthermore, a significant reduction is also achieved in terms of the end energy demand in all pathways. In terms of the gross electricity demand, the long-term and climate protection pathways have an almost unchanged demand (including electricity import) in 2010 and 2050 at around 600 TWh. The transformation pathway, however, exhibits an increase of 26 % in 2050 at 800 TWh. As mentioned earlier, the electricity demand due to classical application actually reduces by 25 % in 2050 compared to 2015, which is in concordance with the climate protection goals. Almost half of the electricity demand in 2050 in the transformation pathway is contributed by new electricity applications such as the strong electrification of the heating and transportation sector, production of hydrogen as well as methanisation as part of the power-to-X applications. Although the long-term and climate protection pathways also considered new electricity applications, their demand is not as high compared to that of the transformation pathway and is therefore compensated by the demand reduction in the classical application.

Besides that, the more aggressive energy efficiency measures, such as demographic degrowth and higher refurbishment rates implemented by the pathways in comparison to the transformation pathway also contributes further to the compensation of the demand from new applications, thus maintaining the gross electricity demand as a relatively lower level. Another important detail to mention is that the nature of the long-term and the climate protection pathway which model each sector in detail in separate sub-models enables them to define sector-specific restrictions. Nonetheless, to a certain extent, this actually limits the optimization model to finding more favourable results. For example, coal is still used for heating demand in 2050 but only limited to

sectors that are difficult to be electrified, such as the steel industry. On this basis, complete electrification of the steel industry is not possible. On the contrary, the transformation pathway only applies cross-sectoral restrictions such as the complete phase-out of coal in 2040. This leads to a deeper decarbonisation and electrification of all sectors in the transformation pathway.

With regard to the electricity generation capacity, wind energy and PV have the largest net installed capacity. In the long-term and transformation pathways, wind energy has the largest installed capacity in 2050, followed by PV. The share of these technologies is switched in the climate protection pathway, as PV was pre-defined to have the larger installed capacity than wind energy. While the climate protection pathway only proposed 500 MW of biomass and biogas power plants, the other pathways have a similar installed capacity of 6 GW. The capacity of hydro power plants remains constant in all pathways. Among conventional power plants, gas-fired plants have the largest share in the long-term and the transformation pathways, with 21 and 67 GW installed respectively. In contrast, only 4 GW of gas-fired power plants are installed in the climate protection pathway, with an additional 70 GW of back-up capacity. This capacity may consist of gas turbines, oil-fired power plants or even measures of demand-side-management (DSM), with no specification provided by the pathway. The transformation pathway completely phases out coal-fired power plants, while these are still to be seen in the remaining pathways. However, these are the remaining power blocks from existing power plants today. No new plants are built in both pathways as most of the capacities have been decommissioned once the maximum lifespan is reached. Only hard coal is still in use in 2050 with very low full load hours. Brown coal power plants have been completely displaced by the very high CO_2 emission certificate prices[1]. The complete installed capacities of electricity generating capacities in 2050 are displayed in Figure 2-1.

In terms of the electricity generation, all pathways share the common fact that wind turbines provide the largest share of electricity generation in 2050, as illustrated in Figure 2-2. PV provides the second largest share among electricity generation. A very contrasting result is reported in terms of the electricity exchange with the neighbouring countries. In total, more electricity was exported to neighbouring countries until 2030 in the climate protection pathway and until 2040 in the long-term pathway. This however changed beyond that as Germany becomes a net electricity importer. In the long-term pathway, the net electricity import in 2050 is even greater than what is generated by PV or onshore wind turbines in Germany. In the climate protection pathway, almost 10 % of the total electricity demand is imported. It is explained in the pathways that the reason for this is the cheaper generation of renewable energies in other countries due to more favourable weather conditions. In contrast, the transformation pathway exports a total of 5 TWh of electricity in 2050 and does not allow for any import from the neighbouring countries.

[1] In January 2019, the Commission on Growth, Structural Change and Employment has agreed to phase out all coal-fired power stations in Germany by 2038 at the latest.

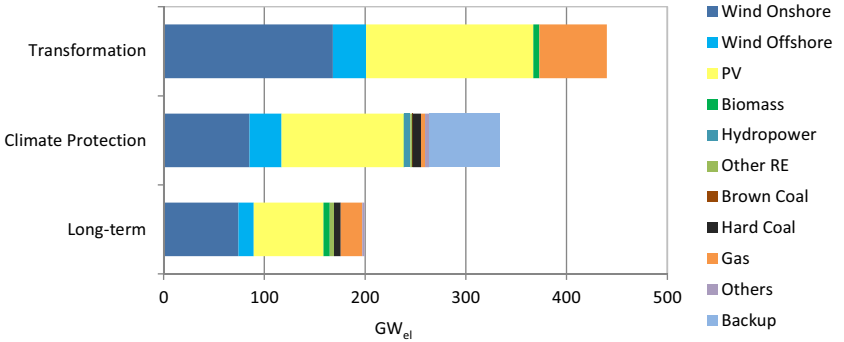

Figure 2-1: Cumulative installed electricity generation capacity in 2050. The "Backup" in the Climate Protection scenario refers to a generic backup power plant that offers a multitude of possible options, such as gas turbines or agreements on load shifting. The "Others" in the long-term scenario refers to other types of conventional and renewable power plants such as the waste-fired power stations or plant-oil-fired power plants.

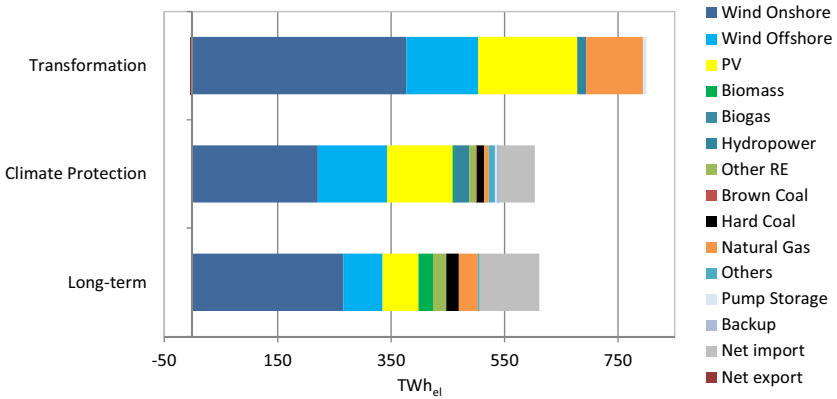

Figure 2-2: Total electricity generation in 2050 in all scenarios. The description of "Others" and "Backup" power plant types can be found in the description of Figure 2-1. The huge difference between the electricity generation in the transformation and the rest of the scenario is contributed by the new electricity applications such as the strong electrification of the heating and transportation sector.

One of the main requirements of achieving an energy system with a large share of renewable energies is electricity storages to compensate for the intermittent nature of the PV and wind energy. Interestingly though, the long-term pathway does not propose any installation of stationary electricity storage. Only the existing 7.4 GW of pump storage capacity is available until 2050. The reason for this is that enough flexibility is provided to the system by the power-to-heat applications, preventing stationary storages to reach economically viable full load hours. In the climate protection pathway, where the installed capacity of power plants and infrastructure are exogenously specified, a

total capacity of 15.7 GW of hydro pump storage and 13.5 GW of power-to-heat plants is set for 2050, with no additional stationary storages. In the transformation pathway however, additional electricity storages in the form of stationary batteries are built. In 2050, 74 GWh of battery capacity is available to the system. This may be attributed to the larger installed capacities of wind and PV to accommodate much higher electricity demand as well as the inability to import electricity from neighbouring countries.

Although stationary batteries are not built in the long-term and climate protection pathway, electric vehicles (EVs) that contain batteries are expanded massively. The electric vehicles considered in this thesis also contain fuel cell powered vehicles due to the application of batteries. In the long-term pathway, 30 million EVs are available in 2050 whereas 32.3 million are reported in the climate protection pathway. The transformation pathway reported around 34 million EVs in 2050. However, not all of the battery capacity is available as a flexibility option for the energy system in the transformation pathway, as this is only limited to 81 GWh (corresponding to 30 % of the total capacity of the full battery EVs). This information is not provided by the long-term and climate protection pathways and it remains unclear if the entire capacity is utilized for flexibility purposes.

Considering all aspects, it can be concluded that PV, wind turbines and batteries will be some of the main pillars of the future energy system in Germany. Therefore, the deployment of these technologies, as proposed by the selected energy pathways, will be analysed in detail in this thesis. In the following sections, technical descriptions and overview regarding the configurations of these technologies are provided, which are vital in determining the material efficiency measures and projections of future market shares in the subsequent chapters.

2.3.1 Wind turbines[2]

The power generation from the wind can be materialized through two different physical concepts; drag and lift forces. The latter can achieve a higher energy yield than the former which makes it widely used in wind turbines. The power available to a wind turbine is proportional to the cube of the kinetic energy of the wind, although the theoretical maximum energy that can be converted from the wind energy is limited by the Betz limit at 59.3 %. Modern-day grid-connected wind turbines are predominantly 3-bladed horizontal-axis machines (Spera 2009). The main components of a modern turbine are shown in Figure 2-3. The mechanical energy of the blades is transmitted via the low-speed shaft through the gearbox to the high-speed shaft that is attached to the generator, where electricity is generated. The yaw system controls the alignment to the direction of the wind by rotating the nacelle.

[2] Some parts of this sub-chapter have been published in (Shammugam et al. 2019a). These contents have been revised and editorially amended as part of this thesis.

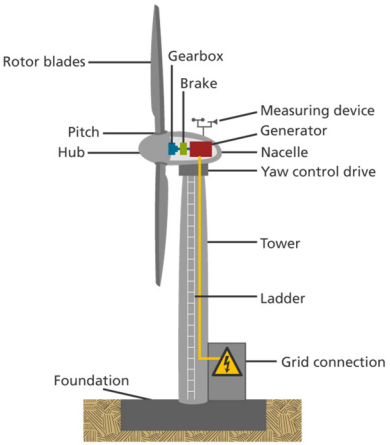

Figure 2-3: Schematic overview of wind turbine components © Fraunhofer ISE

In this thesis, the most common designs in the wind energy sector in Germany, namely horizontal axis design, lift-based, with a three blades rotor and variable speed generator are considered. Among the different factors affecting the material composition of a wind turbine, the drive train system stands out as the most important one that decides the material composition of a wind turbine. Therefore, the scenario definitions for the development of wind turbines in this thesis are depended on the drive train systems (see chapter 6.4 for development scenarios). The six current most commonly used wind turbine drive train systems are listed in Table 2-3.

The drive train systems are differentiated by their generator design (synchronous or induction), excitation (electrical or permanent magnet), number of gear stages (multiple-stage, single-stage or direct-drive) and power converter types (partial or full scale). Each of the drive train systems has its own advantages and disadvantages, which provides a high degree of freedom to the manufacturers to select a system configuration that best suits their business portfolios. According to the data registers from the Bundesnetzagentur (2017), these drive train systems accounted for at least 98 % of the turbines installed in Germany in recent years. Other concepts, such as the electrically-excited synchronous generator with gearbox, or the squirrel cage induction generator with constant speed, are not considered in the present study due to their negligible market share.

In terms of the generator design, the difference between induction and synchronous generators is that a synchronous generator's rotor rotates at the same rate as the synchronously rotating stator field while an induction generator's rotor rotates faster than the stator field. Induction generators, such as DFIG and SCIG, are less expensive than the synchronous generators at the cost of their efficiency (Cheng and Zhu 2014a).

Table 2-3: Types of wind energy conversion systems considered in this thesis

Drive train systems	Doubly-Fed Induction Generator	Electrically-Excited Synchronous Generator-Direct-Drive	Permanent Magnet Synchronous Generator – High Speed	Permanent Magnet Synchronous Generator-Middle Speed	Permanent Magnet Synchronous Generator-Direct-Drive	Squirrel Cage Induction Generator Variable Speed
Acronyms	DFIG	EESG-DD	PMSG-HS	PMSH-MS	PMSG-DD	SCIG
Type of generators	Induction	Synchronous	Synchronous	Synchronous	Synchronous	Induction
Type of excitation	Electrical	Electrical	Permanent Magnet	Permanent Magnet	Permanent Magnet	Electrical
Type of gearbox	3-stage	-	3-stage	1-stage	-	3-stage
Converter	Partial-scale	Full-scale	Full-scale	Full-scale	Full-scale	Full-scale

Induction generators can only be electrically excited, whereas the synchronous generators can be either electrically or permanently excited via magnets. PMSGs are lighter than electrically excited synchronous generators (Arnold et al. 2014; Polinder et al. 2006) and do not require an additional power supply for the magnetic field excitation, which leads to higher efficiency. On top of that, there is no need to transfer this excitation power with slip rings and brushes, which may cause failures and electrical losses (Cheng and Zhu 2014b). However, rare earth elements (REE) such as Neodymium makes the PMSG critical and difficult to handle during manufacturing (Chen and Li 2008) and prone to high price volatility of REE.

A further distinction is made between generators with gearbox and direct-drive ones. The direct-drive concepts, such as EESG-DD and PMSG-DD, feature a reduced number of rotating mechanical parts compared to a geared technology, thus limiting failure risks. This higher reliability has a cost: the generator, directly coupled to the hub, rotates slowly with the rotor speed of about 25 rpm, which causes the direct-drive generators to be larger and heavier than geared generators. A PMSG can feature either direct-drive (PMSG-DD) or geared configurations with single-stage (PMSG-MS) and multiple-stage (PMSG-HS) gearbox. Among geared generators, PMSG-MS represents a good trade-off between generator size and reliability. This so-called "multigrid system" has fewer mechanical components than the multiple-stage geared concept and, with a speed of up to 500 rpm, the generator still has a higher rotation speed than a direct-drive generator, which causes it to be smaller and lighter (Arnold et al. 2014).

In terms of power converters, the DFIG has the particularity of having a partial-scale power converter, meaning that only a part of about 20 to 40 % of the generated power goes through the converter, whereas the other generator types require a full-scale converter for the grid connection (Polinder et al. 2013). This partial-scale converter has the advantage of being smaller, cheaper and has fewer losses. However, compared to the full-scale converters, the partial-scale converters are more vulnerable to grid failures.

2.3.2 Photovoltaic

Ever since the discovery of the silicon p-n junction for converting solar radiation into electricity by Chapin et al. (1954), solar cells have been developing tremendously. Historically, solar cells have been used in fields that do not have access to electricity from the power grid, most notably in outer space as well as remote areas. Today, solar cells in the form of PV modules have become an important sustainable energy technology and are expected to contribute significantly to the future electricity generation. Solar cells convert solar radiation directly into electricity via the photovoltaic effect (see Klassen (2011) for the general principle of a solar cell). Since a solar cell can only generate a limited amount of electricity, a number of cells are usually interconnected in a weatherproof encapsulation and used together. This is known as a PV module. The number of cells in a module can vary, typically between 36, 60 and 72 cells. A PV system consists of PV modules, inverter, cable system and balance of systems (BOS), which usually represents the mounting system. The inverter converts the direct current that is produced in the PV modules into alternating current, to enable a feed-in into the power grid (Jülch et al. 2015). Among the various types of solar cells, the crystalline silicon (c-Si) and thin-film solar cells are the most mature technologies and have an average global production capacity of approximately 93 GW_p and 5 GW_p respectively (Fraunhofer ISE 2018). C-Si solar cells generally consist of either mono- or multi-crystalline silicon cells whereas thin-film solar cells are usually based on copper-indium-gallium-diselenide (CIGS) and cadmium-telluride (CdTe). The historical global market shares of the c-Si and thin-film modules are displayed in Figure 2-4.

Apart from c-Si and thin-film solar cells, various other cells do exist, which are either currently only deployed at a smaller scale (e.g. dye-sensitized and organic cells) or are still under development and not commercially available at a large scale (e.g. perovskite and III-V). Therefore, only c-Si and thin film solar cells are considered in the metal demand analyses of this thesis.

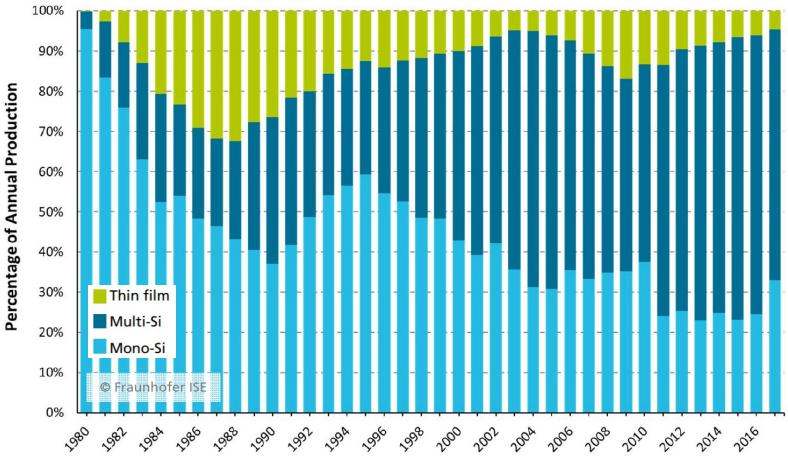

Figure 2-4: Global market share of c-Si and thin film PV module production. Source: Fraunhofer ISE (2018)

Crystalline silicon solar cells

A c-Si solar cell is generally based on a p-n junction, which is made into either p-type or n-type high-purity silicon substrate. Several variations of c-Si concepts are detailed in Polman et al. (2016). Among them, the Tunnel-Oxide-Passivated-Contact (TOPCon) concept is the most common type of c-Si solar cell in the market (ITRPV 2017) and will be used in the analyses in this thesis. The cross-section of a TOPCon cell is shown in Figure 2-5. Typical cell dimensions are 156 x 156 mm^2 and a thickness of 150-200 µm. The front side of the silicon layer is coated with a layer of silicon nitride in order to reduce the front reflection and passivate the emitter surface. The back side of the silicon layer is commonly coated with aluminium which forms the back contact and also acts as a passivation agent. The front contact usually consists of silver. The silicon layers are known as wafers and are either made of monocrystalline silicon (mono-Si) or multi-crystalline silicon (mc-Si), which is differentiated by the way they are prepared and cut. The former silicon is made out of a single continuous crystal lattice structure whereas the latter has crystalline grains with random orientations. A detailed description of the functionality of a c-Si solar cell is provided elsewhere by Glunz et al. (2012).

Thin film solar cells

Although c-Si cells are a robust and proven technology, producing a much cheaper solar cell has always been the constant motivation to develop thin film solar cells (Aberle 2009). Since a large share of energy and costs of production goes into processing the silicon wafer (Kazmerski 2006), the idea was to replace it with other materials, thus automatically reducing the associated costs. This was

first achieved through the development of the Cu_2S/CdS cell, which was significantly thinner than a c-Si cell at that time (Chopra et al. 2004). Ever since, thin-film solar cells have been subject to intense research, leading to the discoveries of many viable materials to be used in making a solar cell. Thin-film solar cells have high optical absorption coefficients, which makes very thin absorber layers possible. The basic principle of thin-film solar cells is that two electronically different material layers, namely the transparent conducting oxides (TCO) and the absorber layer, are placed together. A buffer layer of CdS between them ensures that the charges are separated (Chopra et al. 2004) and forms a junction between the TCO and absorber. Besides that, the buffer layer also improves the interface properties and chemically protects the absorber layer during the high-temperature manufacturing process (Naciri et al. 2007). However, the energy band gap of a buffer layer has to be much higher than that of the absorber so that it can minimize absorption and recombination losses. The ohmic back contact is often realized by a layer of molybdenum.

CdTe represents the largest share of thin-film modules worldwide. The current record efficiency for CdTe solar cells is held by First Solar at 22.1 %, who is also the largest producer of CdTe modules in the world. CdTe solar cells have an energy band gap of 1.5 eV, which is very close to the ideal band gap for photovoltaic conversion efficiency of 1.45 eV (Morales-Acevedo 2006). CIGS thin-film solar cell currently holds the official record for the highest laboratory efficiency of thin-film solar cells at 22.9 % (Green et al. 2018). The p-type absorber layer of $Cu(In_{1-x}, Ga_x)Se_2$ has a high absorptivity and an energy band gap in the range of 1.06-1.7 eV, depending on the composition of indium and gallium in the layer. The exact structures of CIGS and CdTe solar cells and their general principle are explained elsewhere by Polman et al. (2016).

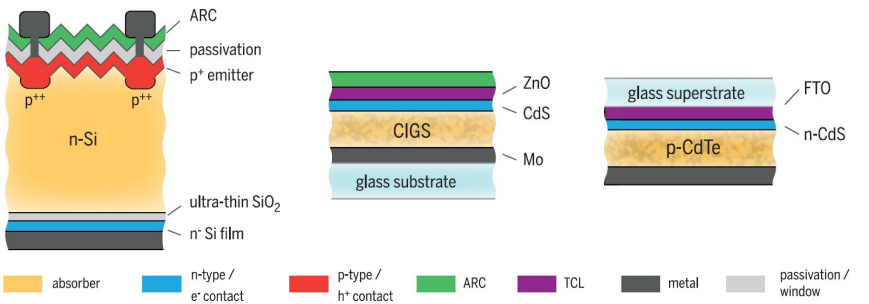

Figure 2-5: Cross-section of a c-Si TOPCon (left), CIGS (middle) and CdTe (right) solar cells. ARC refers to anti-reflection coating while TCL refers to the transparent conductive layer, also known as the transparent conductive oxides. Source: (Polman et al. 2016)

2.3.3 Batteries

Batteries are expected to become a crucial technology in the energy transformation process which will facilitate the decarbonisation of the energy sector. The transportation sector contributes around 22 % of the total energy-related green-house-gas (GHG) emission in Germany. Although the emissions have been reducing –compared to the emission levels in 1990- mainly due to more efficient combustion engines, a more drastic reduction to meet the climate goals would require the electrification of the transportation sector. Therefore, the biggest demand for batteries in the future will most likely come from the transportation sector. Besides the use in electric vehicles (EV), batteries are also important in an energy system with a high share of renewables, mainly as a flexibility option due to the intermittency of PV and wind energy. From the generation point of view, batteries enable excess electricity from PV and wind to be stored and used at later times. They provide valuable support for the power grid by catering balancing energy in order to control the frequency and voltage to ensure the stability of the power grid. In terms of consumption, they enable demand-side-management, which includes measures such as shifting the demand to off-peak period or peak shaving. In combination with PV systems, batteries also increase the electricity self-consumption rate while benefiting the owners through additional revenue and avoided costs of utilizing electricity from the power grid (Kost et al. 2018). Further comprehensive descriptions of the application and benefits of batteries are provided by Klausen (2017).

The most basic element of a battery is a cell, which consists of an anode, cathode and the electrolyte. Metals contained in these components are denoted as the active metals in this thesis, which represents the most important elements for the functionality of the cell. Multiple cells that are wired in series are known as a module. Ultimately, a collection of modules packed in the final shape of a battery is known as a pack (Andrea 2010). There are currently various types of batteries in the market, each with a different layout and chemical composition. This leads to a wide range of parameters such as energy density and cycle numbers, which makes specific batteries to be used in targeted application (Stenzel et al. 2015). However, there are generally five types of batteries that are currently most commonly used for electricity storage purposes in EVs as well as in stationary applications. These are lead-acid, nickel metal hydride, redox-flow, high-temperature and lithium-ion batteries. The general characteristics of the batteries are explained in the following sections and are summarized in Table 2-4.

Lead-acid (Pb-acid) batteries

Invented at the end of the 19th century, the lead-acid battery is one of the very first rechargeable batteries. Since then, it has been one of the major means of electricity storage and has been used in

various applications, from the 12 V starting-lighting-ignition (SLI) system in automobiles (Chumchal and Kurzweil 2017) to standby application such as in telecommunications, data networks and energy sector (May et al. 2018). A cell of the lead-acid battery consists of flat plates made out of lead that is submerged in an electrolyte consisting of water and sulfuric acid. The detailed functionality of a Pb-acid battery can be found in (Johnson 2014).

Pd-acid batteries are a reliable, robust and mature technology as the characteristics have been intensively researched and highly optimized over the years. The major advantages of Pb-acid batteries include the use of relatively cheap materials, simple battery management system as well as the very high safety levels. With a recycling rate of over 99 % (SmithBucklin Statistics Group 2017), Pb-acid batteries are the most recycled consumer product in the western countries and have reached an almost complete closed-loop recycling system. The simple construction of Pb-acid batteries makes the dismantling and recovery of materials to be possible with minimal energy requirement, which further increases the sustainability of the batteries. However, one of the biggest drawbacks of Pb-acid batteries is the toxicity of lead. Poor working conditions in recycling plants of Pb-lead acid plants in some low to middle-income countries have led to lead poisoning. In fact, the entire industry of recycling lead-acid batteries has been ranked the most polluting industrial process worldwide according to disability-adjusted years of life lost (Ballantyne et al. 2018). Other disadvantages of Pb-acid batteries are low gravimetric and volumetric energy density (May et al. 2018) as well as low efficiency and cycles life (Stenzel et al. 2015).

Nickel-metal hydride (NiMH) batteries

NiMH batteries were first patented in 1986 and are a result of the further development of the proven nickel-cadmium (Ni-Cd) battery. Similar to Ni-Cd, NiMH batteries consist of nickel-hydroxide as cathodes while the electrolyte is made out of aqueous potassium hydroxide. The difference is that the active material in the negative electrode is hydrogen-absorbing alloy instead of cadmium. Further working principles of NiMH batteries are detailed in (Chang et al. 2016). The main advantages of NiMH batteries are the long cycle life and high power density compared to Pb-acid and most of the Li-Ion batteries. However, the main disadvantages of NiMH batteries are the susceptibility to memory effect (Sato et al. 2001) and the high self-discharge rate at 30 % of capacity fade per month as opposed to only 5 % in Li-Ion batteries (Julien et al. 2016). In addition to that, NiMH batteries have high costs mainly due to the intensive nickel requirements (Johnson 2014). Although NiMH used to be applied in portable applications in the past, this has been taken over by the much cost effective Li-Ion batteries (Pillot 2017). At the moment, the major use of NiMH batteries is in hybrid electric vehicles (HEV).

Lithium-ion (Li-Ion) batteries

The first commercial Li-Ion battery was introduced by Sony Corporation in 1991 (Blomgren 2017). A Li-Ion cell consists of an anode and cathode contacted by an electrolyte, which carries the positively charged lithium ions between the electrodes. A separator ensures that the electrodes are isolated while still allowing the transfer of lithium ions (Deng 2015). There are two main reasons as to why lithium is primarily used as the ionic charge carriers. Firstly, an extremely high cell potential can be reached since lithium has the lowest reduction potential of any elements. Secondly, lithium, being one of the lightest elements, enables exceptionally high gravimetric and volumetric energy density (Nitta et al. 2015). Consequently, a battery with high energy density makes it an increasingly preferred technology in various electric applications such as in portable electronic devices and electric vehicles (EVs).

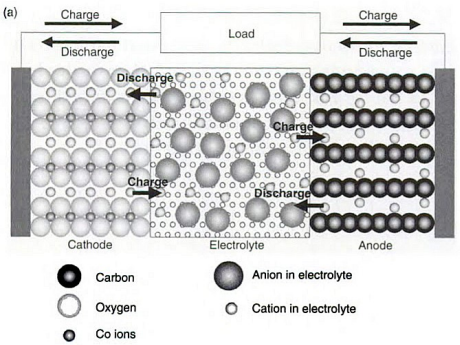

Figure 2-6: Cross section representation of a LCO Li-ion cell. Source: (Kanamura 2005)

The anode of conventional Li-Ion batteries is generally made out of graphite. In terms of the cathode, there are various metal compositions which provide distinctive characteristics to the different types of Li-Ion batteries. The earliest battery commercialized by Sony was based on lithium-cobalt-oxide ($LiCoO_2$). This battery, also known as LCO, was very attractive at the point of introduction as it boasted high volumetric and gravimetric energy density with reasonable cycle lifespan relative to Pb-acid batteries. At present, LCO is still the preferred candidate for portable electronic applications such as cell phones and laptops. The disadvantage of LCO batteries, apart from higher losses during deep cycling, is the high cost of material due to the presence of cobalt. Efforts in reducing the cobalt demand lead to the development of a lithium-nickel-cobalt-aluminium-oxide ($LiNi_{0.8}Co_{0.15}Al_{0.05}O_2$) based cathode, also known as the NCA battery. While cobalt

was partially substituted with nickel, aluminium was introduced to improve the thermal stability. NCA batteries have a superior lifespan than LCO and are primarily used in EVs, most notable by Tesla. Batteries with lithium-manganese-oxide ($LiMn_2O_4$) cathode, also known as the LMO, are cheaper than the LCO or NCA as it has neither nickel nor cobalt. LMO batteries are also safer due to higher thermal stability and the spinel structure of the cathode allows for lower internal resistance. The disadvantage of LMO batteries is that it has a lower energy density compared to NMC or NCA. Another type of Li-Ion battery that is manufactured with abundant materials is the lithium-steel-phosphorous ($LiFePo_4$) battery, known as the LFP. The biggest advantage of LFP batteries is high safety and a relatively high cycle life. However, the biggest drawback of LFP batteries is low energy density. Last but not least, the lithium-nickel-manganese-cobalt-oxide ($LiNiMnCoO_2$) battery, known as the NMC, is the youngest among all aforementioned batteries as it was only commercialized in 2004. Nonetheless, it has experienced the highest growth in terms of application as it is being intensively used in EVs as well as in electronic applications. Although the energy density of NMC is lower than the NCA, it has higher cycle-life and power density.

Although Li-Ion batteries have a higher energy density, better efficiency and favourable calendar lifespan than most of the commercially available secondary batteries, safety is still a major concern (Deng 2015; Wen et al. 2012). The main reason for this is the thermal runaway which occurs when there are irregularities in an exothermic reaction in the battery due to overcharging or other flaws (Liu et al. 2018a). Since the liquid electrolyte of a Li-Ion battery is flammable, a significant increase in temperature eventually leads to fire and explosions. Some of the more prominent incidents related to Li-Ion batteries are the grounding of Boeing 787 Dreamliners due to fires in the aeroplane batteries (Williard et al. 2013) as well as the multiple reported explosions in cell phones and portable devices (Wang et al. 2012).

However, this disadvantage related to the aqueous electrolyte can be addressed with the development of solid-state batteries, which uses solid-electrolytes. Besides providing the benefit of removing the flammable liquid electrolyte, solid-state batteries also have other advantages, such as allowing for higher energy density, longer cycle life (Luntz et al. 2015) as well as reducing material and fabrication cost since the cells are not required to be separated within a module (Sun et al. 2017). Due to these reasons, solid-state batteries are seen as a promising technology to be implemented in EV. The cathode chemistry remains the same with LCO, NCA and LFP being some of the more researched cathode composition for solid-state batteries (Kurzweil and Garche 2017). As for the solid electrolytes, various chemical compositions either in the form of ceramic or polymer electrolytes have been successfully tested (see (Xu et al. 2018; Takada 2013; Sun et al. 2017; Gao et al. 2018)). Despite overwhelming advantages, solid-state batteries are still at an early stage of research. Disadvantages of solid-state batteries include lower power density, low ionic conductivity and high resistance at the interface between the electrolyte and electrodes, which hinders fast charging and discharging (Kawasoko et al. 2018). Furthermore, the cost of manufacturing a solid-state battery is currently high as it is mainly manufactured under controlled laboratory conditions.

Sodium high-temperature batteries

Unlike conventional batteries, the electrolytes of a sodium-based high-temperature battery are solid whereas the anode and cathode are in liquid form (see Figure 2-7). Due to the high melting point of sodium (in the cathode), typically between 310 and 350 °C, this battery system has to be operated at high temperature. Nonetheless, the long cycle life has made it attractive for the use of grid-connected applications. Sodium-sulphur (Na-S) batteries are currently commercially available (Stenzel et al. 2015), with a capacity of 1.8 MW already installed in Germany (DOE 2018). One of the major advantages of Na-S batteries is the use of non-expensive and non-critical materials. However, Na-S batteries have considerably lower energy density compared to Li-Ion batteries. The need for high temperature also proves to be one of the biggest drawbacks of this battery due to two main reasons. Firstly, additional energy is required in order to maintain this operating temperature, which reduces the overall efficiency of the battery. Secondly, the molten salt is corrosive at high temperatures, which calls for additional material and measures to ensure that the encapsulation and housing of the batteries are not harmed (Hueso et al. 2013).

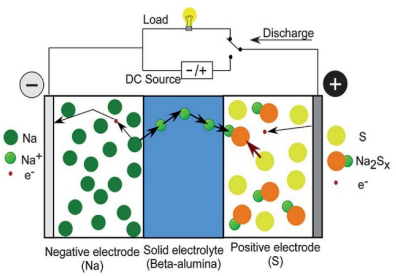

Figure 2-7: Cross section representation of a Na-S cell. Source: (Hueso et al. 2013)

Redox-flow batteries

While small-scale redox-flow batteries (<1 MW) are already commercially available, large-scale batteries are currently at a demonstration stage and have the potential to be applied widely as stationary storage systems in the future. As opposed to the conventional batteries, where one compact cell contains the electrolytes and electrodes, the redox-flow batteries consist of two liquid electrolytes in separate tanks and a stack of cells in which the redox process occurs (see Figure 2-8). One of the advantages of redox-flow batteries in comparison to Na-S is that the former only needs to be operated close to room temperature in order to main the electrolytes in liquid form, which consequently reduces the additional energy requirement and improves the safety quality (Alotto et al. 2014). Currently, there are several redox-flow batteries that are often discussed in the literature.

(Leung et al. 2012) provide a comprehensive overview of the various types of redox flow batteries and their characteristics. The Vanadium/Vanadium (V-V), also known as the Vanadium Redox-Flow battery (VRFB) was discovered in the late 1980s and has ever since become one of the most promising and researched concepts of all redox-flow batteries. The main disadvantage of redox-flow batteries is the extremely low energy and power density. Due to the nature of the system that is not compact, they are not suitable for mobile applications. However, in terms of stationary grid-connected battery systems, where the area of installation is not an issue, redox-flow batteries are suitable candidates as it is easily scalable and has extremely high cycle numbers which can accommodate the intermittency of PV and wind energy generation.

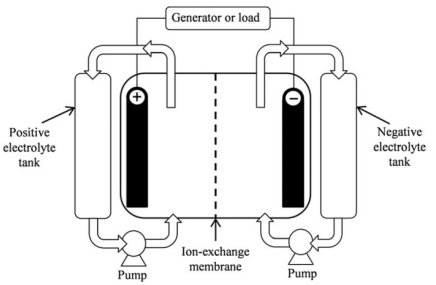

Figure 2-8: Cross section of a V-V redox flow battery. Source: (Kear et al. 2012)

Post Li-Ion battery concepts

At the moment, further development in batteries is mainly driven by the automobile industry to extend the range of electric cars while improving the safety aspects. Despite having the highest energy density among current battery types, Li-Ion batteries cannot meet the increasing demand for energy density, especially for pure electric vehicles, as it is already reaching the limits that intercalation material can achieve (Ji and Nazar 2010; Suo et al. 2013). Therefore, research works are going on in search of next-generation batteries with considerably higher energy density. Two of the most discussed concepts in the literature with the best chances of a market entry are lithium-sulphur (Li-S) and lithium-air (Li-Air) batteries.

Lithium-Sulphur (Li-S) batteries

The Li-S batteries have lithium metal as an anode while the cathode comprises of sulphur, graphite and a binder. Both electrodes are separated by either an organic-solvent aqueous electrolyte and a polymer separator (Fotouhi et al. 2017; Liu et al. 2018b). Li-S batteries have a theoretical maximum energy density of around 2500 Wh/kg, with an achievable energy density estimated around 500

Wh/kg (Stenzel et al. 2015). As opposed to the other alkali metal-sulphur batteries, such as the Na-S, Li-S batteries can be operated at room temperature. The cost of Li-S is estimated to be around 200-400 USD/kWh. However, it has the potential of having lower specific costs compared to conventional Li-Ion batteries such as the NMC or NCA since it only utilizes inexpensive materials. Furthermore, Li-S is also more robust to deep-cycling and has a higher shelf life. Although Li-S batteries have been researched for the past two decades, they exist currently only in laboratories and commercialization still has not materialized. The major drawback of Li-S batteries is the active formation of lithium dendrites in the anode solid-electrolyte-interphase (SEI) due to the high electronegativity of lithium, which causes poor cycle-numbers and increases the possibility of short circuit. However, intensive research activities are currently going on to improve these issues, for instance adding a stabilizing agent such as $LiNO_3$ in the electrolyte (Suo et al. 2013) and protecting the lithium anode using inorganic solid electrolytes.

Lithium-Air (Li-Air) batteries

A Li-Air battery consists of a Li-based anode and an air cathode, separated by either an aqueous or solid electrolyte layer. These batteries have the highest theoretically maximum energy density among any other electrochemical battery concepts at more than 11 kWh/kg, which even rivals the energy density of petroleum (Lee et al. 2011). However, the achievable energy density is estimated to be around 5.2 kWh/kg, which is still considerably higher than Li-Ion batteries available today. The concept of Li-Air has already been around since 1996. However, only through the discovery of the porous electrodes in favour of the intercalation electrode, which showed increased electrochemical performance, did the research works on Li-Air began to grow rapidly (Ogasawara et al. 2006). Li-Air batteries are currently still in relatively early stages of research and development. Some of the challenges faced by Li-Air batteries currently are low power density, low round-trip efficiency, stability issues and safety issues due to high sensitivity to temperature and humidity (Kraytsberg and Ein-Eli 2011). If these problems can be solved, Li-Air batteries have the potential to be intensively applied in the future not only in EVs but also in stationary applications.

Table 2-4: Characteristics of selected battery types compiled based various literature source: (Wietschel et al. 2015; Nitta et al. 2015; Zubi et al. 2018; Bergholz 2015; Iclodean et al. 2017; IRENA 2017; Kumar 2013; Omar et al. 2014; Fetcenko et al. 2007; Zhu et al. 2013; Kear et al. 2012; Nordling et al. 2016; Hannan et al. 2017; Glöser-Chahoud 2017; Xue et al. 2017)

	Pb-acid	**NCA**	**NMC**	**LMO**	**LFP**	**Na-S**	**VRF**	**NiMH**	**Li-S**	**Li-Air**
Gravimetric Energy density [Wh/kg]	30-50	200 - 250	140-200	100-140	90-140	115	15-70	54-110	250-400[a]	450-550[a]
Volumetric Energy density [Wh/l]	50-100	282	240-290	240-290[b]	214-246	150-300	50-100	46-435	350-720[a]	n.a
Power density [W/kg]	75-300	200-1080	270-1400	270-1400[b]	2400-2500	120	20-150	800-1200	250-350[a]	low
Cycle numbers	100-150	1000-1500	1000-3000	1000-1500	2000	2500-4500	13000-20000	500-1800	<100[a]	500[a]
Calendar lifespan [a]	3-15	5-20	5-20	5-20	5-20	15	20	3-15	n.a	n.a
Thermal runaway [°c]	-	150	210	250	270	290-350	-	-	n.a	n.a
Operating temp. [°c]	-20 until +50	-40 until +65	-40 until +65	-40 until +65	-40 until +65	+290 until +350	+20 until +35	-30 until +70	-20 until +50	n.a
Efficiency [%]	60-90	95	95	95	92	80	70-80	60-80	85[a]	<70[a]
Battery cost [€/kWh]	50-150	200-230	200-410	200-245	200-350	360-450	300-450	400-750	200-400[c]	n.a

[a] – Refers to the current values reported in the literature. The actual values upon commercialization can be much higher
[b] – Due to the lack of exact values in the literature, the energy density is assumed similar to NMC, as applied by (IRENA 2017). Exact values in reality might be lower.
[c] – Estimated cost in 2025 by (Stenzel et al. 2015)

3 Theoretical basis of metal prices

According to the concept of general economic equilibrium, the price of a commodity in a free market depends on the quantity that is demanded by consumers and is supplied by producers (Gale 1955). The equilibrium between the supply and demand of a metal in relation to the price is exemplarily illustrated in Figure 3-1. The demanded quantity Q1 and price P1 represent the state of equilibrium between the demand and supply. On the figure in the left, it can be seen that the price increases from P1 to P2 when the demand shifts upwards from D1 to D2 while supply S remains constant. Meanwhile, on the figure in the right, assuming that the demand remains constant, an increase of supply from S1 to S2 eventually reduces the price from P1 to P2. However, commodity markets will eventually regulate themselves in order to reach an economic equilibrium in the long-run (Gale 1955). For instance, once the price of a metal increases as a consequent of growing demand, supply will eventually increase to meet the demand. As a result, market equilibrium will be eventually achieved, thus causing the price to theoretically drop to the initial equilibrium price.

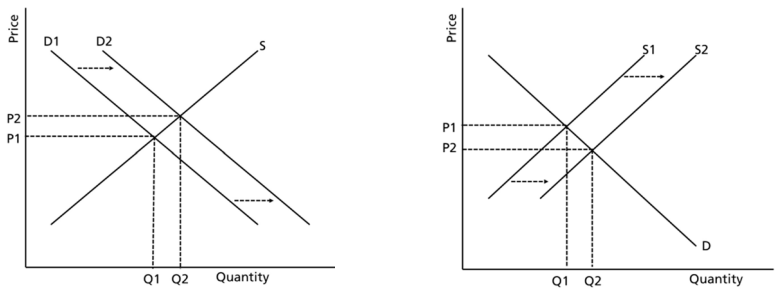

Figure 3-1: The figure on the left illustrates the shift in the market equilibrium when the demand increases (from D1 to D2) while supply (S) remains constant. The figure on the right shows the shift in the market equilibrium when the supply increases (from S1 to S2) while the demand (D) remains constant.

Metals are physically related to each other in terms of production and consumption. On one hand, since most of the metals occur together in mineral deposits, they are very often mined together. On the other hand, metals are almost always used together in order to manufacture any end-use product due to their different characteristics which serve different purposes in the product. Therefore, the behaviours of the metal prices which are either jointly produced or jointly consumed are theoretically explained in this chapter.

3.1 Joint production of metals[3]

In general, metals that are jointly produced can be divided into three categories, namely the primary metal, co-product and by-product. The price relationships of the metals can be systematically deduced based on these classifications. In addition to that, the relationships can further be categorized according to the proportionality of the prices. In economics, the terms substitutes and complements are usually used for this purpose. However, since these terms are more commonly used in explaining the relationship in terms of the consumption, the terms directly proportional or inversely proportional is used in this thesis when explaining joint-production effects. Prices which are directly proportional means that they move in the same direction whereas inversely proportional means that when the price of one metal increases, the price of another metal decreases.

A primary metal is the main product of a mine which has the largest mining volume. In most of the cases, its market price alone determines the mining strategy and is responsible for the economic viability of a mine (Tilton and Guzmán 2016). Some of the metals that are usually classified as primary metals in a mine include iron, copper, aluminium and gold. A by-product is a secondary product from the mining process and does not affect the profit-maximizing decision of the production and the output of the main product (Brooks 1965). This is owed to the significantly smaller production volume and much lower turnovers of the by-products compared to the primary metal. By-products are sold, stored or discarded off, depending on the market price and their specific operational expenditures (Rankin 2011). The secondary production of bismuth in a lead mine is an example of a by-product. The third group of metals, also known as the co-products, can somewhat be categorized between primary metals and by-products. Although co-products are also recovered as secondary products, they are economically valuable and influence the mining strategy regarding the profit maximization production level of the ores (Campbell 1985). Another difference between by- and co-products is that the former do not share any operational costs of a mine as this is solely borne by the primary metal. On the contrary, co-products share the joint production costs with the primary metal (Fizaine 2013; Tilton and Guzmán 2016). One of the most well-known co-products is molybdenum, which is recovered as a secondary product in a copper mine.

As previously mentioned, by-products are secondary products and their production is not driven by their own demand, instead of the production of primary metals and co-products. This implies that the price of a by-product is inelastic to its own prices. Even if the price of a by-product increases due to the increase in demand, the productions remains unchanged if the production of the primary metal remains unchanged. This means that the price of by-products is driven by the price of their respective primary metals and co-products, but the opposite is not true. Co-products on the other hand, have the ability to alter the mining strategy, which means that the production of the main product is depended on the price of co-products. Unlike by-products, whose production is

[3] Some parts of this sub-chapter have been published in (Shammugam et al. 2019b). These contents have been revised and editorially amended as part of this thesis.

constraint by the output of the primary metal, the production of a primary metal can be increased with the increasing price of co-products, until the mine reaches its maximum capacity. This effect is illustrated in Figure 3-2 as previously explained by Shammugam et al. (2019). Therefore, it can be deduced that the price of primary metals is driven by the price of co-products and vice versa.

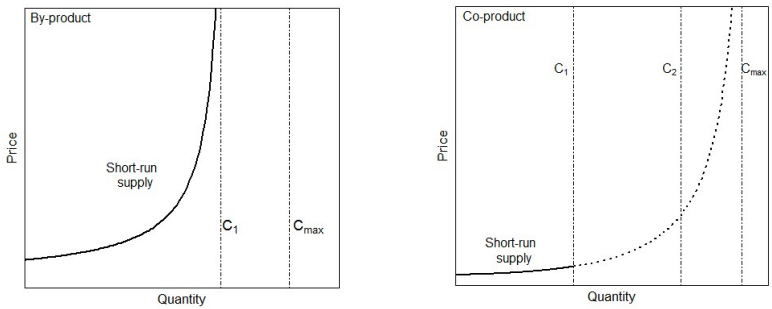

Figure 3-2: Supply curve of a by-product (left) and the supply curve of a co-product (right). C_1 and C_2 refer to the short run constraints whereas C_{max} refers to the maximum production capacity of a mine. Source: Shammugam et al. (2019)

In terms of the direction of the relationships, the prices of the metals that are jointly-produced should theoretically be inversely proportional to each other. This is mainly caused by the overproduction of a metal due to the increased demand for its companion product. For example, as the price of molybdenum increases, mine owners will increase the production of copper ores. Consequently, this will cause an oversupply of copper, assuming that the demand remains unchanged, and ultimately decreasing the copper price. However, this notion is only valid if the metals are strictly related via joint-production and not via joint-consumption as well as this might change the equilibrium of the relationship. The price relationships between metals that are jointly consumed are detailed in the next subchapter.

In Table 3-1, metals that are found in PV, wind turbines and batteries are paired with their respective companion metals in production. Based on this table, metal pairs will be built and tested for any dependencies in their prices.

Table 3-1: Categorisation of selected metals found in PV, wind turbines and batteries into primary metals, co-products, by-products and their companion metals.

Primary metal	Co-Product	By-Product	Source
Al	-	Ga	(Nassar et al. 2015)
Ag	Au	Zn	(Campbell 1985)
Au	Ag	Cu	(Campbell 1985)
Cu	Mo, Ag, Au	Se, Co	(Campbell 1985; Ayres et al. 2003; Rankin 2011; Hustrulid and Bullock 2001)
Fe		Dy, Nd	(Graedel and Nassar 2015)
Li		K, B	(Boryta et al. 2011)
Ni	-	Cu, Co	(Rankin 2011; Nassar et al. 2015)
Pb	Zn, Ag	Cu	(Rankin 2011; Nassar et al. 2015; Hustrulid and Bullock 2001; Campbell 1985)
Zn	Ag, Pb	Cd, In, Ge, Ga	(Rankin 2011; Nassar et al. 2015; Campbell 1985; Hustrulid and Bullock 2001)

3.2 Joint consumption of metals[4]

In order to derive the theoretical relationship between the prices of metals that are jointly consumed, the terms complements and substitutes have to be understood. Substitutes in demand refer to a competing relationship between two metals. This means that if the demand for one metal increases, the demand for the other decreases. As an example, silver has been historically used for electrical contacts in c-Si PV modules. However, since the price of silver is significantly higher than any other metal in a c-Si module, research activities are being conducted in order to replace silver with a much cheaper metal, such as copper. Therefore, in the long run, the demand for silver in PV will decrease upon being substituted by copper, which in turn will lead to an increase in copper demand. Therefore, silver and copper can be categorized as substitutes in demand in the long-run. Hypothetically, substitutes should have an inversely proportional price relationship. In the previous example, the price of copper should increase due to the increasing demand whereas the price of silver should decrease, given that every other variable such as production and the demand in other end-products where the metals are used remains constant.

Complements, on the other hand, refer to metals that are used together in a product and are not substitutable. Nickel and cadmium are a good example of this. Almost 75 % of the global cadmium demand is used for manufacturing nickel-cadmium (Ni-Cd) batteries (USGS 2018). Since both metals are important for the functionality of the batteries and are not easily substitutable, nickel and cadmium are considered complements in demand. Therefore, if the demand for Ni-Cd batteries increases, the demand for both nickel and cadmium will simultaneously increase, given that production remains constant. Therefore, metals that are complements in demand should hypothetically have a directly proportional price relationship.

[4] Some parts of this sub-chapter have been published in (Shammugam et al. 2019b). These contents have been revised and editorially amended as part of this thesis.

However, the relationships between metal prices cannot be defined straightforward in reality. This is owed to the fact that unlike joint-production, where the conditions are binary (two metals are either jointly-produced or not), the definition of joint-consumption depends very much on the level of consumption aggregation. As an example, Ni-Cd batteries have a competing relationship with lead-acid batteries. Therefore, both nickel and cadmium can be classified as substitutes of lead. However, if one aggregates different battery types into one field of consumption, say electricity storages, then both types of batteries are considered complements. Therefore, any hypothesis regarding the price relationships of metals that are jointly-consumed has to be made relative to a predefined aggregation level of consumption. In this thesis, the joint-consumption of metals is considered for the end-products of PV modules, wind turbines and batteries particularly. However, the analysis is also extended to a higher level of aggregation to investigate where a joint implementation of these technologies in Germany will have a simultaneous effect on metal prices.

In general, prices of jointly-produced metals should have an inversely proportional relationship whereas joint-consumption would lead to a proportional relationship between metal prices. Nonetheless, this only holds if the metals are either strictly jointly-produced or consumed. If two metals are related in production and consumption at the same time, then a clear sign cannot be imposed. For instance, silver and copper are both jointly-produced (Campbell 1985) and used in electronic applications such as in capacitors and electrical switches (Thomson Reuters and The Silver Institute 2018; ICSG 2017). An increase in demand for electronic devices will consequently increase the demand for both copper and silver. Therefore, an increased production in a copper mine will not lead to an oversupply of silver, since its demand increases as well, thus moving the price of both metals in a similar direction. However, this will not be true if the substituting relationship between silver and copper in the joint production is significantly stronger and overwhelms the equilibrium provided by the simultaneous joint-production and consumption.

4 Literature review

Based on the research questions, three main literature streams are looked into in detail within the framework of this thesis. In the first section, the estimation of material demand and the corresponding bottleneck risks of PV, wind turbines and batteries for stationary storages and electric vehicles (EVs) are discussed. The second literature stream is the relationship between metal prices. Within this context, the application of Granger-causality test in determining the price relationships between metals are analysed. This is followed by a more detailed discussion of literature sources that investigated the effects of joint production and joint consumption on metal prices. Last but not least, the vector-autoregressive (VAR) analysis of metal prices completes the literature streams analysed. Based on the literature review, research gaps in each literature stream are identified, which serve as the basis in formulating the research design in the succeeding chapter for further analysis.

4.1 Raw material demand in renewable energy technologies

4.1.1 Photovoltaics

PV modules are by far the most-researched renewable energy technology in terms of the material demand and availability due to the utilization of various critical metals. One of the earliest empirical analysis was conducted by Andersson et al. (1998), in which the authors compared the cumulative material demand of a complete market capitalisation by thin-film modules until 2100 to the known reserve levels and production rate at that time. Their results indicated that indium is the most critical metal, followed by tellurium and germanium. One year later, the lead author released another paper (Andersson 2000), in which he argues that the short term deployment of thin-film modules until 2020 will not be constraint by the metal availability, but rather by the increasing metal prices. Majority of studies thenceforth focused on the bottleneck or supply risk faced by critical metals in PV modules. For example, Zuser and Rechberger (2011) analysed the global demand for selected metals in c-Si, a-Si, CdTe and CIGS modules. Total installed capacity in 2040 is assumed to be between 5908 and 8368 GW_p. Upon comparing the total demand with the reserve levels from 2010, tellurium and indium are identified as critical whereas silver is concluded to be critical in terms of production since more than 50 % of the annual production would be required to fulfil the maximum annual demand. Feltrin and Freundlich (2008) also reported possible bottleneck risks of tellurium and indium which could prevent a global large scale deployment of CdTe and CIGS. Helbig et al. (2016a) investigated the supply risks of the metals present in thin-film modules using several other indicators than the physical availability, such as concentrations and political risks. Using a weighted

average of the indicators, the authors reported that indium has the highest supply risk, followed by gallium, molybdenum and tellurium. On a technology level, CdTe has therefore a slight advantage over CIGS due to the utilization of less risky metal.

Furthermore, Kavlak et al. (2015) investigated the metal production requirements for the deployment of PV modules until 2030. Their study was focused on the demand of critical metals in CdTe and CIGS modules, as well as silicon in c-Si modules for global cumulative installed capacities ranging from 720 to 5500 GW_p in 2030. The authors compared the required production growth rate of the metal demands with the historical growth rate in order to test the feasibility of achieving the cumulative installed capacities. The central take away from this paper is that indium, tellurium and selenium will not be able to keep up with the required growth in production. On the contrary, c-Si modules are reported to be able to contribute to 100 % of the global electricity production from PV since silicon is not subject to any constraints. However, the validity of this message would have been much stronger if the authors considered other metals in c-Si modules, especially silver, in order to identify any possible bottleneck risk. As an example, Kleijn et al. (2011) investigated the material requirement for mono c-Si modules in order to achieve the electricity mix in 2050 according to the IEA Blue Map Scenario (IEA 2010). The authors estimated that the demand for silver in 2050 will reach up to more than 44 % of the current global production level, which will certainly face strong competition from other end-use of silver.

On the contrary to the above studies, Candelise et al. (2011) came to the conclusion that the global deployment of thin-film PV modules will be constraint by the availability of neither tellurium nor indium. The authors argue that only at a very conservative assumption, i.e. complete market dominance by thin-film modules, will there be any supply risk. The authors' main critic on other studies is that the estimates of future availability of materials are not robust and contains high uncertainties that overestimated the bottleneck risks. However, no empirical evidence is given by the authors to support this view, as this notion was derived subjectively based on a review of existing literature at that time. A similar statement was also made by Fthenakis (2009), who analysed the sustainability and material requirement of a large scale deployment of thin-film PV cells. The authors showed that the installation of manifold cumulative installed capacity is possible without any bottleneck risk, given that the manufacturing process is improved and more importantly, a sound recycling process of old modules are established. An interesting take on this subject matter was provided by Raugei and Fthenakis (2010) by analysing the global cadmium flows and emissions due to the deployment of CdTe PV modules in the future. The authors estimated that over 2.4 kt of cadmium will be required in 2050 alone, which is derived upon the assumption that the efficiency will be 16 % and the specific material demand to be 54 g/kWp in 2050. Although no scarcity analysis was conducted, the authors argue that the increased use of CdTe PV modules is beneficial to the global environment due to the utilization of cadmium as by-products from the production of zinc ores, which will otherwise be discarded.

While the above studies analysed the global demand of metal, there are only very few studies on the material requirement on a national scale. One of the more prominent studies is by Goe and Gaustad (2014), who analysed the possible criticality of 17 different metals relevant for the development of PV in the US. The analysis was carried out based on a multi metric criticality analysis that involved several economic and environmental criticality indicators, which however does not take the increasing metal demand into consideration. Germanium, indium, tin and silver were identified to be the most critical metals. In terms of Germany, a similar analysis was done by Erdmann et al. (2011), which in addition to PV, also considered a wide range of clean technologies. The authors identified gallium, germanium and indium as the most critical metals for the development of PV in Germany. Viebahn et al. (2015) on the other hand, analysed the material requirements and bottleneck analysis for the deployment of renewable technologies, among others c-Si and thin film modules. Their results show that indium, gallium, selenium and tellurium face a possibility of bottleneck risk, assuming that the annual production and available static reserves be fairly allocated to Germany according to the share of the population.

Based on the majority of the publications reviewed in this sub-chapter, it can be concluded that thin-film PV modules are more likely to face a supply risk than the c-Si modules in the future due to the criticality of various metals such as tellurium, indium, gallium and germanium. However, there are also several studies that propose that the supply risks of metals in PV modules can be mitigated via improved manufacturing process and an efficient recycling process.

4.1.2 Wind turbines

Since the majority of a wind turbine consists of bulk metals such as steel and cast iron, the research on the material demand for future deployment has been focused on the use of REE in the PMs of the generators. Buchholz and Brandenburg (2018) analysed the trends of the demand and supply of neodymium and dysprosium in wind turbines to fulfil a global energy transformation process. The authors estimated that by 2035, the total demand for both metals in wind turbines will account for one third and one-quarter of the current global production level, respectively. They further mentioned that the German manufacturing industry especially, which heavily relies on raw material imports, should invest in improving its local recycling and refining sectors in order to be better prepared to face possible supply chain challenges in the future. Besides that, Viebahn et al. (2015) analysed the neodymium and dysprosium availability for the deployment of wind turbines in Germany based on 6 different drive train concepts, which includes the innovative high-temperature superconducting generators. They reported that both metals are critical relative to the current production level. When compared to the static reserve levels, only dysprosium remains critical.

Besides that, Lacal-Arántegui (2015) investigated the material requirements of generators for future wind turbines and suggested that active substitution measures of REEs in the permanent magnets

should be undertaken for sustainable development. The bottleneck risk of neodymium and dysprosium has also been previously reported by, but not limited to, Buchert (2011), Moss et al. (2013), McLellan et al. (2016) and Dutta et al. (2016). Contrary to these studies, Watari et al. (2018) detected no bottlenecks for neodymium and dysprosium in terms of the cumulative demand in wind turbines. This result was obtained under the assumption of 25 to 50 % market share of wind turbines with a permanent magnet for the globally installed capacities proposed by IEA (2017). One of the main contributors to the mitigation of bottlenecks is the assumption of a closed-loop recycling. In fact, the authors further argue that if any supply risk is to occur, it will be in the form of production constraint due to the sharp increase in demand, and not the reserve availability.

In terms of a more detailed analysis on a national level, Wilburn (2011) investigated the material requirements for onshore turbines in the US until 2030 without any differentiation between the drive trains or changing size of the turbines. Assuming that wind turbines provide 20 % of the electricity produced in 2030, the demand of all bulk metals such as copper and steel will be less than 3 % of the current total consumption of each metal. Furthermore, the main supply risk in terms of REE is a possible export restriction by China. For Germany, apart from Viebahn et al. (2015), who as mentioned earlier investigated the REE requirements, Zimmermann et al. (2013) provided by far the most comprehensive study on the material demand due to the future deployment of wind turbines. The authors conducted a detailed analysis of turbine upscaling and accounted for additional material requirements due to premature decommissioning and component exchanges. Nonetheless, only three different drive-trains were considered, which do not cover the entire German market, and no bottleneck analysis was conducted on the estimated material demands.

Most of the bottleneck risks in the literature are conducted based on the comparison of demands to the reserve levels at the time of the research. However, reserve levels gradually increase in general mainly due to the discovery of more reserves and more importantly, reclassification of resources as reserves due to improvements in the mining techniques and increasing metal prices. Therefore, comparing the estimated demand with current reserve levels can lead to an overestimation of the bottleneck risks. To improve this, Habib and Wenzel (2016) proposed a dynamic approach, in which the cumulative demand is compared to the reserve base of a metal. This methodology was applied to assess the reserve depletion of REEs, iron and copper for direct-drive wind turbines. In this thesis, this approach is applied to all technologies to assess the bottleneck risks under the assumption of increasing reserve levels.

Based on the review of published works in this sub-chapter, it can be concluded that the research on material availability for wind turbines is dominated by REEs in particular. A great number of studies indicated that a large scale deployment of wind turbines with PMs will consequently lead to the supply risk of REEs. Similar to the findings related to PV, several studies do mention that an efficient recycling process can contribute to mitigating the risks.

4.1.3 Batteries

The availability of lithium on a global scale for EVs has been previously analysed by Narins (2017). The author argues that the global transition towards EVs will not be constraint by the availability by lithium mainly owed to the abundant reserves and resources that will be available in the future due to improvements in extracting methods and strong support from government actors. On top of that, the demand growth will be slowed down by the substitution of lithium with other non-critical metals such as zinc. Therefore, the authors claim that if a supply risk were to occur, it will merely be a logistic one and not related to the physical availability of the metal. Speirs et al. (2014) analysed the future demand for lithium according to the Blue Map and Blue EV shift scenarios from the IEA (2010) and analysed it with respect to the future development of global lithium production. Although their results show that the future demand far outweighs the supply in the future, the authors argue that there is no strong evidence that the production cannot be increased more aggressively in order to meet the future demand, since estimated resource levels outweigh the cumulative demand of lithium. Similarly, Kushnir and Sandén (2012) conducted a dynamic material flow analysis to investigate possible constraints by lithium until 2100. The authors argue that the lithium resources, especially when taking the brine and ocean resources into account will not be exhausted by a large scale deployment of EVs. The possibility of a bottleneck can further be reduced if the batteries are recycled. Further studies that also investigated the availability of lithium include Yaksic and Tilton (2009), Gruber et al. (2011), Grosjean et al. (2012) and Vikström et al. (2013).

In addition, the importance of recycling and material substitution in batteries has been previously analysed by Dewulf et al. (2010), who determined the impacts of recycling cathode materials of Li-Ion batteries on natural resources saving. They compared the material demand using scenarios with and without recycling and modelled the entire material flow using a life-cycle-assessment. Although results indicated that recycling cannot shift the production to independency of virgin material demand, it could however reduce the virgin supply by more than 50 %. In addition to that, Månberger and Stenqvist (2018) investigated the supply risk of battery-related metals under various technological and recycling scenarios until 2060. The results indicated that the cumulative demand for lithium and cobalt will exceed the currently known reserve levels in the majority of the scenarios. Although recycling of batteries does reduce the primary metal demand, it does not completely remove the supply risks in the related scenarios. Sommer et al. (2015) emphasized on the need for recycling batteries as they conducted a material flow analysis to estimate the amount of cobalt that can be extracted from old nickel-metal hydride (NiMH) and portable Li-Ion batteries. They estimated that in 2011, approximately 325 t of cobalt was disposed of with waste electrical and electronic equipment, which includes batteries. On a different note, Vaalma et al. (2018) analysed the potential of Na-Ion batteries in reducing cost and supply risks of Li-Ion batteries. Considering current battery topologies, lithium and cobalt will face scarcity problems until 2050. When taking extreme material efficiency measures for future battery designs into consideration, only the demand

for cobalt is reduced significantly. However, the authors argued that substituting lithium with sodium is only economically beneficial if lithium is facing a supply shortage and an increased price.

On a much smaller scale, Miedema and Moll (2013) analysed the requirement and availability of lithium for the electrification of the vehicle fleet in the EU-27 until 2050. Plug-in hybrid electric vehicle (PHEV) is assumed to contribute up to 75 % of the market in 2050 while full battery electric vehicle (BEV) takes up the rest. Interestingly, the authors also considered the substitution of lithium in the production of glass and ceramic with less critical metals and allocated the supply to Li-Ion batteries in the future. By means of a dynamic flow analysis and a consideration of closed-loop recycling, the total demand is then estimated. Results showed that the lithium demand required for the complete electrification of passenger vehicles is considerably high, that one-fifth of the annual global production is needed at certain years. Considering the fact that EU-27 does not even produce enough lithium to satisfy this demand, the authors stated their scepticism of a large scale development of BEVs in the EU. Instead, they called for the adoption of PHEV in the middle-term, due to the smaller lithium requirement and the ability to reduce the lithium supply risks, but not completely removing them. Similar analysis on EU level was also conducted by Simon et al. (2015), who analysed the requirements of lithium, cobalt, nickel and manganese for EV until 2050. Their results show that cobalt faces a severe supply risk even without considering the demand for Li-Ion batteries due to the low reserve and production levels. While other metals are found to be not critical, lithium and nickel become critical once a closed European market and their respective reserves only in the EU are considered. In terms of Germany, Viebahn et al. (2015) analysed and ascertained the bottleneck risk of vanadium, assuming that the entire need for stationary storages in Germany is satisfied by vanadium redox flow batteries.

In conclusion, most of the studies reviewed regarding the supply risks of metals related to batteries suggest that lithium and cobalt will most likely face supply constraints in the future, whereas nickel and vanadium are identified as critical in certain studies. Similar to PV and wind turbines, the studies on batteries also emphasize the importance of recycling in reducing the supply risks.

Based on the studies reviewed in chapter 4.1 regarding PV, wind turbines and batteries, several research gaps could be identified. To begin with, the majority of the studies reviewed in the previous sections only focus their analysis on a selected group of metals, especially REEs and critical metals. Furthermore, the research boundaries for each technology are relatively small. This leads to the omission of infrastructures, which are essential in ensuring the functionality of the technologies, such as the inverters and balance-of-system (BOS) in PV as well as control electronics in wind turbines and batteries. Therefore, this thesis aims at improving the findings in the literature by considering a broader research boundary and conducting a comprehensive analysis of all involved metallic elements in the technologies.

Overestimation of the bottleneck risks is another shortcoming in the literature that is addressed in this thesis. There are two main factors that contribute to this. Firstly, the demand is often estimated

for the complete market dominance of a critical technology. This is improved in this thesis by carefully projecting future market shares of a wide range of sub-technologies based on sound economic and technical arguments as well as expert interviews. Therefore, potential bottlenecks that are presented and discussed in this thesis represent a more realistic demand rather than the theoretical worst-case scenario. Secondly, the demand is often compared to the static production and reserve levels. This shortcoming is improved in this thesis by complementing the static analysis with a dynamic analysis as proposed by Habib and Wenzel (2016). Furthermore, the potential of closed-loop recycling in easing bottleneck risks are also discussed to combat the issue of overestimating potential risks. Additionally, the results in this thesis contribute to the assessment of metal demand for Germany, which is relatively scarce in the literature. On the other hand, the methodology for each technology coupled with country-specific assumptions and input parameters, can be applied to other countries in order to analyse their demand and bottleneck risks.

Another research gap in the literature is the cross-relationship between the technologies. Although studies such as Månberger and Stenqvist (2018), Buchholz and Brandenburg (2018) and Viebahn et al. (2015) analysed the demand for various technologies within a system, the implications of metal use between the technologies were not analysed. The question remains if the use of common metals in various technologies would lead to a symbiotic or antibiotic relationship. This is made possible in this thesis by analysing the full range of metals in the technologies, as a comprehensive picture of all involved metals and their interconnection between the technologies can be established. Last but not least, the possibility of an economic constraint of the raw materials has been relatively underrepresented in the existing literature, since most of the studies have been emphasizing on the supply availability of the raw materials. This thesis contributes to this discipline by investigating the price relationships and the market mechanisms, such as the price impacts due to changes in the supply and demand equilibrium of metals relevant to PV, wind turbines and batteries.

4.2 Price relationship between metals

In answering the second research question, three literature sub-streams are looked into detail, which deals with the price relationship between metals. The first sub-stream is the Granger-causality of metal prices. Granger causality has been widely applied in economics to investigate causality between economic time-series. One of the main reasons for the prominence of this methodology is the simplicity (Hu et al. 2012) and the ability to identify directional influences of variables purely based on the data-driven methodology without any prior knowledge on the subject matters (Beharelle and Small 2016). The tendency for metal prices to move in a similar trend may be due to the effects of markets reacting in a similar way to the same information (Buti and Sapir 1998). Two of the most common ways of how metals are related and react to the same information are via joint-production and joint-consumption. Therefore, the literature regarding the price relationship between jointly

produced and consumed metals are reviewed as the second and third sub-stream of literature in this section.

4.2.1 Granger-causality between metal prices

Studies on causality have been pioneered by works like Tinbergen (1951) and Simon (1952). One of the most widely used methodologies to causality testing is the Granger-causality test (Granger 1969). This approach has been previously applied, for example, by Chan and Mountain (1988), who analysed the causality between the prices of gold and silver. The authors reported that the gold price is a useful determinant in improving the predictability of silver prices. Ciner (2001) and Krawiec and Górska (2015) obtained similar results in their analyses. The latter study also additionally identified causal relationships between silver-platinum and silver-palladium prices using monthly data between 2008 and 2013. Escribano and Granger (1998) used monthly data between 1971 and 1990 to test the long-run relationship and the impact of a financial bubble between 1979 and 1980 on the cointegration nature between gold and silver prices. The authors established the possibility of causality running from log gold price towards log silver prices before the bubble.

There are several variations to the classical Granger-causality test. The approach proposed by Toda and Yamamoto (1995) is one of the more widely applied approaches which overcomes some of the shortcomings of the conventional Granger-causality test (Dolado and Lütkepohl 1996). The differences between both approaches are detailed in chapter 5.2.3. The Toda-Yamamoto approach to Granger-causality testing has been previously applied by Śmiech and Papież (2012), who analysed causality between the monthly prices of gold, silver, platinum and copper for the period from 2000 to 2012. The authors reported causal links flowing from copper price to the other metals until 2003. Beyond this time period, the dynamics of the relationship changed as platinum became the significant driver of other prices. A causality involving platinum price was also reported by Jain and Ghosh (2013), who analysed the causality of gold, platinum and silver prices in India together with the exchange rate and oil price. The authors used daily nominal prices between 2009 and 2011 due to the unavailability of the consumer's price index. A bi-directional causality relationship is established between gold and platinum prices, which were explained by the use of platinum as an alternative investment commodity to gold in India. Similarly, Mishra (2014) also focused her analysis on the Indian market by analysing the causality between gold prices and capital market movement for the period of 1978 to 1979 and 2010 to 2011, conditioned by the wholesale price index of India. A bi-directional causality was identified, which shows that gold and capital investments are equally sought after during the capital market crisis.

On a much broader scale, Chang et al. (2013) applied the Toda-Yamamoto approach to analyse the inter-relationships among gold prices on the markets in London, New York, Japan, Hong Kong and Taiwan using daily prices between 2007 and 2010. Interestingly, the authors not only tested one VAR model with all of the variables but segmented their analysis by focusing on different regions, such as markets in Asia, western countries and a mixture of both regions. Their results show that the

gold price in New York is the most dominant driver as significant causality flows to other markets in all combinations of variables in the VAR models. On the contrary, the price of the Japanese market has the weakest predictive power since most of the gold is imported into Japan, which causes their price to be highly depended on foreign markets. Basoglu et al. (2014) focused their causality analysis on all non-ferrous metals traded at the London Metal Exchange (LME) using daily price series for the period of 2000 and 2013, fuelled by the motivation to propose risk mitigation strategies for traders at the LME. Some of the more notable results are the existence of causality flowing from aluminium to copper, lead to nickel as well as from copper to lead and to nickel.

Based on the literatures that have been reviewed in this section, it becomes noticeable that most of the analyses involve either precious or industrial metals. Historically, the focus on these metals has been driven by their nature as financial assets or economic importance to the industry, which is in close relation to macroeconomic factors such as the inflation rate (Ghosh et al. 2004) and growth of GDP (Binder et al. 2006). However, causality analysis involving minor metals are equally important due to increased use in emerging technologies. Therefore, the knowledge regarding price dependencies between metals that are relevant to renewable energy technologies is necessary in order to be able to anticipate price changes to ensure an economic large-scale deployment of the technologies in the future. This thesis aims to contribute to this research gap by systematically analysing the causal relationships between metals in renewable energy technologies with respect to their nature of production and consumption.

4.2.2 Price relationship of jointly-produced metals

One of the pioneering works in the field of joint-production of metals is the study regarding the role of co-products in stabilising the economic feasibility of the metal mining industry in the US by Campbell (1985). The author used the non-parametric sign test to investigate whether the price movements between metals in a particular direction are significantly different from a random movement. According to the results, co-products do add economic stability to a mine in the short-term. This effect is weakened in the long-run for metals involving lead, zinc, silver and gold. Ever since however, the research on the price relationship between jointly-produced metals never really took off. The reason for this, as mention by Fizaine (2013), is the insignificant role of by-product metals in the past global economies and lack of data. However, as the use of minor metals in key technologies began to intensify, the research in that field also began to grow at the beginning of the last decade. An example of such a study was conducted by Kim and Heo (2012), who found that the price of zinc between 2004 and 2011 Granger-causes the price of its by-products, namely cadmium and germanium. Besides that, the authors also found evidence of a causal link flowing from copper to selenium. Another frequently cited study in this field is the work of Afflerbach et al. (2014), who conducted a simple regression analysis to test the price correlation of primary products and their respective by-products. According to their results, significant relationships exist between tin-copper

and germanium-zinc, whereas weak relationships were identified between aluminium-gallium and cobalt-nickel.

Besides that, Farrow and Krautkraemer (1989) analysed the price changes of silver, lead and zinc that are produced together in a mine and their respective impacts on the ore quality selection. The authors discuss the economic feasibility of varying the ore grades in a mine in anticipation of the price movements. Similarly, Osanloo and Ataei (2003) also propose ways to optimize the extracted ore grade in a multi-metal deposit order to maximize the total net present values of the mine. Last but not least, Redlinger and Eggert (2016) analysed the price volatility of by-products with respect to primary metals over the past 50 years using regression analysis. Their results show that by-products tend to have, on average, more than 50 % higher price volatility than primary metals, with metals such as cadmium, vanadium, indium and selenium showing some of the highest volatilities.

Jordan (2018) provided a sound comparison of the literature involving joint-production of metals. According to his findings, it can be seen that a large number of studies focus on the demand constraints and availability of by-products. Interestingly, most of the studies also reported that supply will highly likely to be constraint by the prices rather than the availability of the metals, which strengthens the need for the deeper analysis of the price relationship between metals. Furthermore, previous studies were conducted using limited sets of metals and were often carried out using qualitative, analytical or even simple statistical approaches such as correlation or sign test. A consistent causality analysis using the improved Toda Yamamoto approach among jointly-produced metals is unavailable, to which this thesis is able to contribute.

4.2.3 Price relationship of jointly-consumed metals

The price relationship between jointly-consumed metals is much more underrepresented in the literature than its counterpart. The possible existence of a relationship between jointly-consumed metals has been previously mentioned by Jerrett and Cuddington (2008), who analysed the price trends and cycles of steel, iron and molybdenum. According to the authors, the possibility of similar trends in the prices of these metals due to a demand shock is significantly higher than a supply shock. In agreement to that, Rossen (2015) and Pradhananga (2016) also stated that a demand shock can be transmitted to the companion metals and that metals that share common application field may have a co-movement between their prices. Furthermore, Fizaine (2013) hypothesized that a co-integrating relationship might be present between metals that share a same field of consumption and that the balance ratio of the demands of two metals in a product is a key driver in determining the market price. Although these studies did mention the possibility of significant relationships between the prices of jointly-consumed metals, substantial empirical evidence was not provided to support their arguments. Therefore, this thesis aims at contributing to this research gap by providing some empirical evidence to support the views of these studies. On a different note, Kim and Heo (2012) is

the only study that analysed the Granger-causality between metals that are found in renewable energy technologies to the best knowledge of the author. However, the focus of their analysis was only the metals found in solar cells. The inter-dependency of metal prices between different renewable energy technologies is a huge gap in the literature, to which this thesis also aspires to contribute.

4.3 VAR analysis of metal prices

The short and middle-term effects of the changing demand on the commodity price can be investigated by forecasting the commodity price in relation to other related economic variables. As mentioned by Chen et al. (1991), there are generally two approaches in the field of forecasting microeconomic properties of commodities, namely the intensity of use and the econometric approach. The former approach gained momentum in the literature when applied by Malenbaum (1973), who forecasted the material requirements in the US in 2000. The core principle of this approach is the assumption that the intensity of use of metals and the income of a country has a relationship according to the Kuznets curve (Leontief 1983). This assumption was empirically proven by Tilton (1989), who established this relationship by analysing the trends in metal demand and GDP with respect to the mining activities in North America. Studies such as McKay (2008) and McKay et al. (2010) have applied this approach to forecast steel prices in selected countries. Although this approach has been proven and applied in the past, it remains however, inferior to the econometric methods of forecasting, which is a more common practice in the current literature. One of the most widely used econometric approaches in analysing the interdependencies between economic variables as well as the short and long-term evolution of the variables forecasting is the vector autoregressive (VAR) analysis. The ability of a multivariate VAR model in improving the predictability of commodity prices has been previously ensured by Gargano and Timmermann (2012). Since commodity prices are strongly affected by macroeconomic variables (Borensztein and Reinhart 1994; Frankel and Rose 2010), the VAR models involving commodity prices are often complemented by macroeconomic variables. Some of the examples of the application of the VAR analysis in investigating commodity variables are Kilian and Park (2009) and Kang et al. (2016), who analysed the influence of macroeconomic variables on the oil price.

The VAR analysis in investigating metal prices has been previously applied by Eryiğit (2017), who investigated the short-term price relationship between the prices of palladium, platinum, gold and silver between 1990 and 2014. By conducting a Granger-test as part of the structural analysis, their results indicated that a short-term correlation is present between gold-silver, gold-platinum and silver-palladium prices. Similar methodology was also used by Mutafoglu et al. (2012), who employed a VAR model to test the relationship between trader's positions and market returns of gold, silver and platinum. The analysis was done for two different time periods determined using a generalised structural break test with unknown break points. The subsequent Granger-causality

analysis showed that while the traders' positions have a slight causal effect on the returns during the pre-break period, no significance could be detected during the post-break period, as only extreme positions were identified to have some predictability power on the market returns. In Labys et al. (1999) the authors determined the impact of macroeconomic influences on LME metal price fluctuations using a dynamic factor analysis. In addition to that, Soytas et al. (2009) examined the effects on the Turkish interest rate, domestic spot gold and silver price by the world oil price and found that that the oil price has no predictive power over the aforementioned local economic factors in Turkey.

Besides Granger-causality, the impulse response function (IRF) and the forecast error variance decomposition (FEVD) are further tools to conduct a structural analysis within a VAR analysis. This approach has been applied, for example in Lee and Ni (2002) and Mork (1989), to investigate the effects of oil price shocks on the demand and supply in various industries. In Dotsey and Reid (1992), the authors used a VAR model and IRF to show that federal fund shocks can be a good predictor of economic outputs. In terms of the application of these approaches to analyse metal prices, Akram (2008) investigated the impact of real interest rates and the US dollar on commodity prices using a structural VAR model. The authors conducted a structural analysis of the model by inducing shocks to the macroeconomic variables. The corresponding effects on the commodity prices were analysed using IRF and FEVD. The results indicated that shocks on both variables do have a substantial effect on commodity prices. Besides that, Xiarchos (2005) investigated the relationship between the price of primary steel and the price of scrap. The IRF and FEVD were conducted to investigate how the volatility in either variable can be transmitted between them. Based on the results, the author established that the change in steel scrap prices significantly affects the changes in primary prices, and that the variability of prices is strongly transmitted to each other. Similarly, Antonakakis and Kizys (2015) used weekly spot price of gold, silver, platinum and palladium dating from 1987 to 2014 to analyse the dynamic transmission as well spillover effects of returns and volatilities of the prices. The authors set up a reduced VAR model with 9 variables, which, apart from the prices of aforementioned metals, includes the oil price as well as the exchange rates between of EUR/USD, GBP/USD, JPY/USD and CHF/USD. The spillovers were then estimated using the FEVD. According to their results, the gold price is the main contributor of return and volatility spillovers to the other investigated metals and that the information regarding gold, silver and platinum can be used to improve the predictability of the volatility of palladium prices. Similar research involving spillover effects have also been done by Kang et al. (2017) and Diebold and Yilmaz (2012). Other studies that apply IRF and FEVD to investigate the implications of a shock on one economic factor on other macroeconomic variables are Lee and Ni (2002), Mork (1989), Dotsey and Reid (1992) and Anzuini et al. (2012).

Majority of the literature mentioned in this section only considers the impact of macroeconomic variables on metal prices. The effect of increasing demand for metals has not been analysed in detail, although the framework of the VAR analysis enables such an investigation. In addition to that, one

of the biggest gaps in the literature is the analysis of the increasing metal demand due to large scale deployment of renewable energy technologies on metal prices. This analysis is of utmost importance for the technologies since metal prices contribute to a significant share of their end prices. The only study, to the best knowledge of the author, who investigated the impact of renewable energy technologies on metal prices is Mo and Jeon (2018), who used a vector error correction model (VECM) to analyse the impact of increasing demand for batteries in electric vehicles on the prices of cathode metals in Li-Ion batteries. Their results show that cobalt prices are the most sensitive to the impact of changes in EV demand. However, their analysis only considered one particular type of Li-Ion battery (NMC 1:1:1). In this thesis, the total demand of various sub-technologies from PV, wind turbines and batteries will be used to analyse the impact on prices and evidently contributing to closing this gap in the literature.

5 Research design

Based on the findings from the literature review, the research design of this thesis in answering the research questions is formulated and introduced in this chapter. Firstly, two main scientific hypotheses are defined, which enables the scientific questions to be tested and answered empirically. The hypotheses also lay out the foundation in selecting the applied methodology and relevant data.

5.1 Scientific hypotheses

In general, this thesis is divided into two main research focuses according to both research questions. Correspondingly, two scientific hypotheses (H_0) are defined for each research focus, based on the findings in the current literature discussed in chapter 4.

- $H_{0,I}$: Increasing metal demand from PV, wind turbines and batteries for the deployment in stationary storages and electric vehicles in Germany will lead to supply bottlenecks
- $H_{0,II}$: Increasing deployment of PV, wind turbines and batteries on a global scale will lead to price dependencies between the jointly-consumed metals in the technologies

5.2 Methodology

There are four groups of methodologies applied in this thesis in order to test the scientific hypothesis. As shown in Figure 5-1, the dynamic metal flow analysis and the assessment of material availability are used to test the first scientific hypothesis whereas the Granger-causality test and a VAR analysis, which includes IRF and FEVD, are applied to test the second hypothesis. The detailed explanations of each group of methodologies are provided in the following sections.

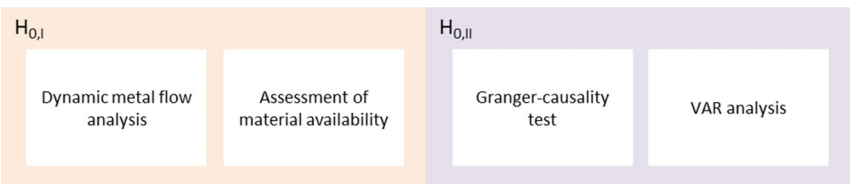

Figure 5-1: Main groups of methodologies in this thesis

5.2.1 Dynamic metal flow analysis

In order to determine the total metal demand for the deployment of PV, wind turbines and batteries until 2050, a dynamic metal flow analysis is conducted. This method has been widely applied in the literature to estimate the flows of metals within a predefined temporal or spatial resolution (Park et al. 2011). Some of the examples of the application of this methodology include Choi et al. (2016), who analysed the flow of indium due to the application in LEDs and GIGS modules as well as Elshkaki and Graedel (2013), who conducted the dynamic analysis of the global metals flows and stocks in electricity generation technologies. The basic principle of this methodology is that the difference between the dynamic inflow and outflow of metal represents the metal stocks in a system. The metal inflow can be calculated using the annual installed capacity, specific metal demands and the market share of the technologies. The outflow, on the other hand, is represented by the decommissioned capacity at maximum lifespan or due to maintenance and repair works. The flow chart of the dynamic metal flow analysis applied in this thesis is briefly illustrated in Figure 5-2.

Figure 5-2: Flow chart of the dynamic metal flow analysis

5.2.1.1 Metal composition and market development

The status quo of the metal compositions of investigated technologies is compiled based on various sources in the literature. These include scientific studies, life-cycle-assessment (LCA) reports as well as manufacturer sheets. The metal compositions of all technologies are then compared and contrasted, before deriving the actual values used in the calculations, based on careful consideration of the framework conditions of each literature sources. In order to determine the future material compositions, material efficiency measures as well as other technological developments of the technologies, such as, but not limited to, the development in PV module efficiency, change in wind turbines sizes as well as an increase of energy density in batteries are considered. A unified methodology to derive the specific metal demand of all technologies is unavailable due to the differences in the structure and the operation conditions of the technologies. Therefore, the exact methodology and applied data are detailed in chapter 6, 7 and 8 according to respective technologies.

Literature research is conducted to determine the current market shares of the sub-technologies as well as to compile proposed market projections from various studies. Based on these projections, a development of the future market shares is proposed upon careful consideration of the possible

economic and technical development of the technologies and expert interviews. In order to account for the uncertainties in the projections, two development scenarios are proposed for each technology. The conservative scenario represents a business-as-usual case, in which the most likely development scenario of the technologies are described. On the other hand, the alternative scenario represents a different technology development case, which can however, still be realised in the future under certain market conditions. Detailed justifications for the market share projections of all scenarios and technologies are listed in chapter 6, 7 and 8 accordingly. The metal demand is then presented as a range between these scenarios, which captures any possible deviations in the assumptions with regard to the market share and technical developments of the technologies.

5.2.1.2 Capacity input-output

The annual installed capacity, $P_{inst,T}(t)$, and decommissioned capacity, $P_{decomm,T}(t)$, where T denotes a technology, of the transformation pathway is used in the calculations without any modification. On the contrary, the long-term and climate protection pathways only provide the cumulative capacities, $P_{cum,T}(t)$, for selected years until 2050. Therefore, $P_{cum,T}(t)$ for each year is obtained by linear interpolation between current capacity and $P_{cum,T}(2050)$. The difference between $P_{cum,T}(t-1)$ and $P_{cum,T}(t)$ provides the annual installed capacity. The decommissioning of a technology is assumed to take place at the end of a year, which means that this capacity will be added to the system again in the following year. The installed capacity of a technology in year *t* is hence represented by the following equation.

$$P_{inst,T}(t) = P_{cum,T}(t) - P_{cum,T}(t-1) + P_{decomm,T}(t-1) \quad \text{, with } t > 0 \tag{5-1}$$

Two different approaches are applied in order to determine the decommissioned capacity of the technologies. The Weibull distribution is applied to PV and wind turbines whereas the simultaneous exit function is only applied to batteries. The Weibull distribution has been widely used in many sectors to model the lifespan of various products, mainly due to the versatile fitting characteristics and the relatively high precision of lifespan estimation (Smith and Naylor 1987). This approach has also been used by (Zimmermann 2013; Laronde et al. 2010a) and Zimmermann et al. (2013) to model the lifespan and premature decommissioning of PV modules and wind turbines, respectively. It is not uncommon for a technology to constantly undergo maintenance works that need component exchanges or even to be prematurely decommissioned before its maximum lifespan. There are two main reasons for this. Firstly, the cost of repair might be too high compared to the replacement of a technology, especially if the technology is already nearing its maximum lifespan. Secondly, spare parts of the malfunctioning components might have been outdated and might not be commercially available anymore. Therefore, the Weibull distribution is applied in this thesis in

order to model a more accurate life span of PV modules and wind turbines by taking premature decommissioning and component failures into account. The probability distribution function of the Weibull distribution is shown in equation (5-2),

$$f_T(t) = \lambda k(\lambda t)^{k-1} e^{-(\lambda t)^k} \tag{5-2}$$

where k represents the shape parameter and λ the scale parameter. The term $f_T(t)$ denotes the share of an installed capacity that fails at time t. The shape parameter determines the slope of the probability function and is determined in this thesis based on values reported in the literature. The scale parameter, which determines the amplitude and the width of the probability function, is calculated using the following equation,

$$\lambda = \frac{1}{\bar{T}} \Gamma(1 + \frac{1}{k}) \tag{5-3}$$

where $\bar{T}$ represents the average lifespan of a product and Γ denotes a gamma function. No decommissioning or additional metal demand due to repair works are assumed in the installation year. In the final year of the lifespan, the total remaining capacity will be decommissioned as it is assumed that the technology will be repowered in the following year. This is achieved via equation (5-4), where all remaining capacity is set to be decommissioned once the lifespan is achieved. The decommissioned capacity at any time t can therefore be calculated as shown in equation (5-5).

$$f_T(\bar{T}) = 1 - \sum_{i}^{\bar{T}-1} f_T(i) \quad \text{, with } 1 \leq i < \bar{T} \tag{5-4}$$

$$P_{decomm,T}(t) = \sum_{i}^{t} P_{inst,T}(i) * f_T(t-i) \quad \text{, with } i > 1 \tag{5-5}$$

Although the Weibull distribution provides a more realistic representation of the lifespan estimation of energy technologies, this method is not a common practice in energy system modelling, since the precision that can be achieved is often not justified by the increase in model complexity and computational time. In energy systems models, the total amount of installed capacity in a certain year will be discarded completely once the lifespan has been achieved, without any consideration of premature decommissioning or component exchanges. This method is known as the simultaneous exit function and can be represented by the equation (5-6).

$$P_{decomm,T}(t) = P_{inst,T}(t - \bar{T}) \quad \text{, with } t = \bar{T} + 1 \tag{5-6}$$

In this thesis, the simultaneous exit function is applied to batteries. Since batteries are undergoing massive research and development, no data regarding the Weibull distribution of the calendar lifespan or failure rates of batteries can be found in the literature. Studies such as Ossai and Raghavan (2017), Harris et al. (2017) and Liu et al. (2016) do apply the Weibull distribution to analyse the lifespan of a battery, but the subject matter is the state-of-health and the cycle-life of the batteries. The results of these studies cannot be applied to the methodology here since failure rates and reliability based on cycle numbers cannot be directly converted to calendar lifetime and a detailed simulation of batteries is not conducted within the framework of this thesis. Therefore, the simultaneous exit function is used instead. Similar to the Weibull distribution methodology, the decommissioned capacity is assumed to be reinstalled in the following year, which means that equation (5-1) is also valid for batteries.

5.2.1.3 Total metal demand

In this thesis, the material demand is differentiated between the sub-technologies (ST). As an example, mono and multi c-Si, CIGS and CdTe represents the sub-technologies of PV. Therefore, the annually installed capacities have to be broken down to each sub-technology. This is done according to equation (5-7), where $P_{inst,ST}$ represents the installed capacity of a sub-technology and $\alpha_{ST}(t)$ represents the market share of the sub-technology at time t.

$$P_{inst,ST}(t) = \alpha_{ST}(t) * P_{inst,T}(t) \quad \text{, with } t > 0 \tag{5-7}$$

The annual metal demand $D_{m,ST}$ is calculated according to equation (5-8), where m denotes a metal while $d_{m,ST}$ represents the specific material demand in a sub-technology. The sum of the metal demand across all sub-technology then gives the total annual metal demand of a technology $D_{m,T}$. Consequently, the cumulative metal demand $D_{total,m,T}$ is provided by the sum of annual metal demand of a technology.

$$D_{m,ST}(t) = d_{m,ST} * P_{inst,T}(t) \tag{5-8}$$

$$D_{m,T}(t) = \sum_{i=ST} D_{m,i}(t) \tag{5-9}$$

$$D_{total,m,T} = \sum_{t} D_{m,T}(t) \tag{5-10}$$

5.2.2 Assessment of material availability

The availability of metals is assessed by comparing the virgin metal demands to their respective supplies. This demand is calculated by subtracting the recycled content, RC_m, from the total material demand, which is assumed constant until 2050. The recycled content represents the amount of scrap that is used in the production of a metal. The RC_m for all metals used in this thesis is obtained from Graedel et al. (2011). The availability of the metals is assessed using three indicators. Firstly, the demand-to-production (D/P) ratio is derived by comparing the annual metal demand to the annual production rate of each metal. This indicator provides an insight of the possible supply risk due to increasing demand, given that the production of metals remains at the current level in the future. The second indicator is the demand-to-reserve (D/R) ratio, where the cumulative demand is compared to the static reserve levels of each metal. This indicator aims to test whether the total cumulative demand exceeds the physical availability of the metals based on the current known reserve levels.

The third indicator is proposed by Habib and Wenzel (2016), whereby the cumulative demand will be compared to the reserve base. The static reserve is given reserve levels that are considered to be economical to be mined based on current mining technologies and demand requirements. On the other hand, the reserve base includes parts of the resources that are currently either geographically not accessible or are sub-economic but have the potential to be mined in the future due to technological advancements and increasing metal prices. Although the static reserve has been gradually increasing in the past years (USGS 2018, 2009), there is no certainty that all of the reported reserve base will be available for mining in the future. Nonetheless, the demand-to-reserve base ($\mathrm{D/R_{base}}$) ratio provides an insight regarding the possible supply risk assuming that more metals will be economically feasible to be mined in future. The production, reserve and reserve base levels that are applied in this thesis are listed in Table 15-1 in Appendix.

$$\mathrm{D/P\ Ratio} = \frac{D_{m,T}(t) * (1 - RC_m)}{Production_M(t)} \tag{5-11}$$

$$\mathrm{D/R\ Ratio} = \frac{D_{total,m} * (1 - RC_m)}{Reserve_m} \tag{5-12}$$

$$\mathrm{D/R_{base}\ Ratio} = \frac{D_{total,m} * (1 - RC_m)}{Reserve\ base_m} \tag{5-13}$$

In the next step, the ratios are then compared to certain maximum limits. If the ratios exceed the maximum limits, then a bottleneck risk is assumed to be present. In this thesis, the maximum

amount of metals that is allocated to Germany is set at 1 % of the global production and reserve levels. This is derived based on the German population, which accounts for approximately 1 % of the global population (World Bank 2018). Of this amount, Viebahn et al. (2015) proposed that 10 % is allocated for renewable energy technologies and batteries (excluding portable devices), an assumption that is also applied in this thesis. Ultimately, the maximum allocation limit to which the indicators are compared to is set at 0.1 %. The implications of this cut-off point and the possibility for the metals to take over the end-usage share of other products or sectors to compensate for the demand in renewable energy technologies is discussed in chapter 10.

5.2.3 Granger-causality

The basic principle of the Granger-causality, as introduced by Granger (1969), is based on the notion that a variable is said to Granger-cause another variable if past values of the former variable can be used to predict the current values of the latter variable. Despite the prominence of this method, several studies have reported the weaknesses of this methodology, which includes the occurrences of spurious results (Chowdhury 1987) as well as the extreme sensitivity towards the form of time series (Roberts and Nord 2006; Fizaine 2015) and model specifications (Yakubu and Abdul Jalil 2016). Therefore, in this thesis, the Granger-causality test as proposed by Toda and Yamamoto (1995), which is an extension of the conventional Granger-causality test, is applied. This modified approach improves the conventional methodology by ensuring the asymptotic distribution of the Wald statistic since it is robust to the integration and cointegration properties of the time series (Dolado and Lütkepohl 1996; Esso 2010). This approach has since been applied in the literature, among others to analyse causalities between macroeconomic factors and commodity prices (Nazlioglu and Soytas 2011; Jain and Ghosh 2013; Klotz et al. 2014). In this thesis, the pair-wise Granger-causality test as proposed by Toda and Yamamoto (1995) is applied to investigate the price dependencies between jointly-produced and jointly-consumed metals in PV, wind turbines and batteries. The methodology is briefly illustrated in the flowchart in Figure 5-3.

In the first step, a pair of price series of metals has to be set up. Since the time series of two metals have different temporal availability, they are trimmed to ensure similar time period without any gaps in-between. The actual sample period for each metal pairs is listed in Table 15-3 in the Appendix. In the next step, each time series of the metal-pair is tested for unit roots. This is only required to determine the order of integration (I) and not for the transformation of the price series. For the unit root test, the Augmented Dickey-Fuller (ADF) (Dickey and Fuller 1979) and Kwiatkowski-Phillips-Schmidt-Shin (KPSS) (Kwiatkowski et al. 1992) tests are applied, which are complementary to each other according to their null hypotheses. The higher order of the integration between the pair of time series is selected as the maximum order of integration (m) for the corresponding metal pair.

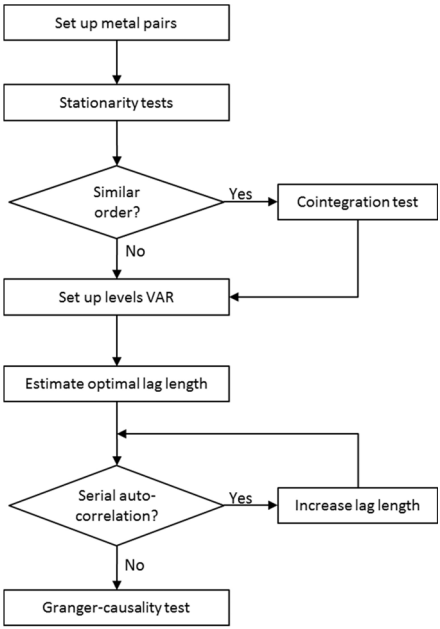

Figure 5-3: Flow chart of the Granger-causality test procedure based on (Toda and Yamamoto 1995)

If both price series have the same order of integration, trace cointegration test as proposed by Johansen (1991) is conducted, in which a vector error correction model (VECM) is estimated. However, the cointegration test does not affect the results of the causality at this point since it is used to cross-check the causality results in the end. According to Engle and Granger (1987), if a co-integration is present, there should be causality at least in one direction. Although this step was not mentioned initially in Toda and Yamamoto (1995), it has become a common practice (e.g. see (Wolde-Rufael 2006; Alimi and Ofonyelu 2013)) since it reduces the probability that the results are spurious due to omitted variables (Stern 2011).

In the next step, a levels vector autoregressive (VAR) model, as presented in equation (5-14) and (5-15), is set up. The variables of both time series are represented by X and Y respectively whereas α, θ, β and δ are the estimated coefficients. The term p is the optimal lag length while ε_x and ε_y are the residuals assumed to have zero mean, constant variance and no autocorrelation. The VAR model is estimated by ordinary least squares (OLS) for each equation in the model separately. In this approach, a VAR$(p + m)$ is estimated in contrast to the VAR(p) model in the conventional approach.

$$X_t = \sum_{i=1}^{p+m} \alpha_i X_{t-i} + \sum_{j=1}^{p+m} \beta_j Y_{t-j} + \varepsilon_{xt} \quad (5\text{-}14)$$

$$Y_t = \sum_{i=1}^{p+m} \theta_i Y_{t-i} + \sum_{j=1}^{p+m} \delta_j X_{t-j} + \varepsilon_{yt} \quad (5\text{-}15)$$

The optimal lag length (p) of the VAR model is chosen using the Bayesian Information Criteria (BIC) (Schwarz 1978). The model is ensured to be well specified by testing for serial autocorrelation in the residuals using the Lagrange Multiplier (LM) test based on Breusch (1978) and Godfrey (1978), also known as the BG-test. Since monthly data is used, the lag length for the BG-test is chosen to be 12. The null hypothesis, H_0, of the BG test is defined that the error process is a white noise whereas the alternative is that a serial autocorrelation is at least present in any order of the error process. If H_0 is rejected, the order of the VAR models is increased and the BG test is repeated, until H_0 is failed to be rejected at a defined significance level. The lag length, at which no serial autocorrelation among residuals is observed, is selected to be the final optimal lag length, p.

A causal link, say Y (or X) Granger-causes X (or Y), is said to be present if the variance of ε_x and ε_y can be reduced by including the lagged terms of Y (or X). In equations (5-14) and (5-15), causality exists if coefficients β_j or δ_j are significantly different from zero. This can be tested by performing a Wald-test under the null hypothesis that the coefficients β_j or δ_j are zero, assuming a covariance stationarity of X and Y. It is important not to include the additional lags, m, in the Wald-test since the Toda-Yamamoto approach utilizes a modified Wald-test which only includes the optimal lag length. This ensures that the Wald statistics remain asymptotically χ^2 distributed with p degrees of freedom regardless of the order of integration and the cointegration nature of the time series. The results are cross-checked with the co-integration of the metal pairs to ensure that causality is present whenever a co-integration is present.

$$H_0 = \sum_{j=1}^{p} \beta_j \ (or\ \delta_j) = 0 \quad ; Y \text{ (or } X\text{) does not Granger-cause } X \text{ (or } Y\text{)} \quad (5\text{-}16)$$

$$H_1 = \sum_{j=1}^{p} \beta_j \ (or\ \delta_j) \neq 0 \quad ; Y \text{ (or } X\text{) Granger-causes } X \text{ (or } Y\text{)} \quad (5\text{-}17)$$

5.2.4 VAR analysis

The influence of the increase in metal demand on their prices is investigated via a vector autoregressive (VAR) analysis. The equations presented in this chapter are based on the works by Johnston and DiNardo (2004) and Lütkepohl (2013). The flow chart of the test procedures in the VAR analysis as applied in this thesis is briefly illustrated in Figure 5-4.

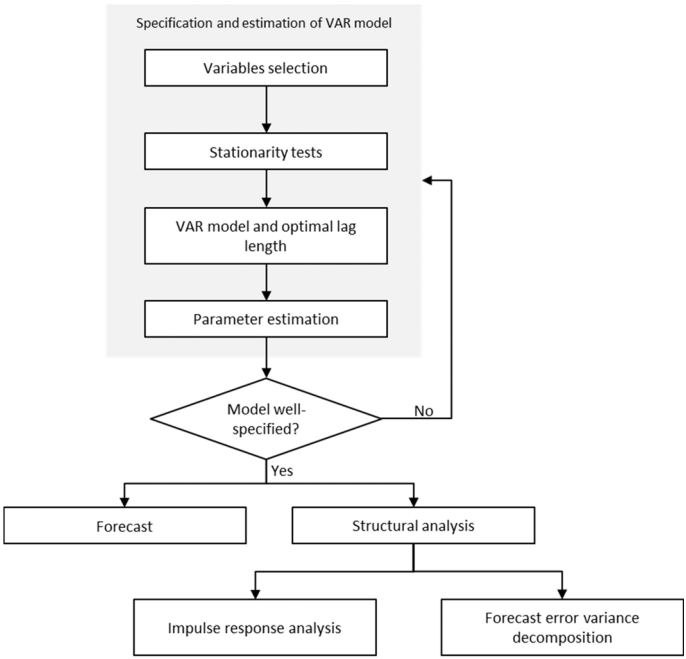

Figure 5-4: Flow chart of the VAR analysis test procedures applied in this thesis

5.2.4.1 Specification and estimation of VAR model

Firstly, all time series are tested for unit roots using the ADF and KPSS tests. Since the presence of a unit root is an undesirable trait in the VAR analysis, the data are transformed by calculating the log differences in case a unit root is present. The ADF and KPSS tests are then repeated to ensure that the transformed time-series are stationary. In the next step, the following VAR-model is set up.

$$y_t = m + A_1 y_{t-1} + A_2 y_{t-2} + \cdots + A_p y_{t-p} + \varepsilon_t \quad (5\text{-}18)$$

The term m is a [K × 1] vector of constants, A_i (for i = 1, . . . , p) is a [K × K] matrix of coefficients and the error process ε_t represents the K-dimensional zero mean white noise process, E(ε_t) = 0, with a time invariant positive definite covariance matrix of E($\varepsilon_t \varepsilon_t'$) = $\sum_\varepsilon$. The model is then specified by selecting an optimal lag length according to the Bayesian information criterion (BIC). Similar to the previous approach, the VAR model is estimated by ordinary least squares (OLS) for each equation in the model separately. Although the model is estimated using integrated variables, the asymptotic inference of the structural analysis will still remain valid (Lütkepohl 2013). Once the model has been estimated, its specifications are checked. For this purpose, the BG-test, as applied in the Granger-causality test procedure, is conducted to test for serial-autocorrelations in the error terms. If the H_0 of no serial autocorrelations is rejected, the lag length of the VAR is increased and the BG-test is repeated until all serial autocorrelations issues are resolved.

The main assumption of an OLS process is that the variance of the error terms remains constant for all time period. However, if the variance changes over time, then they are said to be heteroscedastic. Heteroscedasticity is an undesirable trait since it violates the explicit assumptions of the OLS process and leads to misleading regular standard error of the estimates (Gelfand 2015). Therefore, its presence is tested using the multivariate autoregressive conditional heteroscedasticity (ARCH) test, as introduced by Engle (1982). The H_0 of the ARCH test is that the residuals are homoscedastic. Therefore, if the H_0 is rejected at selected significance levels, the model specification is adjusted and the test is repeated until the heteroscedasticity issues are resolved. In this thesis, different combinations of the macroeconomic variables are chosen to be included in the VAR model and tested for heteroscedasticity. The combination of the variables given in Table 5-5 fails to reject the H_0 of homoscedasticity for all investigated metals, and hence is used to fit the VAR models for all metals in this thesis.

The final test, which evaluates the constancy of the coefficients of the models, is the OLS-CUSUM test, as initially proposed by Durbin et al. (1975) and extended by Ploberger and Kramer (1992). Unlike previous tests, the test for structural stability in this thesis is an informal one, where the plots of the cumulative sums of the OLS residual are inspected. If the sums exceed the boundaries set according to a certain confidence level (95 % in this thesis), then there is evidence for a structural change in the time series and the model has to be specified again. One of the possible alterations that can be undertaken is to implement a Markov-switching model which allows for time-varying coefficients and error covariance, as previously applied by Hamilton (1989) and Sims et al. (2008).

5.2.4.2 Forecasting

Once the specification of the model has been checked and verified, the next step is to conduct a structural analysis of the model. The first part of the structural analysis is forecasting. It should be mentioned that this process is theoretical and relies completely on the notion that economic variables can be autocorrelated and move together over time (Johnston and DiNardo 2004). Making a forecast for h-step ahead, it is assumed that no information is available beyond what is known at the end of the period where empirical data is available. Therefore, the optimal forecast of y_{T+h}, given that $t \leq T$, is the conditional expectation of y_{T+h}, as follows,

$$y_{T+h|T} = E(y_{T+h}|y_T, y_{T-1}, \dots) = m_0 + A_1 y_{T+h-1|T} + \cdots + A_p y_{T+h-p|T} \quad (5\text{-}19)$$

whereby $y_{T+i|T} = y_{T+j}$ for $j \leq 0$. The forecast is done recursively for any positive integer of h. Therefore, the forecast error of any h-step forecast can be represented by equation (5-20). The term Φ_i represents the coefficient matrix, which is basically the multiple of the initial coefficient matrix from equation (5-18) and can be derived using equation (5-21), where $\Phi_0 = I_K$ and $A_j = 0$ for $j > p$. The term I_K represents a [K × K] identity matrix.

$$y_{T+h} - y_{T+h|T} = \Phi_1 \varepsilon_{T+1} + \cdots + \Phi_{h-1} \varepsilon_{T+h-1} + \varepsilon_{T+h} \quad (5\text{-}20)$$

$$\Phi_i = \sum_{j=1}^{i} \Phi_{i-j} A_j , \qquad i = 1,2 \dots \quad (5\text{-}21)$$

Therefore, the variance-covariance matrix of the forecast errors for h-steps ahead can be represented by equation (5-22), where the errors are assumed to have a zero mean.

$$\sum_y (h)\, y = \sum_{j=0}^{h-1} \Phi_j \sum_\varepsilon \Phi_j' \quad (5\text{-}22)$$

5.2.4.3 Impulse response function

The impulse response function is used to investigate the chain reactions between the endogenous variables in the VAR model, when a unit shock is introduced to one of the variables. A unit shock is chosen over the common standard deviation shocks to enable the comparability between various metals. The effects of a unit shock can be modelled through the residual vector of ε_t and be investigated by inverting the VAR representation and the corresponding moving average.

$$y_t = \Phi(L)\varepsilon_t = \sum_{j=0}^{\infty} \Phi_j \, \varepsilon_{t-j} \tag{5-23}$$

Where L represents the lag operator, and $\Phi(L) = \sum_{j=0}^{\infty} \Phi_j L^j$. The response of $y_{n,t+j}$ to a unit impulse, say ε_m, is given by the (n,m)-th elements of the coefficient matrix Φ_j. Therefore, in equation (5-23), Φ_j already represents the responses in the systems. To differentiate this between the original coefficient matrixes from forecasting, Φ_j is henceforth represented by ψ_j. Therefore, the response of $y_{n,t+j}$ to a unit impulse in $y_{m,t}$, with all other variables at t remaining constant, can be represented by equation (5-24), where $\psi_{nm,j}$ represents the (n,m)-th element of ψ_j.

$$\psi_{nm,j} = \frac{\partial y_{n,t+j}}{\partial \varepsilon_{m,t}} \tag{5-24}$$

5.2.4.4 Forecast error variance decomposition

The forecast error variance decomposition is another form of structural analysis within the VAR framework, in which not only the shock effect of one variable can be tested on other variables but the contributions of all endogenous variables on each other's forecast errors, based on the orthogonal impulse response of the coefficient matrices. The methodology of an orthogonal impulse response function is detailed in Lütkepohl (2013). Assuming that ψ_j is still the matrices of the impulse responses, the forecast variance error, σ_k^2, of any k-th component of y_{T+h}, can be represented by equation (5-25).

$$\sigma_k^2(h) = \sum_{j=0}^{h-1} (\psi_{k1,j}^2 + \cdots + \psi_{kK,j}^2) \tag{5-25}$$

5.3 Empirical data

The monthly nominal metal prices used for the Granger-causality test are obtained from the German Federal Institute for Geosciences and Natural Resources (BGR, "Bundesanstalt für Geowissenschaften und Rohstoffe"). In order to calculate the real prices, the nominal prices are divided with the seasonally adjusted consumer price index (CPI) obtained from the Federal Reserve Bank of St. Louis. The period of the time series for the Granger-causality test is defined to be from

1990 until 2013. The reason for defining the year 1990 as the start of the analyses in this thesis is owed to the electricity feeding act, also known as the "Stromeinspeisungsgesetz" (StrEG), which was introduced in Germany in 1990. The act obligated power utilities to allow for electricity feed-in from renewable technologies into the power grid. This law eventually led to the introduction of the Renewable Energy Act (EEG) and a large scale deployment of renewables in Germany. Since the aim of this thesis is to analyse the impact of renewable energy technologies on metal prices, only the time period where the technologies are actually deployed is chosen for the analysis. For metals such as dysprosium, gallium and neodymium, for which the data from 1990 is unavailable, different start period, as shown in Table 5-1, are selected. The results that are presented in this thesis are only based on these specific time periods, which mean that possible relationship beyond this period is not captured by the analysis. The descriptive statistics of the data are listed in Table 5-1, including mean, maximum and minimum price, mean, median, standard deviation, standard error, skewness, and excess kurtosis. All values shown in Table 5-1 are obtained for the price levels, as the Toda-Yamamoto approach calls for the use of price levels without any data transformation. Based on the data, it can be seen that the price of dysprosium has the biggest standard deviation relative to the mean among all metals. The high skewness of the data also reflects the dysprosium price that soared in 2011 and 2012. Besides that, aluminium price is one of the most stable price series during this time period based on the relatively small values of skewness, kurtosis and standard deviation.

Table 5-1: Descriptive statistics of monthly prices for all of the analysed metals according to their respective available sample period. "n" is the available number of monthly price values. The monetary unit $ refers to US dollars. Min and Max refer to the minimum and maximum price respectively in the entire time series whereas Std. Dev., Ex. Kurt. And Std. Error refers to the standard deviation, excess kurtosis and standard error, respectively.

	Period	Unit	n	Min	Max	Mean	Std. dev.	Median	Skew	Ex. Kurt.	Std. error
Ag	01.1990-12.2013	$/oz	288	5.06	40.84	11.34	7.88	7.65	1.75	2.22	0.46
Al	01.1990-12.2013	$/t	288	1363.21	3401.14	2094.75	405.55	1992.54	0.79	-0.09	23.90
Au	01.1990-12.2013	$/oz	288	322.31	1712.86	688.92	367.48	554.61	1.34	0.64	21.65
Cd	01.1990-12.2013	$/kg	288	0.49	18.81	3.33	3.07	2.23	2.12	5.67	0.18
Co	01.1990-12.2013	$/kg	288	17.24	115.22	51.79	23.04	45.59	0.68	-0.41	1.36
Cr	01.1990-12.2013	$/t	288	782.69	6400.98	1904.13	919.59	1736.77	1.91	5.55	54.19
Cu	01.1990-12.2013	$/t	288	1690.61	9696.52	4413.12	2235.51	3658.94	0.69	-0.90	131.73
Dy	04.2001-12.2013	$/kg	153	32.15	2923.74	405.90	678.46	124.40	2.48	5.43	54.85
Fe	01.1990-12.2013	$/t	288	15.21	183.94	45.12	45.98	20.57	1.58	1.07	2.71
Ga	01.2003-12.2013	$/kg	132	219.35	909.89	429.67	158.56	363.42	1.22	0.77	13.80
In	01.1990-12.2013	$/kg	288	102.11	1168.70	455.29	253.92	384.98	0.79	0.03	14.96
Li	01.1990-12.2013	$/t	288	2530.17	6782.35	3908.00	1509.59	2964.84	0.81	-1.09	88.95
Mo	01.1990-12.2013	$/kg	288	7947.35	105820.11	28855.03	24517.29	16014.97	1.32	0.52	1444.70
Nd	01.2005-12.2013	$/kg	108	82.99	1739.87	358.64	346.02	247.92	2.33	5.41	33.30
Ni	01.1990-12.2013	$/t	288	5144.20	55010.37	14528.91	8026.37	12254.43	2.06	5.56	472.96
Pb	01.1990-12.2013	$/t	288	502.71	3876.27	1230.60	688.52	970.86	1.16	0.71	40.57
Se	01.1990-12.2013	$/kg	288	5.36	145.87	41.02	39.41	17.83	1.02	-0.20	2.32
Sn	01.1990-12.2013	$/t	288	4518.85	30971.16	11201.35	5785.98	8869.23	1.26	0.62	340.94
V	01.1990-12.2013	$/lb	288	7.60	138.47	26.80	17.88	23.22	2.75	11.26	1.05
Zn	01.1990-12.2013	$/t	288	897.76	4729.35	1762.01	688.44	1547.91	1.72	3.49	40.57

While the Granger-causality test involves pair-wise testing of metal prices, the VAR analysis involves more variables, which includes both micro and macroeconomic variables. The former is represented by the metal-specific price, demand and production whereas the latter involves the GDP, inflation rate, interest rate and exchange rate, all of which are included in the VAR model as endogenous variables. In contrast to the Granger-causality test, the VAR analysis is carried out using annual data. The reason for this is the unavailability of the macroeconomic data in a monthly resolution. Therefore, the arithmetical average annual prices are calculated from the monthly prices provided by BGR. Since the VAR analysis serves to understand the market dynamics of the metals -independent of the deployment of renewable energy- longer time-series, chosen based on data availability, is applied to fit the VAR model. Based on the descriptive statistics listed in Table 5-2, cobalt has by far the biggest standard deviation relative to the mean price, followed closely by indium. Meanwhile, copper, being an industrial metal that is widely available and extensively used, has the lowest price, followed by another industrial metal, nickel.

Table 5-2: Descriptive statistics of the annual prices for metals used in the VAR analysis. The monetary unit $ refers to US dollars. Min and Max refer to the minimum and maximum price respectively in the entire time series whereas Std. Dev., Ex. Kurt. And Std. Error refers to standard deviation, excess kurtosis and standard error, respectively.

	Unit	Time period	n	Mean	Min	Max	Std. dev.	Median	Skew.	Ex. Kurt.	Std. error
Ag	$/oz	1970-2013	44	14.39	5.38	55.22	9.80	12.23	1.97	4.89	1.48
Co	$/kg	1970-2013	44	52.22	18972.46	21.97	34.65	40.04	2.78	10.10	5.22
Cu	$/kg	1970-2013	44	4.33	1.89	9.12	1.92	3.66	0.78	-0.41	0.29
In	$/kg	1975-2012	38	531.99	105.53	1473.08	343.81	464.96	0.94	0.09	55.77
Ni	$/kg	1970-2013	44	14.81	6.19	39.14	6.25	14.84	1.43	3.20	0.94

In terms of the annual production, the data for silver, copper, indium and nickel are provided by BGR whereas the production of cobalt is obtained from the annual mineral commodity summaries of the USGS. As for the consumption, data of copper and nickel are provided by BGR. For the rest of the metals, the apparent consumption data from the USGS are used as a proxy due to the unavailability of the complete data from BGR. The descriptive statistics of the production and consumption data are listed in Table 5-3 and Table 5-4 respectively. Copper and nickel have the highest production and consumption levels whereas indium is on the other end of the scale. Nonetheless, indium has the standard deviations relative to the mean in both levels.

Table 5-3: Descriptive statistics of the annual production of metals used in the VAR analysis. Min and Max refer to the minimum and maximum price respectively in the entire time series whereas Std. Dev., Ex. Kurt. And Std. Error refers to standard deviation, excess kurtosis and standard error, respectively.

	Unit	Time period	n	Mean	Min	Max	Std. dev.	Median	Skew.	Ex. Kurt.	Std. error
Ag	t	1970-2013	44	15728.38	9352.97	25352.69	4789.09	14510.38	0.44	-1.09	721.98
Co	t	1970-2013	44	44771.60	17962.20	145402.72	34041.57	30765.57	1.91	2.48	5131.96
Cu	kt	1970-2013	44	12542.12	7383.70	20962.36	3982.53	11127.14	0.63	-0.95	600.39
In	t	1975-2012	38	264.15	21.37	784.68	248.77	145.64	0.75	-0.98	40.36
Ni	kt	1970-2013	44	971.64	582.40	1962.37	335.40	850.36	1.02	0.34	50.56

Table 5-4: Descriptive statistics of the annual consumption of metals used in the VAR analysis. Min and Max refer to the minimum and maximum price respectively in the entire time series whereas Std. Dev., Ex. Kurt. And Std. Error refers to standard deviation, excess kurtosis and standard error, respectively.

	Unit	Time period	n	Mean	Min	Max	Std. dev.	Median	Skew.	Ex. Kurt.	Std. error
Ag	t	1970-2013	44	5288.86	3260.00	8000.00	1209.10	5025.00	0.46	-0.63	182.28
Co	t	1970-2013	44	8782.05	5070.00	11800.00	1719.79	8780.00	-0.02	-0.83	259.27
Cu	kt	1970-2013	44	12496.65	7291.40	21089.60	3985.88	10906.39	0.63	-0.91	600.89
In	t	1975-2012	38	51.82	3.50	125.00	39.15	37.50	0.63	-1.14	6.35
Ni	kt	1970-2013	44	956.17	526.40	1774.90	317.51	846.81	0.79	-0.32	47.87

Apart from the microeconomic variables, the VAR model is complemented with macroeconomic variables which serve as control variables in order to capture further economic effects. The inflation rate is represented by the US consumer price index (CPI) whereas the US federal fund rates represent the interest rates. Global GDP and the exchange rate of the national currencies between the US and Germany complete the list of macroeconomic variables. All data are obtained from the Economic Research Division of the Federal Reserve Bank of St. Louis. The descriptive statistics of the variables from 1970 to 2013 are listed in Table 5-5. The statistics indicate that the federal fund rates have the highest volatility based on the standard deviation with respect to the mean values while the exchange rate series, on the other hand, has the smallest volatility.

Table 5-5: Descriptive statistics of the macroeconomic variables used in the VAR analysis. The monetary unit $B refers to billion US dollars, min and max refer to the minimum and maximum price respectively in the entire time series whereas Std. Dev., Ex. Kurt. And Std. Error refers to standard deviation, excess kurtosis and standard error, respectively

	Unit	Mean	Min	Max	Std. Dev.	Median	Skew.	Ex. Kurt.	Std. error
Gross Domestic Product (GDP)	$B	9787.86	4722.01	15612.18	3559.26	9110.80	0.21	-1.45	536.58
Consumer Price Index (CPI)	-	0.62	0.18	1.07	0.27	0.63	-0.05	-1.25	0.04
Federal Fund Rate (FedFund)	%	5.73	0.10	16.38	3.74	5.41	0.52	0.10	0.56
US-Germany national currency exchange rate (ExchangeRate)	-	1.36	0.91	2.47	0.39	1.22	1.08	0.39	0.06

6 Wind turbines[5]

This chapter summarizes the methodology and input parameters presented in Shammugam et al. (2019a). The exact methodology from the authors is also applied in this thesis for the analysis of the raw material demand for the deployment of wind turbines in Germany until 2050.

6.1 Material composition of wind turbine components

The material demand for each component of the wind turbines is determined based on their respective weight percentage. The weight percentage of the rotor, nacelle and tower are presented in Table 6.1 whereas the weight percentage of the foundation is presented in Table 6-2. In this thesis, stainless steel 18/8 is considered as high alloyed steel, as presented in Eymann et al. (2015) and Vestas (2006), whereas low alloyed steel is assumed to be the structural steel S355 that makes up to 70 % of the total low alloyed steel amount of a wind turbine (Pereg and Hoz 2013). The full list of the metal composition of the steel-alloying elements, electrical and electronic components as well as their corresponding references are provided by Shammugam et al. (2019a)

Table 6-1: Average weight composition [%] of materials in rotor, nacelle and tower of a wind turbine. The material composition is relative to the respective components and is assumed to be similar for all nacelle sizes according to respective drive train systems. Other materials include concrete and high-density polyethylene.

	Rotor	Nacelle					Tower	
		DFIG	EESG-DD	PMSG-HS/MS	PMSG-DD	SCIG	Steel tower	Hybrid
Low alloyed steel	9.8	20.7	8.9	10.3	8.9	12.5	97.1	11.3
High alloyed steel	9.4	36.1	29.8	39.3	29.8	41.1	-	-
Cast iron	25.8	35.6	52.6	41.5	52.6	35.6	-	-
Aluminium	0.1	1.1	0.9	0.9	0.9	1.0	1.0	-
Copper	0.1	2.1	7.7	2.2	2.2	3.2	0.9	-
Electrics/Electronics	-	0.3	0.1	0.4	0.1	0.6	1.0	1.0
Other materials	54.8	4.1	0	5.4	5.5	6.0	0	87.7

Table 6-2: Average weight composition [%] of materials in the foundation of a wind turbine. Other materials include concrete and high-density polyethylene.

	Onshore	Offshore			
Foundation	Flat	Monopile	Jacket	Tripod	TLB
Steel	4.5	100	85.8	62.7	87.5
Other materials	95.5	0	14.2	37.3	12.5

[5] Some parts of this sub-chapter have been published in (Shammugam et al. 2019a). These contents have been revised and editorially amended as part of this thesis.

Historically, wind turbines have been growing in size with larger rotor diameter and taller towers. The main reason for this is that higher full-load hours can still be reached despite low wind speed. This is achieved by maintaining the nominal power of the generator at a fairly low level while increasing the rotor diameter or the hub height. Therefore, the requirement of REE in generators is considered to be linearly dependent on the nominal power of the turbines in this thesis. The specific content of dysprosium and neodymium are obtained from Viebahn et al. (2015), who provided the REE content of the NdFeB-PM, which is the most predominant type of magnet used in wind turbines.

Table 6-3: Specific weight [kg/MW] of dysprosium and neodymium in permanent magnets in different drive train concepts (Viebahn et al. 2015).

Drive train	Nd	Dy
PMSG-DD	202	15
PMSG-MS	50	4
PMSG-HS	25	2

In order to obtain the weights of rotor, nacelle and tower for future wind turbines, which are expected to grow larger, the upscaling method is applied. This method has been previously applied in works such as Nijssen et al. (2001) and Caduff et al. (2012) to estimate the increase in wind turbine component mass. This method dictates that the mass of the turbine components can be explained in relation to the rotor diameter, as shown in equation 6-1. The term M describes the mass of each component, a is a constant factor, D is the rotor diameter and b is the scaling factor. The complete coefficients used in this study for the upscaling of the rotor, nacelle and tower are provided in table 6-4. The development of future turbine sizes are discussed briefly in chapter 6.4.

$$\log(M) = \log(a) + \log(D) * b \tag{6-1}$$

Table 6-4: Scaling factors (b) and constants (a) for the upscaling of rotor, nacelle and tower (Shammugam et al. 2019a)

	Rotor	Nacelle						Tower	
Type	-	DFIG	SCIG	PMSG-MS	PMSG-HS	EESG-DD	PMSG-DD	Steel	Hybrid
$\log(a)$	-3.34	-2.28	-1.24	-2.20	-2.33	-3.29	-3.40	-4.22	-3.53
b	2.56	2.13	1.59	2.13	2.17	2.70	2.70	3.22	3.22

The foundation mass of future wind turbines is determined via the foundation-to-turbine mass ratios, which are listed in Table 6-5. The foundation of onshore turbines weighs in average 3.5 times heavier than the combined mass of rotor, tower and nacelle. As for the foundation types of offshore turbines, the ratios are calculated separately based on existing data from wind farm operators. According to the planned projects, offshore turbines will be built in areas of average depth of 35 m

until 2035 (see Deutsche Windguard (2017) for the detailed information regarding the water depth of planned offshore wind turbine projects in Germany). However, the average water depth of where offshore turbines will be built beyond 2035 will increase to 45 m. Therefore, the foundation mass is assumed to increase linearly with the water depth to account for the additional depth that needs to be covered to anchor the turbines to the seabed. Regarding the tension-leg-buoy foundation, since the mooring cables are made of high-density polyethylene, the additional water depth would not affect the metallic material requirements.

Table 6-5: Average ratios of foundation mass to turbine mass for different foundation types

	Onshore	Offshore						
	Flat	Monopile		Tripod		Jacket		TLB
Year	-	2020 - 2035	2036 - 2050	2020 - 2035	2036 - 2050	2020 - 2035	2036 - 2050	-
Foundation-to-turbine mass ratio	3.5	2.2	2.8	1.5	1.9	1.5	1.9	0.9

6.2 Material efficiency measures

One of the most important material efficiency measures in wind turbines would be the reduction of the specific content of REEs. Several strategies regarding the substitution of REEs in PMs and their impact on future demand in wind turbine industry has been extensively discussed by Pavel et al. (2017). The reduction in the specific content of dysprosium and neodymium that is applied in this thesis due to improved production processes and substitution of neodymium and dysprosium with less critical metals is listed in Table 6-6.

Table 6-6: Reduction of the specific content [kg/MW] of REEs in a PM of a generator due to material efficiency measures based on (Viebahn et al. 2015).

	2025		2050	
	Nd	Dy	Nd	Dy
PMSG-DD	163	12	130	12
PMSG-MS	40	3	32	3
PMSG-HS	20	1	16	1

Besides REE, measures in reducing the steel demand for wind turbines are also being actively researched. For instance, the Pile Soil Analysis (PISA) project is a joint industry project that aims at developing a new design methodology for monopile wind turbine foundations (Burd et al. 2017). The findings from the project suggested that traditional monopile manufacturing processes are very conservative: a steel saving could be achieved by using thinner and shorter piles. Monopiles of various sizes have been tested onshore on representative sites of the North Sea to demonstrate the

viability of these lighter designs. Similar research was also conducted by Hamm et al. (2015), who proved the feasibility of a lighter tripod structure. In terms of the tower, World Steel Association (2012) reported that the utilization of higher grade steels such as S460 or S500 instead of S355 can save up to 30 % of the total steel demand in a tower. Last but not least, alternative structures, such as the lattice structure (Trabish 2014) or the bolted steel shell tower (Siemens AG 2011) could also lead to a significant reduction in steel demand. The expected savings and their market shares are shown in table 6-7.

Table 6-7: Savings of low-alloyed steel and the rate of implementation

Innovation	Higher grade steel		Alternative structures		PISA		OFE	
Year	2020	2050	2025	2050	2025	2050	2030	2050
Savings on total low-alloyed steel demand	10 %		30 %		25 %		40 %	
Market share of efficiency measure	40 % of steel towers	80 % of steel towers	1 % of steel towers	25 % of steel towers	10 % of monopiles	80 % of monopiles	5 % of tripods	25 % of tripods

6.3 Lifespan of wind turbines

The lifespan of wind turbines is modelled according to the Weibull distribution using equation (5-2). The average life span of a wind turbine is generally assumed to be 25 years (Kost et al. 2018). The shape parameter, k is assumed to be 2 in this thesis, similar to that applied in Zimmermann et al. (2013). With the average product lifespan of a wind turbine $\overline{T} = 25$ and $k = 2$ by equation (5-3), a scale parameter $\lambda = 0.443$ is obtained. Using equation (5-5), the decommissioning capacity is obtained, which is assumed to be installed again in the next year via repowering.

Besides decommissioning, additional material demand due to repair and maintenance works is also considered in this thesis. Due to the complexity and the large variety of the wind turbine components, only the components with the most frequent failure rates are considered in the material requirement calculation, namely the pitch, gearbox and yaw (Sheng 2013; Carroll et al. 2016). Additionally, the generator failures are also included due to the presence of REEs. The failure rates per year and per turbine of the selected components are adapted based on Carroll et al. 2017 and Carroll et al. (2016) and are listed in table 6-8. Considering the uncertain future evolution of components reliability, constant failure rates per turbine per year are considered for the material requirements calculation up to 2050. Turbines that undergo maintenance include those which have been repowered in each year, as failures can occur from the very first year of installation. Additional material demand from maintenance is not considered on the decommissioning year of turbines. In order to calculate the future demand for maintenance operation precisely, each component listed in table 6-8 is upscaled separately according to the upscaling parameters presented in Shammugam et

al. (2019a). For each minor repair, 10 % of the material will be replaced whereas a major repair requires 20 % of the additional material.

Table 6-8: Annual failure rates per turbine for pitch, yaw, gearbox and generator for different drive train systems

	Pitch	Yaw	Gearbox		Generator					
	-	-	Multiple-stage	Single-stage	DFIG	PMSG-HS	PMSG-DD	PMSG-MS	EESG-DD	SCIG
Major replacement	0.001	0.001	0.059	0.042	0.109	0.007	0.009	0.008	0.109	0.109
Major repair	0.179	0.006	0.042	0.03	0.356	0.024	0.03	0.026	0.356	0.356
Minor repair	0.824	0.162	0.432	0.305	0.538	0.437	0.546	0.473	0.538	0.538

6.4 Further development scenarios of wind turbines

In order to calculate the annual material demand until 2050, two technological roadmaps, namely the conservative and advanced, which differ in terms of the nominal power of the turbines, rotor diameter and the market share of drive trains, are considered in this thesis. The conservative scenario represents a copper-intensive scenario with large market shares of PM-free generators such as DFIG and EESG, whereas the advanced scenario represents a REE-intensive scenario. The exact market shares of the drive train systems for all scenarios are provided by Shammugam et al. (2019a).

6.4.1 Conservative scenario

The basic principle of the conservative scenario is the stagnation of onshore turbine sizes. The reason for this can be factors such as legally binding height limitations, urban space competition and infrastructural restrictions bound to the transportation of sizable components. However, these challenges can be far less relevant for offshore turbines. As the offshore market becomes more mature, it can be assumed that the logistical difficulty of transportation with high lifting facilities will be overcome. Due to this reason, the conservative scenario is not applicable to offshore turbines in this thesis. In this scenario, the average size of a wind turbine in 2050 is expected to not exceed the current biggest wind turbine adapted to low wind sites in Germany. This refers to the E-141 EP4 by Enercon, with a rotor diameter of 141 m and a 4.2 MW nominal power[6]. The reason for this is that onshore turbines are mostly installed on low wind sites and are equipped with small generator designs compared to the size of the rotor. In addition to that, market entry of innovative drive-train systems is not assumed in this scenario since the pressure for innovation is very low. Since EESG-

[6] In 2019, Enercon announced that a much larger EP5 series for low wind sites are being developed. However, no information was given on the completion date of models.

DD currently dominates the onshore market in Germany (see (Bundesnetzagentur 2017), it is assumed to remain a major technology in this scenario.

Upon the merging of Siemens and Gamesa, DFIG turbines in Germany are expected to benefit from the strategic leadership of Siemens on the offshore market and the experience of Gamesa with the onshore DFIG technology in the rest of Europe. Regarding wind turbines with PMs, Vestas has already replaced its PMSG-HS portfolio with SCIG in order to limit its dependency towards REEs. Moreover, the high costs of PMSG-DD will further suppress a large scale deployment. Therefore, PMSG-DD and PMSG-HS are assumed to phase out completely by 2020, replaced by SCIG generators. The PMSG-MS, which is currently only applied offshore, is not expected to enter the onshore market before 2030. It is expected to gradually take over the market shares from the induction generators due to a better energy yield performance at similar manufacturing costs.

6.4.2 Advanced scenario

In the advanced scenario, the barriers addressed in the conservative scenarios are assumed resolved through increasing experience over time. Consequently, wind turbines are expected to grow in size substantially. This assumption is backed by the results of Ashuri (2012), who proved the technical feasibility of a 20 MW offshore wind turbine with an optimized 286 m rotor diameter. The advanced scenario assumes a technology shift towards lighter drive-train types to avoid technically, logistically and economically challenging turbine masses. As a result, EESG-DD is expected to lose onshore market shares whereas much lighter direct-drive systems such as the PMSG-DD and PMSG-MS should largely benefit from this. The possibility of Vestas returning to manufacturing PMSG-HS remains open, which can provide an additional light synchronous generator to the market. However, due to its relatively low efficiency, PMSG-HS will remain sparsely implemented. The DFIG is assumed to dominate the wind energy market in the advanced scenario since it is among the lightest available technologies and is already manufactured by several suppliers. Based on the planned offshore projects, only three types of drive train systems are planned from 2017 to 2019, namely PMSG-DD, PMSG-MS and DFIG (Deutsche Windguard 2017). These turbines have the lowest failure rates compared to other drive train systems and are therefore expected to remain the solely deployed drive train systems offshore up to 2050. The reason for this is that the reliability of offshore turbines is a crucial parameter since maintenance operation during failures requires special equipment and is subject to accessibility restrictions tied to weather condition. Due to its higher efficiency and reliability, PMSG-DD is therefore assumed to dominate the offshore market, followed by the PMSG-MS and DFIG.

7 Photovoltaic

Since the early 1990s, Germany has been one of the leading countries in the world in terms of installed PV capacities. Currently, Germany has the fourth largest cumulative installed PV capacity in the world with 42 GW_p. This is mainly owed to the success of the feed-in-tariffs introduced in the renewable energy act (EEG). In terms of the type of plants installation, rooftop PV plants have been the major plant type in Germany in terms of the installed capacity, followed by the ground-mounted plants, as shown in Figure 7-1. However, the actual market share was mixed in the past years as a significant temporal trend with respect to the year of installation cannot be identified. As illustrated in Figure 7-2, this is not the case regarding the type of modules installed as there is a clear tendency towards c-Si PV modules over the past few years.

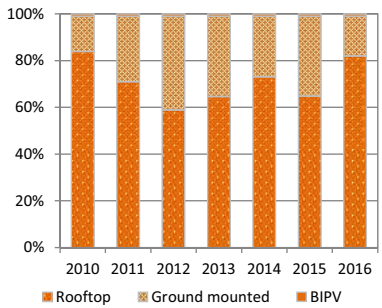

Figure 7-1: Market shares of the installed capacity of rooftop, ground-mounted and building integrated PV (BIPV) plants (ZSW 2014; Hein Concept 2016, 2017). Due to lack of data for building integrated PV from 2013 onwards, a market share of 1 % is assumed for 2013-2016, which is similar to the years before.

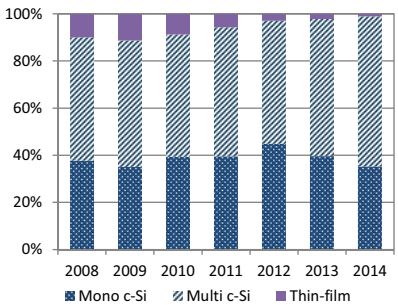

Figure 7-2: Market shares of the installed capacity of thin film modules as well as mono- and multi c-Si modules in Germany (PSE internal data 2018).

Increasing the efficiency of PV modules has been the focus of research as it is one of the most important factors that influence the financial viability of PV modules. In this thesis, the specific material demand is decreased according to the improvements in efficiency since lesser material will be required to generate electricity at higher module efficiency. The theoretical maximum efficiency for single-junction silicon solar cells is 33.3 % (Polman et al. 2016). However, the maximum achievable efficiency is calculated to be much lesser at 29.4 % for a 110-µm-thick solar cell made of undoped silicon (Richter et al. 2013). As to now, the record lab efficiency is 26.7 % for mono-crystalline and 22.3 % for multi-crystalline (Green et al. 2018). This proves that there is enormous

potential to further increase the efficiency in the coming years. As for CIGS and CdTe solar cells, the highest achievable efficiency lies slightly below 25 % (Polman et al. 2016). Since the material demand of the entire PV system is considered in this thesis, the module efficiency is used to determine the development of the specific material demand. The module efficiency is usually lower than the cell efficiency due to additional losses for the cell connections as well as optical losses from the module glass and encapsulation.

Table 7-1 lists the increase of average PV module efficiencies, derived based on literature and discussion with PV experts. Besides increasing the efficiency, reducing the cell thickness is of special interest as it is one possible way of reducing material consumption and subsequently the production costs, especially due to the presence critical metals in the absorber layer of thin-film cells. The reduction of the absorber layer thickness is obtained also based on expert interviews and projections by ITRPV (2017).

Table 7-1: Current and future average module efficiencies of different types of solar cells in the German market

	Mono		Multi		CdTe		CIGS	
	2015	2050	2015	2050	2015	2050	2015	2050
Efficiency [%]	17.5	25.0	16.0	24.0	14.4	22.0	14.0	22.0
Absorber layer thickness [µm]	180	120	180	120	2.0	1.0	1.6	1.0

7.1 Material composition of PV systems

In obtaining the current material composition of c-Si modules, several studies as listed in Table 7-2 are considered. It can be clearly seen that a wide range of material composition is available in the literature. Besides different sources of data, the discrepancy can be owed to the different module types that were analysed by the studies. These however, are not mentioned exactly in the studies. Therefore the internal data from Fraunhofer ISE, which represents the exact composition of a standard aluminium back surface field (Al-BSF) top contact module, is used for the calculation of the material demand for c-Si modules. Al-BSF type modules currently dominate the PV market in Germany (ITRPV 2017). Nonetheless, since the data only represents the final content of a module and not the total material demand in manufacturing them, 5 % additional material demand for the manufacturing losses is assumed.

Table 7-2: Current material composition of crystalline PV modules (excluding the frame) according to studies in the literature and the internal data of Fraunhofer ISE.

c-Si [kg/MWp]	Fthenakis et al. (2011)[7]	Moss et al. (2013)	Schriefl et al. (2013)	ITRPV (2017)	Fraunhofer ISE internal	This thesis
Al	319	-	-	-	322	338
Ag	52	24	11	27	22	23
Cu	667	2741	800	-	499	534
Pb	19	336	-	-	64	67
Si (Mono)	7587	-	19600	-	2244	2356
Si (Multi)	8577	-	-	-	2274	2388
Sn	33	577	-	-	61	64
Ni	< 1	-	-	-	-	-

The material composition of CdTe modules is obtained via literature and discussions with PV experts. Except Viebahn et al. (2014), other studies listed in Table 7-3 state a combined cadmium demand for the absorber and the buffer layer. However, since the efficiency measures of each of these layers are looked into detail in this thesis, the specific material demand of each layer is required. Therefore, instead of considering the average values for cadmium, only values from Viebahn et al. (2014) are considered. For every other material, the average values are calculated. However, due to unavailability of much newer data, the uncertainty of the results involving CdTe modules could be high, should the current composition of a CdTe module differ significantly with the composition that is presented in Table 7-3.

Table 7-3: Current material composition of CdTe modules (excluding the frame) according to studies in the literature and their average values, which are used for further analysis in this thesis

CdTe [kg/MWp]	Moss et al. (2011)	Zimmermann (2013)	Schlegl (2013)	Schriefl et al. (2013)	Viebahn et al. (2014)	This thesis
Cd	-	153.4	143	240	93.2	93
Te	93.3	137.7	135	240	99.7	153
Cd in buffer layer	-	-	-	-	23.5	24
In in TCO	15.9	16.9	-	-	15.5	16
Sn in TCO	21.4	-	-	24	-	23

The material composition of CIGS modules is taken based on actual production data from Fraunhofer ISE. Since the market share of CIGS modules is relatively small, the data of a single manufacturer is considered and not the average value as opposed to CdTe modules. However, the TCO of this particular module is based on the novel ZAO concept which is currently not very common. Therefore, the more frequent indium-based TCO is selected as the status quo TCO layer. The ZAO concept is however considered with increasing market share in the future.

[7] The values from Fthenakis (2011) have been adjusted to represent the module efficiency of 17.5 % (see Table **7-1**) as opposed to the efficiency of only 13.2 % used in their study.

Table 7-4: Current material composition of CIGS modules (excluding the frame) based on Fraunhofer ISE internal data. The composition of indium and tin in TCO is based on (Moss et al. 2013)

CIGS [kg/MWp]	Fraunhofer ISE internal (2017)
Copper	48
Indium	26
Gallium	14
Selenium	130
Cadmium (Buffer layer)	8
Indium in TCO	44
Tin in TCO	6

Since there is a huge difference between the support structures of different PV plant types, the material demand of the mounting structure is differentiated between rooftop, ground-mounted and BIPV plants. The complete material demand for the mounting structure is listed in Table 7-4. The material composition of inverters is very limited in the literature. The data of a 2.5 kW module inverter according to Fthenakis et al. (2011) is applied for BIPV and rooftop plants in this thesis. For ground-mounted PV plants, the specific material demand of a 1 MW inverter is applied in order to calculate the total demand. The number of inverters is scaled according to the installed capacity of the PV plants. The complete material compositions are provided in Table 7-6. The material demands for cabling are also differentiated between the plant types. The only metallic element in a cable that is of interest in this thesis is copper. The specific weight of cables in a PV system is provided by Schlegl (2013). According to Fthenakis et al. (2011), the copper demand accounts for approximately 50 % of the total cable weight. Therefore, half of the specific weight reported by Schlegl (2013) is attributed to the specific copper demand in cables for PV systems, as listed in Table 7-7.

Table 7-5: Specific material demand (kg/MW_p) of mounting structures

		Mono	Multi	CIGS	CdTe	Source
Rooftop	Low alloy steel	0	0	0	0	(Fthenakis et al. 2011)
	Stainless steel	50	55	73	73	
	Aluminum	62	68	91	91	
BIPV	Low alloy steel	162	177	237	237	(Jungbluth et al. 2012)
	Stainless steel	0	0	0	0	
	Aluminum	234	256	342	342	
Ground-mounted	Low alloy steel	507	554	739	739	(Jungbluth et al. 2012)
	Stainless steel	21	23	30	30	
	Aluminum	328	359	478	478	

Table 7-6: Specific material demand (kg/ MW_p) of inverters.

	Rooftop and BIPV	Ground-mounted
Steel	156	94
Aluminum	1364	543
Copper	501	288
Printed circuit board	225	103

Table 7-7: Specific copper demand (kg/ MW_p) of cabling of a PV system

	Mono	Multi	CIGS	CdTe
Rooftop and BIPV	974	1065	1420	1420
Ground-mounted	1850	1691	2467	2467

7.2 Material efficiency measures in PV modules

Future material compositions of solar cells are subject to innovations and cell topologies such as absorber layer thickness and the use of novel materials. In the following section, these measures and their influence on the material composition of solar cells are described.

Crystalline silicon solar cells

Being the most expensive metal in a c-Si solar cell, the amount of silver used as metallization paste in a cell is assumed to decrease in the future. Firstly, the reduction will come as a result of improvements in the screen printing process, which reduces metal losses during the plating process (Cimiotti et al. 2015). Secondly, the demand of silver can not only be reduced by improving the production techniques, but also by replacing silver with nickel and copper, which is able to reduce the costs of metallization by almost 50 % without affecting the efficiency of a solar cell (Meyer et al. 2014; Appleyard 2012). Currently, 5 % of all PV modules in the global market use nickel-copper metallization paste. This share is expected to increase up to 20 % in 2027 (ITRPV 2017). Consequently, almost 65 % of all PV modules are assumed to have nickel-copper metallization paste by 2050. A complete phase-out of silver until then is not expected since the use of nickel-copper metallization paste is not a mature process that still requires proper equipment and solutions regarding reliability issues (Rahman and Lee 2015; Bartsch et al. 2010). These measures lead the average specific demand of silver of all PV modules in the market to drop from around 99 mg/cell today to around 50 mg/cell in 2035 and 26 mg/cell[8] in 2050.

Secondly, the use of lead-free paste is expected to increase, as they already represent 10 % of all c-Si modules in 2018. The use of lead in solar cells is currently excluded from the list of hazardous substances in the EU "Restriction of Hazardous Substances in Electrical and Electronic Equipment" Directive 2 (RoHS) (EU 2017). However, the directive has to be reviewed upon certain years, with the next review being in 2021. Due to this constant uncertainty, lead-free pastes are expected to be applied rapidly in the PV industry. Furthermore, the efficiency of the solar cells remains fairly unchanged with the substitution of lead-free paste (Hoornstra et al. 2005; Sridharan et al. 2012). Therefore, a complete phase-out of lead in 2030 is assumed in this thesis. However, it should be noted that most of the widely used lead-free solders available today contain silver, which

[8] Calculated based on a PV module with 60 cells and a nominal power of 240 W_p.

contradicts the assumption regarding the reduction of silver usage in PV modules. Nonetheless, there are also other types of solders being researched which contains neither silver nor lead, such as tin-bismuth or zinc-based solders (Wu et al. 2015; Dharma et al. 2009; Siewert et al. 2002), which can be used once reliability issues are solved and proven marketable.

Table 7-8: Development of the specific material composition of multi and mono c-Si modules upon consideration of material efficiency measures and improvements in module efficiency

	Multi					Mono				
	2015	2020	2030	2040	2050	2015	2020	2030	2040	2050
Al	370	345	304	272	246	338	319	286	259	237
Ag	25	22	15	10	6	23	20	14	10	6
Cu	584	547	486	439	400	534	505	456	417	384
Pb	73	48	0	0	0	67	45	0	0	0
Si	2388	2101	1500	1159	980	2356	1869	1350	1076	982
Sn	70	65	58	52	47	64	60	54	49	45
Ni	0	0.16	0.53	0.82	1.06	0	0.15	0.50	0.78	1.02

Thin-film solar cells

The optimal absorber thickness in a thin-film solar cell is a fine balance between minimizing recombination effects while improving absorption. While the former can be achieved by minimizing absorber thickness, the latter is achieved by increasing the absorber thickness. The average thickness of CIGS and CdTe absorber layers are reported to be 1.5 µm and 2.0 µm respectively (Ali et al. 2016). (Marscheider-Weidemann et al. 2016) assume in their ambitious projections that the absorber thickness will be reduced to 0.5 µm in 2050. However, according to PV experts, the absorber layer thickness will not necessarily decrease significantly. This is due to the already low cost of PV modules, which does not amortize the efforts of extremely reducing the absorber thickness. Furthermore, Mykytyuk et al. (2012) showed that the total power loss can reach up to 20 % with a layer thickness of 0.5 µm, as opposed to around only 5 % with 1 µm. This is another key factor against a massive reduction of the absorber thickness. Therefore, the absorber thickness of both CIGS and CdTe cells is assumed to reduce only down to 1 µm until 2050 in this thesis.

The buffer layer of thin film PV modules is predominantly made out of the well-established cadmium sulphide (CdS) layer. However, there are two main motivations in finding alternatives to be used as a buffer layer. Firstly, the toxicity of cadmium makes thin films undesirable in comparison to modules with materials that are less hazardous to human health. Besides that, although the use of cadmium in PV is currently exempted from the RoHS 2 Directive, similar to lead, uncertainty exists as to whether this would still be the case in the future since the exemptions have to be renewed periodically. Secondly, the recombination losses in the CdS is high in the wavelength regions between 350 and 550 nm (Witte et al. 2014). Solving this problem means that thin film modules can be applied in a much wider range of conditions. For CIGS cells, there are

several options to substitute CdS as the buffer layer, as shown by Witte et al. (2014), who presented 6 different material compositions that can be used as a buffer layer. Most of them are based on ZnS(O,OH) layers. Similar research has also been conducted by Bhattacharya and Ramanathan (2004). Contreras et al. (2003) even showed that comparable efficiencies can be achieved using ZnS(O,OH) based alternative buffer layers. In terms of CdTe cells, magnesium-doped zinc oxide (MZO) can be used as an alternative to the buffer layer (Bittau et al. 2018b; Bittau et al. 2018a). Therefore, assumptions regarding the reduction of cadmium are made within this thesis, with a complete phase-out from the buffer layer in 2030.

Last but not least, efficiency measures are also considered for the TCO layer with the substitution of indium due to its criticality. For CIGS solar cells, a further advantage of using ZnS(O,OH) as a buffer layer as discussed earlier, is that the TCO layer that is deposited onto the buffer layer can be substituted with the indium-free layer as well. This can be done by using the (Zn,Mg)O layer. For CdTe cells, the MZO buffer layer can be combined with either aluminium-doped zinc oxide (AlZnO) or fluorine-doped tin oxide (FTO) while not significantly compromising the efficiency of the cells. Due to the various possibilities, a phase-out of indium in the TCO is also expected in 2030.

Table 7-9: Development of the specific material composition of CI(G)S modules upon consideration of material efficiency measures and improvements in module efficiency

CIGS [kg/MW]	2015	2020	2030	2040	2050
Cu	48	42	32	25	19
In	26	23	18	14	10
Ga	14	12	9	7	5
Se	130	113	87	67	52
Cd (Buffer layer)	8	5	0	0	0
In (TCO)	44	30	0	0	0
Sn (TCO)	6	6	5	4	4

Table 7-10: Development of the specific material composition of CdTe modules upon consideration of material efficiency measures and improvements in module efficiency

CdTe [kg/MW]	2015	2020	2030	2040	2050
Cd	90	78	58	42	30
Te	149	128	95	69	49
Cd (Buffer layer)	21	14	0	0	0
In (TCO)	14	10	0	0	0
Sn (TCO)	22	20	18	16	14

Aluminium frames currently dominate the PV market, mainly due to the low cost and high mechanical strength. Nonetheless, there are other types of module frames that are being researched, which can be represented much stronger in the market in the future. According to ITRPV (2017), alternative modules frames, particularly steel and plastic, are expected to progressively gain market shares with around 26 % in 2027. Plastic or polymer-based frames represent a lighter alternative, which reduces grounding costs and current leakage risk occurring with aluminium frame due to its conductive nature (Ehbing et al. 2013; Wu et al. 2016). Moreover, plastic frames might feature

similar durability and weather resistance as their aluminium counterparts (BASF 2017). They are therefore assumed to reach around 45 % of the frame shares in 2050, based on the linear trend assumed by ITRPV. Another feasible alternative to aluminium frames is stainless steel frames, which can be made thinner than aluminium frames. This causes steel frames to possess the potential of reducing shadowing effects on the edges of the modules besides being capable of withstanding robust environment conditions (ISSF 2010). However, being slightly more expensive, steel frames are assumed to represent only up to 20 % of the shares in 2050. A linear interpolation is used to determine the type of frame share for each year.

7.3 Lifespan of photovoltaics

Some of the main causes of failures in PV modules are junction box failure, frame and glass breakage, cell cracks and shunt hot spots (Köntges et al. 2014). However, due to the modular nature of PV power plants, defect modules can be replaced easily without affecting the entire operation of a plant for an extended period. This is different in wind turbines as it is a common practice that some of the malfunctioning components will be repaired for days or even weeks. Therefore, as opposed to wind turbines, where different types of repair works are defined (minor, major and replacement), only component replacements are considered for PV plants. The exact amount of capacities that needs to be replaced is determined by the Weibull distribution and is augmented to the annual installed capacity. Thorough literature research on the Weibull distribution of the PV lifespan shows that the shape parameter, k, ranges between 2 and 14.41, whereas the scale parameter, λ, lies between 25 and 29.6. The full list of studies investigating the Weibull-distribution of PV plants can be found in (Collins et al. 2009; Laronde et al. 2010a; Kleiss 2016; Klise 2016; Laronde et al. 2010b; Zimmermann 2013). In this thesis, the average value of $k = 5.3$ and $\lambda = 27.3$ are used.

7.4 Further development scenario of photovoltaics

The market shares of the individual PV technology types are vital factors in determining future material demand. In reality, the development of the PV market in Germany will be heavily affected by the global market. In order to account for the uncertainties on how the PV market in Germany will develop in the future, two possible market development scenarios are proposed, which allow for the consideration of a range of various possible developments. These scenarios are inspired by the market developments proposed by Viebahn et al. (2014). In all scenarios, the market share of c-Si modules is shared equally by mono and multi-crystalline PV modules.

7.4.1 Conservative scenario

The conservative scenario assumes low dynamics in terms of the technology mix in the PV market, where the trends of the past are expected to continue in the future. The continuing decrease in the feed-in-tariff is expected to result in a higher domestic self-consumption. This would lead to an increased adaptation of decentralised energy systems. Therefore, rooftop PV plants are assumed to continue their dominance in the market with a share of 85 % in 2050. Besides that, rooftop PV plants are currently not subjected to implantation restriction as opposed to ground-mounted plants (see (EEG 2017)), which makes the designing and installation of rooftop PV plants to be less complicated than its counterpart. The decreasing market shares of ground-mounted plants between 2011 and 2012 can be explained by the removal of subsidies dedicated to plants on croplands from 2011 onwards, and those dedicated to the large plants of more than 10 MW. A further low share of ground-mounted plants can be expected in the future due to land use competition that could be exacerbated in the future. However, a complete phase-out of ground-mounted PV plants is not foreseeable mainly due to the decrease of BOS-costs, making ground-mounted plants economically attractive. A share of 10 % is therefore assumed for ground-mounted plants in 2050. In terms of BIPV, only a 5 % market share is assumed for 2050 as in Viebahn et al. (2014). It should, however, be noted that an error in the BIPV shares would have a limited impact on the material composition as mounting structures for BIPV only contain steel and aluminium, both noncritical and according to Jungbluth et al. (2010), in similar proportions as flat roof mounting structures.

Following the clear trend of the past years, crystalline modules are assumed to be a dominant market leader in the future, as shown in Figure 7-4. There are two main points to support this. Firstly, the argument that thin-film modules are cheaper than c-Si modules is not valid anymore, as shown in Figure 7-5. The price difference between thin film and c-Si modules has decreased over the past years and since 2015, the average global c-Si module prices have been lower than that of thin-film modules. Secondly, thin-film modules feature a lower efficiency and are not expected to surpass the efficiencies of c-Si modules until 2050 (IEA 2014). Therefore, the savings offered by lighter thin-film panels are somewhat offset by the additional costs of the BOS, if required to produce the same amount of energy as c-Si modules. Thin films can, therefore, be unsuited for limited roof areas.

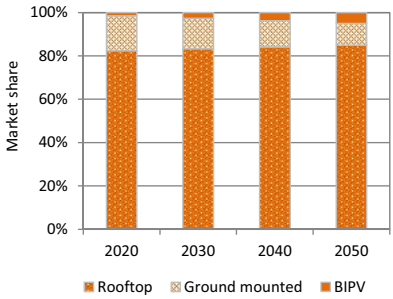

Figure 7-3: Market share development of PV plant types according to the conservative scenario

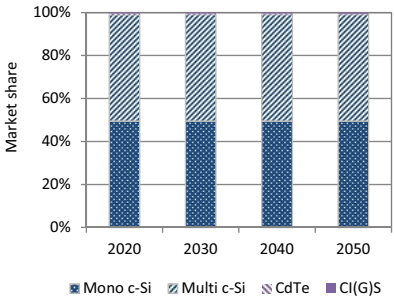

Figure 7-4: Market share development of PV modules according to the conservative scenario

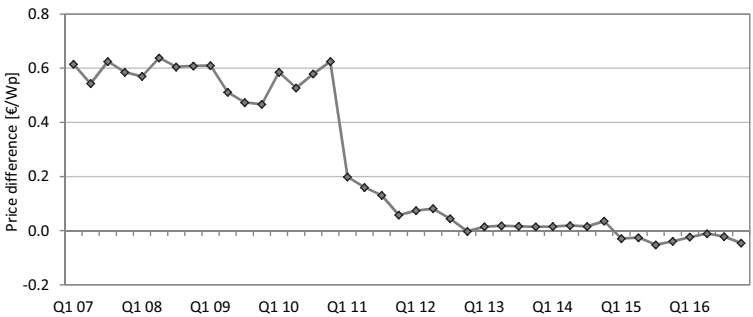

Figure 7-5: Difference between quarterly global average c-Si and thin-film module prices (PSE internal data 2018)

7.4.2 Alternative scenario

The thin-film scenario describes an overall trend toward large rooftop and ground-mounted plants, associated with a growing share of thin-film modules. It is assumed that the decreasing price of PV-plants motivates investors to install larger plants. Such a centralized energy system was already discernible in 2012 with a record 40 % share of ground-mounted plants. In this scenario, ground-mounted PV plants are assumed to reach this record value of 40% in 2050 again. The growing land-use competition, mentioned in the previous section, could be reduced through emerging PV-systems such as agro-photovoltaic plants (Rösch 2016) or even floating PV systems (Choi 2014). Another plausible argument for the increasing share of ground-mounted PV is the interest in manufacturing larger PV modules. Although larger PV modules are not a success story yet and are often associated

with the bankruptcy of "Applied Material" who was the pioneer of this idea, research on this idea has gained momentum in recent years. This is mainly due to the massive cost reduction that can be achieved by reducing the capital equipment expenditure (Horowitz et al. 2017). If this can be realized in the future, then the lower cost will be a further catalyst for ground-mounted PV plants. Therefore, the market share of ground-mounted plants is projected to reach 40 % in the alternative scenario. Rooftop plants are assumed to represent 55 % of the PV-plants in 2050 and remain as market leader, with growing installations of medium (10-100 kWp) and large (>100 kWp) sized rooftop plants such as industrial and commercial buildings. Similar to the conservative scenario, BIPV is assumed to have 5 % of market share in 2050.

As the efficiency of thin films will not surpass that of c-Si PV modules, thin film plants are more likely to be competitive only for large PV plants where land use is not an issue. Besides, the resurgence of thin films could also be enabled by a stronger drop in the module costs. The roadmaps of Viebahn et al. (2014) and Marscheider-Weidemann et al. (2016) assumed a 40 % market share of thin-film modules in 2050, which has been assessed as too ambitious by PV experts that were interviewed within the framework of this thesis. As a more reasonable estimate, thin film plants are assumed to reach 25 % market shares in 2050.

The further leadership of CdTe over CIGS in Germany remains unclear, as there are strong arguments for both technologies. CdTe and CIGS are quite similar in terms of module efficiency, with the highest recorded efficiencies of 18.6 % and 19.2 % respectively (Green et al. 2018). However, CdTe modules currently represent 60 % of all thin-film modules produced worldwide. Moreover, the replacement of cadmium, whose toxicity led to the growing unpopularity of CdTe, is currently an object of research (Marscheider-Weidemann et al. 2016) and there are plausible ways to successfully reduce a significant amount of cadmium in the modules. Besides that, another important argument for CdTe is the main manufacturer, the American company First Solar, who is the only thin-film manufacturer among the top-10 module suppliers globally in 2016. If First Solar remains a major player in the PV industry, CdTe would be expected to continue having significant market shares. Two main arguments can be put forward to support this hypothesis as follows:

- First Solar benefits from a mature manufacturing process. This is shown through the launching of its Series 6 of CdTe modules in Q2 2018, which offer better efficiency at a reduced cost.
- The partnership between First Solar and GE can further accelerate the development of thin-film modules in terms of increasing efficiency and increasing costs competitiveness.

CIGS modules on the other hand, only contain a fraction of the cadmium found in CdTe, specifically in the buffer layer, which can be easily replaced by other elements. The main manufacturer of CIGS modules is the Japanese Solar Frontier, which is reported to have a high potential to become a main player in the manufacturing market in the future. Furthermore, the German-based CIGS research and manufacturing company, Manz CIGS Technology GmbH, was

recently sold to Shanghai Electric and Shenhua, with the objective of building a single global leading research pole for the CIGS industry. This could further catalyst the development of the CIGS modules.

As a conclusion, CdTe and CIGS are both assumed to be well implemented on the market in 2050 in the thin-film scenario, with a slight advantage for CIGS due to the absence (see chapter 7.2) of toxic materials and the manufacturing in Germany via Manz which could cater for the local market. CdTe is therefore assumed to represent 40 % of the thin film modules in 2050, and CIGS 60 % of the thin film modules.

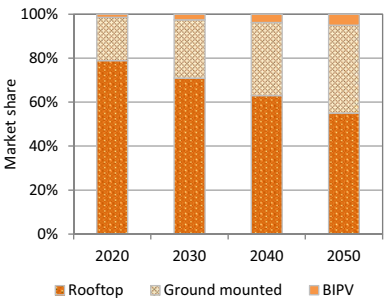

Figure 7-6: Market share development of PV plant types according to the thin-film scenario

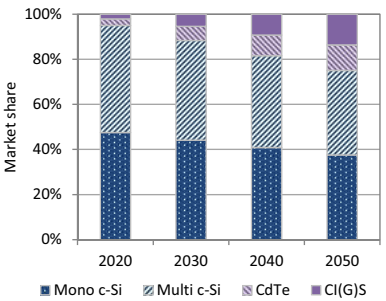

Figure 7-7: Market share development of PV modules according to the thin-film scenario

8 Batteries

In this chapter, the current status and the development of traction batteries in EVs and batteries in stationary applications in Germany are described. Stationary batteries are differentiated between home batteries and stand-alone battery power plants.

8.1 Home battery system

Home batteries are generally installed together with a PV rooftop system in order to increase the self-consumption rate of electricity in households. According to the annual monitoring report of PV home storage systems in Germany by (Figgener et al. 2018), every second installed PV rooftop plant in 2017 was installed together with a battery. Currently, there is a total installed battery power of 280 MW, with a storage capacity of approximately 600 MWh in Germany. This can be expected to increase in the future since the cost of PV home storage systems will be significantly lower in the future, which makes installing a battery together with a PV system very cost efficient according to the economic benefit that they can provide (Agora Energiewende 2013). Figure 8-1 shows the market shares of the type of newly installed batteries from 2013 until 2017. It can clearly be seen that the market shifted from Pb-acid to Li-Ion batteries, such that almost all of the newly installed batteries by the end of 2017 only consist of the latter type. The staggering dominance of Li-Ion batteries can be attributed mainly to the rapidly falling price and the high energy density that makes it possible to be compact and easy to be installed at homes.

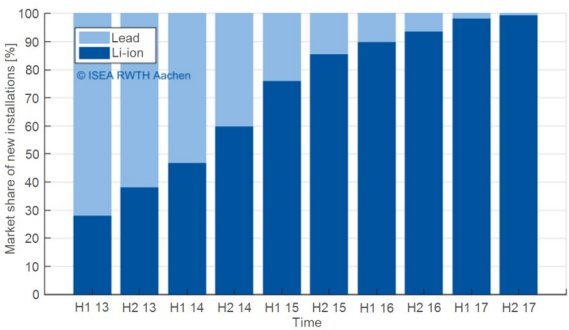

Figure 8-1: Market shares of the number of Pb-acid and Li-ion batteries in PV home battery systems in Germany. Figure translated into English from (Figgener et al. 2018)

8.2 Stationary battery power plants

The fundamental use of stationary battery power plants in Germany is to provide primary control for frequency regulation in the power grid (Stenzel et al. 2018). The fast reaction time of a battery to store and provide electricity in a very short time makes it a suitable technology to balance out the constant feed-in and off-take of electricity in the power grid. Apart from that, large battery systems are also used for the decentralized integration of renewables within a smart-grid system, for instance as district storages (Brautigam et al. 2018). Similar to home battery systems, the installation of stationary batteries has been growing significantly mainly due to the large penetration of intermittent renewable energy sources in the energy system. The development of the cumulative installed capacity of stationary storages in Germany is shown in Figure 8-2. 430 MW of battery power is currently installed, providing a capacity of slightly more than 550 MWh (Stenzel et al. 2018). By the end of 2017, almost 96 % of all stationary batteries consist of Li-ion batteries, with a small share of redox-flow, Na-S and lead-acid batteries.

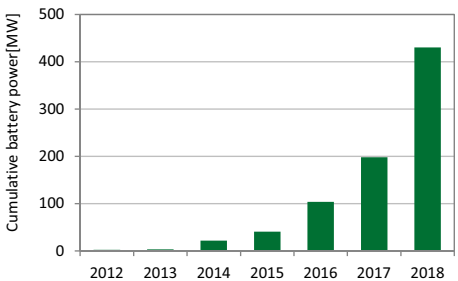

Figure 8-2: Cumulative installed capacity of stationary battery systems in Germany. Data from 2012 until 2017 is provided by the (DOE 2018). Missing year-of-commissioning in the dataset was assumed two years after the date of announcement. Data of 2018 is provided by (Stenzel et al. 2018) since the (DOE 2018) did not continue their data monitoring in 2018.

8.3 Batteries in electric vehicles

By the end of 2017, the share of EVs in Germany only amounted to less than 1 % of the total number of vehicles. The newly registered EVs in 2017 represent 3.2 % of the total vehicles registered in the same year. Some of the challenges that are faced by EVs, apart from the short millage due to limitations of the batteries, are the higher prices compared to conventional vehicles and lack of public charging infrastructures, which limits the travel distance unpreventably. For example, 4730 charging poles (12500 charging points), of which only 850 are fast charging poles, were publically available in 2017, which is extremely low compared to the 290000 of EVs currently in Germany. Nonetheless, EVs are expected to significantly expand in Germany due to three main reasons. First and foremost, EVs profit from the support of the German government via regulatory

incentives. The Electric Mobility Act was introduced in 2015 and defined some incentives and privileges for EVs. Furthermore, the government also pledged to invest € 1bn in order to provide subsidies to purchasers of EVs and to expand the charging infrastructure throughout the country (BMWi 2018). Secondly, the automobile industry in Germany is actively investing in EVs, that increasing number of models can be expected in the near future. For instance, VW and BMW have pledged 127 billion USD until 2025 in order to develop new EV models and expand production capacity (DW 2018). Thirdly, the prices of EVs are expected to drop considerably in the near future and become competitive with conventional vehicles. The main reason for the high price of EVs in the past has been the high price of Li-Ion batteries. For instance, BNEF (2018) reports that the average price of batteries for EVs in 2010 was around 1000 USD/kWh. Seven years later, the average price for batteries in EVs dropped to 209 USD/kWh. Additional improvements in energy density and cost reduction are expected to suppress the cost of EVs even further.

In order to accurately estimate the market share of the battery types in the German EV fleet the registration of vehicles provided by the Federal Motor Vehicle Transport Authority (known as the Kraftfahrt-Bundesamt (KBA) in German) is analysed in detail. Statistics collected on the number of EVs are shown in Figure 8-3. The differences between the types of EVs are as follows:

- Hybrid electric vehicles (HEV): The main power source of a HEV is the internal combustion engine (ICE), while a battery is used to complement the ICE. Therefore, batteries in a HEV have much smaller capacity compared to other types of EVs. The battery cannot be plugged in as it is purely charged by the regenerative braking.
- Plug-in hybrid electric vehicle (PHEV): The main power source of a PHEV is the battery-powered electric motor, while an ICE is used to complement the battery, especially when the battery is fully discharged or even in some cases when extra power is needed. The battery of a PHEV can be charged by regenerative braking as well as by plugging it in.
- Battery electric vehicle (BEV): A BEV is solely powered by the battery-powered electric motor without an ICE, which has to be charged by plugging it in.

With 70 % market share among EVs by the end of 2017, the German market is currently dominated by HEVs. Toyota Yaris, Toyota Auris, Honda Jazz and Lexus models are the highest selling HEVs which makes up to 75% market. As mentioned earlier, since batteries are only of secondary importance in HEVs, they do not need to have a high energy density or capacity but a high cycle life due to the extremely high frequency of charging and discharging is of utmost importance. NiMH batteries fulfil these requirements and hence have been the preferred choice of batteries for HEVs. On the contrary, BEVs and PHEVs only use Li-Ion batteries. Marscheider-Weidemann et al. (2016) and Glöser-Chahoud (2017) reported that the global market share for BEV and PHEV are similar, with NMC having the largest share followed by LMO, NCA and LFP. In order to estimate the market shares of the battery types in Germany, it is therefore assumed that NMC and LMO are also the market leaders in Germany regarding BEV and PHEV. Since LFP is currently only used by

Chinese EV manufacturers (Azevedo et al. 2018), it is completely removed from the market share in Germany. In terms of NCA, the only known model in Germany that utilized this technology is Tesla, specifically Model S and Model X, of which there are only 7500 units in total in Germany. The complete current market share of the battery types in the German EV fleet is illustrated in Figure 8-4.

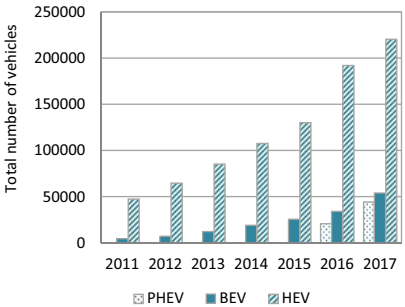

Figure 8-3: Total number of registered EVs in Germany from the beginning of 2012 until the beginning of 2018 (KfB 2018)

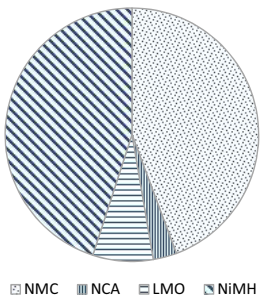

Figure 8-4: Market share of battery types in the German EV fleet in 2017

8.4 Material composition of batteries

The specific material demands of the batteries are presented in this chapter for the materials in the cell, housing (including wirings), and the battery management system. Since this thesis only analyses the demand for traction batteries, lead Pb-acid batteries for SLI purposes in EVs are not considered. Firstly, the specific material demands of the cathode in Li-Ion batteries according to various studies are listed in Table 8-3. The material composition relates to Li-Ion batteries that are currently available, which means that the NMC refers to the NMC111 concept whereas the NCA refers to the typical NCA batteries that utilize 80 % nickel, 15 % cobalt and 5 % aluminium. All anode materials are assumed to be graphite, which represents almost 90 % of the global market share of anodes in Li-Ion batteries (Pillot 2017). The cathode and anode in a battery cell are connected to aluminium and copper current collectors respectively. The specific demand of copper is 0.45 kg/kWh whereas the aluminium demand is 0.78 kg/kWh for the current collectors, both taken from the average values of the specific demand of collectors from Stahl et al. (2016). In terms of the electrolyte, Lithium-hexafluorophosphate ($LiPH_6$) is generally used in Li-ion batteries. Stahl et al. (2016) reported that 0.7 kg/kWh of electrolytes are used on average by Li-ion batteries, which corresponds to 0.03 kg/kWh of lithium.

The specific demands of all other investigated battery types are listed in Table 8-4. In terms of the specific nickel demand in NiMH, values vary between 40 kg/kWh (Angerer 2009) and 26.4 kg/kWh. In this thesis, the specific demand proposed by Mudgal et al. (2011) is applied, as this represents the life-cycle-inventory that considers each step in the manufacturing process. Correspondingly, the cobalt content is also chosen from Mudgal et al. (2011). For the specific demand of Vanadium in VRFB, the average values are used from the listed literature sources in Table 8-4. The specific lithium demand in Li-S and Li-Air are extremely scarce in the literature since these batteries are still under research. Gerssen-Gondelach and Faaij (2012) reported that both battery concepts contain 0.52 kg/kWh of lithium. However, these values were taken from Andersson and Råde (2001), who mentioned that the lithium demand of Li-Metal batteries, which includes Li-S and Li-air, can vary between 0.26 and 0.52 kg/kWh. Deng et al. (2017) conducted an LCA on a 61.8 kWh Li-S battery and found out that it contains 0.24 kg/kWh of lithium, which is close to the minimum value reported by Andersson and Råde (2001). Therefore, the lithium demands for post-Li-ion concepts are assumed to 0.24 kg/kWh since it is based on an actual life-cycle-inventory of a battery. An additional demand of 4 g/kWh of lithium is considered as the amount of lithium in the electrolyte of Li-Ion batteries (Deng et al. 2017). Apart from the cells, a battery also requires materials for its housing as well as casing and interconnections of the cells. These demands are listed in Table 8-1. For Li-ion batteries, the material demand may slightly vary in reality according to the cell types. However, for the estimation of the total material demand, this is simplified where the average specific demand of various Li-Ion cell types is applied.

Table 8-1: Specific material demand (kg/kWh) of the battery housing and wirings of Li-Ion, NiMH, Na-S and VRF batteries. Source: (Stahl et al. 2016)

	Fe	Al	Cu
Li-ion	2.9	0.3	0.3
Na-S	1.3	2.7	0.3
V-V	0.5	1.6	0.9
NiMH	16.7	-	-

Another important infrastructure in a battery system is the battery management system (BMS), which is important to ensure that the battery is functioning in a safe operating area. Some of the more specific functions of a BMS are controlling the charging current to prevent an overcharge, controlling the needs for cooling to prevent overheating and balancing the operation of various cells to maximize the capacity of the battery (Andrea 2010). The weight percentage of a BMS is dominated by aluminium, copper and steel, which is used for the housing and wiring (Stahl et al. 2016). Moreover, it also consists of electronic components such as integrated circuits and transistors. The specific material demand of BMS, as listed in Table 8-2, is used in this thesis as a proxy for the BMS for all types of batteries.

Table 8-2: Material composition of battery management system (BMS) for all types of batteries. Source: (Stahl et al. 2016)

Metal	Fe	Al	Sn	Cu	Au	Ni	Ag	Zn	Mn	Mo	Ta
g/battery	74.0	235.0	5.9	31.9	0.1	0.4	3.6	0.1	0.1	1.3	0.5

Table 8-3: Specific material demand [kg/kWh] of cathodes in Li-ion batteries according to various literature sources

Cell type	Metal	(Buchert et al. 2011)	(Kushnir 2015)	(Marscheider-Weidemann et al. 2016)	(Stahl et al. 2016)	(Glöser-Chahoud 2017)	(Pertti 2017)	(Olivetti et al. 2017)	(Månberger and Stenqvist 2018)	This thesis
NMC	Li	0.16	-	-	0.17	-	0.16	0.14	-	0.16
	Ni	0.45	-	0.29	0.45	-	-	0.39	-	0.40
	Co	0.45	-	0.59	0.45	0.40	0.36	0.39	-	0.44
	Mn	0.42	-	0.27	-	-	-	0.37	-	0.35
NCA	Li	0.14	-	-	0.14	-	0.16	0.11	-	0.14
	Ni	0.90	-	0.66	0.9	-	-	0.76	-	0.81
	Co	0.17	-	0.124	0.17	0.17	0.22	0.14	-	0.17
	Al	0.03	-	-	0.03	-	-	-	-	0.03
LMO	Li	-	0.12	-	-	-	-	-	-	0.12
	Mn	-	0.96	0.61	-	-	-	-	-	0.79
	Co	-	-	-	-	0.07	-	-	-	0.07
LFP	Li	0.11	-	-	0.12	-	0.16	-	0.17	0.14
	Fe	0.86	-	-	0.86	-	-	-	-	0.86

Table 8-4: Specific demand [kg/kWh] of active materials in various battery types according to different literature sources

Cell type	Metal	(Angerer 2009)	(Mudgal et al. 2011)	(Marscheider-Weidemann et al. 2016)	(Stahl et al. 2016)	(Viebahn et al. 2014)	(Gerssen-Gondelach and Faaij 2012)	(Deng 2015)	This thesis
NiMH	Ni	40.00	26.40	-	-	-	-	-	26.4
	Co	2.40	0.61	-	-	-	-	-	0.61
VRF	V	-	-	2.92	4.87	3.14	-	-	3.64
Na-S	Na	-	-	-	1.07	-	-	-	1.07
Li-S	Li	-	-	-	-	-	0.52	0.24	0.24
Li-air	Li	-	-	-	-	-	0.52	-	0.24

8.5 Material efficiency measures in batteries

Explicit material efficiency measures in terms of specific types of batteries are not available in the literature to the best knowledge of the author. The reason for this is that batteries such as Li-ion and VRFB are relatively young, where the priorities in research lie elsewhere. Majority of the current research involving batteries is primarily focused on increasing the performance and safety of the batteries while reducing the specific costs. Nonetheless, focusing on these fields can indirectly reduce specific material demands. As an example, there are several types of "next generation" NMC cathode compositions currently being actively researched and developed. Some of the more prominent ones are the NMC 622 and NMC 811[9], which have superior energy density compared to the usual NMC 111. As can be seen from the specific material demand of both former concepts in Table 8-5, more advanced NMC cell concepts reduce the specific demand for lithium, manganese and cobalt but at the expense of nickel. The drive to increase the nickel share in the NMC battery is motivated by the potential to increase the battery capacity and energy density (Manthiram 2017). In addition to that, it reduces the total cost since cobalt is the most expensive metal in that composition. However, increasing the nickel content deteriorates the thermal stability of the battery, which is otherwise provided by manganese and cobalt (Bak et al. 2014). In this thesis, it is assumed that this challenge will eventually be overcome, based on promising research developments (see (Dixit et al. 2017; Visser and Gao 2018)). The expected market shares of the advanced NMC cell concepts derived based on a projection by IEA (2018b) are shown in Figure 8-5.

Table 8-5: Specific material composition [kg/kWh] of various NMC cathodes. The values for NMC 111 are obtained from Table 8-3 whereas the rest of the material compositions is obtained from Olivetti et al. (2017)

	Li	Mn	Ni	Co
NMC 111	0.16	0.35	0.40	0.44
NMC 622	0.13	0.20	0.64	0.21
NMC 811	0.11	0.09	0.75	0.09

In terms of developments in NCA, the progress is mainly driven by Tesla. According to several reports, the latest NCA batteries of Tesla already requires less cobalt compared to the NMC 811 batteries. In addition to that, the CEO of Tesla, Elon Musk, mentioned that Tesla aims to completely remove the cobalt content from their batteries by 2019. However, since there are no scientific evidence at the time of the completion of this thesis to support these statements, complete removal of cobalt from the NCA batteries is not considered. Nonetheless, the cobalt content is assumed to decrease down to the content of a NMC 811 by 2020.

[9] The digits represent the composition of nickel, manganese and cobalt respectively. For example, a NMC 811 means that the cathode consists of 80% of nickel, 10% of manganese and 10% of cobalt.

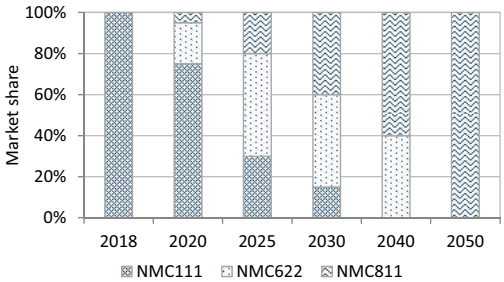

Figure 8-5: Projected market share of NMC cell concepts in Germany

Further reduction of specific material demand will come as a result of the increasing energy density of the batteries. A new cell concept that can contribute to significantly higher energy density is the use of alloy materials as anodes in Li-Ion batteries. Among alloy metals such as germanium, tin and antimony that are considered suitable, silicon stands out to be the most promising candidate (Goriparti et al. 2014). Compared to graphite, which has a theoretical gravimetric capacity of 372 mAh/g, silicon's capacity is approximately 4200 mAh/g (Casimir et al. 2016). However, the biggest drawback of silicon is the extreme expansion (~400% of original volume) of silicon during the charge and discharge process, which eventually causes cracks and degradation in the electrode, unstable SEI and loss of contact with the charge collectors. Ultimately, this lowers the cycle life of the battery and fades the capacity considerably. One of the propositions to mitigate this problem is to use the mixture of silicon and graphite (Si/C anodes) as opposed to pure silicon anode. Besides that, the use of novel structures such as thin-films (Tocoglu et al. 2013) or nanotubes (Wen et al. 2013) can support and distribute the stress resulting from the expansion during the charge and discharge process (Liao et al. 2018). Jin et al. (2017) provide a comparison of these measures in improving the capacity and cycle life of the batteries. Although there is currently no best solution that can overcome all the problems faced by silicon-based anodes, positive progress has been made in the past and further intensive research can lead to the successful commercialization of silicon-based Li-Ion batteries that can reach energy density over 400 Wh/kg (Placke and Winter 2018).

Besides that, post-Li-ion batteries also contribute to the reduction of metal demands by removing the needs for nickel and cobalt as well as having superior energy density. However, while this might be true for Li-S batteries, Li-Air batteries might contain some traces of critical metals still. As mentioned in chapter 2.3.3, the formation of lithium peroxides in Li-Air batteries reduces the performance by covering the active reaction surface of the electrodes. In order to combat this, certain elements are introduced to the anode as catalysts, which also improves the cycle life additionally (Kraytsberg and Ein-Eli 2011). Several metals have been discussed as a possible catalyst for Li-Air batteries, such as tin, platinum group elements (PGE), gold (Mei et al. 2016; Lu et al. 2011) or even the combination of nickel, cobalt and manganese (Ates et al. 2016). Since a single

solution is not available, it is too early to assume which catalyst will be the most effective and economical when Li-Air is commercialized. Due to this uncertainty, no metals for catalyst are considered in this thesis.

Considering all aspects, the material efficiency measure is considered to be directly proportional to the improvements in energy density that can be achieved by the batteries. In this thesis, different rates of reduction are considered for the battery types, derived based on their potential to increase their respective energy density, as opposed to Månberger and Stenqvist (2018), who assumed a flat rate for all technologies. In this thesis, 1.5 % of reduction in specific material demand per annum is assumed for Li-Ion batteries. This corresponds to the average energy density of NMC and NCA batteries in the German market in 2050 reaching between 320 and 250 Wh/kg and over 400 Wh/kg respectively. This can be made possible by the combined use of graphite and silicon in the anode, assuming that the technical challenges can be overcome. Na-S and VRFB are assumed to experience 1.5 % and 3 % reduction of material intensity, which corresponds to the average battery energy density reaching up to 200 and 100 Wh/kg respectively, as mentioned by Stenzel et al. (2015). As for Li-S battery, the energy density is assumed to increase from 250 to around 480 Wh/kg, which corresponds to 2 %/a reduction in material intensity. Last but not least, Li-Air batteries, which reportedly have the highest potential in terms of energy density among other batteries, are assumed to undergo 3 % of reduction specific material demand. This is in line with the assumption that the energy density will reach approximately 1100 Wh/kg in 2050, which might seem very conservative compared to the reported maximum achievable energy density of around 5000 Wh/kg. Nonetheless, the energy densities assumed in this thesis represent the average market values. This means that while much higher values can be implemented by 2050, its application may be very limited in certain fields of application such as cross-continental trucks. Nonetheless, a sensitivity analysis is conducted to investigate the impact of the rate of reduction on the total demand in chapter 9.5.3.

8.6 Further development scenarios of the battery market

Similar to PV and wind turbines, two development scenarios are proposed for batteries in stationary and EVs applications. However, before deriving the possible development of the battery types in the future, it is important to understand the battery requirements for different applications. For EVs, the maximum driving range is the most vital factor, which can be improved by increasing the energy density of the batteries. Therefore, batteries for EVs are limited to high energy density batteries such as Li-Ion, Li-S and Li-Air. For stationary applications, the energy density is not as important as the cycle life, as a grid-connected or PV home battery will be charged and discharged at a high frequency due to the intermittency of the electricity generation. In this case, the cycle life is a more important factor to be addressed.

8.6.1 Stationary applications

The starting point in deriving the development of Li-Ion batteries in stationary applications is the current market shares for PV home battery systems in Germany. Table 8-6 lists the top battery types and their respective providers whereas the market share of the battery types is illustrated in Figure 8-6. The German market is currently dominated by LFP, followed by NMC and NCA batteries. In terms of the manufacturers of NCA batteries for stationary purposes, SENEC is currently the only manufacturer who applies this technology in their "SENEC.Home V2.1" systems. Although Tesla is known for their use of NCA batteries for their electric cars, the Tesla Powerwall storage units consist of NMC batteries.

Due to the lack of market players, it is assumed that NCA batteries will completely phase out in stationary applications by 2030, where the market will converge towards LFP and NMC. A further convergence towards a single battery type is not expected since both batteries have strong arguments to be implemented in the future. While LFP has superior cycle life and is the safer option among both batteries, NMC is cheaper (Patry et al. 2015) and has a higher energy density. The price of LFP is expected to sink in the future due to the learning effects thanks to the planned gigafactories by CATL and BYD, two of the leading LFP battery manufacturer in the world. With BYD already present in the German market, their share is expected to grow in the future if they can offer their product at a much-reduced price. Besides that, independent of the production capacity, there are currently more German manufacturers for LFP batteries than NMC, who could cater to the local needs more effectively and remain competitive, given that their products can also be offered at low prices. Therefore, while both batteries are expected to stay in the German market, LFP is expected to have a higher market share than NMC. The complete market shares are shown in Figure 8-7 and Figure 8-8.

Table 8-6: Market shares of the top battery providers in the German PV home storage market (EuPD Research 2018)

Rank	Manufacturer	Country	Battery type
1	Sonnen	Germany	LFP
2	LG Chem	S. Korea	NMC
3	E3/DC	Germany	NMC
4	SENEC	Germany	NCA
5	Solarwatt	Germany	NMC
6	Varta	Germany	LFP
7	Daimler	Germany	NMC
8	BYD	China	LFP

Figure 8-6: Market shares of the battery types in the German PV home storage system

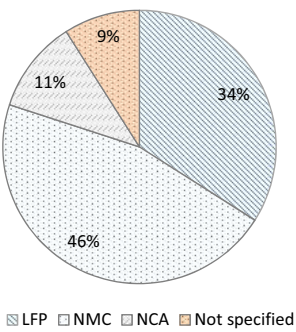

8.6.1.1 Conservative

The basic principle of the conservative scenario is that the future market for stationary batteries will be dominated by posts Li-Ion batteries. All technical challenges in developing the advanced batteries are expected to be timely solved. Although high energy density is not an important requirement for stationary batteries, the decreasing cost of Li-Ion batteries and the compact construction make them the primary choice for stationary batteries in the future. In addition to that, the requirement for high cycle life to match that of high-temperature and flow batteries is assumed to be fulfilled by the breakthrough of Li-S, Li-air as well as solid-state concepts. The market entry for Li-S battery is expected in 2025, as proposed by Thielmann et al. (2015a) and Tomboy (2018), and is assumed to reach up to 10 % of all installed batteries in 2030. Thielmann et al. (2015a) also mention that Li-S will be fully capable to take over the role of Na-S and VRF batteries as mid-range storages, which further justifies the low need for high-temperature and redox flow batteries in this scenario. Therefore, both latter batteries are expected to phase out completely by 2025. Li-Air batteries are expected to enter the market in 2030 (Thielmann et al. 2015a; Pillot 2017; IEA 2018b; Tomboy 2018) and is assumed to take up to 50 % of the stationary battery demand in 2050. Part of the Li-air and Li-S will be in all-solid-state form, which enables the batteries to be built very compact and will be highly suitable for PV home storage systems. Advanced Li-Ion batteries are expected to still remain in 2050 at a significantly reduced market share and are expected to phase out beyond 2050.

8.6.1.2 Alternative

In the alternative-scenario, it is assumed that the technical problems faced by the Li-S and Li-Air batteries will not be solved, hindering a timely commercialization. Instead, the market will be dominated by non-Li-ion batteries. This represents the extreme scenario in order to assess the maximum demand for vanadium as well as the minimum amount of metals related to Li-ion batteries. The maximum demand for vanadium has been previously estimated by Viebahn et al. (2014), in which the authors assumed a complete market share of VRF batteries. This is an exaggerated estimation since a complete market capitalization by VRF is highly unlikely. Firstly, they can never be used for PV home storage system due to the high requirement for area of installation. Li-Ion batteries are expected to be solely used for this purpose due to their compact nature and easy installation. Secondly, VRF will have to compete with the Na-S battery for market shares in applications as stand-alone battery power plants. Both batteries have high cycle numbers and are suitable for grid-connected applications. VRF batteries are slightly more advanced in terms of R&D and are expected to be fully commercialized by 2025 whereas Na-S is not expected to experience a significant market uptake until 2035. Nonetheless, Na-S is projected to have energy density between 200-250 Wh/kg and a cost of production of around 80 €/kWh by 2050, which will be a major catalyst in opting for Na-S batteries (Stenzel et al. 2015). Furthermore, Na-S does not contain any critical metals, which makes securing raw materials for Na-S less challenging than VRF batteries.

Nonetheless, VRF batteries can be scaled much easier without having to increase the price linearly (DOE 2013). Furthermore, VRF batteries have the advantage of easy recyclability, such that most of the components can be dismantled and used in a new battery with minimal effort. Although the energy density of VRF cannot match that of Na-S in the future, advanced concepts such as V-Air can reach up to 100 Wh/kg of energy density with much superior cycle life than Na-S (Stenzel et al. 2015). Due to these reasons, the market share of non-Li-Ion batteries is expected to be shared by Na-S and VRF batteries, with a slight advantage to the latter battery due to faster commercialization and more cost-effective scalability.

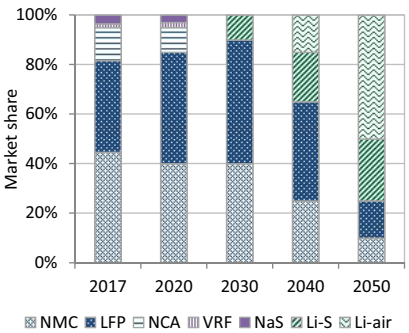

Figure 8-7: Market shares of the installed capacity of stationary batteries in the conservative scenario

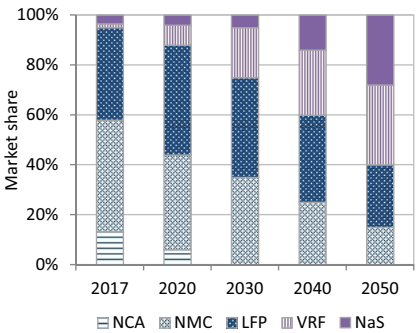

Figure 8-8: Market shares of the installed capacity of stationary batteries in the alternative scenario

8.6.2 Batteries in electric vehicles

Regarding the future market shares of EVs, HEV is expected to lose market shares and inevitably disappear completely by 2030 (Thielmann et al. 2015b; Tomboy 2018). This is also in line with the government incentives mentioned in chapter 8.3, which are only valid for BEV and PHEV, thus making them more competitive in the future. Until then, the NiMH batteries in BEV will also be partially substituted with Li-ion batteries mainly due to economic reasons (Opitz et al. 2017; Michaelis et al. 2016).

Although NCA has the highest energy density among present Li-ion batteries, it is mainly used by Tesla, while most of the other manufacturers use NMC batteries. The reason as to why NMC is preferred by most of the manufacturers is detailed by Zubi et al. (2018), who mentioned that the longer lifespan of the NMC brings more advantages than the weight that can be saved by NCA through its higher energy density. Faster charging time, contributed by the higher power density, is another advantage of NMC over NCA. The strategy of Tesla to create EVs with extended driving

mileage leaves them no choice but to use the NCA batteries. Due to this, Tesla's EVs have a maximum mileage of more than 400 km, but they also have the heaviest batteries among their competitors. The maximum driving range of EVs from other manufacturers is generally less than 200 km. Therefore, it is assumed that NMC will continue to be the preferred candidate of Li-ion batteries, while NCA will only have a small market share in the future in Germany.

Until recently, NMC has been used together with LMO as a hybrid solution to profit from the advantages of both batteries. However, this has changed as manufacturers are only using NMC to prevent any additional weight from the relatively lower energy density LMO battery (Timofeeva 2017). Mitsubishi i-Miev, Renault Zoe and Fiat 500 are some of the examples of models that have opted only for NMC batteries, having previously utilized the hybrid solution (Lluc and Beatriz 2015). As a result, LMO is not expected to be applied in future EVs. In terms of LFP batteries, it is currently solely used in China, particularly in the E6 models of BYD. Although BYD has one of the biggest market shares in China, it does not have any significant market in the rest of the world in terms of EVs. Therefore, no future market entry is assumed for LFP.

8.6.2.1 Conservative scenario

The conservative scenario differs from the alternative scenario by the use of Li-S and Li-Air batteries. Both batteries are expected to overcome the technical and economic challenges and will be introduced to the market in the near future. Similar to the market shares discussed in chapter 8.6.1.1 based on the projections of (Pillot 2017; Tomboy 2018; Azevedo et al. 2018; IEA 2018b, 2018a), Li-S is expected to be commercialized by 2025, while the commercialization of Li-Air batteries will happen in 2030. Furthermore, all-solid-state batteries, which can be materialized latest by 2030 (Thielmann et al. 2015b), will further magnify the superiority of post-Li-Ion batteries, causing Li-Ion batteries to be completely obsolete for EVs by 2050. NCA is expected to phase out much faster than the NMC since Tesla is expected to adopt the Li-S or Li-Air batteries if they are proven successful.

8.6.2.2 Alternative scenario

In the alternative scenario, the technical problems faced by Li-S and Li-air batteries are assumed to remain until 2050 and the market requirements will be fulfilled by Li-ion batteries. Although this is highly unlikely, this scenario serves as the extreme scenario in order to identify the maximum cobalt and nickel demand if a technological breakthrough in batteries does not materialize. The market will continue to be dominated by NMC batteries. NCA is not expected to phase out in the German market, as it is assumed that Tesla will have the staying power in the German market as a provider of long-range EVs. Reports such as (Bloomberg 2018b; Clean Technica 2018) show that Tesla's

model 3 is outselling every other small and midsize luxury cars, including Audi, BMW and Mercedes and is even nearing the sales of bestselling conventional cars of Toyota and Honda in the US. The success of Tesla's Model 3 in the US is assumed to be transferred to Europe as well, when the expansion of Tesla's Model 3 to Europe takes place in 2019. In addition, Tesla aims to bring down battery prices to less than 100 USD/kWh by 2021 (Bloomberg 2018a). In comparison, (Pillot 2017) estimated that NMC cell-price will reduce from 380 USD /kWh to 150 USD /kWh in 2025 whereas pack cost will reduce from 370 to 210 $/kWh. However, since the production capacity of Tesla is very limited and is the only major manufacturer that applies this technology, the market share of NCA batteries is assumed to remain only at 15 %.

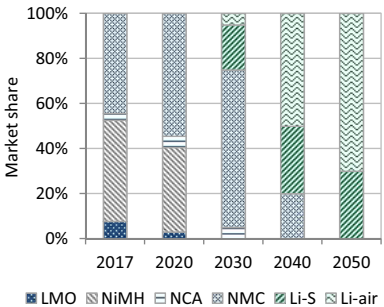

Figure 8-9: Market shares of the installed capacity of batteries for EVs in the conservative scenario

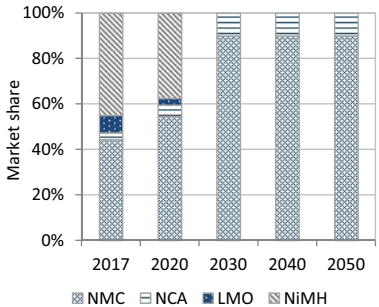

Figure 8-10: Market shares of the installed capacity of batteries for EVs in the alternative scenario

9 Results

9.1 Primary metal demand

The cumulative material demands from 2020 to 2050 resulting from the deployment of PV, wind turbines and batteries in Germany according to all investigated energy pathways and scenarios are listed in Table 9-1. Generally, the material demand correlates with their respective market shares and installed capacities of each energy pathway. In terms of PV and wind turbines, the highest metal demand is obtained for the transformation pathway whereas the long-term pathway requires the least amount. For batteries, the climate protection pathway has the highest demand for most of the metals.

Breaking down the metal demand of each technology in detail, the biggest demand in PV is contributed by the metals found in the mounting structure and module frames, namely steel and aluminium. In contrast, the metals found in the power electronics, such as gold, titanium and platinum require the least amount. The difference between demands for the conservative and the alternative scenario is smaller within the cell metals of c-Si modules as opposed to the cell metals within thin-film modules. For instance, in the transformation pathway, the silver demand in the alternative scenario is 12 % lower than the conservative scenario. However, the former scenario sees the requirement of indium to be 12 times more than the latter scenario. This inconsistency is owed to the assumed market shares in the scenarios and the skewed pattern of the installed capacity. The market share of c-Si modules in the alternative scenario reduces gradually from 99 % as of 2017 to 45 % in 2050. However, the annual installed capacity is on average much higher from 2035 onwards compared to the year before that. As the material efficiency increases each year and is much greater in the later years, the higher installed capacity beyond 2035 suppresses the difference between the metal demands in the cell metals of c-Si modules in both conservative and alternative scenario.

In terms of wind turbines, steel is the most intensively required metal followed by copper and alloying elements such as chromium, manganese and nickel. The conservative-scenarios generally require the lesser material amount. However, there is an exception in terms of copper, where the demand is higher in the conservative scenario in all pathways. This is due to the fact that the conservative scenario is characterized by the intensive use of EESG-DD drive train, which is bound to a nacelle containing at least twice more copper than other systems in the form of generator windings. This leads to an overall high demand for copper in the conservative scenarios. Another result that stands out is the higher demand for dysprosium and neodymium in the conservative-climate protection scenario than the demand in the conservative-transformation scenario. Although the total installed capacity is lower in the climate protection scenario, it has the higher installed

capacity of offshore turbines, where the deployment of turbines with PM is the most intensive. However, this effect is not seen in the alternative scenario. This can be explained by the shift in the market towards drive train systems with PMs in the alternative scenarios. Since turbines with PMs will also be widely installed on shore in the alternative scenario, the demand for REEs increases with respect with the total installed capacity, which causes the transformation scenario to have the highest demand for REEs.

Last but not least, steel, aluminium and copper are the most intensively required metals in batteries, which is a result of the demand for battery housing and wirings. In terms of the active metals, nickel has the highest demand, followed by lithium and cobalt. In general, the alternative scenario has a higher demand compared to the conservative scenario in all energy scenarios. This is owed to the assumption that Li-S and Li-Air will be successfully implemented in the conservative scenario and their potential of high energy density can be taken advantage of, thus reducing the specific metal demand drastically. In terms of the vanadium demand from the VRF batteries, the demand in the conservative scenario is the highest since they are assumed to phase out once Li-S and Li-Air batteries are commercialized.

Table 9-1: Overview of the cumulative demand of all selected investigated metals in PV, wind turbines and batteries for stationary application and in EVs in Germany for all energy pathways from 2020 until 2050. Con and Alt represent the conservative and alternative scenarios respectively. Bulk metals such as steel, aluminium and copper are generally the most required metals in all technologies. On the contrary, the metal requirements of power electronics, such as palladium, platinum and titanium are the least. The demands of rest of the investigated metals are listed in Table 15-2 in the Appendix.

		Photovoltaic						Wind turbine						Batteries					
		Long-term		Climate protection		Transformation		Long-term		Climate protection		Transformation		Long-term		Climate protection		Transformation	
Metal	Unit	Con	Alt	Con	Alt	Con	Alt	Con	Alt	Con	Alt	Con	Alt	Con	Alt	Con	Alt	Con	Alt
Ag	t	1048	913	1873	1633	2379	2075	0.3	0.4	0.5	0.6	0.9	1.2	213	213	219	219	231	226
Al	kt	537	552	960	987	1217	1252	205	256	327	373	553	709	666	648	734	714	707	709
Cd	t	22	280	40	505	50	638	0	0	0	0	0	0	0	0	0	0	0	0
Co	kg	60	60	107	107	132	132	152	211	221	289	423	604	39	109	42	119	57	118
Cr	kt	12	13	22	23	27	29	454	528	712	763	1255	1488	0	0	0	0	0	0
Cu	kt	76	117	136	210	170	258	743	629	1202	979	2222	1818	465	450	512	496	497	475
Dy	t	0	0	0	0	0	0	336	627	621	987	589	1440	0	0	0	0	0	0
Ga	t	3	46	6	83	7	101	0	0	0	0	0	0	0	0	0	0	0	0
In	t	30	374	53	679	66	854	0	0	0	0	0	0	0	0	0	0	0	0
Li	kt	0	0	0	0	0	0	0	0	0	0	0	0	146	110	161	121	150	113
Mn	kt	2	4	3	7	4	9	467	563	796	901	1111	1400	34	92	37	101	49	99
Nd	t	0	0	0	0	0	0	4252	7855	7825	12388	7428	18093	0	0	0	0	0	0
Ni	kt	6	6	10	11	13	13	202	235	317	340	560	664	175	593	195	662	246	604
Pd	kg	25	25	44	44	55	55	64	88	92	120	176	252	0	0	0	0	0	0
Pt	kg	3	3	5	5	6	6	7	9	10	12	18	26	0	0	0	0	0	0
Se	t	30	438	53	787	66	961	0	0	0	0	0	0	0	0	0	0	0	0
Sn	t	3312	3347	5937	5999	7388	7501	1302	1799	1886	2467	3610	5156	349	349	359	359	379	370
St	kt	156	292	280	524	350	641	34779	41663	57721	65236	85005	105868	1941	1887	2118	2058	2280	2189
Te	t	2	27	3	49	4	59	0	0	0	0	0	0	0	0	0	0	0	0
Va	kt	0	0	0	0	0	0	0	0	0	0	0	0	0	0	0	0	0.3	36

9.2 Bottleneck analysis

Figure 9-1 shows the range of demand-to-reserve ratio of the metals related to PV systems according to the static (D/R ratio) and the dynamic approach (D/R_{base}). The top and bottom of the range represent the scenarios with the maximum and minimum demand respectively. The maximum demand is obtained in the transformation scenario whereas the long-term scenario provides the minimum demand, which corresponds to the proposed installed capacity in the scenarios. These limits can be further differentiated between the conservative and alternative scenarios. Results indicate that indium is the most critical metal with a D/R ratio between 0.17 % and 3.76 %, which way exceeds the maximum allocation limit of 0.1 %. Similarly, the range of silver also completely exceeds the allocation limit for PV. Since the minimum criticality limits of both metals exceed the maximum allocation limit, even the low installed capacity proposed by the long-term scenario is unable to prevent a supply risk. Metals such as selenium, tellurium and tin are only partially critical as the lower limit, provided by the long-term conservative scenario, is well below the PV allocation limit. Other metals in solar cells, such as nickel and gallium, as well as metals from the BOS and electronics, do not face any supply bottlenecks. In the dynamic approach, the maximum criticality of indium can be reduced significantly down to a D/R_{base} of 1.9, which however, still exceeds the maximum limit for Germany. Similarly, the bottleneck risks of selenium and silver also could not be completely mitigated. Only tin is completely risk-free considering the reserve base whereas tellurium only barely exceeds the upper limit of the allocation limit.

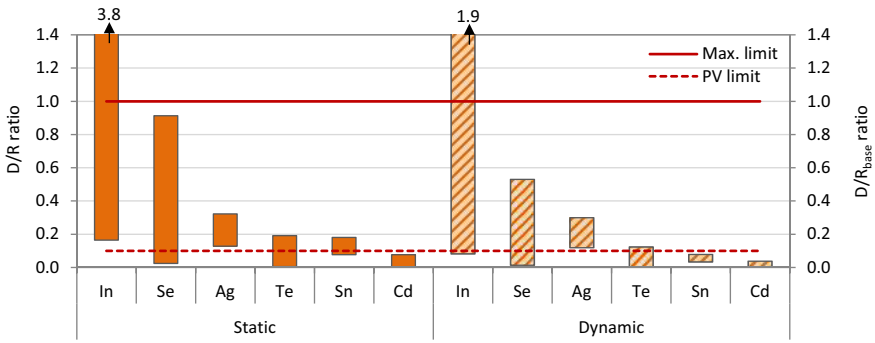

Figure 9-1: Demand-to-reserve ratio for the cumulative demand of selected metals in PV for all energy pathways and scenarios between 2020 and 2050. 'Max. Limit' represents the maximum allocation limit for Germany whereas 'PV limit' represented the maximum allocation for PV modules in Germany. In the static approach, the reserve levels of 2017 are used whereas in the dynamic approach, the reserve base levels are used to obtain the ratios.

Regarding wind turbines, the requirements of 5 particular metals exceed the allocated budget of static geological reserves, in either all or some of the scenarios. The advanced-transformation

scenario, based on the assumption of significantly larger turbines in the future, presents the highest risk among these metals, with the requirements for nickel reaching more than 7 times of the allocated budget. In the dynamic approach, the supply needs of manganese and antimony lie beneath the allocated budget, with the demand of nickel, copper and dysprosium still remaining higher than the allocation limit. Despite posing the greatest risk, it should be mentioned that nickel is predominantly used as an alloying element and does not contribute directly to the functionality of a wind turbine. Since the high risk of nickel is as a consequent of high steel demand, the usage of nickel can be reduced by increasing the share of concrete towers and the share of steel lattice towers. Furthermore, increasing the deployment of floating, jacket and tripod foundations in offshore turbines will also help in reducing nickel demand, as these measures are able to reduce the steel demand drastically. Substituting the currently used stainless steel to ferrite grade stainless steel, which requires significantly lesser nickel, is also possible when fabricated and applied accordingly. On the contrary, the high demand of copper and dysprosium is more alarming since these metals are fundamental to the functionality of a wind turbine, with one being the alternative for the other, in terms of generators with copper windings or with PM.

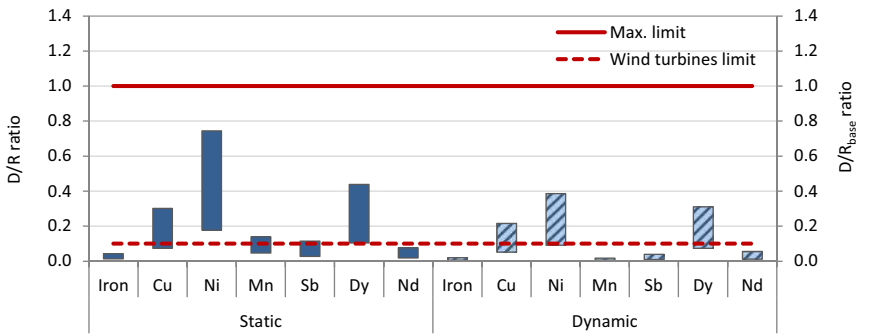

Figure 9-2: Demand-to-reserve ratio for the cumulative demand of selected metals in wind turbines for all energy pathways and scenarios between 2020 and 2050. 'Max. Limit' represents the maximum allocation limit for Germany whereas 'Wind turbines limit' represents the maximum allocation for wind turbines. In the static approach, the reserve levels of 2017 are used whereas in the dynamic approach, the reserve base levels are used to obtain the ratios.

Figure 9-3 shows the demand-to-reserve ratio of active metals for batteries in Germany. The total material demand for stationary storages was added to the demand for EVs in the transformation scenario to obtain the total material demand that is used in this analysis. Based on the results of the static approach, cobalt is the most critical metal since the maximum demand exceeds the allocation limit. This is given by all energy scenarios according to the alternative scenario. While the demands of lithium and nickel lie beneath the maximum allocation limit for Germany, they still exceed the allocation limit for batteries. The illustrated demand range for vanadium is only provided by the

transformation scenario since no stationary storages are proposed by the long-term and climate protection pathways. According to the alternative-transformation scenario, the maximum demand exceeds the allocation limit for batteries. While the demand-to-reserve ratios can be reduced in the dynamic approach, the demands for lithium and cobalt still remain critical, while the least nickel demand lies slightly below the allocation limit for batteries.

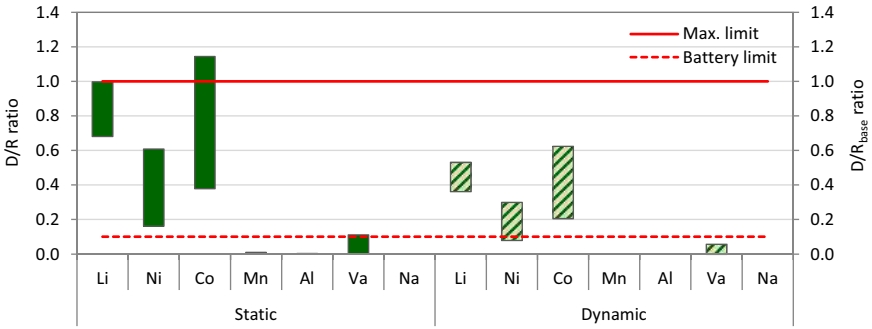

Figure 9-3: Demand-to-reserve ratio for the cumulative demand of selected metals in batteries for all development and energy scenarios between 2020 and 2050. 'Max. limit' represents the maximum allocation limit for Germany whereas 'Battery limit' represented the maximum allocation for batteries in stationary applications and electric vehicles in Germany. In the static approach, the reserve levels of 2017 are used whereas in the dynamic approach, the reserve base levels are used to obtain the ratios.

9.3 Production constraints

The demand-to-production (D/P) ratio is used to investigate whether the annual demands can be met by the current levels of production. The D/P ratios according to the maximum annual demand of all critical metals for all technologies are listed in Table 9-2. In terms of PV, the maximum demand occurs around 2040 when the installed capacity peaks to compensate for the large decommissioned capacity. Alarmingly, some of the critical metals include aluminium and tin, which are bulk metals that are produced in a large amount globally. Looking at the results in detail, indium, gallium and selenium are the most critical metals in all alternative scenarios as they exceed the maximum allocation limit for Germany. In the conservative scenario, indium and silver are the most critical metals. While the maximum demand of gallium, selenium, cadmium and tellurium exceed the limit in the long-term and climate protection alternative scenarios, a conservative development of PV will completely mitigate bottlenecks of these metals. Both of these pathways also do not display any risks in terms of aluminium.

Regarding wind turbines, dysprosium and neodymium are by far the most critical metals, with demands way exceeding the maximum allocation for Germany in all scenarios and pathways. In the

previous chapter, it was mentioned that the high D/R ratio of nickel is not considered problematic since it is not fundamental to the functionality of a wind turbine and that the demand can be reduced once the application of steel is scaled down. The results given in Table 9-2 accentuate the need to reduce the use of steel and its alloying elements since their demands exceed the allocation limit for wind turbines in Germany. Similar criticality is also exhibited by copper. For batteries, a severe production constraint will most likely occur in lithium if the current production level is maintained since the maximum D/P ratio ranges between 12.9 and 22.5 across all scenarios. The maximum demand for cobalt also exceeds the maximum allocation limit for Germany. Another metal that is expected to face production constraints is vanadium. However, in the conservative scenario where the use of VRF batteries is limited, the bottleneck risk is fairly low.

Table 9-2: D/P ratios of the maximum annual demand for each metal in all energy pathways and scenarios

	Metal	Transformation		Long-term		Climate protection	
		Alternative	Conservative	Alternative	Conservative	Alternative	Conservative
PV	In	8.91	0.58	4.21	0.3	4.95	0.31
	Ag	0.42	0.48	0.23	0.27	0.27	0.32
	Sn	0.23	0.24	0.12	0.12	0.14	0.14
	Al	0.12	0.11	0.07	0.06	0.08	0.08
	Ga	2.72	0.14	1.19	0.07	1.49	0.09
	Se	2.48	0.13	1.08	0.07	1.36	0.08
	Si	0.14	0.17	0.08	0.09	0.09	0.11
	Cd	0.21	0.01	0.10	0.01	0.12	0.01
	Te	1.18	0.06	0.52	0.03	0.64	0.04
Wind turbines	Cu	0.43	0.49	0.19	0.21	0.20	0.24
	Cr	0.19	0.15	0.08	0.07	0.08	0.08
	Fe	0.24	0.17	0.11	0.08	0.12	0.10
	Ni	1.29	1.00	0.57	0.48	0.56	0.50
	Nd	5.22	2.17	2.70	1.27	3.01	1.80
	Dy	20.30	8.58	9.94	4.69	11.20	6.67
Batteries	Li	12.86	16.03	14.60	20.07	16.36	22.49
	Ni	0.86	0.45	1.15	0.28	1.28	0.29
	Co	3.14	2.19	3.14	1.39	3.49	1.52
	Cu	0.09	0.09	0.11	0.11	0.12	0.12
	Ta	0.10	0.10	0.11	0.11	0.11	0.11
	Va	2.66	0.14	0.00	0.00	0.00	0.00

9.4 Potential of material recycling

The secondary metal flow is defined as the metal demand that will be available at the end-of-life of a technology. This demand is determined according to the decommissioned capacity each year, which can be traced according to their year of installation. The material composition of their respective year of installation is then used to calculate the actual material amount that is decommissioned. Recycling of the investigated technologies is not a well-established process since the volume of technologies to be recycled is currently very low to encourage the uptake of the recycling industry.

Nonetheless, recycling can be an effective instrument in the future to reduce the primary material demand due to the deployment of these technologies. In order to assess the full potential of recycling in reducing the criticality of metals established in chapter 9.2, it is assumed that the entire secondary metal flow can be reused in manufacturing new units in a closed-loop recycling process. This will consequently reduce the primary metal demand.

The secondary metal flow of critical metals in PV is shown in Table 9-3. Comparing these demands with the primary demands as listed in Table 9-1 shows that a development of the PV market in Germany according to the conservative scenarios will eventually lead to a surplus of recycled metals, especially in gallium, selenium, cadmium and tellurium. This occurs as a result of the low market share of thin-film modules in the future, which does not require a significant amount of material as opposed to the current in-use stock. Tellurium stands out in this case as a surplus is expected even in the alternative scenario. This can be explained by the tremendous material reduction potential that CdTe modules have, where the specific demand of tellurium can be reduced from 149 kg/MW to less than 49 kg/MW due to improvement in efficiency and reduction of cell thickness. Other critical metals such as selenium, tin and silver no longer face a bottleneck risk once a closed loop recycling is considered. As for the alternative scenario, surplus demand from recycling occurs for silver in the climate protection and long-term scenario. Although the bottleneck risk of all metals can be mitigated by considering closed-loop recycling of PV modules, indium still remains critical in the alternative scenarios with D/R ratios between 1.4 - 2.8 as well as D/R_{base} ratios between 0.7 - 1.4.

Table 9-3: Cumulative secondary metal flow of selected metals in PV according to all investigated scenarios from 2020 until 2050. The secondary metal flow that is available for recovery is depending on the year of installation of the power plants.

		Transformation		Climate Protection		Long Term	
		Alternative	Conservative	Alternative	Conservative	Alternative	Conservative
Si	[kt]	161	168	146	151	116	119
In	[t]	323	79	243	73	142	61
Ga	[t]	31	9	24	8	15	7
Se	[t]	299	78	225	73	139	63
Cd	[t]	339	155	277	151	201	142
Sn	[t]	5334	5372	4505	4533	3103	3122
Te	[t]	182	168	177	167	171	167
Ag	[t]	1768	1848	1608	1661	1271	1398

The D/R and D/R_{base} ratios of the metal demands upon recycling for wind turbines and batteries are displayed in Figure 9-4. Regarding wind turbines, the supply risk of copper is partly mitigated according to the static approach and almost completely removed in the dynamic approach. However, the low recycling potential limits the risk mitigation of dysprosium in both approaches as the remaining material demand upon recycling still remains above the allocation limit. Results of the metals in batteries indicate that metal recycling can reduce the total metal demand tremendously, especially of lithium and cobalt, which previously exceeded the maximum allocation limit for

Germany. Nonetheless, the lithium demands for all energy pathways as well as nickel and cobalt demands in the climate protection and long-term scenarios still lie above the allocation limit for batteries in Germany. This improves slightly in the dynamic approach as the nickel and cobalt demands for the long-term scenario lies beneath the allocation limit. The bottleneck risk of lithium, on the other hand, is still not mitigated.

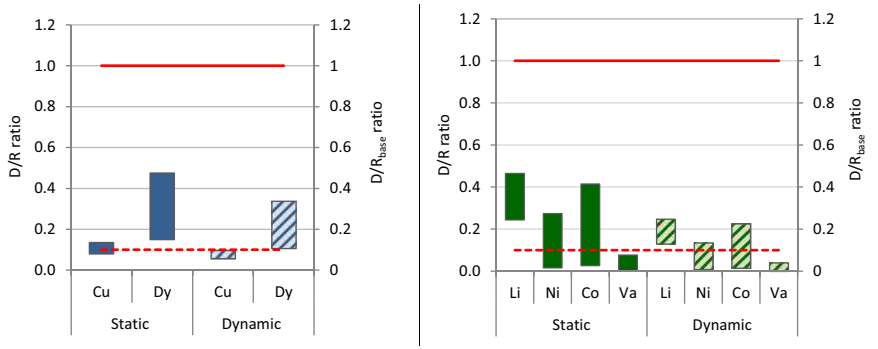

Figure 9-4: Share of the cumulative demand compared to the global static reserve (static) and reserve base (dynamic) upon considering the total recyclable metal demand for wind turbines (left) and batteries (right). The red continuous line represents the maximum allocation limit for Germany whereas the dashed line represents the maximum allocation limit for wind turbines and batteries respectively.

Although the results above prove that a closed loop recycling is able to mitigate the bottleneck risks in most cases, the question remains as to which extent is recycling able to reduce the production constraints to satisfy the annual metal demands. In order to investigate this matter, the D/P ratios of the annual demand before and after recycling are plotted for selected metals in Figure 9-5 to illustrate the impact of recycling in reducing production constraints. For silver, gallium and cobalt, the demand upon recycling creates a surplus of the metals, mostly owed to the material efficiency measures in producing the technologies. In terms of dysprosium, the recycled material demand eventually reaches surplus levels around 2048. This shows that most of the dysprosium demand will still be in in-use stocks by 2050 and will be available for recovery and recycling beyond 2050.

On a different note, only beyond 2035, with the introduction of Li-air and Li-S batteries, will the demand for cobalt reduce and compensate for the high demands in the earlier years. Correspondingly, the annual demand for lithium exhibits the highest increment among all metals. However, it can be seen that the demand upon recycling moves downwards in the later years. Considering that this trend continues even beyond 2050, it is safe to assume that the production constraints of annual lithium demand will be minimal in the long-term future. In terms of copper, the demand upon recycling constantly remains below the allocation limit for wind turbines in Germany.

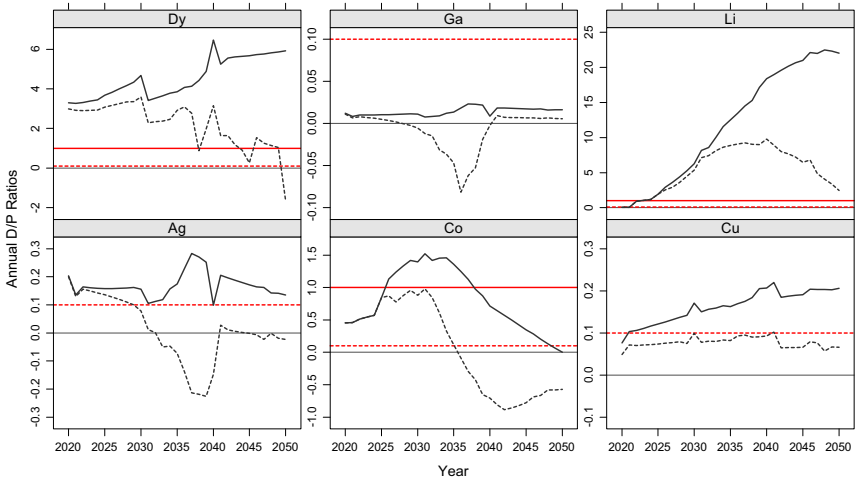

Figure 9-5: Comparison of demand-to-production ratios of primary annual demand (black continuous line) and annual demand upon considering a closed loop recycling (black dashed lines) in the conservative climate protection scenario. The red continuous line represents the maximum allocation for Germany whereas the red dotted line represents the maximum allocation for renewable energy technologies in Germany. The allocation limits are not shown for all metals due to the clarity of illustration purposes.

9.5 Further material efficiency measures

9.5.1 Wind turbines

Although only two materials (copper and dysprosium) are proven to be critical in the results, the need to intensify research efforts and to further reduce the total material demand should not be undermined to continue increasing the holistic sustainability of the electricity production from wind turbines. Improving manufacturing techniques will clearly help in reducing the production losses, which currently amounts to an average of 5 % of the total material demand (Shammugam et al. 2019a). Another strategy is to make efforts in improving the reliability of wind turbine components, which would reduce the additional demand due to repair and component exchanges. Improved reliability might also indirectly lead to the reduction of REE demand. Turbines with PM benefit, among others, from their higher reliability and lesser maintenance costs especially for deep-sea offshore turbines. By improving the reliability of electrically-excited turbines, the requirements for turbines with PMs can be suppressed, thus reducing the demand for REE. This however might incidentally lead to the increase of copper demand, a possible effect which has to be considered and analysed in detail.

In addition to that, improving material efficiency can lead to the reduction of material demand in particular components. As an example, Yang et al. (2017) showed that an improved design or even lowering the working temperature of a turbine can reduce the amount of REE in a PM. Besides that, material substitution is also able to contribute in reducing potential supply risks. Measures such as substituting dysprosium with cerium and cobalt while reducing the amount of neodymium in NdFeB magnets (Pathak et al. 2015) or even completely replacing the common NdFeB magnets with ferrite magnets (Campos et al. 2018) can ultimately reduce the REE demand. Nonetheless, it is important to note that these measures are still in a research phase and require significantly more advancement before market entry.

On top of that, the raw material requirements in this thesis have been estimated under the fundamental assumption that the general design and material composition of wind turbines will not radically transform in the next decades. However, ground-breaking designs such as the bladeless design developed by Vortey Bladeless, helium-filled floating wind turbines by the MIT startup Altaeros Energies or even more sustainable horizontal-axis wind turbines (Aso and Cheung 2015) are currently being researched and tested. If these concepts are proven to be technically and economically viable, they can clearly rival the conventional three-blade wind turbines in the future and reduce the material demand in the wind energy sector.

9.5.2 Photovoltaic

Accelerated substitution of silver

The criticality of silver strongly depends on the assumption of the rate of silver substitution by copper. In order to test the impacts of an accelerated substitution of silver, is it assumed that the entire c-Si modules in the German market in 2050 will be silver-free, as opposed to only approximately 65 % of the modules to be silver-free in the previous analysis. The accelerated substitution will lead to the average silver usage per cell to reduce from 95 g/cell to around 20 g/cell in 2035 and less than 10 g/cell by 2040. The comparison of the accelerated substitution and the conservative one used in the previous section are shown in Figure 9-6. The accelerated substitution is then applied to all conservative scenarios, which has the highest silver intensity due to c-Si implementation. Results show that around 50 % of the total silver demand can be reduced with the proposed accelerated rate of substitution, as shown in Figure 9-7. This would mean that silver no longer faces supply risk in the long-term scenario, while the risks of the climate protection and transformation scenario can be reduced tremendously even before considering recycling. This sensitivity analysis further strengthens the conclusion that a c-Si module based deployment of PV is a highly sustainable solution in the future.

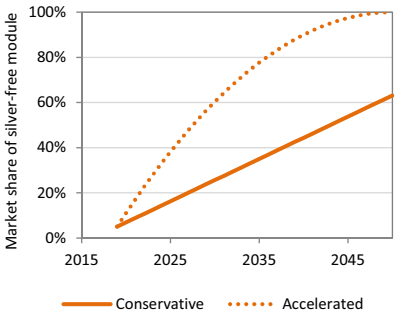

Figure 9-6 Comparison between the conservative and accelerated rate of silver substitution in PV modules

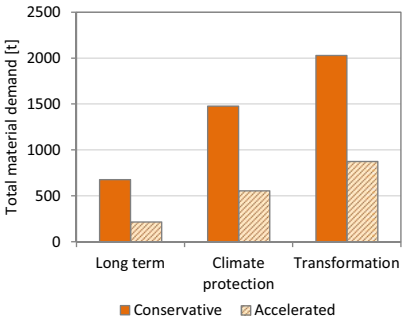

Figure 9-7: Reduction of the total silver demand based on the accelerated silver substitution in comparison to the conservative substitution rate

CZTS solar cell

Another way of reducing the supply risks related to PV is by utilizing emerging cell technologies that contain less critical metals. Copper-zinc-tin-sulphur (CZTS) based technology is an example of a thin-film solar cell similar to CIGS with indium and gallium replaced by zinc and tin respectively. Since it only contains relatively inexpensive metals, the production cost of CZTS cells can be very low and has the potential to be manufactured at a large scale in the future (Ravindiran and Praveenkumar 2018; Karimi et al. 2016). However, the efficiency of CZTS, currently at 12.6 %, is much lower than that of CdTe and CIGS (Green et al. 2018), as it still suffers from high optical losses and losses due to recombination effect (Lee and Ebong 2017). This proves to be a huge hindrance in the large scale implementation of the CZTS solar cells as the low efficiency overpowers the advantage of lower cost of production. If these issues are addressed soon and a higher efficiency can be achieved in the near future, CZTS cells can certainly pose a serious challenge to the current thin-film technologies and further reduce the demand for critical metals.

Tandem solar-cell

As the efficiency of a c-Si solar cell is practically limited to 27 %, efforts are being carried out to produce multi-junction solar cells, where a set of absorbers with varying bandgaps are used in order to overcome the efficiency limit. According to Cariou et al. (2018), two material systems that are currently discussed as suitable absorbers on silicon are the perovskite and III-V materials.

Perovskite solar cells have gained much attention lately as cell efficiency of more than 20 % is achieved in less than four years of development (Green et al. 2014; Lee and Ebong 2017). The highest recorded cell efficiency of a single-junction perovskite cell is 22.7 %, which is even higher

than the efficiency of CdTe solar cells (Green et al. 2018). Other advantages of perovskite cells include low recombination losses (Ball et al. 2013) and wide light absorption range (Grätzel 2014; Snaith 2013), which enables the absorber thickness to be much lesser than the ones by CdTe and CIGS cells. On the flipside, perovskite cells have high photocurrent losses due to parasitic absorption and a fairly low fill factor (Lee and Ebong 2017). In addition to that, perovskite cells also display stability issues and are very sensitive to moisture during manufacturing and operation (Troughton et al. 2017; Song et al. 2016), which is why the high-efficiency perovskite cells are currently only made in highly controlled conditions. This proves to be a serious problem as a large-scale production under such condition can be financially unattractive. However, ongoing efforts in the research is determined in finding ways of achieving this high efficiency in a more efficient manufacturing process which would suit a large-scale production (Fakharuddin et al. 2016; Seok et al. 2018; Saliba et al. 2018; Luo et al. 2015; Lei et al. 2015). Another major issue that can hinder the application of perovskite cells, especially in the EU, is the usage of the toxic metal lead. To address this matter, alternatives are currently being intensively researched, with tin, bismuth and antimony all proving to be a viable substitution of lead in the perovskite cells (Kamat et al. 2017; Wang et al. 2018; Ali et al. 2018). If all of these shortcomings of perovskite cells can be overcome in the near future, it has the potential to be strongly commercialized and compete even with c-Si cells for market shares.

The second concept involves a combination of III-V semiconductors with silicon substrates (III-V//Si). This concept is highly attractive since the multi-junction architecture enables high efficiency in combination with the low cost of Si substrates (Feifel et al. 2018). The highest recorded efficiency of such a concept is 35.9 % measured at standard conditions (Essig et al. 2017), which however involves complex module integration. Cariou et al. (2018) managed to achieve a cell efficiency of 33.3 % using a less complex process involving direct wafer bonding. Nonetheless, both processes are highly expensive and are currently not suitable for large-scale industrial application. According to Essig et al. (2017), the price of III-V//Si solar cell lies between 4.85 and 8.24 USD/W_p, depending on the particular III-V metals applied. This proves to be extremely high in comparison with the commercially available single-junction c-Si solar cell, estimated to be between 0.3 and 0.35 USD/W_p. The authors also further predict that the cost can be reduced to 0.66 USD/W_p in the long term and further improve the competitiveness of the III-V//Si solar cell.

9.5.3 Batteries

Increase in energy density

The results presented in chapter 9 reflect the consequences of a reduction in specific material demand orientated on the improvement in energy density as detailed in chapter 1.9. In this section, the implications of an even aggressive increase in energy density on the total material demand are

investigated by conducting a sensitivity analysis to the rate of reduction of material intensity. This is carried out exemplarily for Li-Air batteries since they still have much room for improvements according to their maximum achievable energy density. In the previous analysis, a 3 % reduction in material density is assumed, corresponding to an increase from 450 Wh/kg to 1100 Wh/kg in 2050. The reduction in the total material demand is shown exemplarily for lithium in the conservative climate protection scenario for each unit increment of the material intensity reduction. Results show that at 4% reduction of material intensity, the material demand of lithium upon recycling already lies beneath the allocation limit. This shows the importance of continuing the intensive research and development in batteries in order to increase the energy density, which not only improves the mileage in EVs but also indirectly contributes to the reduction of total material requirement.

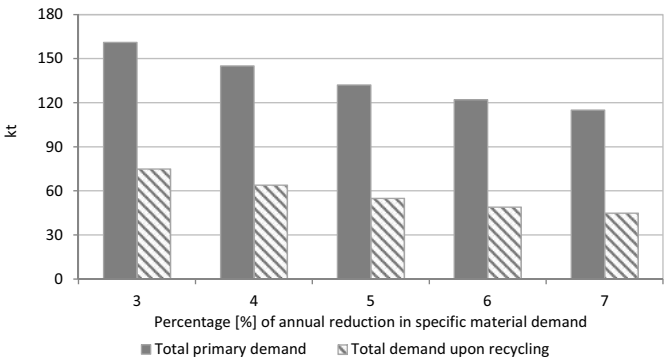

Figure 9-8: Reduction of the total lithium demand for every increment in the reduction of specific material demand, shown exemplarily for the conservative climate protection scenario. Maximum allocation limit is at 64 kt.

Second-life batteries

Another way of decreasing the material demand is the deployment of used batteries for a second life application, also known as second life batteries. In EVs, Li-Ion batteries will have to be replaced once the capacity of the batteries have reached between 70 to 80 % of their initial capacity (Casals et al. 2017) since the driving range will be extremely limited at that capacity. This usually occurs between 7 to 10 years upon usage. Instead of dismantling and recycling the batteries while it still has 80 % of the initial capacity, they can be further used in other applications until their maximum lifespan is reached, especially as stationary storages. It is a win-win situation for both fields of applications since the second life batteries can be purchased at a lower price, which then, in turn, reduces the cost of ownership of EVs (Jiao and Evans 2016). Fischhaber et al. (2016) identified possible application fields for second life batteries and reported that they can be used for various stationary applications such as providing spinning reserves, load-shifting and even for energy trading

on the day-ahead or intraday platforms. Reid and Julver (2016) investigated the process of remanufacturing used batteries from EVs for second life purposes and reported that the batteries can be used 10 to 15 years more before being recycled.

The potential of second-life batteries in reducing material demand is tested for the transformation scenario since it is the only scenario that expands battery capacity for stationary applications. The total capacity of all decommissioned NMC batteries in the conservative transformation scenario after 10 years of usage in EVs is approximately 229 GWh. Even after considering that they only possess 70 % of their initial capacity, 160 GWh of battery capacity will be available, which is considerably higher than the 79 GWh of proposed total battery capacity for stationary applications. This proves the enormous potential of second life batteries in reducing the material demand of batteries in stationary applications.

9.6 Granger-causality between metal prices[10]

Once the supply bottlenecks have been identified, the relationship between the prices of active metals in PV, wind turbines and batteries are investigated and presented in this sub-chapter. This is achieved by conducting a pair-wise Granger-causality test for predefined metal pairs based on their nature of joint production and joint consumption. The results of unit root and cointegration tests for all metal pairs are presented independently of their production or consumption behaviour. The results of the ADF and KPSS tests are presented in Table 15-3 (in the Appendix). The price series of all metals are stationary at first order according to the ADF test at 1 % significance level and insignificant KPSS statistic. Only the gold price is accepted to be stationary at a 10 % significance level according to the KPSS test. Based on these results, the maximum order of integration of all pairs of time series is set to be one. The optimal lag lengths chosen based on BIC is listed in Table 15-4. The results of the Breusch-Godfrey (BG) test are also listed in Table 15-4 (Appendix), which indicate that the final lag lengths of all metal pairs do not have serial autocorrelations in the residuals at 5 % significance level. The trace and the maximum eigenvalue statistics of the Johansen's cointegration test are listed in Table 9-4. The cointegration results are used to cross-check the final Granger-causality results, where causality in any direction has to be present if a cointegration is detected between the metals. Results show that 10 metal pairs have a cointegration relationship at the first rank, with lead-copper and steel-dysprosium showing the most significant cointegration relationship according to both trace and maximum eigenvalue tests.

[10] Some parts of this sub-chapter have been published in (Shammugam et al. 2019b). These contents have been revised and editorially amended as part of this thesis.

Table 9-4: Results of the Johansen cointegration test. In summary, cointegration exists between 10 metal pairs. This result will be cross-checked and validated with the results in chapter 9.5.1 and 9.5.2 as causal links are expected between these metal pairs.

* represents 10% significance level, ** 5% significance level and *** 1% significance level.

Metal pair	Rank	Trace statistic	Max. eigenvalue statistic	Metal pair	Rank	Trace statistic	Max. eigenvalue statistic
Al-Ga	0	8.89	8.58	Ag-Cu	0	7.13	7.02
Al-Ga	1	0.30	0.30	Ag-Cu	1	0.11	0.11
Ag-Au	0	11.44*	11.22*	Ag-Ni	0	6.86	6.54
Ag-Au	1	0.21	0.21	Ag-Ni	1	0.33	0.33
Ag-Zn	0	5.25	4.88	In-Ga	0	2.94	2.78
Ag-Zn	1	0.37	0.37	In-Ga	1	0.16	0.16
Au-Cu	0	13.41**	13.31**	In-Se	0	6.14	5.67
Au-Cu	1	0.09	0.09	In-Se	1	0.48	0.48
Cu-Mo	0	6.04	5.58	In-Cu	0	6.84	6.58
Cu-Mo	1	0.46	0.46	In-Cu	1	0.26	0.26
Cu-Se	0	10.61*	10.44*	Ga-Se	0	8.39	7.56
Cu-Se	1	0.17	0.17	Ga-Se	1	0.83	0.83
Cu-Co	0	3.55	3.27	Ga-Cu	0	6.73	6.63
Cu-Co	1	0.28	0.28	Ga-Cu	1	0.10	0.10
Fe-Dy	0	18.53***	18.52***	Ag-Ga	0	5.78	5.32
Fe-Dy	1	0.01	0.01	Ag-Ga	1	0.46	0.46
Fe-Nd	0	16.22**	16.21**	Ag-In	0	3.84	3.74
Fe-Nd	1	0.01	0.01	Ag-In	1	0.10	0.10
Ni-Cu	0	14.52**	14.10**	Li-Ni	0	14.24**	13.15**
Ni-Cu	1	0.42	0.42	Li-Ni	1	1.09	1.09
Ni-Co	0	7.90	6.38	Li-Co	0	5.85	4.41
Ni-Co	1	1.52	1.52	Li-Co	1	1.44	1.44
Pb-Ag	0	9.13	9.01	Mn-Li	0	10.06	8.79
Pb-Ag	1	0.11	0.11	Mn-Li	1	1.27	1.27
Pb-Cu	0	22.85***	22.64***	Mn-Ni	0	17.25**	16.34***
Pb-Cu	1	0.20	0.20	Mn-Ni	1	0.91	0.91
Pb-Zn	0	10.01	8.17	Mn-Co	0	8.33	5.68
Pb-Zn	1	1.84	1.84	Mn-Co	1	2.65	2.65
Zn-In	0	12.48*	12.04**	Cu-Nd	0	9.25	9.18
Zn-In	1	0.43	0.43	Cu-Nd	1	0.07	0.07
Zn-Ga	0	8.74	8.53	Cu-Dy	0	7.20	7.18
Zn-Ga	1	0.20	0.20	Cu-Dy	1	0.02	0.02

9.6.1 Joint-production

As listed in Table 9-5, 14 out of the 26 metal pairs analysed under the premise of joint production have a Granger-causality relationship at least at a 10 % significance level. A bidirectional Granger-causality is present between the prices of gold and silver, which are each other's primary metal and co-product simultaneously (see Table 3-1). Significant causalities are also observed between copper and its companion metals. For instance, bidirectional causalities are present between copper and its co-products, gold and molybdenum while a unidirectional Granger-causality is present between copper and selenium. In addition to that, the price of copper is also Granger-caused by nickel and lead, where copper is a by-product. In terms of other minor metals, mixed results are obtained. To begin with, the prices of dysprosium and neodymium are Granger-caused by the price of steel. This

comes as a result of more than 50 % of all REEs being produced together with steel (Graedel and Nassar 2015). On the other hand, although more than 90 % of gallium is produced together with either aluminium or zinc (Nassar et al. 2015), no causal links are present between their prices. Similarly, the price of indium is not Granger-caused by the price of Zinc although 75 % of indium is produced as companion metals of zinc. Causality involving Zinc is only present between lead and cadmium. Furthermore, the price of cobalt is neither Granger-caused by copper nor nickel, despite being almost entirely produced together with both metals. Therefore, it remains to see if the prices of minor metals such as indium, cobalt and gallium are driven by their joint-consumption characteristics. Generally, results indicate that metals that are present in PV, wind turbines and batteries are significantly affected by their companion metals in terms of production. While this can definitely be said for industrial and precious metals, the same conclusion cannot be made for minor metals.

Table 9-5: Test statistics of the χ^2 Wald-test for metals that are jointly produced. X -> Y represents the null hypothesis of X does not Granger-cause Y, whereas Y -> X represents the null hypothesis of Y does not Granger-cause X.β and δ represent the corresponding sum of coefficients whenever causality is present.

* represents 10% significance level, ** 5% significance level and *** 1% significance level.

X	Y	$\chi^2(X \rightarrow Y)$	Sum of β	X	Y	$\chi^2(X \rightarrow Y)$	Sum of β
Al	Ga	0.14	-	Pb	Ag	4.24	-
Ag	Au	44.60***	-3.79	Pb	Cu	23.75**	-0.21
Ag	Zn	6.56*	14.21	Pb	Zn	22.71	-
Au	Ag	25.59***	0.00	Zn	Ag	1.53	-
Au	Cu	26.23**	-1.23	Zn	Pb	120.20***	0.08
Cu	Mo	26.67**	-0.04	Zn	Cd	70.26***	0.00
Cu	Ag	14.52	-	Zn	In	8.88	-
Cu	Au	21.21*	-0.01	Zn	Ga	2.22	-
Cu	Se	45.13***	0.00	Mo	Cu	46.69***	-0.01
Cu	Co	0.25	-	Ag	Cu	17.90	-
Fe	Dy	306.57***	0.79	Au	Pb	4.62	-
Fe	Nd	7.68*	-1.57	Ag	Pb	4.13	-
Ni	Cu	92.94***	0.02	Au	Zn	5.62	-

The results of the Granger-causality analysis of jointly-produced metals show that 6 of the cointegration relationships, identified in Table 9-4, can be confirmed via the presence of a causal link. These metal pairs are gold-silver, gold-copper, steel-dysprosium, steel-neodymium, nickel-copper and lead-copper. In addition to that, the cointegration between zinc and indium can also be confirmed by the existence of Granger-causality flowing from indium to zinc[11].

[11] A unidirectional Granger-causality is identified flowing from indium to zinc with a test statistic of χ^2=10.88 at 10 % significance level.

9.6.2 Joint-consumption

The results of the Granger-causality test among metals in PV, wind turbines and batteries are listed in Table 9-6, Table 9-7 and Table 9-8, respectively. The tests are only conducted for the active metals in the technologies that are fundamental to the functionality. For PV, these include metals in the solar cells whereas for batteries, active metals in the cells are considered. Regarding wind turbines, copper and REEs are considered in the tests.

In terms of c-Si modules, a unidirectional causality is observed flowing from silver to nickel and copper to silver whereas a bi-directional causality is present between copper and nickel. Since silver is being gradually substituted in solar cells by copper and nickel, a negative relationship is expected. However, this is only true between silver and nickel, as a positive relationship is present between copper and silver. This can be attributed to the small market share of silver-free modules in the market at the moment. A much significant negative relationship can be expected in the future when silver is substituted on a large scale. With regards to thin-film modules, the price of gallium is Granger-caused by selenium. In combination with the lack of Granger-causality between the prices of gallium and zinc as well as aluminium, this shows that the joint-consumption drives the price of gallium much stronger than joint-production. Besides that, Granger-causality is also present between selenium-indium and selenium-copper. The positive relationship between these metal pairs shows that their prices move in the same direction, i.e. when the demand for thin-film modules increases, the demand for all relevant metals increases simultaneously. Assuming a constant production, the prices of all metals increases as well.

In wind turbines, no causality is observed between copper and REEs. The significant causality between neodymium and dysprosium cannot be completely attributed to joint consumption since both metals are also produced together. For active metals of batteries, bi-directional casualties are present between lithium and nickel as well as lithium and manganese, which can be explained by the large scale use in NMC type Li-ion batteries. Apart from that, the price of manganese is Granger-caused by the price of cobalt.

The presence of causal links between the metal pairs of copper-selenium, lithium-nickel and manganese-nickel completes the cross-checks of the cointegration test as all the co-integrating metal pairs have Granger-causality between their prices at least in one direction.

Table 9-6: Test statistics of the χ^2 Wald-test for metals that are jointly consumed in PV modules. X -> Y represents the null hypothesis of X does not Granger-cause Y, whereas Y -> X represents the null hypothesis of Y does not Granger-cause X.β and δ represent the corresponding sum of coefficients whenever causality is present.

* represents 10% significance level, ** 5% significance level and *** 1% significance level.

X	*Y*	χ^2 (*X* ->*Y*)	Sum of β	χ^2 (*Y* ->*X*)	Sum of δ
Cu	Ni	97.11***	-0.34	100.63***	-0.02
Ag	Ni	25.38***	-229.48	10.51	-
Cu	Ag	36.79**	0.00	26.24	-
In	Ga	0.05	-	1.79	-
In	Se	22.10	-	61.46***	23.89
In	Cu	12.77	-	10.61	-
Ga	Se	0.50	-	5.72*	0.12
Ga	Cu	0.99	-	1.55	-
Se	Cu	29.43***	1.34	45.13***	0.00
Ag	Ga	1.78	-	0.48	-
Ag	In	4.14	-	14.25**	0.00
Ag	Cd	2.39	-	0.80	-
In	Cd	1.84	-	1.13	-
Se	Cd	16.44***	-0.01	4.66	-

Table 9-7: Test statistics of the χ^2 Wald-test for metals that are jointly consumed in wind turbines. X -> Y represents the null hypothesis of X does not Granger-cause Y, whereas Y -> X represents the null hypothesis of Y does not Granger-cause X.β and δ represent the corresponding sum of coefficients whenever causality is present.

* represents 10% significance level, ** 5% significance level and *** 1% significance level.

X	*Y*	χ^2 (*X* ->*Y*)	Sum of β	χ^2 (*Y* ->*X*)	Sum of δ
Cu	Nd	1.73	-	-	-
Cu	Dy	8.27	-	-	-
Nd	Dy	117.18***	0.01	54.12***	-0.45

Table 9-8: Test statistics of the χ^2 Wald-test for metals that are jointly consumed in batteries. X -> Y represents the null hypothesis of X does not Granger-cause Y, whereas Y -> X represents the null hypothesis of Y does not Granger-cause X. β and δ represent the corresponding sum of coefficients whenever causality is present.

* represents 10% significance level, ** 5% significance level and *** 1% significance level.

X	*Y*	χ^2 (*X* ->*Y*)	Sum of β	χ^2 (*Y* ->*X*)	Sum of δ
Li	Ni	141.18***	0.80	60.24***	0.01
Li	Co	2.53	-	1.22	-
Ni	Co	3.90	-	0.72	-
Mn	Li	1.93	-	1.47	-
Mn	Ni	19.97**	-2.23	27.74***	-0.01
Mn	Co	7.48	-	52.38***	0.01

Overall, it can be seen that significant Granger-causalities between jointly used metals within the technologies do exist, especially in PV and batteries. However, it is important to mention that the effect of joint-consumption has to be analysed with respect to the level of aggregation. By increasing the consumption aggregation to a higher level, all technologies are aggregated into one application field. While a universally accepted term to classify all three technologies is not present, they can be classified as technologies relevant to the energy transition process. This allows for an inter-technology Granger-causality analysis to test if the energy transition process leads to price dependencies among PV, wind turbines and batteries in general. The results presented in Table 9-9 clearly shows that an inter-technology dependency of metal prices does exist. For instance, the price of silver used in c-Si PV modules Granger-causes the prices of REEs in wind turbines. A bi-directional causality is also present between the prices of silver and lithium. In terms of thin-film modules, the price of indium is Granger-caused by lithium whereas the price of gallium is Granger-caused by the price of cobalt and nickel. In some cases, more significant relationships among metals in different technologies are observed than within a single technology. As an example, lithium has significant predictive power over the price of indium. However, no causal links are identified between indium and gallium as well as copper despite being used together in CIGS modules. Regarding wind turbines, the link to PV modules is given by significant relationships between REEs and silver as well as gallium. On the other hand, there is no link between REEs and metals in batteries. Copper is an exception since it is used in both wind turbines as well as in the wirings and charge collectors in batteries. Overall, 55 % of the tested metal pairs exhibit causality between their prices.

Table 9-9: Test statistics of the χ^2 Wald-test for jointly consumed metals in all technologies. The metals in a column Granger-causes the metals in corresponding metal in a row. "NA" refers to metal pairs whose serial autocorrelation could not be resolved even upon increasing the lag length of the bivariate VAR model up to 30 lags. These metal pairs are excluded from the causality test as it was assumed that a lag length more than that would be overfitting the model and the results would be unreliable.
* represents 10% significance level, ** 5% significance level and *** 1% significance level.

	Ag	Cd	Co	Cu	Dy	Ga	In	Li	Mn	Nd	Ni	Se
Ag	-	2.4	1.4	26.2	96.6***	1.8	4.1	87.2***	2.2	46.2***	25.4***	NA
Cd	0.8	-	3.2	44.0***	0.5	2.9	1.1	0.5	93.2***	0.4	46.5***	4.7
Co	4.3	1.4	-	6.1	0.8	12.3***	4.5	1.2	52.4***	0.3	0.7	1.5
Cu	36.8***	59.1***	3.4	-	8.3	1.5	10.6	115.2***	26.3***	1.7	97.1***	45.1***
Dy	34.6***	0.5	0.5	11.2	-	0.6	7.3	0.5	0.1	54.1***	1.8	17.2*
Ga	0.5	1.4	0.2	1.0	25.2***	-	1.8	0.5	1.6	17.0***	3.9	0.5
In	14.3**	1.8	2.0	12.8	5.9	0.0	-	7.6	1.5	10.4***	3.0	22.1
Li	71.6***	0.3	2.5	118.7***	2.1	0.3	12.7**	-	1.5	0.1	141.2***	23.0*
Mn	2.7	30.2**	7.5	8.2	0.5	0.7	8.1	1.9	-	0.5	20.0**	0.7
Nd	3.0	0.3	0.8	1.9	117.2***	0.2	5.2*	1.8	0.5	-	0.3	0.4
Ni	10.5	75.1***	3.9	100.6***	2.1	4.7*	18.5***	60.2***	27.7***	1.4	-	54.9***
Se	NA	16.4***	4.3	29.4***	33.6***	5.7*	61.5***	75.8***	23.9***	4.9*	31.2***	-

9.6.3 Robustness test

The results presented in chapter 9.5 are assumed to be robust since the improved Toda-Yamamoto approach is applied to test for Granger-causality besides additional tests to eliminate serial autocorrelations in the residuals. As a final step to ensure the robustness of the results, a placebo test according to Afflerbach et al. (2014) is conducted. This involves the test for Granger-causality of every other metal pair that has not been tested under the definitions in chapter 9.6. A separate hypothesis is defined for the robustness test, which states that the number of causal relationships among random metal pairs should be lower compared to the metals pairs that are jointly consumed or produced. According to the results in Table 15-5 (Appendix), it can be seen that only 40 % of the metal pairs exhibit causal relationship, which is lower than the reported value in the previous sections and aligns with the hypothesis of the placebo test. This reassures that the results are not spurious and that the methodology applied is robust and not biased.

Nonetheless, the question remains as to why a significant amount of causalities exists in the placebo test. The main reason for this could be the existence of a price dependency in other fields of application, in which the amount of metals that are utilized could be much greater than in renewable energy technologies. As an example, copper and aluminium are generally used together in construction and transportation sector, which explains the causal link between their prices in the placebo test. On a different note, the existence of Granger-causality can also be contributed indirectly by certain factors, such as the inflation rate or economic growth. For instance, if the general economy of a country is on a rise, demand for industrial production or construction of infrastructures will increase. Consequently, the demand for industrial metals, in general, will rise, which might lead to a Granger-causality pattern in their prices despite not being used together in a single end-product. Besides that, the dynamic nature of metal application in various sectors and products can also play a role in existing causalities beyond the definitions in this thesis. As an example, before being largely used in batteries, cobalt was mainly used in superalloys together with chromium. This can explain the significant Granger-causality observed between chromium and cobalt (see Table 15-5). Nonetheless, with the strong application in batteries, especially in EVs, the relationship between cobalt and chromium can be expected to weaken in the future, with more significant causalities exiting between cobalt and battery-related metals such as lithium and nickel.

9.7 VAR analysis of metal prices

The final section of this chapter involves the results of the VAR analysis of metal prices, where the impacts of a shock to the price, supply and demand will be analysed. For this purpose, silver, cobalt, copper indium and nickel are chosen to be investigated further due to data availability as well as to represent all investigated technologies in this thesis. The results of indium and nickel are provided in the Appendix.

The results of the ADF and KPSS tests of all relevant variables in the VAR analysis are listed in Table 9-10. The results of the macroeconomic variables are divided into two time periods since the data for indium is only available from 1975 onwards whereas for other metals, 1970 is applied as the start year. Based on the metal-specific variables, the log differences of all time-series are stationary. In terms of the macroeconomic variables, the log difference of CPI does not remove the unit root in the time series, as opposed to the first difference. Therefore, the latter criterion is chosen to transform the time series of CPI whereas the log difference of other variables is applied further in the VAR analysis. The optimal lag length of all VAR models chosen based on BIC is 1.

Table 9-10: Test statistics of unit root tests of all relevant variables in the VAR analysis.
* represents 10% significance level, ** 5% significance level and *** 1% significance level.

Metal	Time period	Variables	ADF	KPSS
Ag	1970 - 2013	Δ log (Price)	-5.16***	0.12*
		Δ log (Con)	-6.75***	0.03
		Δ log (Prod)	-6.17***	0.04
Co	1970 - 2013	Δ log (Price)	-5.81***	0.04
		Δ log (Con)	-8.59***	0.03
		Δ log (Prod)	-4.89***	0.05
Cu	1970 - 2013	Δ log (Price)	-6.03***	0.05
		Δ log (Con)	-6.78***	0.03
		Δ log (Prod)	-6.61***	0.04
In	1975 - 2013	Δ log (Price)	-4.54***	0.04
		Δ log (Con)	-8.93***	0.05
		Δ log (Prod)	-7.61***	0.07
Ni	1970 - 2013	Δ log (Price)	-5.63***	0.04
		Δ log (Con)	-8.06***	0.02
		Δ log (Prod)	-5.97***	0.04
-	1970 - 2013	Δ log (GDP)	-4.86***	0.09
		Δ CPI	-4.19**	0.10
		Δ log (FedFund)	-5.07***	0.04
		Δ log (ExchangeRate)	-4.67***	0.06
-	1975 - 2013	Δ log (GDP)	-4.63***	0.06
		Δ CPI	-4.16**	0.08
		Δ log (FedFund)	-4.44***	0.05
		Δ log (ExchangeRate)	-4.22**	0.06

The results of the model checking according to the BG-test and the ARCH-test in Table 9-11 shows that all models are adequately specified. The null hypothesis of no serial autocorrelations is failed to be rejected at 10 % in the BG-test. According to Lütkepohl (2013), although serial autocorrelation is important while specifying a VAR model, it does not affect the results of the structural analysis. Hence the test is only conducted for 10 % significance level in this thesis. In the ARCH-test, homoscedasticity of the residuals is not rejected at least at the 5 % significance level for all models.

Table 9-11: Test statistics (χ^2) of the BG-test and the ARCH test for heteroscedasticity
* represents 10% significance level, ** 5% significance level and *** 1% significance level.

Model	Serial autocorrelation	Heteroscedasticity
VAR(Ag)	294*	1036
VAR(Co)	336	1332
VAR(Cu)	336	1332
VAR(In)	252	868
VAR(Ni)	294*	1036

Last but not least, the OLS-CUSUM figures of all variables are shown exemplarily for the VAR model of copper in Figure 9-9. The boundaries (dotted horizontal lines) are calculated at 5 % confidence levels. Since the empirical fluctuation process does not exceed the boundaries, no structural breaks are present in the time series. This is valid in all the VAR models of the metals. This completes the model checks and establishes the fact that all models are well-specified.

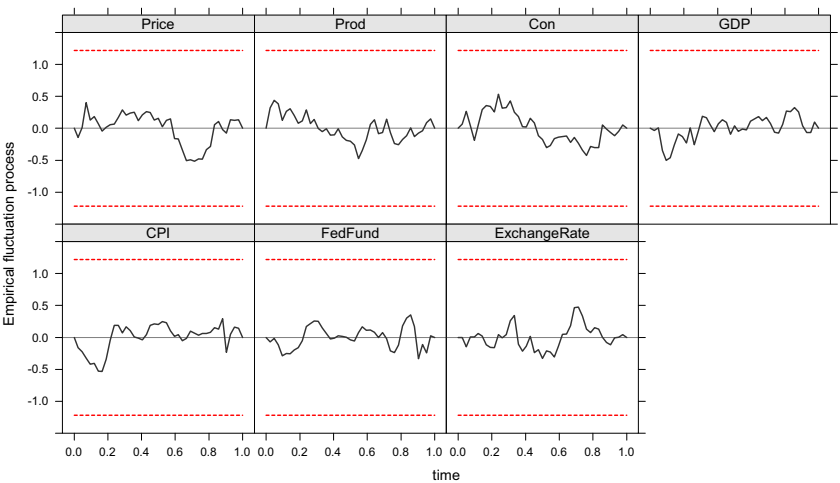

Figure 9-9: OLS-CUSUM of the VAR model of copper. Dotted lines represent the boundaries of the empirical fluctuation process calculated at 5 % confidence level.

Next, metal prices are forecasted for 10 steps beyond the last period in the time series. Figure 9-10 depicts the forecast ranges of the prices of all metals. The plots are visually examined to determine whether the forecasts are likely to be accurate. Based on the results, it is seen that forecast follows the trends of the training data consistently. The forecast lies close to the mean values and no significant change in trend is observed. Only the forecast of indium tends to slightly move upwards, probably due to the historical peaks. However, the increase is relatively small and the confidence

intervals still remain within an acceptable range compared to the mean. Overall, the forecasts of all metals are accepted to be within the expected ranges.

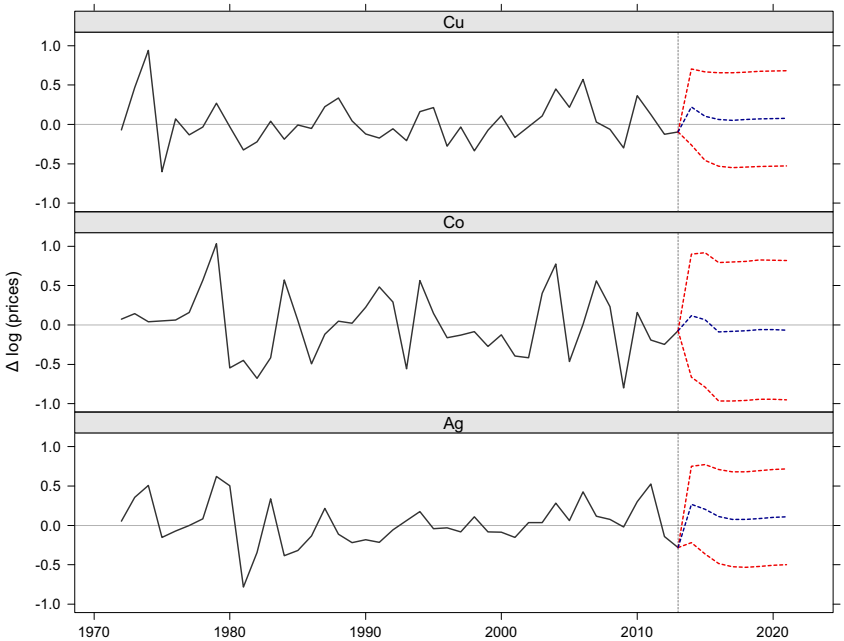

Figure 9-10: Forecast (dotted lines) of the Δ log price of copper (Cu), cobalt (Co) and silver (Ag). The blue dotted lines represent the mean values of the forecast whereas the red dotted lines represent the 10 % and 90 % confidence intervals of the forecast values.

In the next step, the impulse responses based on the VAR models are calculated and analysed. A unit shock is induced in the consumption of all metal in order to test the impact on the price and production levels. The results are illustrated in Figure 9-11. It can be clearly seen that an impact in the metal demand has an immediate positive impact on the price. A positive demand shock appreciates all prices in the following time period and depreciates in the following period, before oscillating and returning to zero eventually. The reason as to why the price drops in the second time period are that the consumption itself reduced in the second period and remains there until a certain period before moving back to zero. The change in the price of all metals remains negative for at least 2 time periods except for cobalt, which immediately becomes positive in the following time period. However, cobalt remains the only metal whose price oscillates around the zero changes. In the medium run however, the effect is reabsorbed when production increases to compensate the increasing demand which causes the price to converge back to zero.

Based on the results, an increase in demand affects the price of copper the most based on the amplitude of the impacts and the time it takes for the transitionary shocks to die out. For instance, a 1 % increase in the change of demand causes the change in copper price to increase by 1 %. Silver and cobalt on the other hand, only experience a 0.3 and 0.5 % increase respectively. In order to further understand the difference between the price impacts, the effects are compared to their monetary market volume, which is given by the product of the average market price and the production volume in 2017 of the metals obtained from (USGS 2018). The market volume of copper in 2017 was approximately 79 billion USD compared to 11 billion USD of silver and 6 billion USD for cobalt. Interestingly, the impacts of a demand shock on metal prices are directly proportional to the market volume. This is also valid for the responses of nickel and indium.

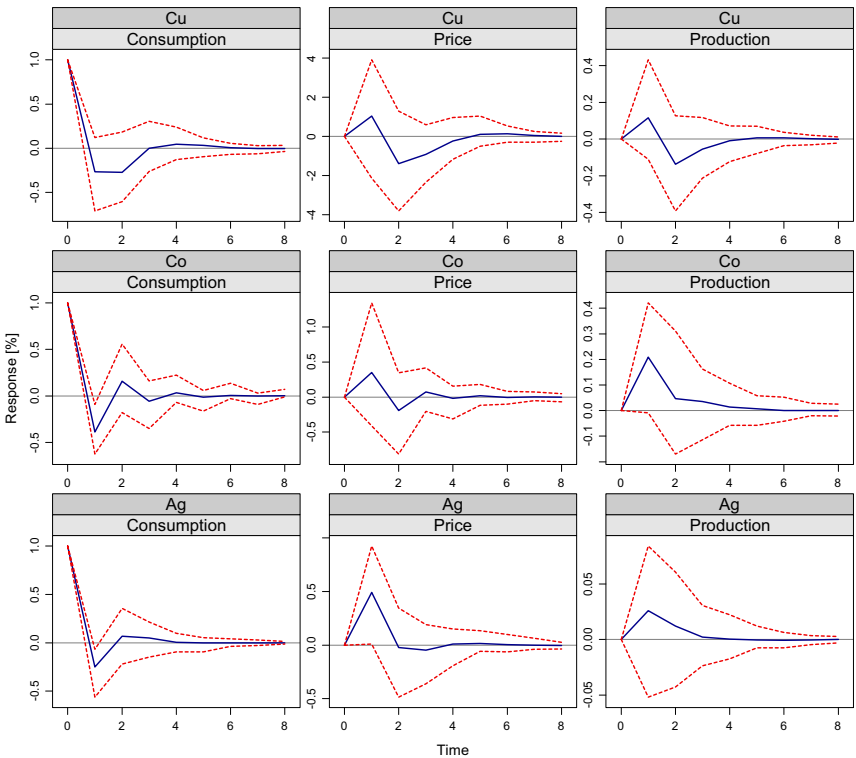

Figure 9-11: Responses of the change in log differences of price and production to a unit shock in the log differences of the consumption of copper, cobalt and silver. The dotted lines represent the 95% confidence intervals obtained by bootstrapping together with the impulse responses at 100 replications.

A plausible explanation for this could lie within the role of the market liquidity and the flexibility of the metals to adjust towards market distortions. Metals such as copper and nickel have always had a relatively stable demand and production in the past. The high liquidity of these metals ensures market equilibrium, which means that their storage capacity is not built to sustain a sudden unexpected short-term shock. On the contrary, metals such as indium and cobalt are by-products of other metals. This means that the overproduction of these metals can be stored and regulated based on their market prices. Furthermore, since the data applied in this thesis goes back to 1970, it could have been that the use of these metals in the past was not as significant as today. Therefore, minor could have been stored in the past until the appropriate market for them has been established, which consequently causes their storage capacity to be relatively larger than their respective demands. Therefore, minor metals can be more flexible in adjusting towards market disruption, given that their storage capacity is large enough. Furthermore, it is also seen that a shock to copper demand depresses itself over a relatively longer period compared to other metals. The fluctuations are evaluated in this thesis based on the time it takes for the shocks to return to less than 25 % of the maximum amplitude of the response. In these terms, silver has the smallest fluctuations as the fluctuation stabilizes after two time period. Cobalt requires 3 time period whereas for the other metals, the change in price stabilizes after 4 time periods.

The IRF analysis is continued with a unit shock to the production of the metals. The impact of this on the consumption and metal prices are illustrated in Figure 9-12. Expected results in terms of the responses in the prices are obtained, as they decrease in the subsequent time step. The biggest response is observed in silver, where a 1 % increase in the change of production depreciates the change of price by 1.2 %. In contrast, the change on cobalt price only decreases by 0.7 %, which is the least among the investigated metals. In terms of consumption, mixed results are obtained. Hypothetically, a positive shock in production should decrease the price due to oversupply, which consequently increases the demand. While this is observed in copper and silver, the consumption of cobalt decreases. An explanation for this could be that the price of cobalt has been affected by various factors other than the supply and demand fundamentals in the past. Events such as political unrests and strong governmental regulation in the US market have caused what is today known as the cobalt crisis in the 1970s. As a direct result of this crisis and the recession in the early 1980s, the demand for cobalt began to reduce massively as recovery from secondary materials began to increase. At the same time however, the cobalt production in Congo and Zambia continued, which ultimately lead to an oversupply situation in the cobalt market ((Plunkert and Jones 1999). Since the data applied in the VAR analysis starts from 1970, the aforementioned incidents and the effects on the market is visible in the results. This shows that the cobalt crisis in the 1970s did actually have a long-term impact on the market. However, significant amount of cobalt is being traded on the free market in recent times, such as at the London Metal Exchange (LME) since 2010. Therefore, the results of the VAR analysis regarding cobalt in this thesis have to be treated with caution.

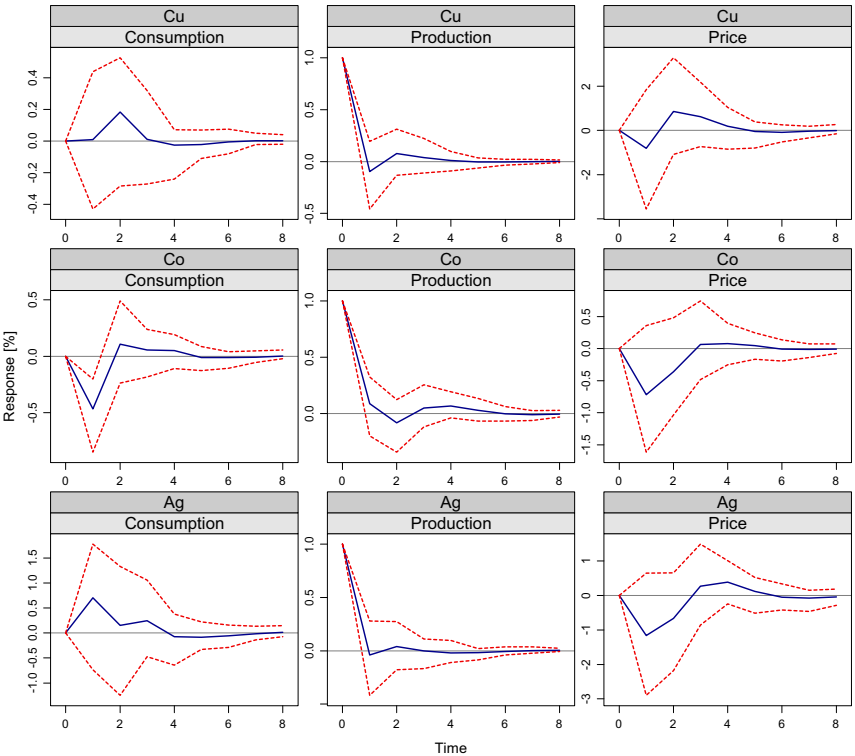

Figure 9-12: Responses in log differences of price and consumption to a unit shock in the log differences of the production of copper, cobalt and silver. The dotted lines represent the 95% confidence intervals obtained by bootstrapping together with the impulse responses at 100 replications.

In the following step, a unit shock is induced to the price in order to investigate how this affects the supply and demand equilibrium of the metals. A positive price shock should hypothetically reduce the demand. On the other hand, production will increase since producers have more incentives to bring their products to the market. However, as displayed in Figure 9-13, mixed results are obtained. Most notably, silver consumption increases as a result of a positive price shock. This is owed to the fact that silver is treated as a financial asset since its price is robust towards inflation. This effect will be explained in detail in chapter 10.4. Nonetheless, this effect eventually dies off once the production is increased to compensate for the increased price. Another odd result is the decrease in production once the price increases for copper. The reason for this could be that the production level of copper is more significantly affected by the consumption rather than the price. Therefore, once the price increases, the expected decrease in consumption will eventually lead to a decrease in copper production. This effect is further demonstrated in the forecast error variance decomposition

and will be explained in the following section. Overall, the general trend remains valid for other metals that an increase in price will lead to a decrease in consumption and an increase in production. The changes observed in the consumption and production of the metals as a result of a price shock is relatively lower compared to the effects of a demand shock.

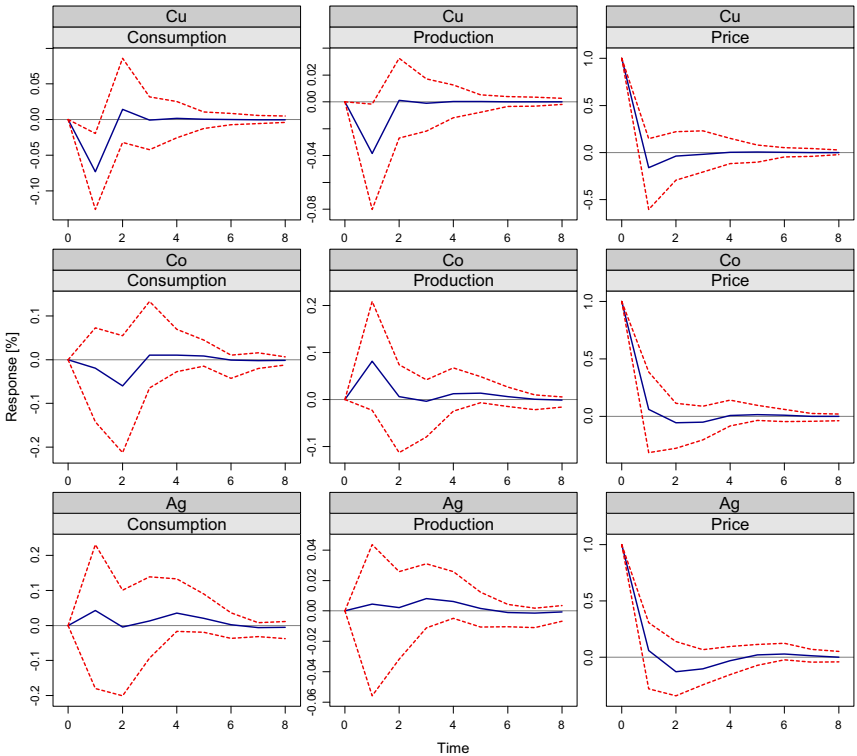

Figure 9-13: Responses of the change in log differences of consumption and production to a unit shock in the log differences of the price of copper, cobalt and silver. The dotted lines represent the 95% confidence intervals obtained by bootstrapping together with the impulse responses at 100 replications.

The final step of the structural analysis is the forecast error variance decomposition (FEVD), which is illustrated in Figure 9-14 for copper, cobalt and silver. The most significant observation is that all variables are affected the most by their own lag values. In terms of the prices of all metals, macroeconomic variables prove to be important drivers, particularly the inflation rate and the exchange rate. This proves the hypothesis mentioned in chapter 9.6.3, that the Granger-causality

observed among the metals in the placebo test could have been caused by an indirect joint-consumption effect such as by macroeconomic variables.

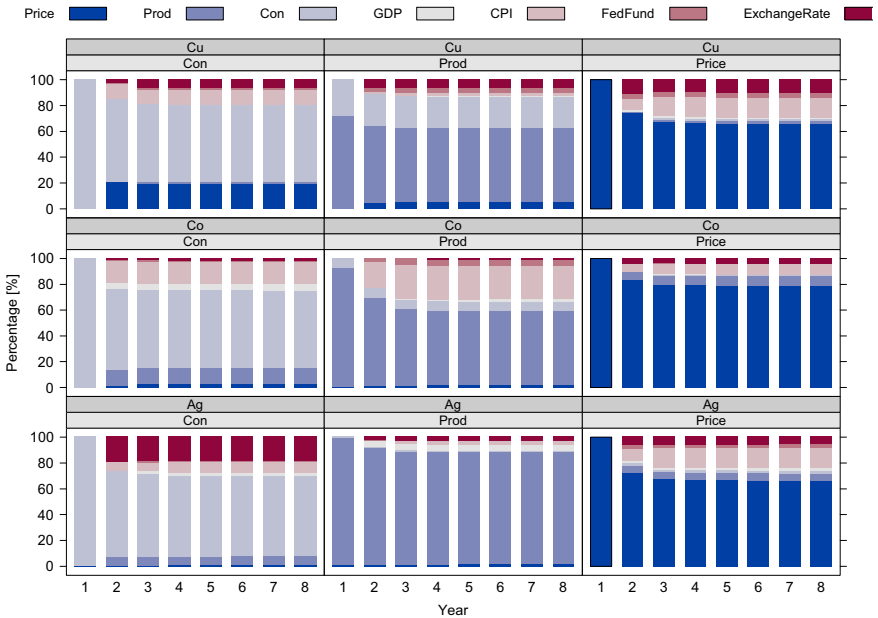

Figure 9-14: FEVD of the consumption, production and price of copper (Cu), cobalt (Co) and silver (Ag). "Con" refers to consumption whereas "Prod" refers to production. The rest of the abbreviations refers to the macroeconomic variables as listed in Table 5.5.

Apart from that, no general trends can be derived from the results. In terms of copper, the price proves to be a significant driver of the demand. However, for cobalt and silver, production levels affect the demand much stronger than the price. Besides that, the FEVD of copper production shows that the demand drives the production more significantly than the price or any other macroeconomic variable. This explains the results observed in Figure 9-13, where the production depreciates when the price increases. The FEVD proves that the decrease in production is a result of the decrease in consumption rather than the increase in price. For cobalt, the production is affected the most by the inflation rate. On the other hand, the production of silver seems to be very stable and is independent of any micro or macroeconomic variables, which further strengthens the argument for silver being used as a stable financial asset.

10 Discussion

10.1 Bottleneck risks of metals

With regards to the bottleneck risk in metals related to PV, the results in this thesis agree with most of the literature that detected bottlenecks in silver (Kleijn et al. 2011; Zuser and Rechberger 2011), indium (Kavlak et al. 2015; Feltrin and Freundlich 2008) and selenium (Kavlak et al. 2015). However, no risk was detected for tellurium, as previously reported by (Zuser and Rechberger 2011; Viebahn et al. 2015). This is owed to the much-reduced market share of thin-film technologies in this thesis, which is derived based on interviews with PV experts from the research and industry. The literature review in chapter 3 reveals that most of the bottlenecks reported in the literature represent a theoretical maximum of considering a complete market dominance of thin-film modules. One of the biggest challenges faced by thin-film modules is the lack of manufacturers, whose current production capacity is unlikely to completely satisfy the future needs of PV in Germany. Therefore, c-Si modules will most likely dominate the PV market in the future. Therefore, the development of PV in the future will not be deterred by bottleneck risk of metals relevant to the thin-film modules, which agrees to the findings of Candelise et al. (2011). However, silver still remains as a critical metal in c-Si modules. Nonetheless, substitution measures are already available and if it can be implemented on a large scale in the near future, the sustainability of c-Si modules with respect to raw materials usage can be further increased since the criticality of silver can be mitigated.

Regarding batteries, lithium is expected to face a severe bottleneck risk considering the current reserve and production levels. However, as previously discussed by Kushnir and Sandén (2012) and Speirs et al. (2014), the future reserve levels of lithium can be extremely large once lithium content in the ocean resources is taken into account. Once an economically feasible technology in extracting lithium is commercially available, the demand for lithium in meeting the requirements for EV can be fulfilled. This is highly likely to be achieved in the future since promising works have already been proposed in the research, for example works by Hoshino (2015) and Virolainen et al. (2016). Apart from lithium, cobalt is also most likely to face a bottleneck in terms of both reserves and production levels. However, the development of cobalt-free post Li-Ion batteries coupled with either a closed-loop recycling or dynamic reserve levels can mitigate all bottleneck risks of cobalt. In fact, Azevedo et al. (2018) reported that the use of cobalt in batteries for EVs can have a 50 to 60 % market share by 2025. This shows the importance of cobalt in EVs will grow in the future and the demand from other sectors such as superalloys and hard materials can be allocated to the EV sector. Similarly, nickel is also risk-free if post Li-Ion batteries can be realized in a timely manner.

In terms of wind turbines, dysprosium is identified as critical in this thesis, which agrees to the findings of most of the literature such as Dutta et al. (2016) and Viebahn et al. (2015). However, unlike the results of Watari et al. (2018), who reported that a closed-loop recycling can completely remove bottleneck risks of metal in wind turbines, the risk of dysprosium is not completely mitigated in this thesis even upon considering a closed-loop recycling and material efficiency measures. Since most of the wind turbines with PMs are expected to be installed offshore in the future, a large stock of dysprosium will still be in use in 2050, which will be available for recycling beyond that. This effect can be seen in Figure 9-5, where a surplus of recycled demand can be achieved between 2048 and 2050. Apart from dysprosium, the supply risk of copper is of particular interest as it has not been identified before in the literature within the context of the deployment of wind turbines in Germany. The bottleneck of copper is a severe problem since it is also used in many other sectors, particularly in building, construction, transportation as well as power transmission and distribution network (IWCC and ICA 2017). The major problem in wind turbines is that copper and dysprosium are substitutes in terms of their usage in generators either with PM or copper windings. This means that the reduction of one metal will eventually lead to the increase of the other if the proposed installed capacities of the energy pathways are fulfilled.

Therefore, unlike PV, a conclusion regarding the better development scenario cannot be proposed for wind turbines. However, the conservative scenario of installing smaller turbines with copper windings onshore, while installing larger turbines offshore, seems to be the better option since the bottleneck risk of copper is relatively lower than dysprosium. However, this will pose a major risk in terms of land competition with other sectors, such as agriculture. Another possible way of reducing the risk faced by the metals relevant to wind turbines is by substituting part of the generation capacity of wind turbines with PV. Fath (2018) proved in her thesis that the maximum rooftop PV potential for Germany amounts to around 3000 GW_p, which shows that PV is very much capable of accounting for part of the generation capacity of wind turbines. However, this might actually increase the total costs of the energy system due to the higher requirement for storages to even out the peak generation at noon. In order to systematically analyse the implications of this measure, the information regarding the material use has to be included in energy system models. By setting limitations such as the annual material availability, a sustainable pathway that does not violate any metal allocations can be proposed and investigated. This enables the additional systemic costs and technical requirements of such an energy system to be ascertained.

The results of this thesis show that recycling is a key strategy in decreasing the overall primary material demand and improving the sustainability of the technologies. In addition, recycling presents a huge opportunity to ensure that the critical metals remain in Germany upon the lifespan of their respective products and be used in manufacturing new products. This will consequently reduce the material dependency of Germany on foreign countries in the long run. Earliest PV plants and wind turbines in Germany are expected to be decommissioned on a large scale in the next 5 to 10 years. Although there are already established markets for scrap metals, recycling of technologies such as

PV or wind turbine is still at an early stage of development. Moreover, the recycling process of critical metals such as REEs is still highly limited by process costs and output quality (Binnemans et al. 2013; Royen and Fortkamp 2016). On top of that, closed-loop recycling, in reality, may require more energy and more material due to production losses and quality degradation of material (Adibi et al. 2017). These aspects should be assessed in detail in order to prepare the industry to utilize the high material recovery potential that the energy system has to offer in the future that will reduce any possible supply bottlenecks. Closed-loop recycling is much more probable to achieve in batteries than in PV or wind turbines. The knowledge and business models of recycling Pb-acid batteries, which are by far one of the most recycled end-products in the world, can be transferred to Li-Ion batteries in order to establish closed-loop recycling.

Even if certain technologies will not be relevant in the future, such as the thin-film PV modules, recycling them might still be beneficial to other sectors. Currently, there is approximately 2 GW_p of thin-film modules in in-use stocks in Germany. Recycling these modules will ensure that metals such as tellurium and gallium can be reallocated to other sectors such as electronic semiconductors in the future. However, recycling is ultimately a matter of economic feasibility. Therefore, the question remains if an effective recycling process for metal stocks can be established if there is no future application for a particular technology. If the PV market is going to be dominated by c-Si modules in the future, establishing thin-film modules recycling facilities will be extremely difficult due to the absence of the product in the future. Similarly, reducing the demand for the application of critical metals reduces the incentives in recycling them since the amount of recoverable metal might not be justified by the extraction costs. Therefore, reducing the usage of critical metals and increasing the rate of recycling at the same time is a paradox in reality. A concentrated use of a critical metal in a single application will lead to a higher rate of recycling in the future, as compared to a diluted use in various applications. Furthermore, Raugei and Fthenakis (2010) argue that the increased use of cadmium in CdTe modules are in fact beneficial to the environment, which would otherwise be discarded to the environment as a residue to mining zinc ores. Therefore further research is required to address these issues in order to come up with an optimal strategy to mitigate bottleneck risks as well as to institute an effective recycling strategy.

Overall, the bottleneck risks of all metals are significantly lower once the cumulative demands are compared to the reserve base of the metals. Nonetheless, the need to intensify research efforts and to further reduce the total material demand should not be undermined to continue increasing the holistic sustainability of renewable energy technologies and batteries. Improving manufacturing techniques will clearly help in reducing the production losses, which for instance, currently amounts to an average 5 % of the total material demand for wind turbines. Another strategy is to make efforts in improving the reliability of components, which would reduce the additional demand due to repair and component exchanges. On a different note, the long-term pathway seems to be the best option in achieving the German energy transformation process since it has the lowest material demand and bottlenecks. However, this pathway was derived based on the principle that it is more

economical to expand the generation capacities elsewhere in Europe and transfer them to Germany via the power distribution network. In doing so, the installed capacities of renewable energy technologies in Germany can only be lowered. Therefore, the maximum allocation limits for the long-term and climate protection pathways should be lowered since part of the generation capacities are outsourced. In this context, the results of the transformation pathway represent the most accurate analysis of the raw material assessment of the German energy transformation process, since the energy pathway is derived based on the assumption of an import and export transmission capacity of only 5 GW_{el} in 2050.

Comparing the results with existing literature shows that this thesis did indeed contribute to closing the research gaps mentioned in chapter 4.1.3. Firstly, by conducting a comprehensive analysis of all involved metallic elements and a broader research boundary, criticality in various metals has been identified. The possibility of supply bottlenecks of tin in PV or manganese and copper in wind turbines have not been identified in the literature, since the existing literature on this topic predominantly focuses on REEs and critical metals. Besides that, the results in this thesis show that an ex-ante assumption of no bottleneck for non-critical metals can backfire. This applies especially to the results of Viebahn et al. (2015), who excluded silver from their analysis of material criticality in Germany with the assumption that the supply will be enough to satisfy the future demand for PV. Secondly, by considering more realistic development scenarios and technology market shares, overestimation of supply bottlenecks could be avoided. Therefore, no supply bottleneck is identified for Gallium in Germany, as previously reported by Erdmann et al. (2011). Similarly, the application of the reserve base to compare the cumulative metal demand in this thesis massively reduces the supply bottlenecks. For instance, the supply bottlenecks of vanadium in stationary batteries as well as tellurium can be almost completely mitigated, suggesting that these metals might not be critical in the future as opposed to the finding of Viebahn et al. (2015) and (Andersson 2000; Zuser and Rechberger 2011; Månberger and Stenqvist 2018), respectively.

10.2 Joint-production of metal

The results of the Granger-causality test of jointly produced primary metal and co-product agree, to a certain extent, to the findings in the literature. Similar to the results of Ciner (2001) as well as Krawiec and Górska (2015), causality relationship is identified in this thesis between the prices of silver and gold. Furthermore, the causal link between copper and gold prices has also been previously proved by Śmiech and Papież (2012), while the link between copper and molybdenum has been established by Campbell (1985). Causal links are also identified between nickel and copper as well as between zinc and cadmium, as previously proved by Basoglu et al. (2014) as well as Kim and Heo (2012), respectively. Considering these results, as well as the causality identified between metal pairs of lead-zinc and zinc-silver, it can be concluded that the prices of primary metals and co-products do Granger-cause each other. On the other hand, it cannot be conclusively said that

primary metals Granger-causes the prices of by-products due to the lack of strong evidence. On a different note, metals that are produced together should hypothetically have an inversely proportional price relationship. Only five out of 13 causal links between jointly-produced metals have a negative sign.

The reason for the weak relationship of primary metals and their by-products as well as the unexpected directions of the price movements can be explained by the production volume of the by-products that is much lower compared to the primary metals. As detailed in chapter 3.1, when the production of one metal increases, the companion metal is expected to experience an oversupply, assuming that other variables remain unchanged. The results in this thesis however, do not strongly agree with this. There are two main reasons for this. First and foremost, it can be that the demands for both metals increase simultaneously. Therefore, the supply-demand equilibrium can be maintained in both metals and an oversupply does not occur. Secondly, the additional volume of the companion metals is stored, which prevents them from entering the market. Additionally, the companion metals can also be discarded if the available volume is too small or the operational costs of the companion metals cannot be justified by the market prices. Ultimately, this prevents the surplus of the companion products and does not change the price relationship between the metals. Afflerbach et al. (2014) further discussed that the additional production of the primary metal, as a result of increased demand, can lead to higher marginal costs. Consequently, the profit margin of the primary metal can decrease. Therefore, the supply of companion metals into the market will be strictly controlled by mine operators since they are needed to provide additional profit to compensate the losses caused by the primary metals. One common practice of achieving this is to relocate the mining activity to a different area within a mine. Jordan (2017) proved that mine operators utilize the geographical distribution of various ore-grades in a mine since it provides more flexibility to carry out targeted mining in different parts of a mine so that the demand and supply of other companion metals remain unchanged.

In general, the contribution of this thesis to the existing literature on the price relationship between jointly produced metals is the quantitative analysis based on a well-elaborated statistical framework. The results of the Granger-causality test are more informative than the currently available literature utilizing sign test Campbell (1985) or simple correlation test Afflerbach et al. (2014) as it can be used to anticipate the price movements of co- and by-products based on the market situation of primary metals. In addition to that, the causality analysis between jointly-produced metals relevant to wind turbines and batteries is an extension to the works of Kim and Heo (2012), who only considered PV-related metals in their analysis.

10.3 Joint-consumption of metal

The analysis of the price dependencies of jointly consumed metals is one of the major contributions of this thesis since it has not been empirically analysed in the literature. The results of this thesis confirm the assumptions of Jerrett and Cuddington (2008), Fizaine (2013) and Rossen (2015), that a price dependency should theoretically exist between metals that share similar field of application. The second hypothesis in this thesis states that the increasing deployment of renewable energy technologies will lead to price dependencies between the jointly-consumed metals. The results of this thesis show that this hypothesis is true to a certain extent. In terms of PV, the price of indium is Granger-caused by the price of selenium. This shows that joint-consumption has a greater effect on the price of indium compared to the joint production effect, due to the lack of causality with the price of zinc. On the other hand, the bi-directional causalities between copper-nickel and copper-selenium cannot be completely attributed to the joint-consumption effect since they are also related in terms of production. 60 % of the causal relationships have an expected positive sign, which is a result of a simultaneous increase in metal demand if the demand for a common product increases. The negative signs observed between metal pairs such as selenium-cadmium can be explained by the fact that these metals are substitutes in the form of GIGS and CdTe PV modules. Historically, the market share within thin-film modules has been shifting from CdTe towards CIGS, which shows that the share of CdTe has been substituted by CIGS. This explains the negative relationship between selenium and cadmium since the reduced demand for the latter metal will cause the price to drop, assuming that other variables such as production remains constant. Similarly, the price of nickel is negatively Granger-caused by silver, which is used as a substitute in c-Si modules.

In terms of batteries, significant bidirectional causality is observed between lithium-nickel as well as nickel-manganese, all of which are used together in NMC type Li-Ion batteries. The positive coefficient between lithium and nickel indicates that these metals are complements due to their joint-usage in NMC and NCA type Li-ion batteries. As for the negative coefficients between manganese and nickel, the existence of LMO and NCA batteries where only one of the metals is applied in either one of the batteries, causes a significant substituting effect between their prices. Interestingly, the price of cobalt, which is not Ganger-caused by its companion metals in terms of production, is affected by manganese. However, with increasing utilization of lithium, nickel and cobalt in Li-Ion batteries, the price dependencies between these metals can be expected to strengthen in the future. In wind turbines, the relationship between copper and the REEs are tested, which only led to the identification of causality between neodymium and dysprosium prices. Although both metals are used together in manufacturing permanent magnets, their dependencies can also be related to their joint production. This effect cannot be differentiated further within the framework of this thesis. The absence of any relationship between copper and REE can be attributed to the fact that the use in wind turbines and generators are not the main application field of copper.

On a different note, metal pairs that are related in both production and consumption, such as copper and selenium, should hypothetically have positive signs. This is owed to the fact that a change in demand will change the supply simultaneously and vice versa. For example, an increase in demand for CIGS modules will increase the demand for copper and selenium simultaneously. As a result, increasing the production of a copper mine with selenium as a by-product will not lead to a surplus of any metals, which causes the prices of both metals to move in a similar direction. Nonetheless, if the equilibrium between the joint-production and joint-consumption effect is overthrown by any of the criteria, then metal pairs that are related in both production and consumption may have an ambiguous signalled relationship. This may explain the negative Granger-causality between dysprosium and neodymium. While the production of 91 % of global dysprosium occurs as a by-product of other REEs, only 37 % of neodymium is produced as a by-product of other REEs. Therefore, the increasing demand for dysprosium clearly creates a surplus for neodymium, which causes the prices to move in the opposite direction despite being used together in permanent magnets.

Looking at the bigger picture of the interrelationship between the metals, results indicate that a cross-technology dependency of metal prices does exist. The relationships between jointly-consumed metals are strongly depended on the level of consumption aggregations. For instance, at the end-product level, PV and wind turbines can be considered as two different products. However, at a higher level of aggregation, both technologies can be classified into one category, namely renewable energy technologies. Therefore the expansion of the energy system to increase the share of renewables increases the demand for all technologies, thus of all related metals. This explains the predictive power of silver in PV for example, over dysprosium and neodymium that are used in wind turbines. Significant relationships are also present between metals in PV and batteries, such as lithium-silver, silver-nickel, lithium-indium and nickel-indium. Currently, every second rooftop PV system in Germany is installed together with a battery as a PV-home storage system. An intensified application of PV-home storage systems in Germany will further strengthen the relationships between the metals in PV and batteries.

However, it is important to mention that there might be additional relationships beyond the definitions in this thesis that cause dependencies between the metal prices. The presence of Granger-causality at a higher level of consumption does not rule out the possibility of significant relationships at an even higher aggregation level. Indirect joint-consumption is another factor that may cause price dependencies, especially when metal prices react similarly to external macroeconomic factors. This has been previously proven by works of (Labys et al. 1999; Batten et al. 2010; Kyrtsou and Labys 2006; Klotz et al. 2014), who identified significant relationships between commodity prices, including industrial and precious metals, and macroeconomic factors such as inflation rates and business cycles. Besides that, economic prosperity might lead to increased industrial production and demand for metals in general, which may cause metal prices to behave similarly. The effect of an indirect joint-consumption cannot be differentiated in the results and is a

major limitation to the methodology in this thesis. Nonetheless, the central message is still valid, that jointly-consumed metals in renewable energy technologies have a price dependency between them, and that the continuous installation of these technologies will further strengthen this effect.

Overall the price dependencies proven in this thesis show the importance of a systemic analysis while proposing policies for renewable energy technologies in the future. A demand shock in a particular technology might lead to an economic constraint of another technology due to the dependencies of their technologies. A technological breakthrough is an example of a demand shock. For instance, the success of overcoming challenges faced by Li-S or Li-Air batteries might lead to a sudden surge in demand for metals such as lithium, nickel and cobalt. Consequently, the increase in price for the aforementioned metals might affect other metals such as silver and indium, which can in turn, dampen cost reduction measures in PV. Besides that, stronger policies to ensure a higher rate of recycling for jointly-consumed metals with a large market share in an end-use product is necessary as this will ensure a more stable supply of metals. In the long-run, joint-consumption of metals will eventually lead to a joint-production via a functional closed-loop recycling process, thus limiting the impact of price fluctuations of the companion metals.

10.4 Impact of temporary shocks on the metal markets

The approach of conducting a VAR analysis for individual metals with respect to their supply and demand as well as macroeconomic variables is a novel contribution since most of the existing studies predominantly focus on aggregated price indexes (Akram 2008; Anzuini et al. 2012) or only consider the dependency between metal prices without considering their supply-demand equilibrium (Xiarchos 2005; Antonakakis and Kizys 2015). The works of Mo and Jeon (2018), who carried out a VECM analysis to test the impact of increasing demand for EVs on battery-related metals, is the most comparable work to the VAR analysis in this thesis.

The results of the impulse response functions show all metal prices react immediately towards a sudden change in demand or supply of metals. In addition to that, it can be ascertained that a long-run equilibrium is present in the metal market, in which the relationship between the micro and macroeconomic variables causes the market to adjust itself towards equilibrium in case of a temporary shock. This result agrees with the findings of Erbil and Roache (2010), who proved this for metals such as copper, nickel, tin and zinc. Referring back to the previous example of a breakthrough of solid-state batteries, the demand shock for the metals will impact their prices, which however, will eventually return to equilibrium. Nonetheless, based on the results, it may take somewhere between 2 to 5 years for the equilibrium to be reached.

Another important result of this thesis is the evidence of the increasing financialisation of metals, which is clearly shown in silver. The financialisation of commodities has been extensively analysed in the field of research by works such as, but not limited to, (Silvennoinen and Thorp 2013; Henderson et al. 2015; Mayer et al. 2017). The financialisation of metals is caused by activities of investors who take positions in metals and treat them the same as stocks or bonds to capture profits. The increasing investment activities in commodities evidently gave birth to other financial effects, namely momentum investments and herding effect. Lutzenberger et al. (2017) previously proved that the momentum effect is significant in improving the predictive power of metal prices, thus asserting the financialisation of metals. The silver market presents a market anomaly, where the demand keeps increasing independent of the direction of the price movement. This is due to the behaviour of the investors that keep purchasing since they assume that the price of silver will eventually keep increasing and they can find a buyer at a higher price in the future. On the other hand, the herding effect is caused by a group of investors who imitates the activities of other investors, which creates a snowball effect in the investment activities. Babalos et al. (2015) proved that significant herding activities between commodities, including silver, did exist during the global financial crisis in 2008. A comprehensive literature review on this topic is provided by Spyrou (2013). In short, the results indicate that the effect of financialisation is apparent in the silver market. This shows that the use of silver in PV not only pose a physical availability risk for PV modules but also a high economic risk due to the susceptibility towards financialisation of metals. With the increasing importance of critical metals such as cobalt and lithium in the future, increasing activities of financialisation can be expected in the future as well, which might lead to severe uncertainties regarding their prices.

The results of the forecast error variance decomposition show that the movements in metal prices are predominantly affected by their own historical price. While copper price impacts the demand significantly, the same cannot be said for minor metals such as cobalt and silver, where the impact of the price is almost negligible to the demand. This poses a threat to the development of renewable energy technologies since tough competition can be expected with other sectors to secure metal demand. It can be expected that every sector will try to secure their required demand independently of the price. However, this is not the case for industrial metals like copper, where the price is the largest external driver for the demand. Consequently, this opens up the discussion of which sector is willing to pay higher prices in securing the required metal demand. Helbig et al. (2017) have previously investigated this issue using a scale of raw material productivity per sector for 17 mega sectors in the EU as proposed by the EC (2014). The basic principle of this scale is that highly productive mega sectors are able to secure prioritized supply of raw materials due to their high specific value added. While renewable energy is not a sector per se in this categorisation, the next most suitable classification would be "electronics and ICT", which is the third most productive mega sector behind refining and pharmaceuticals. This means that renewable energy technologies have high competitive power in securing metal demand. However, there might still be strong competition within a sector itself, such as the use for gallium in semiconductors.

The results of the forecast error variance decomposition further strengthen the fact that indirect causality effects may be present among metal prices due to dependencies to macroeconomic factors. One of the most significant factors is the inflation rate, which supports the findings by Chen et al. (2010) as well as Jain and Ghosh (2013). One may argue that the impact of inflation rate on metal prices seem counterintuitive since the willingness of consumers to pay more for a product is what defines the inflation rate. However, in the VAR model, all variables are related to each other via certain lag values. This means that an increasing inflation rate will cause consumers to expect a higher inflation rate in the future, thus increasing spending and consumption. This will evidently lead to the increase in metal prices. Therefore, while the results show that the demand does not directly affect the metal prices, it indirectly affects via the linkage with other variables such as the inflation rate.

Due to data unavailability, the VAR analysis is only conducted for selected metals. However, by linking the results with the findings of the Granger-analysis, broader statements regarding the impact on minor metals can be made. Results show that a demand shock in metals relevant to renewable energy technologies has an immediate impact on their respective prices. This means that prices of other metals such as lithium, manganese, nickel and selenium, which are Granger-caused by the price of copper, will also most likely be affected according to their respective temporal lag lengths. Once again, the importance of recycling has to be reiterated in this section. The results show that the prices of metals decreases if the production increases. Therefore, increasing the rate of recycling should contribute to increasing the production indirectly and hence lowering the price. In addition to that, recycling metals also reduces the vulnerability of price volatility towards external impacts, since the supply can be regulated within Germany.

11 Conclusion and further works

As Germany commits to environmental and climate goals, the utilization of clean energy technologies is expected to increase significantly. However, the application of technologies like photovoltaics (PV), wind turbines and batteries comes at a price due to their dependency towards scarce metals, such as rare earth elements (REEs) and cobalt. This means that large-scale deployment of these technologies might cause supply bottlenecks of related metals in the future. Consequently, this might lead to economic implications in the metal market, which can disrupt a cost-efficient transformation of the German energy system. Under this premise, this thesis aimed at answering two main research questions. Firstly, does the increasing metal demand due to the energy transformation process in Germany lead to supply bottlenecks? Secondly, what are the economic implications of the increasing metal demand due to the energy transformation process on the metal market?

In answering the first research question, the metallic raw material demand for photovoltaics, wind turbines and batteries were investigated. In doing so, several development scenarios and material efficiency measures were considered. In terms of PV, results show that thin-film technologies are at high risk of facing supply bottlenecks due to the criticality of indium, selenium, tin and tellurium. Crystalline silicon (c-Si) solar cells on the other hand, only face risk in silver. With regards to wind turbines, copper and dysprosium are identified as the most critical metals according to current production and reserve level due to extremely high demands as well as lack of feasible and economic measures to mitigate the possible supply risks in the future. As for batteries, lithium, nickel and cobalt are identified as the most critical metals. Among them, the demand for cobalt is expected to exceed the maximum allocation limit for Germany, should no technological breakthrough takes place in the near future involving post-Li-Ion batteries.

However, the supply bottlenecks of the metals can be eased if the energy transformation process is steered in the right direction. For example, results proved that deployment of c-Si PV modules is more sustainable in Germany compared to thin-film modules, given that active measures in substituting silver with copper and nickel are undertaken. Regarding batteries, more resources should be invested in developing post-Li-Ion batteries such as the solid-state or Li-Air and Li-S batteries. Results clearly indicate that the market entry of these novel concepts can take the pressure off cobalt and nickel. However, the lithium demand will overshoot as a result. Nonetheless, the lithium content in brine and ocean is reported to be high enough to cover a large-scale deployment of lithium on a global scale. Besides, efforts in increasing the energy density and the use of second-life batteries can contribute to further reducing the metal demand in batteries. In terms of wind

turbines, since the bottleneck risk of copper is substantially lower than that of dysprosium, smaller wind turbines with electrically-excited generators are a better option in the future, considering from the perspective of material availability. Measures such as improving production techniques, increasing the reliability of turbine components and using lightweight support structures will certainly help in reducing the bottleneck risks.

In addition to these efforts, results showed that one of the most effective ways of reducing the supply bottlenecks would be to establish an effective closed-loop recycling process for the metals. A substantial amount of PV and wind turbines will be available for decommissioning in the next 5 to 10 years in Germany. Early policy measures will ensure that the industry is well-prepared to recover the critical metals once they are decommissioned. Even if some of the metals like tellurium or gallium might not be relevant for future PV modules, their recovery will still benefit other manufacturing sectors, most notably the semiconductor industry. Although such a process does not completely mitigate the risk in certain metals such as dysprosium and cobalt, it certainly facilitates in reducing the bottlenecks in the long-term. It can be observed from the results that most of these metals will still be in the in-use stocks by 2050 and that they would be available for recovery beyond that. Therefore, stronger policies to ensure a higher rate of recycling metals in the investigated technologies are necessary as this will ensure a more stable supply of metals.

The second research question was tested using two approaches. In the first approach, the Toda-Yamamoto approach to Granger-causality testing was applied to test the price dependencies among metals that are present in PV, wind turbines and batteries. This test was first conducted for their respective companion metals in terms of production. Results proved that strong causality relationship exists between co-products and primary metals. For minor metals, no general statements can be made as mixed results were obtained. In the next step, the causality between jointly-consumed metals was tested within each technology, which showed evidence of significant relationships among metals in PV and batteries. A test at a higher aggregation level allowed for an inter-technology analysis, where significant Granger-causalities between the technologies could be observed. Although the existence of the causal link among this metal cannot be directly contributed to their application in these technologies, it can be concluded that large-scale deployment of these technologies in the future will only strengthen causality relationships that are already present. Therefore, it is important for manufacturers of these technologies to consider the joint production and consumption nature of these metals and their corresponding price relationships while diversifying their metal portfolios. This will ensure more cost-effective material substitution measures and provide insights regarding the suitable metals to be applied in alternative concepts to the technologies.

The second approach involved the use of a vector autoregressive analysis in order to test the dynamics of selected metal prices in the investigated technologies and their relationship with demand and supply. In case of a sudden increase in demand, the prices of all metals increase

immediately. However, all metal prices try to return to equilibrium once the market is disrupted. The amplitude of the price movements seemed to correlate with the market volume of the metals, with copper and nickel exhibiting the highest changes in price whereas indium the least. Although no definitive conclusion can be made, results point toward the fact that the market for minor metals is more flexible to adapt to sudden changes. Since most of them are produced as by-products of other industrial metals, their storage capacity might be large enough to store excess produced amount, which can effectively balance the market equilibrium in the short-term. In case of a sudden increase in prices, the demand for all metals decreases except for silver. This effect can be attributed to momentum investment activities, which shows that silver behaves like a financial asset. Therefore, its application in c-Si solar cells carries a huge economic risk, as any speculation or disruption in the market might cause the price to surge, which in turn, increases the price of PV modules. Last but not least, macroeconomic variables such as inflation rate and exchange rate do have a noticeable influence on the metal market. Once again, recycling plays an important role to reduce the economic risks of the metals. A high recycling rate will ensure a more stable supply of metals. In the long-run, joint-consumption of metals will eventually lead to a joint-production via a functional closed-loop recycling, thus limiting the impact of price fluctuations of the companion metals. In doing so, the dependency of Germany on the import of scare metals can be reduced.

Upon the analyses and critical appraisal of this thesis, several prospects for further works are identified. Firstly, this thesis only investigated the metals used in three different technologies. However, there are various other technologies relevant to the energy transformation process, especially heating technologies such as heat pump, combined heat and power plants as well as power grid expansion. Therefore, the analyses have to be expanded to include more technologies in order to be able to assess the complete metal demand and the corresponding risks of the energy transformation process. Secondly, the bottleneck analysis could be extended to supply risk analysis according to the definition and methodology of other works such as Graedel et al. (2012) or Helbig et al. (2016b). In doing so, other important risks such as the environmental implications, the concentration of production and political stability of origin country can also be analysed besides the physical availability of the metals. In this context, it is also highly recommended to combine the material criticality research with energy system analysis. By incorporating the information regarding metal use and availability in existing energy system models, a more realistic transformation pathway that is not only cost-minimal but also has a sustainable use of metals can be obtained. To this end, the energy system model REMod is highly suitable as it is able to provide the complete requirements for the energy transformation process in Germany without any outsourcing of generation capacity in neighbouring countries.

In addition to that, the recycling potential estimated in this thesis only represents the maximum recyclable demand. However, in reality, the actual recoverable demand will be much less, as it might be constraint by economic and technical limitations. Therefore, a detailed analysis of the economic

and technical feasibility of recovering and recycling the raw materials from the investigated technologies has to be carried out in order to estimate the recyclable demand more precisely.

Regarding the Granger-causality analysis, the results in this thesis are strongly limited by the choice of metal-pairs in selected technologies. As further works, it is highly recommended to conduct a more detailed analysis of price dependencies of a smaller batch of metals. This should be combined with the use of relevant metals in other main products and manufacturing sectors. As a consequence, this will evidently enable the investigation of price relationships between renewable energy technologies and other products and contribute further to the discussion of competitions and synergies between various manufacturing sectors. On a different note, the impact of macroeconomic variables on the metal market has to be analysed in detail. In this thesis, the VAR models of all metals have been complemented with similar variables for reasons of simplicity. A detailed analysis of each metal based on a much more thorough literature review is highly recommended. In order to further validate the findings and the trends identified in this thesis, the analysis should be extended to a wider range of metals.

12 List of figures

13 List of tables

14 Publication bibliography

Aberle, Armin G. (2009): Thin-film solar cells. In *Thin Solid Films* 517 (17), pp. 4706–4710. DOI: 10.1016/j.tsf.2009.03.056.

Achner, S.; Barzantny, K.; Vomverg, S.; Groscurth, H.; Hassenstein, W.; Böhling, A.; Breuer, T. (2015): Klimaschutz: Der Plan. Energiekonzept für Deutschland. Greenpeace. Hamburg, checked on 01.03.17.

Adibi, N.; Lafhaj, Z.; Yehya, M.; Payet, J. (2017): Global Resource Indicator for life cycle impact assessment. Applied in wind turbine case study. In *Journal of Cleaner Production* 165, pp. 1517–1528. DOI: 10.1016/j.jclepro.2017.07.226.

Afflerbach, Patrick; Fridgen, Gilbert; Keller, Robert; Rathgeber, Andreas W.; Strobel, Florian (2014): The by-product effect on metal markets – New insights to the price behavior of minor metals. In *Resources Policy* 42, pp. 35–44. DOI: 10.1016/j.resourpol.2014.08.003.

Agora Energiewende (2013): Kostenoptimaler Ausbau der Erneuerbaren Energien in Deutschland. Ein Vergleich möglicher Strategien für den Ausbau von Wind- und Solarenergie in Deutschland bis 2033. With assistance of Consentec GmbH, Fraunhofer Institute for Wind Energy and Energy System Technology (IWES). Available online at https://www.agora-energiewende.de/fileadmin2/Projekte/2012/Kostenoptmaler-Ausbau-EE/Agora_Studie_Kostenoptimaler_Ausbau_der_EE_Web_optimiert.pdf.

Akram, Q. Farooq (2008): Commodity prices, interest rates and the dollar. Norges Bank Working Paper. Norges Bank. Sentrum (Norges Bank Working Paper, 12/2008), checked on 5/11/2018.

Ali, N.; Hussain, A.; Ahmed, R.; Wang, M. K.; Zhao, C.; Haq, B. Ul; Fu, Y. Q. (2016): Advances in nanostructured thin film materials for solar cell applications. In *Renewable and Sustainable Energy Reviews* 59, pp. 726–737. DOI: 10.1016/j.rser.2015.12.268.

Ali, Roshan; Hou, Guo-Jiao; Zhu, Zhen-Gang; Yan, Qing-Bo; Zheng, Qing-Rong; Su, Gang (2018): Predicted Lead-Free Perovskites for Solar Cells. In *Chem. Mater.* 30 (3), pp. 718–728. DOI: 10.1021/acs.chemmater.7b04036.

Alimi, Santos R.; Ofonyelu, Chris C. (2013): Toda-Yamamoto Causality Test Between Money Market, Interest Rate and Expected Inflation: The Fischer Hypothesis Revisited. In *European Scientific Journal* 9 (7), pp. 125–142. Available online at http://eujournal.org/index.php/esj/article/view/859, checked on 5/5/2018.

Alotto, Piergiorgio; Guarnieri, Massimo; Moro, Federico (2014): Redox flow batteries for the storage of renewable energy. A review. In *Renewable and Sustainable Energy Reviews* 29, pp. 325–335. DOI: 10.1016/j.rser.2013.08.001.

Andersson, B.A; Azar, C.; Holmberg, J.; Karlsson, S. (1998): Material constraints for thin-film solar cells. In *Energy* 23 (5), pp. 407–411. DOI: 10.1016/S0360-5442(97)00102-3.

Andersson, Björn A. (2000): Materials availability for large-scale thin-film photovoltaics. In *Prog. Photovolt: Res. Appl.* 8 (1), pp. 61–76. DOI: 10.1002/(SICI)1099-159X(200001/02)8:1<61::AID-PIP301>3.0.CO;2-6.

Andersson, Björn A.; Råde, Ingrid (2001): Metal resource constraints for electric-vehicle batteries. In *Transportation Research Part D: Transport and Environment* 6 (5), pp. 297–324. DOI: 10.1016/S1361-9209(00)00030-4.

Andrea, Davide (2010): Battery management systems. For large lithium-ion battery packs. Boston: Artech House.

Angerer, Gerhard (2009): Rohstoffe für Zukunftstechnologien. Einfluss des branchenspezifischen Rohstoffbedarfs in rohstoffintensiven Zukunftstechnologien auf die zukünftige Rohstoffnachfrage. Stuttgart: Fraunhofer-IRB-Verl. (ISI-Schriftenreihe "Innovationspotenziale"), checked on 8/1/2018.

Antonakakis, N.; Kizys, R. (2015): Dynamic spillovers between commodity and currency markets. In *International Review of Financial Analysis* 41, pp. 303–319. DOI: 10.1016/j.irfa.2015.01.016.

Anzuini, Alessio; Lombardi, Marco J.; Pagano, Patrizio (2012): The Impact of Monetary Policy Shocks on Commodity Prices. Bank of Italy Temi di Discussione Working Paper No. 851. In *SSRN Journal*. DOI: 10.2139/ssrn.2030797.

Appleyard, D. (2012): PV Technology: Swapping Silver for Copper. Replacing sliver in PV module contacts with lower-cost copper is a promising route to cheaper large-scale production. Edited by Renewable Energy World. Available online at https://www.renewableenergyworld.com/articles/print/volume-15/issue-3/solar-tech/pv-technology-swapping-silver-for-copper.html, checked on 8/14/2018.

Arnold, Karin; Friege, Jonas; Krüger, Christine; Nebel, Arjuna; Ritthof, Michael; Samadi, Sascha et al. (2014): KRESSE – Kritische mineralische Ressourcen und Stoffströme bei der Transformation des deutschen Energieversorgungssystems. Abschlussbericht an das Bundesministerium für Wirtschaft und Energie (BMWi). Wuppertal Institut. Wuppertal. Available online at http://wupperinst.org/p/wi/p/s/pd/38/, checked on 16.02.17.

Ashuri, Turaj (2012): Beyond classical upscaling. Integrated aeroservoelastic design and optimization of large offshore wind turbines. [S.l.]: [s.n.].

Aso, Raymond; Cheung, Wai Ming (2015): Towards greener horizontal-axis wind turbines. Analysis of carbon emissions, energy and costs at the early design stage. In *Journal of Cleaner Production* 87, pp. 263–274. DOI: 10.1016/j.jclepro.2014.10.020.

Ates, Mehmet Nurullah; Gunasekara, Iromie; Mukerjee, Sanjeev; Plichta, Edward J.; Hendrickson, Mary A.; Abraham, K. M. (2016): In Situ Formed Layered-Layered Metal Oxide as Bifunctional Catalyst for Li-Air Batteries. In *J. Electrochem. Soc.* 163 (10), A2464-A2474. DOI: 10.1149/2.0111613jes.

Ausfelder, Florian; Drake, Frank-Detlef; Erlach, Berit; Fischedick, Manfred; Henning, Hans-Martin; Kost, Christoph et al. (2017): "Sektorkopplung" - Untersuchungen und Überlegungen zur Entwicklung eines integrierten Energiesystems. München, Halle (Saale), Mainz: acetech - Deutsche Akademie der Technikwissenschaften e.V.; Deutsche Akademie der Naturforscher Leopoldina e.V. -

Nationale Akademie der Wissenschaften; Union der Deutschen Akademien der Wissenschaften e.V. (Schriftenreihe Energiesysteme der Zukunft).

Ayres, Robert U.; Ayres, Leslie W.; Råde, Ingrid (2003): The Life Cycle of Copper, Its Co-Products and Byproducts. Dordrecht: Springer (Eco-Efficiency in Industry and Science, 13). Available online at http://dx.doi.org/10.1007/978-94-017-3379-3.

Azevedo, Marcelo; Campagnol, Nicolò; Hagenbruch, Toralf; Hoffmann, Ken; Lala, Ajay; Ramsbottom, Oliver (2018): Lithium and cobalt - a tale of two commodities. Metals and Mining. Edited by McKinsey&Company. Available online at https://www.mckinsey.com/~/media/mckinsey/industries/metals%20and%20mining/our%20insights/lithium%20and%20cobalt%20a%20tale%20of%20two%20commodities/lithium-and-cobalt-a-tale-of-two-commodities.ashx, checked on 8/28/2018.

Babalos, Vassilios; Stavroyiannis, Stavros; Gupta, Rangan (2015): Do commodity investors herd? Evidence from a time-varying stochastic volatility model. In *Resources Policy* 46, pp. 281–287. DOI: 10.1016/j.resourpol.2015.10.011.

Bak, Seong-Min; Hu, Enyuan; Zhou, Yongning; Yu, Xiqian; Senanayake, Sanjaya D.; Cho, Sung-Jin et al. (2014): Structural changes and thermal stability of charged LiNixMnyCozO_2 cathode materials studied by combined in situ time-resolved XRD and mass spectroscopy. In *ACS applied materials & interfaces* 6 (24), pp. 22594–22601. DOI: 10.1021/am506712c.

Ball, James M.; Lee, Michael M.; Hey, Andrew; Snaith, Henry J. (2013): Low-temperature processed meso-superstructured to thin-film perovskite solar cells. In *Energy Environ. Sci.* 6 (6), p. 1739. DOI: 10.1039/c3ee40810h.

Ballantyne, Andrew D.; Hallett, Jason P.; Riley, D. Jason; Shah, Nilay; Payne, David J. (2018): Lead acid battery recycling for the twenty-first century. In *Royal Society open science* 5 (5), p. 171368. DOI: 10.1098/rsos.171368.

Bartsch, J.; Mondon, A.; Bayer, K.; Schetter, C.; Hörteis, M.; Glunz, S. W. (2010): Quick Determination of Copper-Metallization Long-Term Impact on Silicon Solar Cells. In *Journal of The Electrochemical Society* 157 (10), H942. DOI: 10.1149/1.3466984.

BASF (2017): Ultramid and Ultradur. Engineering plastics for photovoltaic mounting system. Available online at www.plasticsportal.eu/solar.

Basoglu, Mustafa Serdar; Korkmaz, Turhan; Cevik, Emrah Ismail (2014): London Metal Exchange. Causality Relationship between the Price Series of Non-Ferrous Metal Contracts. In *International Journal of Economics and Financial Issues* 4 (4), pp. 726–734. Available online at http://www.econjournals.com/index.php/ijefi/article/download/875/pdf.

Batten, Jonathan A.; Ciner, Cetin; Lucey, Brian M. (2010): The macroeconomic determinants of volatility in precious metals markets. In *Resources Policy* 35 (2), pp. 65–71. DOI: 10.1016/j.resourpol.2009.12.002.

Beharelle, Anjali Raja; Small, Steven L. (2016): Imaging Brain Networks for Language. In : Neurobiology of Language: Elsevier, pp. 805–814.

Behn, Ralf; Byfield, Selina (Eds.) (2016): Consulting with energy scenarios: Requirements for scientific policy advice. Position paper. Halle: acatech – National Academy of Science and Engineering; German National Academy of Sciences Leopoldina; Union of the German Academies of Sciences and Humanities (Schriftenreihe zur wissenschaftlichen Politikberatung).

Bergholz, Timm (2015): Lithiumbatterien für stationäre und mobile Anwendungen. Benchmarking und experimentelle Umsetzung. Jülich: Forschungszentrum Jülich (Schriften des Forschungszentrums Jülich Reihe Energie & Umwelt / Energy & Environment, 275).

Bhattacharya, R. N.; Ramanathan, K. (2004): Cu(In,Ga)Se2 thin film solar cells with buffer layer alternative to CdS. In *Solar Energy* 77 (6), pp. 679–683. DOI: 10.1016/j.solener.2004.05.009.

Binder, Claudia R.; Graedel, T. E.; Reck, Barbara (2006): Explanatory Variables for per Capita Stocks and Flows of Copper and Zinc. In *Journal of Industrial Ecology* 10 (1-2), pp. 111–132. DOI: 10.1162/108819806775545475.

Binnemans, Koen; Jones, Peter Tom; Blanpain, Bart; van Gerven, Tom; Yang, Yongxiang; Walton, Allan; Buchert, Matthias (2013): Recycling of rare earths. A critical review. In *Journal of Cleaner Production* 51, pp. 1–22. DOI: 10.1016/j.jclepro.2012.12.037.

Bittau, F.; Artegiani, E.; Abbas, A.; Menossi, D.; Romeo, A.; Bowers, J.; Walls, J. (2018a): Magnesium-doped Zinc Oxide as a High Resistance Transparent Layer for thin film CdS/CdTe solar cells. Presented at the 2017 IEEE 44th. Photovoltaic Specialists Conference (PVSC). Washington, D.C., June 25-30th. Available online at https://dspace.lboro.ac.uk/2134/27046.

Bittau, Francesco; Potamialis, Christos; Togay, Mustafa; Abbas, Ali; Isherwood, Patrick J.M.; Bowers, Jake W.; Walls, John M. (2018b): Analysis and optimisation of the glass/TCO/MZO stack for thin film CdTe solar cells. In *Solar Energy Materials and Solar Cells* 187, pp. 15–22. DOI: 10.1016/j.solmat.2018.07.019.

Blomgren, George E. (2017): The Development and Future of Lithium Ion Batteries. In *Journal of The Electrochemical Society* 164 (1), A5019-A5025. DOI: 10.1149/2.0251701jes.

Bloomberg (2018a): Tesla's Cobalt-Light Batteries Seen Providing Cost Advantage. Edited by Anthony Palazzo. Available online at https://www.bloomberg.com/technology, checked on 10/19/2018.

Bloomberg (2018b): Tesla's Model 3 Is Becoming One of America's Best-Selling Sedans. Edited by Tom Randall, Gabrielle Coppola. Available online at https://www.bloomberg.com/hyperdrive, checked on 10/19/2018.

BMWi (Ed.) (2017a): Langfristszenarien für die Transformation des Energiesystems in Deutschland. With assistance of Fraunhofer ISI, Consentec GmbH, ifeu. Available online at https://www.bmwi.de/Redaktion/DE/Artikel/Energie/langfrist-und-klimaszenarien.html, updated on 2017, checked on 4/12/2018.

BMWi (2017b): Langfristszenarien für die Transformation des Energiesystems in Deutschland. Modul 2: Modelle und Modellverbund. Fraunhofer ISI; Consentec GmbH; IFEU; TU Wien; M-Five; TEP Energy GmbH. Available online at https://www.bmwi.de/Redaktion/DE/Downloads/B/berichtsmodul-2-modelle-und-modellverbund.pdf?__blob=publicationFile&v=6, checked on 4/16/2018.

BMWi (2018): Regulatory environment and incentives for using electric vehicles and developing a charging infrastructure. Federal Ministry for Economics Affairs and Energy. Available online at https://www.bmwi.de/Redaktion/EN/Artikel/Industry/regulatory-environment-and-incentives-for-using-electric-vehicles.html, checked on 11/2/2018.

BNEF (2018): Electric Vehicle Outlook. Bloomberg New Energy Finance. Available online at https://bnef.turtl.co/story/evo2018?teaser=true.

Borensztein, Eduardo; Reinhart, Carmen (1994): The Macroeconomic Determinants of Commodity Prices. Washington, D.C: International Monetary Fund (IMF Working Papers, Working Paper No. 94/9). Available online at http://elibrary.imf.org/view/IMF001/07143-9781451927221/07143-9781451927221/07143-9781451927221.xml.

Boryta, D. A.; Kullberg, T. F.; Thurstion, A. M. (2011): Production of lithium compounds directly from lithium containing brines. Applied for by Chemetall Foote Corporation. App. no. 12/962,423. Patent no. US 8,057,764 B2.

Brautigam, A.; Rothacher, T.; Staubitz, H. (2018): Fact sheet: The energy storage market in Germany. Edited by William McDougall. Germany Trande and Invest. Berlin.

Breusch, Trevor S. (1978): Testing for Autocorrelation in Dynamic Linear Models. In *Australian Economic Papers* 17 (31), pp. 334–355. DOI: 10.1111/j.1467-8454.1978.tb00635.x.

Brooks, David B. (1965): Supply and Competition in Minor Metals. Abingdon, Oxon, New York, NY: RFF Press (Routledge revivals).

Buchert, Matthias (2011): Rare Earths - a Bottleneck for future Wind Turbine Technologies? in Wind Turbine Supply Chain & Logistics, Berlin, 29th of August 2011. Öko-Institut e.V. Available online at https://www.oeko.de/oekodoc/1296/2011-421-en.pdf.

Buchert, Matthias; Jenseit, Wolfgang; Merz, Cornelia; Schüler, Doris (2011): Ökobilanz zum „Recycling von Lithium-Ionen-Batterien" (LithoRec). Endbericht. Edited by Öko-Institut e.V. Darmstadt. Available online at https://www.oeko.de/oekodoc/1500/2011-068-de.pdf, checked on 8/8/2018.

Buchholz, Peter; Brandenburg, Torsten (2018): Demand, Supply, and Price Trends for Mineral Raw Materials Relevant to the Renewable Energy Transition Wind Energy, Solar Photovoltaic Energy, and Energy Storage. In *Chemie Ingenieur Technik* 90 (1-2), pp. 141–153. DOI: 10.1002/cite.201700098.

Bundesnetzagentur (2017): Erneuerbare Energien - Anlagenregister. Veröffentlichung Anlagenregister August 2014 bis Dezember 2016. Available online at https://www.bundesnetzagentur.de/DE/Sachgebiete/ElektrizitaetundGas/Unternehmen_Institutionen/ErneuerbareEnergien/Anlagenregister/Anlagenregister_Veroeffentlichung/Anlagenregister_Veroeffentlichungen_node.html;jsessionid=3FA7D7721B01FBAF5F063C5964E9D636, checked on 2/16/2017.

Burck, Jan; Blücher, Felix von; Fabian, Theresa (2010): Welche Energie-Zukunft ist möglich? Ein Vergleich von vier Niedrig-Energie-Szenarien für Deutschland. Edited by Daniela Baum, Katrin Schilling. Germanwatch e.V. Bonn, Berlin.

Burd, Harvey; Byrne, Byron; McAdam, R. A.; Houlsby, Guy; Martin, Chris; Beuckelaers, William et al. (2017): Design aspects for monopile foundations: TC209 Workshop - Foundation Design of Offshore Wind Structures.

Bürger, V.; Hesse, T.; Andreas Palzer; Benjamin Köhler; Sebastian Herkel; Peter Engelmann; Dietlinde Quack (2017): Klimaneutraler Gebäudebestand 2050. Energieeffizienzpotenziale und die Auswirkungen des Klimawandels auf den Gebäudebestand. Edited by Umweltbundesamt (UBA). Dessau-Roßlau.

Buti, Marco; Sapir, André (Eds.) (1998): Economic policy in EMU. A study by the European Commission services. Oxford: Clarendon Press.

Caduff, Marloes; Huijbregts, Mark A. J.; Althaus, Hans-Joerg; Koehler, Annette; Hellweg, Stefanie (2012): Wind power electricity: the bigger the turbine, the greener the electricity? In *Environmental science & technology* 46 (9), pp. 4725–4733. DOI: 10.1021/es204108n.

Campbell, Gary A. (1985): The role of co-products in stabilizing the metal mining industry. In *Resources Policy* 11 (4), pp. 267–274. DOI: 10.1016/0301-4207(85)90044-3.

Campos, Marcos Flavio de; Rodrigues, Daniel; Castro, Jose Adilson de (2018): Replacement of NdFeB by Ferrite Magnets. In *MSF* 912, pp. 106–111. DOI: 10.4028/www.scientific.net/MSF.912.106.

Candelise, Chiara; Speirs, Jamie F.; Gross, Robert J.K. (2011): Materials availability for thin film (TF) PV technologies development. A real concern? In *Renewable and Sustainable Energy Reviews* 15 (9), pp. 4972–4981. DOI: 10.1016/j.rser.2011.06.012.

Cariou, Romain; Benick, Jan; Feldmann, Frank; Höhn, Oliver; Hauser, Hubert; Beutel, Paul et al. (2018): III–V-on-silicon solar cells reaching 33% photoconversion efficiency in two-terminal configuration. In *Nature Energy* 3 (4), pp. 326–333. DOI: 10.1038/s41560-018-0125-0.

Carroll, James; McDonald, Alasdair; Dinwoodie, Iain; McMillan, David; Revie, Matthew; Lazakis, Iraklis (2017): Availability, operation and maintenance costs of offshore wind turbines with different drive train configurations. In *Wind Energ.* 20 (2), pp. 361–378. DOI: 10.1002/we.2011.

Carroll, James; McDonald, Alasdair; McMillan, David (2016): Failure rate, repair time and unscheduled O&M cost analysis of offshore wind turbines. In *Wind Energ.* 19 (6), pp. 1107–1119. DOI: 10.1002/we.1887.

Casals, C. L.; García, B. A.; Cremades, Lázaro V. (2017): Electric vehicle battery reuse. Preparing for a second life. In *Journal of Industrial Engineering and Management* 10 (2), p. 266. DOI: 10.3926/jiem.2009.

Casimir, Anix; Zhang, Hanguang; Ogoke, Ogechi; Amine, Joseph C.; Lu, Jun; Wu, Gang (2016): Silicon-based anodes for lithium-ion batteries. Effectiveness of materials synthesis and electrode preparation. In *Nano Energy* 27, pp. 359–376. DOI: 10.1016/j.nanoen.2016.07.023.

Chan, M. W. Luke; Mountain, C. (1988): The Interactive and Causal Relationships Involving Precious Metal Price Movements. An Analysis of the Gold and Silver Markets. In *Journal of Business & Economic Statistics* 6 (1), p. 69. DOI: 10.2307/1391419.

Chang, Chia-Lin; Della Chang, Jui-Chuan; Huang, Yi-Wei (2013): Dynamic price integration in the global gold market. In *The North American Journal of Economics and Finance* 26, pp. 227–235. DOI: 10.1016/j.najef.2013.02.002.

Chang, Shiuan; Young, Kwo-hsiung; Nei, Jean; Fierro, Cristian (2016): Reviews on the U.S. Patents Regarding Nickel/Metal Hydride Batteries. In *Batteries* 2 (2), p. 10. DOI: 10.3390/batteries2020010.

Chapin, D. M.; Fuller, C. S.; Pearson, G. L. (1954): A New Silicon p-n Junction Photocell for Converting Solar Radiation into Electrical Power. In *Journal of Applied Physics* 25 (5), pp. 676–677. DOI: 10.1063/1.1721711.

Chen, Dongling; Clements, Kenneth W.; Roberts, E.John; Weber, E.Juerg (1991): Forecasting steel demand in China. In *Resources Policy* 17 (3), pp. 196–210. DOI: 10.1016/0301-4207(91)90003-E.

Chen, Yu-Chin; Rogoff, Kenneth S.; Rossi, Barbara (2010): Can Exchange Rates Forecast Commodity Prices? In *Quarterly Journal of Economics* 125 (3), pp. 1145–1194. DOI: 10.1162/qjec.2010.125.3.1145.

Chen, Z.; Li, H. (2008): Overview of different wind generator systems and their comparisons. In *IET Renewable Power Generation* 2 (2), pp. 123–138. DOI: 10.1049/iet-rpg:20070044.

Cheng, Ming; Zhu, Ying (2014a): The state of the art of wind energy conversion systems and technologies: A review. In *Energy Conversion and Management* 88, pp. 332–347. Available online at http://www.sciencedirect.com/science/article/pii/S0196890414007614, checked on 16.02.17.

Cheng, Ming; Zhu, Ying (2014b): The state of the art of wind energy conversion systems and technologies: A review. In *Energy Conversion and Management* 88, pp. 332–347. Available online at http://www.sciencedirect.com/science/article/pii/S0196890414007614, checked on 16.02.17.

Choi, Chul Hun; Cao, Jinjian; Zhao, Fu (2016): System Dynamics Modeling of Indium Material Flows under Wide Deployment of Clean Energy Technologies. In *Resources, Conservation and Recycling* 114, pp. 59–71. DOI: 10.1016/j.resconrec.2016.04.012.

Choi, Young-Kwan (2014): A Study on Power Generation Analysis of Floating PV System Considering Environmental Impact. In *International Journal of Software Engineering and Its Applications* 8 (1), pp. 75–84. DOI: 10.14257/ijseia.2014.8.1.07.

Chopra, K. L.; Paulson, P. D.; Dutta, V. (2004): Thin-film solar cells. An overview. In *Progress in Photovoltaics Research and Applications* 12 (23), pp. 69–92. DOI: 10.1002/pip.541.

Chowdhury, Abdur R. (1987): Are causal relationships sensitive to causality tests? In *Applied Economics* 19 (4), pp. 459–465. DOI: 10.1080/00036848700000016.

Chumchal, C.; Kurzweil, D. (2017): Lead–acid battery operation in micro-hybrid and electrified vehicles. In Jürgen Garche, Eckhard Karden, Patrick T. Moseley, D. A. J. Rand (Eds.): Lead-acid batteries for future automobiles. Amsterdam, Netherlands: Elsevier, pp. 395–414.

Cimiotti, G.; Bartsch, J.; Kraft, A.; Mondon, A.; Glatthaar, M. (2015): Design Rules for Solar Cells with Plated Metallization. In *Energy Procedia* 67, pp. 84–92. DOI: 10.1016/j.egypro.2015.03.291.

Ciner, Cetin (2001): On the long run relationship between gold and silver prices A note. In *Global Finance Journal* 12 (2), pp. 299–303. DOI: 10.1016/S1044-0283(01)00034-5.

Clean Technica (2018): 7 Charts — Tesla Model 3 vs The Competition (US Sales). Edited by Zachary Shahan. Available online at https://cleantechnica.com/2018/08/06/7-charts-tesla-model-3-vs-the-competition-us-sales/, checked on 10/19/2018.

Collins, Elmer; Dvorack, Michael; Mahn, Jeff; Mundt, Michael; Quintana, Michael (2009): Reliability and availability analysis of a fielded photovoltaic system. In : 34th IEEE Photovoltaic Specialists Conference (PVSC), 2009. Philadelphia, Pennsylvania, USA, 7 - 12 June 2009. 2009 34th IEEE Photovoltaic Specialists Conference (PVSC). Philadelphia, PA, USA, 6/7/2009 - 6/12/2009. Institute of Electrical and Electronics Engineers; IEEE Electron Devices Society; IEEE Photovoltaic Specialists Conference; PVSC. Piscataway, NJ: IEEE, pp. 2316–2321.

Contreras, M. A.; Nakada, T.; Hongo, M.; Pudov, A. O. (2003): ZnS(O,OH)/Cu(In,Ga)Se2 solar cell with 18.6% efficiency. In K. Kurokawa, Lawrence L. Kazmerski, B. McNelis, M. Yamaguchi, C. Wronski, Wim C. Simke (Eds.): Proceedings of 3rd World Conference on Photovoltaic Energy Conversion. Joint conference of 13th PV Science & Engineering Conference : 30th IEEE PV Specialists Conference : 18th European PV Solar Energy Conference : Osaka International Congress Center "Gra. World Conference on Photovoltaic Energy Conversion. Osaka: WCPEC 3 Organizing Committee, pp. 570–573.

CPA Australia (2012): Guide to managing commodity risk. Southbank, Victoria: CPA Australia Ltd. Available online at cpaaustralia.com.au.

Deng, Da (2015): Li-ion batteries. Basics, progress, and challenges. In *Energy Sci Eng* 3 (5), pp. 385–418. DOI: 10.1002/ese3.95.

Deng, Yelin; Li, Jianyang; Li, Tonghui; Gao, Xianfeng; Yuan, Chris (2017): Life cycle assessment of lithium sulfur battery for electric vehicles. In *Journal of Power Sources* 343, pp. 284–295. DOI: 10.1016/j.jpowsour.2017.01.036.

Deutsche Windguard (2017): Status des Offshore Windenergieausbaus in Deutschland. With assistance of S. Lüers, A. Wallasch, K. Vogelsang. Varel, Germany. Available online at http://www.windguard.de/_Resources/Persistent/005f7376fe568db6655015912203b4170c0d17c2/Factsheet-Status-Offshore-Windenergieausbau-2017.pdf, checked on 01.03.17.

Dewulf, Jo; van der Vorst, Geert; Denturck, Kim; van Langenhove, Herman; Ghyoot, Wouter; Tytgat, Jan; Vandeputte, Kurt (2010): Recycling rechargeable lithium ion batteries. Critical analysis of natural resource savings. In *Resources, Conservation and Recycling* 54 (4), pp. 229–234. DOI: 10.1016/j.resconrec.2009.08.004.

Dharma, I. Gusti Bagus Budi; Shukor, Mohd Hamdi Abd; Ariga, Tadashi (2009): Wettability of Low Silver Content Lead-Free Solder Alloy. In *Materials Transactions* 50 (5), pp. 1135–1138. DOI: 10.2320/matertrans.M2009024.

Dickey, David A.; Fuller, Wayne A. (1979): Distribution of the Estimators for Autoregressive Time Series with a Unit Root. In *Journal of the American Statistical Association* 74 (366), pp. 427–431. DOI: 10.1080/01621459.1979.10482531.

Diebold, Francis X.; Yilmaz, Kamil (2012): Better to give than to receive. Predictive directional measurement of volatility spillovers. In *International Journal of Forecasting* 28 (1), pp. 57–66. DOI: 10.1016/j.ijforecast.2011.02.006.

Dixit, Mudit; Markovsky, Boris; Schipper, Florian; Aurbach, Doron; Major, Dan T. (2017): Origin of Structural Degradation During Cycling and Low Thermal Stability of Ni-Rich Layered Transition Metal-Based Electrode Materials. In *J. Phys. Chem. C* 121 (41), pp. 22628–22636. DOI: 10.1021/acs.jpcc.7b06122.

DOE (2013): Grid Energy Storage. U.S. Department of Energy. Available online at http://large.stanford.edu/courses/2016/ph240/smith-c1/docs/gyuk.pdf.

DOE (2018): DOE Global Energy Storage Database. Office of Electricity Delivery and Energy Reliability. Edited by Sandia National Laboratories. Available online at https://www.energystorageexchange.org/, checked on 11/11/2018.

Dolado, Juan J.; Lütkepohl, Helmut (1996): Making wald tests work for cointegrated VAR systems. In *Econometric Reviews* 15 (4), pp. 369–386. DOI: 10.1080/07474939608800362.

Dotsey, Michael; Reid, Max (1992): Oil shocks, monetary policy and economic activity. Economic Review, July/August. Federal Reserve Bank of Richmond, checked on 6/9/2017.

Durbin, J.; Brown, R.; Evans, J. (1975): Testing the Constancy of Regression Relationships Over Time Using Least Squares Residuals. In *Journal of the Royal Statistical Society: Series B (Methodological)* 37 (2), pp. 149–192.

Dutta, Tanushree; Kim, Ki-Hyun; Uchimiya, Minori; Kwon, Eilhann E.; Jeon, Byong-Hun; Deep, Akash; Yun, Seong-Taek (2016): Global demand for rare earth resources and strategies for green mining. In *Environmental research* 150, pp. 182–190. DOI: 10.1016/j.envres.2016.05.052.

DW (2018): Can Germany conquer global e-car markets? | DW | 13.07.2018. As reported by Bloomberg New Energy Finance (BNEF) 2016. Deutsche Welle. Available online at https://www.dw.com/en/can-germany-conquer-global-e-car-markets/a-44666788, checked on 11/2/2018.

EC (2014): Report on Critical Raw Materials for the EU. Report of the Ad hoc Working Group on defining critical raw materials. European Commision.

EEG (2017): Gesetz für den Ausbau erneuerbarer Energien (Erneuerbare-Energien-Gesetz - EEG 2017). Available online at https://www.gesetze-im-internet.de/eeg_2014/.

Ehbing, H.; Schauseil, F.; Hoffman, A.; Seidlitz, D. (2013): Photovolatic Solar Module Having a Polyurethane Frame. Applied for by Bayer Material Science AG. App. no. 12/936,308. Patent no. US 8,381,466 B2.

Elshkaki, Ayman; Graedel, T. E. (2013): Dynamic analysis of the global metals flows and stocks in electricity generation technologies. In *Journal of Cleaner Production* 59, pp. 260–273. DOI: 10.1016/j.jclepro.2013.07.003.

Engle, Robert F. (1982): Autoregressive Conditional Heteroskedasticity With Estimates of the Variance of United Kingdom Inflation. In *Econometrica* 50 (4), pp. 987–1008. DOI: 10.2307/1912773.

Engle, Robert F.; Granger, C. W. J. (1987): Co-Integration and Error Correction. Representation, Estimation, and Testing. In *Econometrica* 55 (2), pp. 251–276. DOI: 10.2307/1913236.

Erbil, Nese; Roache, Shaun (2010): How Commodity Price Curves and Inventories React to a Short-Run Scarcity Shock. In *IMF Working Papers* 10 (222), p. 1. DOI: 10.5089/9781455208876.001.

Erdmann, Lorenz; Behrendt, Siegfried; Feil, Moira (2011): Kritische Rohstoffe für Deutschland. Identifikation aus Sicht deutscher Unternehmen wirtschaftlich bedeutsamer mineralischer Rohstoffe, deren Versorgungslage sich mittel- bis langfristig als kritisch erweisen könnte. Edited by Institut für Zukunftsstudien und Technologiebewertung (IZT), adelphi. Berlin, checked on 8/16/2018.

Eryiğit, Mehmet (2017): Short-term and long-term relationships between gold prices and precious metal (palladium, silver and platinum) and energy (crude oil and gasoline) prices. In *Economic Research-Ekonomska Istraživanja* 30 (1), pp. 499–510. DOI: 10.1080/1331677X.2017.1305778.

Escribano, Alvaro; Granger, Clive W. J. (1998): Investigating the relationship between gold and silver prices. In *J. Forecast.* 17 (2), pp. 81–107. DOI: 10.1002/(SICI)1099-131X(199803)17:2<81::AID-FOR680>3.0.CO;2-B.

Essig, Stephanie; Allebé, Christophe; Remo, Timothy; Geisz, John F.; Steiner, Myles A.; Horowitz, Kelsey et al. (2017): Raising the one-sun conversion efficiency of III–V/Si solar cells to 32.8% for two junctions and 35.9% for three junctions. In *Nat Energy* 2 (9), p. 3. DOI: 10.1038/nenergy.2017.144.

Esso, Loesse Jacques (2010): Threshold cointegration and causality relationship between energy use and growth in seven African countries. In *Energy Economics* 32 (6), pp. 1383–1391. DOI: 10.1016/j.eneco.2010.08.003.

EU (2017): Directive (EU) 2017/2102 of the European Parliament and of the council of 15 November 2017 amending Directive 2011/65/EU on the restriction of the use of certain hazardous substances in electrical and electronic equipment. Official Journal of the European Union.

EuPD Research (2018): sonnen und LG Chem als Führungsduo im deutschen Markt für Heimspeicher. EuPD Research Sustainable Management GmbH. Available online at https://www.eupd-research.com/en/home/view-details/sonnen-und-lg-chem-als-fuehrungsduo-im-deutschen-markt-fuer-heimspeicher/.

Eymann, Lea; Stucki, Matthias; Fürholz, Andreas; König, Alex (2015): Ökobilanzierung von Schweizer Windenergie. Bundesamt für Energie BFE. Bern.

Fakharuddin, Azhar; Rossi, Francesca de; Watson, Trystan M.; Schmidt-Mende, Lukas; Jose, Rajan (2016): Research Update. Behind the high efficiency of hybrid perovskite solar cells. In *APL Mater.* 4 (9), p. 91505. DOI: 10.1063/1.4962143.

Farrow, Scott; Krautkraemer, Jeffrey A. (1989): Extraction at the intensive margin. In *Resources and Energy* 11 (1), pp. 1–21. DOI: 10.1016/0165-0572(89)90002-9.

Fath, Karoline (2018): Technical and economic potential for photovoltaic systems on buildings. Dissertation.

Feifel, Markus; Ohlmann, Jens; Benick, Jan; Hermle, Martin; Belz, Jurgen; Beyer, Andreas et al. (2018): Direct Growth of III–V/Silicon Triple-Junction Solar Cells With 19.7% Efficiency. In *IEEE J. Photovoltaics* 8 (6), pp. 1590–1595. DOI: 10.1109/JPHOTOV.2018.2868015.

Feist, W. (2011): Zertifizierungskriterien für die Modernisierung mit Passivhaus-Komponenten. EnerPHit. Darmstadt. Available online at https://passiv.de/downloads/03_zertifizierungskriterien_enerphit_archiv_2011_de.pdf.

Feltrin, Andrea; Freundlich, Alex (2008): Material considerations for terawatt level deployment of photovoltaics. In *Renewable Energy* 33 (2), pp. 180–185. DOI: 10.1016/j.renene.2007.05.024.

Fetcenko, M. A.; Ovshinsky, S. R.; Reichman, B.; Young, K.; Fierro, C.; Koch, J. et al. (2007): Recent advances in NiMH battery technology. In *Journal of Power Sources* 165 (2), pp. 544–551. DOI: 10.1016/j.jpowsour.2006.10.036.

Figgener, J.; Haberschusz, D.; Kairies, K.; Wessels, O.; Tepe, B.; Sauer, D. U. (2018): Wissenschaftliches Mess- und Evaluierungsprogramm Solarstromspeicher 2.0. Jahresbericht 2018. Institut für Stromrichtertechnik und Elektrische Antriebe, RWTH Aachen. Available online at http://www.speichermonitoring.de.

Fischhaber, S.; Regett, A.; Schuster, S. F.; Hesse, H. (2016): Studie: Second-Life-Konzepte für Lithium-Ionen-Batterien aus Elektrofahrzeugen Analyse von Nachnutzungsanwendungen, ökonomischen und ökologischen Potenzialen. Frankfurt am Main: Begleit- und Wirkungsforschung Schaufenster Elektromobilität (BuW).

Fizaine, Florian (2013): Byproduct production of minor metals. Threat or opportunity for the development of clean technologies? The PV sector as an illustration. In *Resources Policy* 38 (3), pp. 373–383. DOI: 10.1016/j.resourpol.2013.05.002.

Fizaine, Florian (2015): Minor metals and organized markets. News highlights about the consequences of establishing a futures market in a thin market with a dual trading price system. In *Resources Policy* 46, pp. 59–70. DOI: 10.1016/j.resourpol.2015.08.004.

Fleiter, T. (Ed.) (2018): FORECAST/eLOAD (model Website). Fraunhofer ISI. Available online at https://www.forecast-model.eu/forecast-en/index.php, checked on 4/16/2018.

Fotouhi, Abbas; Auger, Daniel; O'Neill, Laura; Cleaver, Tom; Walus, Sylwia (2017): Lithium-Sulfur Battery Technology Readiness and Applications—A Review. In *Energies* 10 (12), p. 1937. DOI: 10.3390/en10121937.

Frankel, Jeffrey; Rose, Andrew K. (2010): Determinants of Agricultural and Mineral Commodity Prices. HKS Faculty Research Working Paper Series RWP10-038. John F. Kennedy School of Government. Harvard University. Available online at http://nrs.harvard.edu/urn-3:HUL.InstRepos:4450126, checked on 5/15/2018.

Fraunhofer ISE (2018): Photovoltaics Report. Fraunhofer Institute for Solar Energy Systems ISE; PSE Conferences & Consulting GmbH. Freiburg. Available online at https://www.ise.fraunhofer.de/content/dam/ise/de/documents/publications/studies/Photovoltaics-Report.pdf.

Fthenakis, V.; Kim, H. C.; Frischknecht, R.; M. Raugei; P. Sinha; M. Stuck (2011): Life Cycle Inventories and Life Cycle Assessments of Photovoltaic Systems. IEA PVPS Task 12, Subtask 20, LCA, Report IEA-PVPS T12-02:2011. Available online at https://www.bnl.gov/pv/files/pdf/226_Task12_LifeCycle_Inventories.pdf.

Fthenakis, Vasilis (2009): Sustainability of photovoltaics. The case for thin-film solar cells. In *Renewable and Sustainable Energy Reviews* 13 (9), pp. 2746–2750. DOI: 10.1016/j.rser.2009.05.001.

Gale, David (1955): The law of supply and demand. In *MATH. SCAND.* 3, p. 155. DOI: 10.7146/math.scand.a-10436.

Gao, Zhonghui; Sun, Huabin; Fu, Lin; Ye, Fangliang; Zhang, Yi; Luo, Wei; Huang, Yunhui (2018): Promises, Challenges, and Recent Progress of Inorganic Solid-State Electrolytes for All-Solid-State Lithium Batteries. In *Advanced materials (Deerfield Beach, Fla.)* 30 (17), e1705702. DOI: 10.1002/adma.201705702.

Gargano, A.; Timmermann, A. (2012): Predictive Dynamics in Commodity Prices. Federal Reserve Bank of San Francisco. Available online at http://www.frbsf.org/economic-research/files/timmermann_presentation.pdf, checked on 6/8/2017.

Gelfand, Sharla Jaclyn (2015): Understanding the impact of heteroscedasticity on the predictive ability of modern regression methods. Dissertation. Department of Statistics and Actuarial Science. Simon Fraser University. Available online at https://www.stat.sfu.ca/content/dam/sfu/stat/alumnitheses/2015/SharlaGelfandProject.pdf.

Gerhardt, N.; Sandau, F.; Scholz, A.; Hahn, H.; Schumacher, P.; Sager, C. et al. (2015): INTERAKTION EE-STROM, WÄRME UND VERKEHR. Analyse der Interaktion zwischen den Sektoren Strom, Wärme/Kälte und Verkehr in Deutschland in Hinblick auf steigende Anteile fluktuierender Erneuerbarer Energien im Strombereich unter Berücksichtigung der europäischen Entwicklung. Ableitung von optimalen strukturellen Entwicklungspfaden für den Verkehrs- und Wärmesektor. With assistance of Norman Gerhardt, Fabian Sandau, Angela Scholz, Henning Hahn, Patrick Schumacher, Christina Sager et al. Fraunhofer IWES; Fraunhofer IBP; IFEU; Stiftung Umweltenergierecht. Available online at https://www.iee.fraunhofer.de/content/dam/iwes-neu/energiesystemtechnik/de/Dokumente/Veroeffentlichungen/2015/Interaktion_EEStrom_Waerme_Verkehr_Endbericht.pdf, checked on 1/19/2018.

Gerssen-Gondelach, Sarah J.; Faaij, André P.C. (2012): Performance of batteries for electric vehicles on short and longer term. In *Journal of Power Sources* 212, pp. 111–129. DOI: 10.1016/j.jpowsour.2012.03.085.

Ghosh, D.; Eric, J. L.; Peter, M.; Robert, E. W. (2004): GOLD AS AN INFLATION HEDGE? In *Studies in Economics & Finance* 22 (1), pp. 1–25. DOI: 10.1108/eb043380.

Glöser-Chahoud, Simon (2017): Quantitative Analyse der Kritikalität mineralischer und metallischer Rohstoffe unter Verwendung eines systemdynamischen Modell-Ansatzes. Dissertation. With assistance of Universitätsbibliothek der TU Clausthal.

Glunz, S. W.; Preu, R.; Biro, D. (2012): Crystalline Silicon Solar Cells. In : Comprehensive Renewable Energy: Elsevier, pp. 353–387.

Godfrey, L. G. (1978): Testing for Higher Order Serial Correlation in Regression Equations when the Regressors Include Lagged Dependent Variables. In *Econometrica* 46 (6), p. 1303. DOI: 10.2307/1913830.

Goe, Michele; Gaustad, Gabrielle (2014): Identifying critical materials for photovoltaics in the US. A multi-metric approach. In *Applied Energy* 123, pp. 387–396. DOI: 10.1016/j.apenergy.2014.01.025.

Goriparti, Subrahmanyam; Miele, Ermanno; Angelis, Francesco de; Di Fabrizio, Enzo; Proietti Zaccaria, Remo; Capiglia, Claudio (2014): Review on recent progress of nanostructured anode materials for Li-ion batteries. In *Journal of Power Sources* 257, pp. 421–443. DOI: 10.1016/j.jpowsour.2013.11.103.

Graedel, T. E.; Allwood, Julian; Birat, Jean-Pierre; Buchert, Matthias; Hagelüken, Christian; Reck, Barbara K. et al. (2011): What Do We Know About Metal Recycling Rates? In *Journal of Industrial Ecology* 15 (3), pp. 355–366. DOI: 10.1111/j.1530-9290.2011.00342.x.

Graedel, T. E.; Barr, Rachel; Chandler, Chelsea; Chase, Thomas; Choi, Joanne; Christoffersen, Lee et al. (2012): Methodology of metal criticality determination. In *Environmental science & technology* 46 (2), pp. 1063–1070. DOI: 10.1021/es203534z.

Graedel, T. E.; Nassar, N. T. (2015): The criticality of metals. A perspective for geologists. In *Geological Society, London, Special Publications* 393 (1), pp. 291–302. DOI: 10.1144/SP393.4.

Granger, C. W. J. (1969): Investigating Causal Relations by Econometric Models and Cross-spectral Methods. In *Econometrica* 37 (3), p. 424. DOI: 10.2307/1912791.

Grätzel, Michael (2014): The light and shade of perovskite solar cells. In *Nature Materials* 13, 838-842. DOI: 10.1038/nmat4065.

Green, Martin A.; Hishikawa, Yoshihiro; Dunlop, Ewan D.; Levi, Dean H.; Hohl-Ebinger, Jochen; Ho-Baillie, Anita W.Y. (2018): Solar cell efficiency tables (version 51). In *Prog. Photovolt: Res. Appl.* 26 (1), pp. 3–12. DOI: 10.1002/pip.2978.

Green, Martin A.; Ho-Baillie, Anita; Snaith, Henry J. (2014): The emergence of perovskite solar cells. In *Nature Photonics* 8 (7), p. 506. DOI: 10.1038/nphoton.2014.134.

Grosjean, Camille; Miranda, Pamela Herrera; Perrin, Marion; Poggi, Philippe (2012): Assessment of world lithium resources and consequences of their geographic distribution on the expected development of the electric vehicle industry. In *Renewable and Sustainable Energy Reviews* 16 (3), pp. 1735–1744. DOI: 10.1016/j.rser.2011.11.023.

Gruber, Paul W.; Medina, Pablo A.; Keoleian, Gregory A.; Kesler, Stephen E.; Everson, Mark P.; Wallington, Timothy J. (2011): Global Lithium Availability. In *Journal of Industrial Ecology* 15 (5), pp. 760–775. DOI: 10.1111/j.1530-9290.2011.00359.x.

Habib, Komal; Wenzel, Henrik (2016): Reviewing resource criticality assessment from a dynamic and technology specific perspective – using the case of direct-drive wind turbines. In *Journal of Cleaner Production* 112, pp. 3852–3863. DOI: 10.1016/j.jclepro.2015.07.064.

Hacker, Florian; Harthan, Ralph; Kasten, Peter; Loreck, Charlotte; Seebach, Dominik; Timope, Christof et al. (2011): Betrachtung der Umweltentlastungspotenziale durch den verstärkten Einsatz von kleinen, Betrachtung der Umweltentlastungspotenziale durch den verstärkten Einsatz von kleinen, batterieelektrischen Fahrzeugen im Rahmen des Projekts „E-Mobility“. Schlussbericht im Rahmen der Förderung der Modellregionen Elektromobilität des Bundesministeriums für Verkehr, Bau- und Wohnungswesen. Öko-Institut e.V. Berlin. Available online at https://www.oeko.de/oekodoc/1344/2011-007-de.pdf, checked on 4/16/2018.

Hamilton, James (2008): Understanding Crude Oil Prices. Cambridge, MA: National Bureau of Economic Research.

Hamilton, James D. (1989): A New Approach to the Economic Analysis of Nonstationary Time Series and the Business Cycle. In *Econometrica* 57 (2), p. 357. DOI: 10.2307/1912559.

Hamm, Christian; Siegel, Daniel; Niebuhr, Nils; Jurkojc, Piotr; Hellen, Rene von der (2015): Offshore Foundation Based on the ELiSE Method. In Christian Hamm (Ed.): Evolution of Lightweight Structures, vol. 6. Dordrecht: Springer Netherlands (Biologically-Inspired Systems), pp. 195–206.

Hannan, M. A.; Hoque, M. M.; Mohamed, A.; Ayob, A. (2017): Review of energy storage systems for electric vehicle applications. Issues and challenges. In *Renewable and Sustainable Energy Reviews* 69, pp. 771–789. DOI: 10.1016/j.rser.2016.11.171.

Harris, S. J.; Harris, D. J.; Li, C. (2017): Failure statistics for commercial lithium ion batteries. A study of 24 pouch cells. In *Journal of Power Sources* 342, pp. 589–597. DOI: 10.1016/j.jpowsour.2016.12.083.

Hein Concept (2016): PV Marktdaten Update 2015 Gesamt. Available online at https://www.heinconcept.de/images/HC_Marktdaten_PV_2015_Gesamt.pdf.

Hein Concept (2017): PV Marktdaten Update Dezember 2016. Available online at https://www.heinconcept.de/images/HC_Marktdaten_PV_2016_Dezember.pdf.

Helbig, Christoph; Bradshaw, Alex M.; Kolotzek, Christoph; Thorenz, Andrea; Tuma, Axel (2016a): Supply risks associated with CdTe and CIGS thin-film photovoltaics. In *Applied Energy* 178, pp. 422–433. DOI: 10.1016/j.apenergy.2016.06.102.

Helbig, Christoph; Kolotzek, Christoph; Thorenz, Andrea; Reller, Armin; Tuma, Axel; Schafnitzel, Mario; Krohns, Stephan (2017): Benefits of resource strategy for sustainable materials research and development. In *Sustainable Materials and Technologies* 12, pp. 1–8. DOI: 10.1016/j.susmat.2017.01.004.

Helbig, Christoph; Wietschel, Lars; Thorenz, Andrea; Tuma, Axel (2016b): How to evaluate raw material vulnerability - An overview. In *Resources Policy* 48, pp. 13–24. DOI: 10.1016/j.resourpol.2016.02.003.

Henderson, Brian J.; Pearson, Neil D.; Wang, Li (2015): New Evidence on the Financialization of Commodity Markets. In *The Review of Financial Studies* 28 (5), pp. 1285–1311. DOI: 10.1093/rfs/hhu091.

Henning, Hans-Martin; Palzer, Andreas (2015): Was kostet die Energiewende? – Wege zur Transformation des deutschen Energiesystems bis 2050. Fraunhofer ISE. Freiburg. Available online at https://www.ise.fraunhofer.de/content/dam/ise/de/documents/publications/studies/Fraunhofer-ISE-Studie-Was-kostet-die-Energiewende.pdf, checked on 1/19/2018.

Hillebrandt, Katharina; Samadi, Sascha; Fischedick, Manfred (2015): Pathways to deep decarbonization in Germany: SDSN - IDDRI, checked on 4/10/2018.

Hoornstra, J.; Schubert, G.; Broek, K.; Granek, F.; LePrince, C. (2005): Lead free metallisation paste for crystalline silicon solar cells. From model to results. In : 2005 31st IEEE Photovoltaic Specialists

Conference. Conference Record of the Thirty-First IEEE Photovoltaic Specialists Conference. Lake buena Vista, FL, USA, 3-7 Jan. 2005. IEEE, Electron Devices Society Staff. [Place of publication not identified]: I E E E, pp. 1293–1296.

Horowitz, K.A.W; Fu, R.; Sun, X.; Silverman, T.; Woodhouse, M.; Alam, M. A. (2017): An Analysis of the Cost and Performance of Photovoltaic Systems as a Function of Module Area. National Renewable Energy Laboratory (NREL) (NREL/TP-6A20-67006).

Hoshino, Tsuyoshi (2015): Innovative lithium recovery technique from seawater by using world-first dialysis with a lithium ionic superconductor. In *Desalination* 359, pp. 59–63. DOI: 10.1016/j.desal.2014.12.018.

Hu, Sanqing; Cao, Yu; Zhang, Jianhai; Kong, Wanzeng; Yang, Kun; Zhang, Yanbin; Li, Xun (2012): More discussions for granger causality and new causality measures. In *Cognitive neurodynamics* 6 (1), pp. 33–42. DOI: 10.1007/s11571-011-9175-8.

Hueso, Karina B.; Armand, Michel; Rojo, Teófilo (2013): High temperature sodium batteries. Status, challenges and future trends. In *Energy Environ. Sci.* 6 (3), p. 734. DOI: 10.1039/C3EE24086J.

Hustrulid, W. A.; Bullock, Richard Lee (2001): Underground mining methods. Engineering fundamentals and international case studies. Littleton, Colorado: Society for Mining, Metallurgy and Exploration.

Iclodean, C.; Varga, B.; Burnete, N.; Cimerdean, D.; Jurchiş, B. (2017): Comparison of Different Battery Types for Electric Vehicles. In *IOP Conf. Ser.: Mater. Sci. Eng.* 252, p. 12058. DOI: 10.1088/1757-899X/252/1/012058.

ICSG (2017): The world copper factbook 2017. Edited by International Copper Study Group. Lisbon. Available online at http://www.icsg.org/index.php/component/jdownloads/finish/170/2462.

IEA (2010): Energy technology perspectives 2010. Scenarios & strategies to 2050. Paris: IEA/OECD.

IEA (2013): World energy outlook 2013. Paris: International Energy Agency (World Energy Outlook).

IEA (2014): World Energy Outlook 2014. International Energy Agency. Paris. Available online at https://www.iea.org/publications/freepublications/publication/WEO2014.pdf, checked on 01.03.17.

IEA (2017): Energy Technology Perspectives 2017. Paris: International Energy Agency.

IEA (2018a): Energy storage. Tracking Clean Energy Progress. Edited by International Energy Agency. Available online at https://www.iea.org/tcep/energy-integration/energystorage/, updated on 5/22/2018, checked on 8/1/2018.

IEA (2018b): Global EV Outlook 2018. Edited by OECD, IEA, checked on 8/21/2018.

IRENA (2015): REmap, Renewable Energy Prospects: Germany. International Renewable Energy Agency (IRENA). Abu Dhabi. Available online at www.irena.org/remap.

IRENA (2017): Electricity Storage and Renewables. Cost and Markets to 2030. Edited by International Renewable Energy Agency. Abu Dhabi. Available online at http://www.irena.org/-/media/Files/IRENA/Agency/Publication/2017/Oct/IRENA_Electricity_Storage_Costs_2017.pdf.

ISSF (2010): Stainless steel in solar energy use. Brussels: International Stainless Steel Forum.

ITRPV (2017): International Technology Roadmap for Photovoltaic. Ninth edition. With assistance of ITRPV, VDMA PV.

IWCC; ICA (2017): Global 2018 Semis End Use Data Set. International Wrought Copper Council; International Copper Association.

Jain, Anshul; Ghosh, Sajal (2013): Dynamics of global oil prices, exchange rate and precious metal prices in India. In *Resources Policy* 38 (1), pp. 88–93. DOI: 10.1016/j.resourpol.2012.10.001.

Jerrett, Daniel; Cuddington, John T. (2008): Broadening the statistical search for metal price super cycles to steel and related metals. In *Resources Policy* 33 (4), pp. 188–195. DOI: 10.1016/j.resourpol.2008.08.001.

Ji, Xiulei; Nazar, Linda F. (2010): Advances in Li–S batteries. In *J. Mater. Chem.* 20 (44), p. 9821. DOI: 10.1039/b925751a.

Jiao, Na; Evans, Steve (2016): Business Models for Sustainability. The Case of Second-life Electric Vehicle Batteries. In *Procedia CIRP* 40, pp. 250–255. DOI: 10.1016/j.procir.2016.01.114.

Jin, Yan; Zhu, Bin; Lu, Zhenda; Liu, Nian; Zhu, Jia (2017): Challenges and Recent Progress in the Development of Si Anodes for Lithium-Ion Battery. In *Adv. Energy Mater.* 7 (23), p. 1700715. DOI: 10.1002/aenm.201700715.

Johansen, Soren (1991): Estimation and Hypothesis Testing of Cointegration Vectors in Gaussian Vector Autoregressive Models. In *Econometrica* 59 (6), p. 1551. DOI: 10.2307/2938278.

Johnson, N. M. (2014): Battery technology for CO2 reduction. In R. Folkson (Ed.): Alternative Fuels and Advanced Vehicle Technologies for Improved Environmental Performance. Towards zero carbon transportation. Amsterdam: Woodhead (Woodhead Publishing Series in Energy, No. 57), pp. 582–631.

Johnston, John; DiNardo, John (2004): Econometric methods. 4. ed., [Nachdr.]. Nex York, NY: McGraw-Hill.

Jordan, Brett (2018): Economics literature on joint production of minerals. A survey. In *Resources Policy* 55, pp. 20–28. DOI: 10.1016/j.resourpol.2017.10.002.

Jordan, Brett W. (2017): Companions and competitors. Joint metal-supply relationships in gold, silver, copper, lead and zinc mines. In *Resource and Energy Economics* 49, pp. 233–250. DOI: 10.1016/j.reseneeco.2017.05.003.

Jülch, Verena; Hartmann, Niklas; Hussein, Noha Saad; Schlegl, Thomas (2015): Photovoltaik. In Martin Wietschel, Sandra Ullrich, Peter Markewitz, Friedrich Schulte, Fabio Genoese (Eds.): Energietechnologien der Zukunft. Wiesbaden: Springer Fachmedien Wiesbaden, pp. 123–138.

Jülch, Verena; Senkpiel, Charlotte; Kost, Christoph; Hartmann, Niklas; Schlegl, Thomas (2018): Meta study on future crosssectoral decarbonization target systems in comparison to current status of technologies. Discussion Paper. Fraunhofer Institute for Solar Energy Systems ISE. Freiburg. Available online at https://www.ise.fraunhofer.de/content/dam/ise/en/documents/publications/studies/Meta_Study_Crossectoral_Decarbonization_Target_Systems.pdf, checked on 4/11/2018.

Julien, Christian; Mauger, Alain; Vijh, Ashok; Zaghib, Karim (2016): Lithium Batteries. In Christian Julien, Alain Mauger, Ashok Vijh, Karim Zaghib (Eds.): Lithium Batteries. Cham: Springer International Publishing, pp. 29–68.

Jungbluth, N.; Stucki, M.; Flury, K.; Frischknecht, R.; Büsser, S. (2012): Life Cycle Inventories of Photovoltaics. Edited by Swiss Federal Office of Energy SFOE. ESU-services Ltd.

Jungbluth, N.; Stucki, M.; Frischknecht, R. (2010): Photovoltaics. Sachbilanzen von Energiesystemen: Grundlagen für den ökologischen Vergleich von Energiesystemen und den Einbezug von Energiesystemen in Ökobilanzen für die Schweiz. Edited by R. Dones, Christian Bauer, Paul Scherrer Institut Villigen. Uster, CH (ecoinvent report No. 6-XII).

Kamat, Prashant V.; Bisquert, Juan; Buriak, Jillian (2017): Lead-Free Perovskite Solar Cells. In *ACS Energy Lett.* 2 (4), pp. 904–905. DOI: 10.1021/acsenergylett.7b00246.

Kanamura, Kiyoshi (2005): Chapter 11 - Electrolytes for lithium batteries. In Tsuyoshi Nakajima, Henri Groult (Eds.): Fluorinated Materials for Energy Conversion. Amsterdam: Elsevier Science, pp. 253–266. Available online at http://www.sciencedirect.com/science/article/pii/B9780080444727500394.

Kang, Sang Hoon; McIver, Ron; Yoon, Seong-Min (2017): Dynamic spillover effects among crude oil, precious metal, and agricultural commodity futures markets. In *Energy Economics* 62, pp. 19–32. DOI: 10.1016/j.eneco.2016.12.011.

Kang, W.; Ratti, R. A.; Vespignani, J. (2016): The impact of oil price shocks on the U.S. stock market. A note on the roles of U.S. and non-U.S. oil production. In *Economics Letters* 145, pp. 176–181. DOI: 10.1016/j.econlet.2016.06.008.

Karimi, M.; Eshraghi, M. J.; Jahangir, V. (2016): A facile and green synthetic approach based on deep eutectic solvents toward synthesis of CZTS nanoparticles. In *Materials Letters* 171, pp. 100–103. DOI: 10.1016/j.matlet.2016.02.065.

Kavlak, Goksin; McNerney, James; Jaffe, Robert L.; Trancik, Jessika E. (2015): Metal production requirements for rapid photovoltaics deployment. In *Energy Environ. Sci.* 8 (6), pp. 1651–1659. DOI: 10.1039/C5EE00585J.

Kawasoko, Hideyuki; Shiraki, Susumu; Suzuki, Toru; Shimizu, Ryota; Hitosugi, Taro (2018): Extremely Low Resistance of Li3PO4 Electrolyte/Li(Ni0.5Mn1.5)O4 Electrode Interfaces. In *ACS applied materials & interfaces* 10 (32), pp. 27498–27502. DOI: 10.1021/acsami.8b08506.

Kazmerski, Lawrence L. (2006): Solar photovoltaics R&D at the tipping point. A 2005 technology overview. In *Journal of Electron Spectroscopy and Related Phenomena* 150 (2-3), pp. 105–135. DOI: 10.1016/j.elspec.2005.09.004.

Kear, Gareth; Shah, Akeel A.; Walsh, Frank C. (2012): Development of the all-vanadium redox flow battery for energy storage. A review of technological, financial and policy aspects. In *Int. J. Energy Res.* 36 (11), pp. 1105–1120. DOI: 10.1002/er.1863.

KfB (2018): Kraftfahrt-Bundesamt - Produkte der Statistik. Flensburg. Available online at https://www.kba.de/DE/Statistik/Produktkatalog/produktkatalog_node.html, checked on 10/15/2018.

Kilian, Lutz; Park, Cheolbeom (2009): THE IMPACT OF OIL PRICE SHOCKS ON THE U.S. STOCK MARKET. In *International Economic Review* 50 (4), pp. 1267–1287. DOI: 10.1111/j.1468-2354.2009.00568.x.

Kim, Haeyeon; Heo, Eunnyeong (2012): Causality Between Main Product and Byproduct Prices of Metals Used for Thin-Film PV Cells. IAEE Asia. Seoul, checked on 5/11/2018.

Klassen, Stephen (2011): The Photoelectric Effect. Reconstructing the Story for the Physics Classroom. In *Sci & Educ* 20 (7-8), pp. 719–731. DOI: 10.1007/s11191-009-9214-6.

Klausen, Mira (2017): Market opportunities and regulatory framework conditions for stationary battery storage systems in Germany. In *Energy Procedia* 135, pp. 272–282. DOI: 10.1016/j.egypro.2017.09.519.

Kleijn, René; van der Voet, Ester; Kramer, Gert Jan; van Oers, Lauran; van der Giesen, Coen (2011): Metal requirements of low-carbon power generation. In *Energy* 36 (9), pp. 5640–5648. DOI: 10.1016/j.energy.2011.07.003.

Kleiss, G. (2016): Estimating Future Recycling Quantities of PV Modules in the European Union. 4 pages / 32nd European Photovoltaic Solar Energy Conference and Exhibition; 2370-2373. DOI: 10.4229/EUPVSEC20162016-5CV.3.30.

Klise, Geoffrey Taylor (2016): Component Reliability and Failure Analysis Modeling. Sandia National Lab. (SNL-NM), Albuquerque, NM (United States). Available online at https://www.osti.gov/servlets/purl/1364818.

Klotz, Philipp; Lin, Tsoyu Calvin; Hsu, Shih-Hsun (2014): Global commodity prices, economic activity and monetary policy. The relevance of China. In *Resources Policy* 42, pp. 1–9. DOI: 10.1016/j.resourpol.2014.08.001.

Köntges, Marc; Kurtz, Sarah; Packard, Corinne; Jahn, Ulrike; Berger, Karl A.; Kato, Kazuhiko (2014): Performance and reliability of photovoltaic systems. Subtask 3.2: Review of failures of photovoltaic modules : IEA PVPS task 13 : external final report IEA-PVPS. [Sankt Ursen]: International Energy Agency, Photovoltaic Power Systems Programme.

Kost, Christoph; Shammugam, Shivenes; Jülch, Verena; Nguyen, Huyen-Tran; Schlegl, Thomas (2018): Levelized Cost of Electricity: Renewable energy technologies. Fraunhofer Institute for Solar Energy Systems ISE. Freiburg. Available online at https://www.ise.fraunhofer.de/content/dam/ise/en/documents/publications/studies/EN2018_Fraunhofer-ISE_LCOE_Renewable_Energy_Technologies.pdf.

Krawiec, Monika; Górska, Anna (2015): Granger Causality Tests For Precious Metal Returns. In *Metody Ilościowe w Badaniach Ekonomicznych* XVI (2), pp. 13–22, checked on 5/11/2018.

Kraytsberg, Alexander; Ein-Eli, Yair (2011): Review on Li–air batteries—Opportunities, limitations and perspective. In *Journal of Power Sources* 196 (3), pp. 886–893. DOI: 10.1016/j.jpowsour.2010.09.031.

Kumar, B. (2013): Ceramic nanocomposites for energy storage and power generation. In Rajat Banerjee (Ed.): Ceramic nanocomposites. 1. publ. Oxford: Woodhead Publ (Woodhead Publishing series in composites science and engineering, 46), pp. 509–529.

Kurzweil, P.; Garche, J. (2017): Overview of batteries for future automobiles. In : Lead-Acid Batteries for Future Automobiles: Elsevier, pp. 27–96.

Kushnir, Duncan (2015): Lithium Ion Battery Recycling Technology 2015. Current State and Future Prospects. ESA REPORT # 2015:18. Environmental Systems Analysis, Chalmers University of Technology. Göteborg, Sweden.

Kushnir, Duncan; Sandén, Björn A. (2012): The time dimension and lithium resource constraints for electric vehicles. In *Resources Policy* 37 (1), pp. 93–103. DOI: 10.1016/j.resourpol.2011.11.003.

Kwiatkowski, Denis; Phillips, Peter C.B.; Schmidt, Peter; Shin, Yongcheol (1992): Testing the null hypothesis of stationarity against the alternative of a unit root. In *Journal of Econometrics* 54 (1-3), pp. 159–178. DOI: 10.1016/0304-4076(92)90104-Y.

Kyrtsou, Catherine; Labys, Walter C. (2006): Evidence for chaotic dependence between US inflation and commodity prices. In *Journal of Macroeconomics* 28 (1), pp. 256–266. DOI: 10.1016/j.jmacro.2005.10.019.

Labys, W.C; Achouch, A.; Terraza, M. (1999): Metal prices and the business cycle. In *Resources Policy* 25 (4), pp. 229–238. DOI: 10.1016/S0301-4207(99)00030-6.

Lacal-Arántegui, Roberto (2015): Materials use in electricity generators in wind turbines – state-of-the-art and future specifications. In *Journal of Cleaner Production* 87, pp. 275–283. DOI: 10.1016/j.jclepro.2014.09.047.

Laronde, R.; Charki, A.; Bigaud, D. (2010a): Reliability of photovoltaic modules based on climatic measurement data. In *Int. J. Metrol. Qual. Eng.* 1 (1), pp. 45–49. DOI: 10.1051/ijmqe/2010012.

Laronde, Rémi; Charki, Abderafi; Bigaud, David; Excoffier, Philippe (2010b): Photovoltaic system lifetime prediction using Petri networks method. In Neelkanth G. Dhere, John H. Wohlgemuth, Kevin Lynn (Eds.): Reliability of Photovoltaic Cells, Modules, Components, and Systems III. SPIE Solar Energy + Technology. San Diego, California, Sunday 1 August 2010: SPIE (SPIE Proceedings), p. 777306.

Lee, Jang-Soo; Tai Kim, Sun; Cao, Ruiguo; Choi, Nam-Soon; Liu, Meilin; Lee, Kyu Tae; Cho, Jaephil (2011): Metal-Air Batteries with High Energy Density. Li-Air versus Zn-Air. In *Adv. Energy Mater.* 1 (1), pp. 34–50. DOI: 10.1002/aenm.201000010.

Lee, Kiseok; Ni, Shawn (2002): On the dynamic effects of oil price shocks. A study using industry level data. In *Journal of Monetary Economics* 49 (4), pp. 823–852. DOI: 10.1016/S0304-3932(02)00114-9.

Lee, Taesoo D.; Ebong, Abasifreke U. (2017): A review of thin film solar cell technologies and challenges. In *Renewable and Sustainable Energy Reviews* 70, pp. 1286–1297. DOI: 10.1016/j.rser.2016.12.028.

Lei, Binglong; Eze, Vincent Obiozo; Mori, Tatsuo (2015): High-performance CH 3 NH 3 PbI 3 perovskite solar cells fabricated under ambient conditions with high relative humidity. In *Jpn. J. Appl. Phys.* 54 (10), p. 100305. DOI: 10.7567/JJAP.54.100305.

Leontief, Wassily W. (Ed.) (1983): The future of nonfuel minerals in the U.S. and world economy. Input-output projections, 1980 - 2030. Lexington, Mass.: Heath (Lexington books).

Leung, Puiki; Li, Xiaohong; Ponce de León, Carlos; Berlouis, Leonard; Low, C. T. John; Walsh, Frank C. (2012): Progress in redox flow batteries, remaining challenges and their applications in energy storage. In *RSC Adv.* 2 (27), p. 10125. DOI: 10.1039/c2ra21342g.

Liao, Dongliang; Kuang, Xuanlin; Xiang, Jiangfeng; Wang, Xiaohong (2018): A Silicon Anode Material with Layered Structure for the Lithium-ion Battery. In *J. Phys.: Conf. Ser.* 986, p. 12024. DOI: 10.1088/1742-6596/986/1/012024.

Liu, Kai; Liu, Yayuan; Lin, Dingchang; Pei, Allen; Cui, Yi (2018a): Materials for lithium-ion battery safety. In *Science advances* 4 (6), eaas9820. DOI: 10.1126/sciadv.aas9820.

Liu, Tianyu; Cheng, Long; Pan, Zhengqiang; Sun, Quan (2016): Cycle life prediction of lithium-ion cells under complex temperature profiles. In *EiN* 18 (1), pp. 25–31. DOI: 10.17531/ein.2016.1.4.

Liu, Yijie; He, Ping; Zhou, Haoshen (2018b): Rechargeable Solid-State Li-Air and Li-S Batteries. Materials, Construction, and Challenges. In *Adv. Energy Mater.* 8 (4), p. 1701602. DOI: 10.1002/aenm.201701602.

Lluc, C. C.; Beatriz, A. G. (2015): A review of the complexities of applying second life electric car batteries on energy businesses. In. Energy Systems Conference. London, 24-25 June. Elsevier.

Lokanc, M.; Eggert, R.; Redlinger, M. (2015): The Availability of Indium: The Present, Medium Term, and Long Term. Edited by NREL National Renewable Energy Laboratory. Colorado School of Mines„ checked on 5/6/2019.

Lu, Yi-Chun; Gasteiger, Hubert A.; Shao-Horn, Yang (2011): Catalytic activity trends of oxygen reduction reaction for nonaqueous Li-air batteries. In *Journal of the American Chemical Society* 133 (47), pp. 19048–19051. DOI: 10.1021/ja208608s.

Luntz, Alan C.; Voss, Johannes; Reuter, Karsten (2015): Interfacial challenges in solid-state Li ion batteries. In *The journal of physical chemistry letters* 6 (22), pp. 4599–4604. DOI: 10.1021/acs.jpclett.5b02352.

Luo, Paifeng; Liu, Zhaofan; Xia, Wei; Yuan, Chenchen; Cheng, Jigui; Lu, Yingwei (2015): Uniform, stable, and efficient planar-heterojunction perovskite solar cells by facile low-pressure chemical vapor deposition under fully open-air conditions. In *ACS applied materials & interfaces* 7 (4), pp. 2708–2714. DOI: 10.1021/am5077588.

Lütkepohl, Helmut (2013): Vector autoregressive models. In : Handbook of Research Methods and Applications in Empirical Macroeconomics: Edward Elgar Publishing, pp. 139–164. Available online at https://EconPapers.repec.org/RePEc:elg:eechap:14327_6.

Lutzenberger, Fabian; Gleich, Benedikt; Mayer, Herbert G.; Stepanek, Christian; Rathgeber, Andreas W. (2017): Metals. Resources or financial assets? A multivariate cross-sectional analysis. In *Empirical Economics* 53 (3), pp. 927–958. DOI: 10.1007/s00181-016-1162-9.

Malenbaum, Wilfred (1973): Materials Requirements in the United States and Abroad in the Year 2000: A Research Project Prepared for the National Commission on Materials Policy in the Wharton School, University of Pennsylvania: National Technical Information Service (PB 219 675). Available online at https://books.google.de/books?id=HSb8OAAACAAJ.

Månberger, André; Stenqvist, Björn (2018): Global metal flows in the renewable energy transition. Exploring the effects of substitutes, technological mix and development. In *Energy Policy* 119, pp. 226–241. DOI: 10.1016/j.enpol.2018.04.056.

Manthiram, Arumugam (2017): An Outlook on Lithium Ion Battery Technology. In *ACS central science* 3 (10), pp. 1063–1069. DOI: 10.1021/acscentsci.7b00288.

Marscheider-Weidemann, Frank; Langkau, Sabine; Hummen, Torsten; Erdmann, Lorenz; Tercero Espinoza, Luis Alberto; Angerer, Gerhard et al. (2016): Rohstoffe für Zukunftstechnologien 2016. Auftragsstudie. Berlin: DERA (DERA Rohstoffinformationen, 28).

Matthes, F. (2010): Energiepreise für aktuelle Modellierungsarbeiten. Regressionsanalytisch basierte Projektionen. Öko-Institut e.V. Available online at https://www.oeko.de//oekodoc/984/2010-004-de.pdf.

May, Geoffrey J.; Davidson, Alistair; Monahov, Boris (2018): Lead batteries for utility energy storage. A review. In *Journal of Energy Storage* 15, pp. 145–157. DOI: 10.1016/j.est.2017.11.008.

Mayer, Herbert; Rathgeber, Andreas; Wanner, Markus (2017): Financialization of metal markets. Does futures trading influence spot prices and volatility? In *Resources Policy* 53, pp. 300–316. DOI: 10.1016/j.resourpol.2017.06.011.

McKay, Huw (2008): Metal intensity in comparative historical perspective. China, North Asia, the United States & the Kuznets Curve. Canberra: ANU Global Dynamic Systems Centre (Global Dynamic Systems Centre working paper series, no. 6).

McKay, Huw; Sheng, Yu; Song, Ligang (2010): China's metal intensity in comparative perspective. In Ross Garnaut, Jane Golley and Ligang Song (Eds.): China: The Next Twenty Years of Reform and Development. Canberra: ANU E Press, pp. 73–98.

McLellan, Benjamin; Yamasue, Eiji; Tezuka, Tetsuo; Corder, Glen; Golev, Artem; Giurco, Damien (2016): Critical Minerals and Energy–Impacts and Limitations of Moving to Unconventional Resources. In *Resources* 5 (2), p. 19. DOI: 10.3390/resources5020019.

Mei, Delong; Yuan, Xianxia; Ma, Zhong; Wei, Ping; Yu, Xuebin; Yang, Jun; Ma, Zi-Feng (2016): A SnO2-Based Cathode Catalyst for Lithium-Air Batteries. In *ACS applied materials & interfaces* 8 (20), pp. 12804–12811. DOI: 10.1021/acsami.6b02402.

Meyer, C.; Breuer, K.; Lackowicz, A.; Hefner, W.; Schum, B.; Metz, A. (2014): Schlussbericht zum Verbundprojekt Langstabile Vorderseitenmetallisierung auf Basis Umweltfreundlicher Galvanischer Schichten (Las VeGaS). With assistance of SCHOTT Solar AG, RENA GmbH, CIS GmbH. Technische Informationsbibliothek (TIB). Erfurt. Available online at

https://www.tib.eu/de/suchen/download/?tx_tibsearch_search%5Bdocid%5D=TIBKAT%3A745183433&cHash=c6bba71dffaddd2ad40a068da238bf09#download-mark.

Michaelis, Sarah; Maiser, Eric.; Kampker, Achim; Heimes, Heiner; Lienemann, Christoph; Wessel, Saskia et al. (2016): Roadmap: Batterie-Produktionsmittel 2030. Frankfurt am Main: VDMA Verlag. Available online at https://battprod.vdma.org/documents/7411591/15357859/VDMA+Roadmap+Batterie-Produktionsmittel+2030+Update/b8c52edd-5c65-4d92-8290-09876153f30b.

Miedema, Jan H.; Moll, Henri C. (2013): Lithium availability in the EU27 for battery-driven vehicles. The impact of recycling and substitution on the confrontation between supply and demand until2050. In *Resources Policy* 38 (2), pp. 204–211. DOI: 10.1016/j.resourpol.2013.01.001.

Mishra, P. K. (2014): Gold Price and Capital Market Movement in India. The Toda–Yamamoto Approach. In *Global Business Review* 15 (1), pp. 37–45. DOI: 10.1177/0972150913515597.

Mo, Jung; Jeon, Wooyoung (2018): The Impact of Electric Vehicle Demand and Battery Recycling on Price Dynamics of Lithium-Ion Battery Cathode Materials. A Vector Error Correction Model (VECM) Analysis. In *Sustainability* 10 (8), p. 2870. DOI: 10.3390/su10082870.

Morales-Acevedo, Arturo (2006): Thin film CdS/CdTe solar cells. Research perspectives. In *Solar Energy* 80 (6), pp. 675–681. DOI: 10.1016/j.solener.2005.10.008.

Mork, Knut Anton (1989): Oil and the Macroeconomy When Prices Go Up and Down. An Extension of Hamilton's Results. In *Journal of Political Economy* 97 (3), pp. 740–744. DOI: 10.1086/261625.

Moss, R. L.; Tzimas, Evangelos; Kara, H.; Willis, P.; Kooroshy, J. (2011): Critical Metals in Strategic Energy Technologies. Assessing Rare Metals as Supply-Chain Bottlenecks in Low-Carbon Energy Technologies. Edited by Publications Office of the European Union. JRC – Institute for Energy and Transport; Oakdene Hollins Ltd; The Hague Centre for Strategic Studies.

Moss, Raymond; Willis, Peter; Tercero, Espinoza Luis; Tzimas, Evangelos; Arendorf, Josephine; Thompson, Paul et al. (2013): Critical metals in the path towards the decarbonisation of the EU energy sector. Assessing rare metals as supply-chain bottlenecks in low-carbon energy technologies. Luxembourg: Publications Office of the European Union (EUR - Scientific and technical research series, EUR 25994).

Mudgal, S.; Le-Guern, Y.; Tinetti, B.; Chanoine, A.; Pahal, S.; Witte, F. (2011): Comparative Life-Cycle Assessment of nickelcadmium (NiCd) batteries used in Cordless Power Tools (CPTs) vs. their alternatives nickel-metal hydride (NiMH) and lithium-ion (Li-ion) batteries. Final Report. European Commission – DG ENV. Available online at http://ec.europa.eu/environment/waste/batteries/pdf/report_12.pdf.

Mutafoglu, T. H.; Tokat, E.; Tokat, H. A. (2012): Forecasting precious metal price movements using trader positions. In *Resources Policy* 37 (3), pp. 273–280. DOI: 10.1016/j.resourpol.2012.02.002.

Mykytyuk, T. I.; Roshko, V.Ya.; Kosyachenko, L. A.; Grushko, E. V. (2012): Limitations on Thickness of Absorber Layer in CdS/CdTe Solar Cells. In *Acta Physica Polonica A* 122 (6), pp. 1073–1076. DOI: 10.12693/APhysPolA.122.1073.

Naciri, R.; Bihri, H.; Mzerd, Ahmed; Rahioui, A.; Abd-Lefdil, M.; Messaoudi, C. (2007): The role of the CdS buffer layer in the CuInS2 Thin film solar cell. Revue des Energies Renouvelables CER'07. Oujda.

Narins, Thomas P. (2017): The battery business. Lithium availability and the growth of the global electric car industry. In *The Extractive Industries and Society* 4 (2), pp. 321–328. DOI: 10.1016/j.exis.2017.01.013.

Nassar, N. T.; Graedel, T. E.; Harper, E. M. (2015): By-product metals are technologically essential but have problematic supply. In *Science advances* 1 (3), e1400180. DOI: 10.1126/sciadv.1400180.

Nazlioglu, Saban; Soytas, Ugur (2011): World oil prices and agricultural commodity prices. Evidence from an emerging market. In *Energy Economics* 33 (3), pp. 488–496. DOI: 10.1016/j.eneco.2010.11.012.

Nijssen, R.P.L.; Zaaijer, M. B.; Bierbooms, W.A.A.M.; van Kuik, G.A.M.; van Delft, D.R.V.; van Holten, Th. (2001): The application of scaling rules in up-scaling and marinisation of a wind turbine. European Wind Energy Conference and Exhibition. Copenhagen,Denmark.

Nitta, Naoki; Wu, Feixiang; Lee, Jung Tae; Yushin, Gleb (2015): Li-ion battery materials. Present and future. In *Materials Today* 18 (5), pp. 252–264. DOI: 10.1016/j.mattod.2014.10.040.

Nordling, Anna; Englund, Ronja; Hembjer, Alexander; Mannberg, Andreas (2016): Energy Storage - Electricity storage technologies. IVA's Electricity Crossroads project. Edited by Royal Swedish Academy of Engineering Sciences. Stockholm. Available online at https://www.iva.se/globalassets/rapporter/vagval-el/201604-iva-vagvalel-ellagring-rapport-english-e-ny.pdf.

Ogasawara, Takeshi; Débart, Aurélie; Holzapfel, Michael; Novák, Petr; Bruce, Peter G. (2006): Rechargeable LI2O2 electrode for lithium batteries. In *Journal of the American Chemical Society* 128 (4), pp. 1390–1393. DOI: 10.1021/ja056811q.

Olivetti, Elsa A.; Ceder, Gerbrand; Gaustad, Gabrielle G.; Fu, Xinkai (2017): Lithium-Ion Battery Supply Chain Considerations. Analysis of Potential Bottlenecks in Critical Metals. In *Joule* 1 (2), pp. 229–243. DOI: 10.1016/j.joule.2017.08.019.

Omar, N.; Firouz, Y.; Monem, M. A.; Samba, A.; Gualous, H.; Coosemans, T. et al. (2014): Analysis of Nickel-Based Battery Technologies for Hybrid and Electric Vehicles. In Jan Reedijk (Ed.): Reference module in chemistry, molecular sciences and chemical engineering. Oxford: Elsevier.

Opitz, A.; Badami, P.; Shen, L.; Vignarooban, K.; Kannan, A. M. (2017): Can Li-Ion batteries be the panacea for automotive applications? In *Renewable and Sustainable Energy Reviews* 68, pp. 685–692. DOI: 10.1016/j.rser.2016.10.019.

Osanloo, M.; Ataei, M. (2003): Using equivalent grade factors to find the optimum cut-off grades of multiple metal deposits. In *Minerals Engineering* 16 (8), pp. 771–776. DOI: 10.1016/S0892-6875(03)00163-8.

Ossai, Chinedu; Raghavan, Nagarajan (2017): Statistical Characterization of the State-of-Health of Lithium-Ion Batteries with Weibull Distribution Function—A Consideration of Random Effect

Model in Charge Capacity Decay Estimation. In *Batteries* 3 (4), p. 32. DOI: 10.3390/batteries3040032.

Palzer, Andreas (2016): Sektorübergreifende Modellierung und Optimierung eines zukünftigen deutschen Energiesystems unter Berücksichtigung von Energieeffizienzmaßnahmen im Gebäudesektor. Dissertation. Stuttgart: Fraunhofer Verlag. Available online at http://publica.fraunhofer.de/eprints/urn_nbn_de_0011-n-408742-11.pdf, checked on 4/13/2018.

Park, Jeong-a; Hong, Seok-jin; Kim, Ik; Lee, Ji-yong; Hur, Tak (2011): Dynamic material flow analysis of steel resources in Korea. In *Resources, Conservation and Recycling* 55 (4), pp. 456–462. DOI: 10.1016/j.resconrec.2010.12.007.

Pathak, Arjun K.; Khan, Mahmud; Gschneidner, Karl A.; McCallum, Ralph W.; Zhou, Lin; Sun, Kewei et al. (2015): Cerium. An unlikely replacement of dysprosium in high performance Nd-Fe-B permanent magnets. In *Advanced materials* 27 (16), pp. 2663–2667. DOI: 10.1002/adma.201404892.

Patry, Gaëtan; Romagny, Alex; Martinet, Sébastien; Froelich, Daniel (2015): Cost modeling of lithium-ion battery cells for automotive applications. In *Energy Sci Eng* 3 (1), pp. 71–82. DOI: 10.1002/ese3.47.

Pavel, Claudiu C.; Lacal-Arántegui, Roberto; Marmier, Alain; Schüler, Doris; Tzimas, Evangelos; Buchert, Matthias et al. (2017): Substitution strategies for reducing the use of rare earths in wind turbines. In *Resources Policy* 52, pp. 349–357. DOI: 10.1016/j.resourpol.2017.04.010.

Pereg, J. R.; Hoz, J. F. (2013): ECOWIND - Life Cycle Assessment of 1 Kwh generated by a Gamesa onshore wndfarm G90 2.0 MW. Gamesa, checked on 03.04.17.

Pertti, Kauranen (2017): Raw material needs by the Li-ion battery industry. Edited by Close Loop. Available online at http://closeloop.fi/wp-content/uploads/2017/05/Li-raw-materials-20170517.pdf, checked on 8/1/2018.

Pillot, Christophe (2017): Lithium ion battery raw material Supply&deman 2016-2025. AVICENNE ENERGY. Available online at http://cii-resource.com/cet/AABE-03-17/Presentations/BRMT/Pillot_Christophe.pdf, checked on 8/8/2018.

Placke, Tobias; Winter, Martin (2018): Progress and Challenges: Generation 3b. European Battery Cell R&I Workshop, 11-12 January 2018. Brussels.

Ploberger, Werner; Kramer, Walter (1992): The Cusum Test with Ols Residuals. In *Econometrica* 60 (2), p. 271. DOI: 10.2307/2951597.

Plunkert, P. A.; Jones, T. S. (1999): Metal Prices in the United States through 1998: U.S. Geological survey.

Polinder, H.; van der Pijl, F.F.A.; Vilder, G.-J. de; Tavner, P. J. (2006): Comparison of Direct-Drive and Geared Generator Concepts for Wind Turbines. In *IEEE Trans. On Energy Conversion* 21 (3), pp. 725–733. DOI: 10.1109/TEC.2006.875476.

Polinder, Henk; Ferreira, Jan Abraham; Jensen, Bogi Bech; Abrahamsen, Asger B.; Atallah, Kais; McMahon, Richard A. (2013): Trends in Wind Turbine Generator Systems. In *IEEE Journal of Emerging and Selected Topics in Power Electronics* 1 (3), pp. 174–185. DOI: 10.1109/JESTPE.2013.2280428.

Polman, Albert; Knight, Mark; Garnett, Erik C.; Ehrler, Bruno; Sinke, Wim C. (2016): Photovoltaic materials. Present efficiencies and future challenges. In *Science (New York, N.Y.)* 352 (6283), aad4424. DOI: 10.1126/science.aad4424.

Pradhananga, Manisha (2016): Financialization and the rise in co-movement of commodity prices. In *International Review of Applied Economics* 30 (5), pp. 547–566. DOI: 10.1080/02692171.2016.1146875.

Rahman, Atteq ur; Lee, Soo Hong (2015): Crystalline Silicon Solar Cells with Nickel/Copper Contacts. In Leonid A. Kosyachenko (Ed.): Solar Cells - New Approaches and Reviews: InTech.

Rankin, William John (2011): Minerals, Metals and Sustainability. Meeting future material needs. Leiden, Netherlands: CRC Press.

Raugei, M.; Fthenakis, V. (2010): Cadmium flows and emissions from CdTe PV. Future expectations. In *Energy Policy* 38 (9), pp. 5223–5228. DOI: 10.1016/j.enpol.2010.05.007.

Ravindiran, M.; Praveenkumar, C. (2018): Status review and the future prospects of CZTS based solar cell – A novel approach on the device structure and material modeling for CZTS based photovoltaic device. In *Renewable and Sustainable Energy Reviews* 94, pp. 317–329. DOI: 10.1016/j.rser.2018.06.008.

Redlinger, Michael; Eggert, Roderick (2016): Volatility of by-product metal and mineral prices. In *Resources Policy* 47, pp. 69–77. DOI: 10.1016/j.resourpol.2015.12.002.

Reid, G.; Julver, J. (2016): Second Life-Batterien als flexible Speicher für Erneuerbare Energien. Edited by Bundesverband Erneuerbare Energie e.V., Hannover Messe.

Repenning, J.; Emele, L.; Blanck, R.; Dehoust, G.; Förster, H.; Greiner, B. et al. (2016): Climate Protection Scenario 2050. Summary of second final report. Study conducted on behalf of the German Federal Ministry for the Environment, Nature Conservation, Building and Nuclear Safety. With assistance of Öko-Institut e.V., Fraunhofer ISI. Edited by BMUB. Berlin. Available online at https://www.oeko.de/fileadmin/oekodoc/Climate-Protection-Scenario-2050-Summary.pdf, updated on 2016.

Richter, Armin; Hermle, Martin; Glunz, Stefan W. (2013): Reassessment of the Limiting Efficiency for Crystalline Silicon Solar Cells. In *IEEE J. Photovoltaics* 3 (4), pp. 1184–1191. DOI: 10.1109/JPHOTOV.2013.2270351.

Roberts, David L.; Nord, Stephen (2006): Causality tests and functional form sensitivity. In *Applied Economics* 17 (1), pp. 135–141. DOI: 10.1080/00036848500000011.

Rodrigo Cerda (2005): Market Power and Primary Commodity Prices: The Case of Copper. In *Journal of Applied Economics Letters* (14(10)), pp. 775–778.

Rongguo, C.; Juan, G.; Liwen, Y.; Huy, D.; Liedtke, M. (2016): Supply and Demand of Lithium and Gallium. Edited by ICMLR, BGR, checked on 5/6/2019.

Rösch, Christine (2016): Agrophotovoltaik - die Energiewende in der Landwirtschaft. In *GAIA - Ecological Perspectives for Science and Society* 25 (4), pp. 242–246. DOI: 10.14512/gaia.25.4.5.

Rossen, Anja (2015): What are metal prices like? Co-movement, price cycles and long-run trends. In *Resources Policy* 45, pp. 255–276. DOI: 10.1016/j.resourpol.2015.06.002.

Royen, H.; Fortkamp, U. (2016): Rare Earth Elements - Purification, Seperation and Recycling. Stockholm: IVL Swedish Environmental Research Institute Ltd. (No. C 211).

Saliba, Michael; Correa-Baena, Juan-Pablo; Wolff, Christian M.; Stolterfoht, Martin; Phung, Nga; Albrecht, Steve et al. (2018): How to Make over 20% Efficient Perovskite Solar Cells in Regular (n–i–p) and Inverted (p–i–n) Architectures. In *Chem. Mater.* 30 (13), pp. 4193–4201. DOI: 10.1021/acs.chemmater.8b00136.

Sato, Yuichi; Takeuchi, Shigeo; Kobayakawa, Koichi (2001): Cause of the memory effect observed in alkaline secondary batteries using nickel electrode. In *Journal of Power Sources* 93 (1-2), pp. 20–24. DOI: 10.1016/S0378-7753(00)00506-1.

Schlegl, Thomas (2013): Entwicklungslinien der PV-Technologien und Materialsubstitutionsmöglichkeiten. Edited by Evangelische Akademie Tutzing. Evangelische Akademie Tutzing. Tuzing (Strategische Metalle für die Energiwende), checked on 6/8/2017.

Schriefl, E.; Bruckner, M.; Bruckner, A.; Windhaber, M. (2013): Metallbedarf von Erneuerbare-Energie-Technologien. Progress Report 2 im Rahmen des Projekts „Feasible Futures for the Common Good". energieautark consulting, SERI. Wien.

Schwarz, Gideon (1978): Estimating the Dimension of a Model. In *The Annals of Statistics* 6 (2), pp. 461–464. DOI: 10.1214/aos/1176344136.

Seok, Sang Il; Grätzel, Michael; Park, Nam-Gyu (2018): Methodologies toward Highly Efficient Perovskite Solar Cells. In *Small (Weinheim an der Bergstrasse, Germany)* 14 (20), e1704177. DOI: 10.1002/smll.201704177.

Shammugam, S.; Gervais, E.; Schlegl, T.; Rathgeber, A. (2019a): Raw metal needs and supply risks for the development of wind energy in Germany until 2050. In *Journal of Cleaner Production* 221, pp. 738–752. DOI: 10.1016/j.jclepro.2019.02.223.

Shammugam, S.; Rathgeber, A.; Schlegl, T. (2019b): Causality between metal prices. Is joint consumption a more important determinant than joint production of main and by-product metals? In *Resources Policy* 61, pp. 49–66. DOI: 10.1016/j.resourpol.2019.01.010.

Sheng, Shuangwen (2013): Report on Wind Turbine Subsystem Reliability ─ A Survey of Various Databases. NREL National Renewable Energy Laboratory.

Siemens AG (2011): Bolted Steel Shell Tower. Erlangen, Germany. Available online at https://www.energy.siemens.com/us/pool/hq/power-generation/renewables/wind-power/Bolted_Steel_Shell_Tower_brochure_EN.pdf, checked on 13.05.17.

Siewert, T.; Liu, S.; Smith, D. R.; Madeni, J. C. (2002): Properties of Lead-Free Solders. Database for Solder Properties with Emphasis on New Lead-free Solders. 4th ed. National Institute of Standards and Technology; Colorado School of Mines. Colorado.

Silvennoinen, Annastiina; Thorp, Susan (2013): Financialization, crisis and commodity correlation dynamics. In *Journal of International Financial Markets, Institutions and Money* 24, pp. 42–65. DOI: 10.1016/j.intfin.2012.11.007.

Simon, Bálint; Ziemann, Saskia; Weil, Marcel (2015): Potential metal requirement of active materials in lithium-ion battery cells of electric vehicles and its impact on reserves. Focus on Europe. In *Resources, Conservation and Recycling* 104, pp. 300–310. DOI: 10.1016/j.resconrec.2015.07.011.

Simon, Frédéric (2018): Race for lithium illustrates EU drive for 'strategic' raw materials. Special Report: The global race for raw materials. With assistance of European Mineral Resources Confederation (EUMICON). EURACTIV. Available online at https://en.euractiv.eu/wp-content/uploads/sites/2/special-report/EURACTIV-Special-Report-The-global-race-for-raw-materials.pdf.

Simon, Herbert A. (1952): On the Definition of the Causal Relation. In *The Journal of Philosophy* 49 (16), p. 517. DOI: 10.2307/2021114.

Sims, Christopher A.; Waggoner, Daniel F.; Zha, Tao (2008): Methods for inference in large multiple-equation Markov-switching models. In *Journal of Econometrics* 146 (2), pp. 255–274. DOI: 10.1016/j.jeconom.2008.08.023.

Śmiech, S.; Papież, M. (2012): A dynamic analysis of causality between prices on the metals market. In : Proceedings of the International Scientific Conference "Quantitative Methods in Economics". Multiple Criteria Decision Making XVI", Bratislava, Slovakia, 30th May-1st June 2012. Bratislava: Vydavatel'stvo EKONÓM, pp. 221–225.

Smith, Richard L.; Naylor, J. C. (1987): A Comparison of Maximum Likelihood and Bayesian Estimators for the Three- Parameter Weibull Distribution. In *Applied Statistics* 36 (3), p. 358. DOI: 10.2307/2347795.

SmithBucklin Statistics Group (2017): National recycling rate study. Edited by Battery Council International (BCI). Chicago.

Snaith, Henry J. (2013): Perovskites. The Emergence of a New Era for Low-Cost, High-Efficiency Solar Cells. In *J. Phys. Chem. Lett.* 4 (21), pp. 3623–3630. DOI: 10.1021/jz4020162.

Sommer, P.; Rotter, V. S.; Ueberschaar, M. (2015): Battery related cobalt and REE flows in WEEE treatment. In *Waste management (New York, N.Y.)* 45, pp. 298–305. DOI: 10.1016/j.wasman.2015.05.009.

Song, Zhaoning; Abate, Antonio; Watthage, Suneth C.; Liyanage, Geethika K.; Phillips, Adam B.; Steiner, Ullrich et al. (2016): Perovskite Solar Cell Stability in Humid Air. Partially Reversible Phase Transitions in the PbI 2 -CH 3 NH 3 I-H 2 O System. In *Adv. Energy Mater.* 6 (19), p. 1600846. DOI: 10.1002/aenm.201600846.

Soytas, Ugur; Sari, Ramazan; Hammoudeh, Shawkat; Hacihasanoglu, Erk (2009): World oil prices, precious metal prices and macroeconomy in Turkey. In *Energy Policy* 37 (12), pp. 5557–5566. DOI: 10.1016/j.enpol.2009.08.020.

Speirs, Jamie; Contestabile, Marcello; Houari, Yassine; Gross, Robert (2014): The future of lithium availability for electric vehicle batteries. In *Renewable and Sustainable Energy Reviews* 35, pp. 183–193. DOI: 10.1016/j.rser.2014.04.018.

Spera, David (2009): Introduction to Modern Wind Turbines. In David A. Spera (Ed.): Wind Turbine Technology: Fundamental Concepts in Wind Turbine Engineering, Second Edition. Three Park Avenue New York, NY 10016-5990: ASME, pp. 47–103.

Spyrou, Spyros (2013): Herding in financial markets. A review of the literature. In *Review of Behavioral Finance* 5 (2), pp. 175–194. DOI: 10.1108/RBF-02-2013-0009.

Sridharan, S.; Pham, T.; Khadilkar, C.; Shaikh, A.; Kim, S. (2012): Lead free solar cell contacts. Applied for by Ferro Corporation. App. no. 11/145.538. Patent no. US 8,093,491 B2.

Stadler, Michael; Kranzl, Lukas; Huber, Claus; Haas, Reinhard; Tsioliaridou, Elena (2007): Policy strategies and paths to promote sustainable energy systems—The dynamic Invert simulation tool. In *Energy Policy* 35 (1), pp. 597–608. DOI: 10.1016/j.enpol.2006.01.006.

Stahl, H.; Bauknecht, D.; Hermann, A.; Wolfgang Jenseit; Andreas R. Köhler; Cornelia Merz et al. (2016): Ableitung von Recycling und Umweltanforderungen und Strategien zur Vermeidung von Versorgungsrisiken bei innovativen Energiespeichern. Edited by Umweltbundesamt (UBA). Öko-Institut e.V. Dessau-Roßlau.

Stenzel, P.; Fleer, J.; Linssen, J. (2015): Elektrochemische Speicher. In Martin Wietschel, Sandra Ullrich, Peter Markewitz, Friedrich Schulte, Fabio Genoese (Eds.): Energietechnologien der Zukunft. Wiesbaden: Springer Fachmedien Wiesbaden, pp. 157–214.

Stenzel, P.; Linssen, J.; Robinus, M.; Stolten, D. (2018): Trends of Stationary Battery Storage Systems in Germany – A Database Analysis. Strommarkttreffen „Batterien: Kostenentwicklung, Technologien, Anwendungen“. Forschungszentrum Jülich: IEK-3: Institut für Elektrochemische Verfahrenstechnik. Berlin.

Stern, David I. (2011): From Correlation to Granger Causality. In *Crawford School Research Paper No. 13*. DOI: 10.2139/ssrn.1959624.

Sun, Chunwen; Liu, Jin; Gong, Yudong; Wilkinson, David P.; Zhang, Jiujun (2017): Recent advances in all-solid-state rechargeable lithium batteries. In *Nano Energy* 33, pp. 363–386. DOI: 10.1016/j.nanoen.2017.01.028.

Suo, Liumin; Hu, Yong-Sheng; Li, Hong; Armand, Michel; Chen, Liquan (2013): A new class of Solvent-in-Salt electrolyte for high-energy rechargeable metallic lithium batteries. In *Nature communications* 4, p. 1481. DOI: 10.1038/ncomms2513.

Takada, Kazunori (2013): Progress and prospective of solid-state lithium batteries. In *Acta Materialia* 61 (3), pp. 759–770. DOI: 10.1016/j.actamat.2012.10.034.

Thielmann, Axel; Sauer, Andreas; schnell, Mario; Wietschel, Martin (2015a): Technologie Roadmap. Stationäre Energiespeicher 2030. Karlsruhe: Fraunhofer-Institut für System- und Innovationsforschung ISI.

Thielmann, Axel; Sauer, Andreas; Wietschel, Martin (2015b): Gesamt-Roadmap Lithium-Ionen-Batterien 2030. Edited by Fraunhofer-Institut für Systemund Innovationsforschung ISI. Karlsruhe, checked on 8/1/2018.

Thomson Reuters; The Silver Institute (2018): World Silver Survey 2018. London. Available online at https://www.silverinstitute.org/wp-content/uploads/2018/04/2018WorldSilverSurvey.pdf, checked on 5/2/2018.

Tilton, John E. (1989): Changing trends in metal demand and the decline of mining and mineral processing in North America. In *Resources Policy* 15 (1), pp. 12–23. DOI: 10.1016/0301-4207(89)90030-5.

Tilton, John E.; Guzmán, Juan Ignacio (2016): Mineral economics and policy. Abingdon: RFF Press Resources for the future.

Timofeeva, Elena (2017): The Spectrum of EV Battery Chemistries. Inlfluit Energy. Available online at http://www.influitenergy.com/the-spectrum-of-ev-battery-chemistries/, checked on 10/19/2018.

Tinbergen, Jan (1951): Econometrics. London: Bradford & Dickens.

Tocoglu, U.; Cetinkaya, T.; Cevher, O.; Oguz Guler, M.; Akbulut, H. (2013): Nanostructured Silicon Thin Film Electrodes for Li-Ion Batteries. In *Acta Phys. Pol. A* 123 (2), pp. 380–382. DOI: 10.12693/APhysPolA.123.380.

Toda, Hiro Y.; Yamamoto, Taku (1995): Statistical inference in vector autoregressions with possibly integrated processes. In *Journal of Econometrics* 66 (1-2), pp. 225–250. DOI: 10.1016/0304-4076(94)01616-8.

Tomboy, Willy (2018): The Batteries Report 2018. Recharge. Brussels. Available online at https://www.rechargebatteries.org/wp-content/uploads/2018/05/RECHARGE-The-Batteries-Report-2018-April-18.pdf, checked on 8/21/2018.

Trabish, Herman K. (2014): Is GE's Space Frame Tower the Future of Wind Power? GE goes back to the roots of wind power—but with a twist. Greentech Media. Available online at https://www.greentechmedia.com/articles/read/Is-GEs-Space-Frame-Wind-Turbine-Tower-The-Future-of-Wind-Power, updated on 3/7/2014, checked on 5/13/2017.

Troughton, J.; Hooper, K.; Watson, T. M. (2017): Humidity resistant fabrication of CH3NH3PbI3 perovskite solar cells and modules. In *Nano Energy* 39, pp. 60–68. DOI: 10.1016/j.nanoen.2017.06.039.

USGS (2009): Mineral Commodity Summaries 2009: U.S. Geological survey.

USGS (2018): Mineral Commodity Summaries 2018: U.S. Geological survey. Available online at https://minerals.usgs.gov/minerals/pubs/mcs/2018/mcs2018.pdf.

Vaalma, Christoph; Buchholz, Daniel; Weil, Marcel; Passerini, Stefano (2018): A cost and resource analysis of sodium-ion batteries. In *Nature Reviews Materials* 3 (4), p. 18013. DOI: 10.1038/natrevmats.2018.13.

Vestas (2006): Life cycle assessment of electricity produced from onshore sited wind power plants based on Vestas V82-1.65 MW turbines. Denmark, checked on 28.02.17.

Viebahn, Peter; Arnold, Karin; Friege, Jonas; Krüger, Christine; Nebel, Arjuna; Samadi, Sascha et al. (2014): KRESSE - kritische mineralische Ressourcen und Stoffströme bei der Transformation des deutschen Energieversorgungssystems. Abschlussbericht. Wuppertal: Wuppertal Institut für Klima, Umwelt, Energie.

Viebahn, Peter; soukup, Ole; Samadi, Sascha; Teubler, Jens; Wiesen, Jens; Ritthoff, Michael (2015): Assessing the need for critical minerals to shift the German energy system towards a high proportion of renewables. In *Renewable and Sustainable Energy Reviews* 49, pp. 655–671. Available online at http://www.sciencedirect.com/science/article/pii/S1364032115003408, checked on 11.05.17.

Vikström, Hanna; Davidsson, Simon; Höök, Mikael (2013): Lithium availability and future production outlooks. In *Applied Energy* 110, pp. 252–266. DOI: 10.1016/j.apenergy.2013.04.005.

Virolainen, Sami; Fallah Fini, Mojtaba; Miettinen, Ville; Laitinen, Antero; Haapalainen, Mika; Sainio, Tuomo (2016): Removal of calcium and magnesium from lithium brine concentrate via continuous counter-current solvent extraction. In *Hydrometallurgy* 162, pp. 9–15. DOI: 10.1016/j.hydromet.2016.02.010.

Visser, Logan; Gao, Yuxin (2018): Stabilized NMC811 to Enable High Energy Density Lithium Ion Batteries. In *Major Qualifying Projects (All Years)*. Available online at https://digitalcommons.wpi.edu/mqp-all/679.

Wang, Qingsong; Ping, Ping; Zhao, Xuejuan; Chu, Guanquan; Sun, Jinhua; Chen, Chunhua (2012): Thermal runaway caused fire and explosion of lithium ion battery. In *Journal of Power Sources* 208, pp. 210–224. DOI: 10.1016/j.jpowsour.2012.02.038.

Wang, Zhuo; Lei, Binglong; Xia, Xiaohong; Huang, Zhongbing; Homewood, Kevin Peter; Gao, Yun (2018): CH 3 NH 2 BiI 3 Perovskites. A New Route to Efficient Lead-Free Solar Cells. In *J. Phys. Chem. C* 122 (5), pp. 2589–2595. DOI: 10.1021/acs.jpcc.7b11849.

Watari, Takuma; McLellan, Benjamin; Ogata, Seiichi; Tezuka, Tetsuo (2018): Analysis of Potential for Critical Metal Resource Constraints in the International Energy Agency's Long-Term Low-Carbon Energy Scenarios. In *Minerals* 8 (4), p. 156. DOI: 10.3390/min8040156.

Wen, Hanjie; Zhu, Chuanwei; Zhang, Yuxu; Cloquet, Christophe; Fan, Haifeng; Fu, Shaohong (2016): Zn/Cd ratios and cadmium isotope evidence for the classification of lead-zinc deposits. In *Scientific Reports* 6, p. 25273. DOI: 10.1038/srep25273.

Wen, Jianwu; Yu, Yan; Chen, Chunhua (2012): A Review on Lithium-Ion Batteries Safety Issues. Existing Problems and Possible Solutions. In *Mat Express* 2 (3), pp. 197–212. DOI: 10.1166/mex.2012.1075.

Wen, Zhenhai; Lu, Ganhua; Mao, Shun; Kim, Haejune; Cui, Shumao; Yu, Kehan et al. (2013): Silicon nanotube anode for lithium-ion batteries. In *Electrochemistry Communications* 29, pp. 67–70. DOI: 10.1016/j.elecom.2013.01.015.

Wietschel, Martin; Ullrich, Sandra; Markewitz, Peter; Schulte, Friedrich; Genoese, Fabio (Eds.) (2015): Energietechnologien der Zukunft. Wiesbaden: Springer Fachmedien Wiesbaden.

Wilburn, D. R. (2011): Wind energy in the United States and materials required for the land-based wind turbine industry from 2010 through 2030. U.S. Geological Survey Scientific Investigations Report 2011–5036. Available online at http://pubs.usgs.gov/sir/2011/5036.

Williard, Nicholas; He, Wei; Hendricks, Christopher; Pecht, Michael (2013): Lessons Learned from the 787 Dreamliner Issue on Lithium-Ion Battery Reliability. In *Energies* 6 (9), pp. 4682–4695. DOI: 10.3390/en6094682.

Witte, Wolfram; Spiering, Stefanie; Hariskos, Dimitrios (2014): Substitution of the CdS buffer layer in CIGS thin-film solar cells. In *Vakuum in Forschung und Praxis* 26 (1), pp. 23–27. DOI: 10.1002/vipr.201400546.

Wolde-Rufael, Yemane (2006): Electricity consumption and economic growth. A time series experience for 17 African countries. In *Energy Policy* 34 (10), pp. 1106–1114. DOI: 10.1016/j.enpol.2004.10.008.

World Bank (2018): Population, total | Data. World Bank Group. Available online at https://data.worldbank.org/indicator/SP.POP.TOTL, checked on 11/29/2018.

World Steel Association (2012): Steel solutions in the green economy. Wind turbines.

Wu, S.; Huo, Y.; Guo, Y.; Yao, W.; Lin, Z.; Cai, J. et al. (2016): Plastic Photovoltaic Module Frame and Rack, and Composition for Making the Same. Applied for by Dow Global Technologies LLC. App. no. US14896471. Patent no. US2016/0134231 A1. Priority no. 28-6-2013.

Wu, Xiaodan; Li, Jianxing; Unuvar, Tora; Manikam, Vemal Raja; Tolentino, Erik Nino (2015): The improvements of high temperature Zn-based lead free solder. In : IEEE 65th Electronic Components and Technology Conference (ECTC), 2015. 26-29 May 2015, San Diego, CA, USA. 2015 IEEE 65th Electronic Components and Technology Conference (ECTC). San Diego, CA. Annual IEEE Computer Conference; IEEE Electronic Components and Technology Conference; ECTC. Piscataway, NJ: IEEE, pp. 1268–1272.

Xiarchos, Irene (2005): Steel: Price Links between Primary and Scrap Markets. Conference Paper: Southern Agricultural Economics Association Annual Meetings. Little Rock, checked on 5/11/2018.

Xu, Lin; Tang, Shun; Cheng, Yu; Wang, Kangyan; Liang, Jiyuan; Liu, Cui et al. (2018): Interfaces in Solid-State Lithium Batteries. In *Joule* 2 (10), pp. 1991–2015. DOI: 10.1016/j.joule.2018.07.009.

Xue, Weijiang; Miao, Lixiao; Qie, Long; Wang, Chao; Li, Sa; Wang, Jiulin; Li, Ju (2017): Gravimetric and volumetric energy densities of lithium-sulfur batteries. In *Current Opinion in Electrochemistry* 6 (1), pp. 92–99. DOI: 10.1016/j.coelec.2017.10.007.

Yaksic, Andrés; Tilton, John E. (2009): Using the cumulative availability curve to assess the threat of mineral depletion. The case of lithium. In *Resources Policy* 34 (4), pp. 185–194. DOI: 10.1016/j.resourpol.2009.05.002.

Yakubu, Yahaya; Abdul Jalil, Suhaila (2016): Modified Wald Test Approach into Causality between Electricity and Manufacturing Sector in Nigeria. In *IOSR Journal of Economics and Finance* 7 (1), pp. 47–61. DOI: 10.9790/5933-07114761.

Yang, Yongxiang; Walton, Allan; Sheridan, Richard; Güth, Konrad; Gauß, Roland; Gutfleisch, Oliver et al. (2017): REE Recovery from End-of-Life NdFeB Permanent Magnet Scrap. A Critical Review. In *J. Sustain. Metall.* 3 (1), pp. 122–149. DOI: 10.1007/s40831-016-0090-4.

Zepf, V.; Reller, A.; Rennie, C.; Ashfield, M.; Simmons, J. (2014): Materials critical to the energy industry. An introduction. Second edition. London: BP p.l.c.

Zhu, Wenhua H.; Zhu, Ying; Davis, Zenda; Tatarchuk, Bruce J. (2013): Energy efficiency and capacity retention of Ni–MH batteries for storage applications. In *Applied Energy* 106, pp. 307–313. DOI: 10.1016/j.apenergy.2012.12.025.

Zimmermann, Till (2013): Dynamic material flow analysis of critical metals embodied in thin-film photovoltaic cells. artec-paper Nr. 194: artec Forschungszentrum Nachhaltigkeit, University of Bremen.

Zimmermann, Till; Rehberger, Max; Göling-Reisemann, Stefan (2013): Material Flows Resulting from Large Scale Deployment of Wind Energy in Germany. In *Resources* 2 (3), pp. 303–334. DOI: 10.3390/resources2030303.

ZSW (2014): Vorbereitung und Begleitung der Erstellung des Erfahrungsberichts 2014 gemäß § 65 EEG. Vorhaben IIc Solare Strahlungsenergie. With assistance of Zentrum für Sonnenenergie- und Wasserstoff-Forschung Baden Württemberg, Fraunhofer Institute for Wind Energy and Energy System Technology (IWES), Bosch & Partner GmbH, GfK SE. Edited by BMWi. Stuttgart. Available online at https://www.clearingstelle-eeg-kwkg.de/files/zwischenbericht-vorhaben-2c.pdf.

Zubi, Ghassan; Dufo-López, Rodolfo; Carvalho, Monica; Pasaoglu, Guzay (2018): The lithium-ion battery. State of the art and future perspectives. In *Renewable and Sustainable Energy Reviews* 89, pp. 292–308. DOI: 10.1016/j.rser.2018.03.002.

Zuser, Anton; Rechberger, Helmut (2011): Considerations of resource availability in technology development strategies. The case study of photovoltaics. In *Resources, Conservation and Recycling* 56 (1), pp. 56–65. DOI: 10.1016/j.resconrec.2011.09.004.

15 Appendix

Table 15-1: Global production, global reserve and global reserve base used for the calculation of bottleneck indicators. The source for global production and global reserve is (USGS 2018) and for the reserve base is (USGS 2009) unless stated otherwise

	Global production in 2017 [t]	Global reserve [t]	Global reserve base [t]
Ag	25000	530000	570000
Al[1]	60000000	7500000000	9500000000
Au	3150	54000	100000
Cd[2]	23000	593400	1200000
Co	110000	7100000	13000000
Cr[3]	31000000	510000000	510000000
Cu	19700000	790000000	1000000000
Dy[4]	420	320000	450000
St	1700000000	83000000000	16000000000000
Ga[5]	315	560000	589440
In[6]	720	15000	30000
Li	43000	16000000	30000000
Mn	16000000	680000000	5200000000
Mo	290000	17000000	19000000
Na	54000000	25000000000	40000000000
Nd[4]	19000	23000000	31500000
Ni	2100000	74000000	150000000
Pb	4700000	88000000	170000000
Pd	210	69000	80000
Pt	200	69000	80000
Sb	150000	1500000	4300000
Se	3300	100000	172000
Si	7400000	NA	NA
Sn	290000	4800000	11000000
Ta	1300	110000	180000
Te	420	31000	48000
Ti	6200000	870000000	1500000000
V	80000	20000000	38000000
Zn	13200000	230000000	480000000

1 – One quarter of bauxite amount is allocated for aluminium reserve and reserve base

2 – Reserve and reserve base calculated based on (Wen et al. 2016)

3 – Due to unavailable data, reserve base is assumed to be similar to reserve levels

4 – Production and reserve are based from (Viebahn et al. 2015) whereas the reserve base is provided by (USGS 2009)

6 – Data for reserve and reserve base are provided by (Lokanc et al. 2015)

5 – Data for reserve and reserve base are provided by (Rongguo et al. 2016)

Table 15-2: Overview of the cumulative demand of selected investigated metals (which are not previously presented in Table 9-1) in PV, wind turbines and batteries for stationary application and in EVs in Germany for all energy pathways from 2020 until 2050. Con and Alt represents the conservative and alternative scenarios respectively.

		Photovoltaic						Wind turbine						Batteries					
		Long-term		Climate protection		Transformation		Long-term		Climate protection		Transformation		Long-term		Climate protection		Transformation	
Metal	Unit	Con	Alt	Con	Alt	Con	Alt	Con	Alt	Con	Alt	Con	Alt	Con	Alt	Con	Alt	Con	Alt
Au	kg	55	55	99	99	123	123	141	196	205	268	392	560	5910	5910	6088	6088	6422	6273
Mg	kt	2	2	3	3	4	4	0	0	0	0	0	0	0	0	0	0	0	0
Mo	t	0	0	0	0	0	0	0	0	0	0	0	0	77	77	79	79	83	82
Na	t	0	0	0	0	0	0	0	0	0	0	0	0	0	0	0	0	162	9662
Pb	t	424	413	726	698	838	795	883	1221	1280	1674	2450	3500	0	0	0	0	0	0
Sb	t	165	165	296	296	367	367	423	585	613	801	1173	1675	0	0	0	0	0	0
Si	kt	102	89	178	154	215	186	0	0	0	0	0	0	0	0	0	0	0	0
Ta	t	0	0	0	0	0	0	0	0	0	0	0	0	30	30	30	30	32	31
Ti	kg	6	6	11	11	13	13	152	211	221	289	423	604	0	0	0	0	0	0
Zn	t	220	220	394	394	489	489	563	778	815	1066	1560	2228	6	6	6	6	6	6

Table 15-3: Test statistics of unit root tests in level series and 1st differenced series.
* represents 10% significance level, ** 5% significance level and *** 1% significance level.

				Metal X				Metal Y			
				Level		First difference		Level		First difference	
X	Y	Timestep	n	ADF	KPSS	ADF	KPSS	ADF	KPSS	ADF	KPSS
Al	Ga	01.2004-12.2013	120	-3.30*	0.90***	-4.16***	0.14	-2.45	0.42*	-3.90**	0.16
Ag	Au	01.1990-12.2013	288	-2.39	4.36***	-5.14***	0.10	-1.65	4.16***	-4.99***	0.41*
Ag	Zn	01.1990-12.2013	288	-2.39	4.36***	-5.14***	0.10	-3.45*	0.87***	-4.63***	0.06
Au	Cu	01.1990-12.2013	288	-1.65	4.16***	-4.99***	0.41*	-2.58	3.89***	-6.90***	0.08
Cu	Mo	01.1990-12.2013	288	-2.58	3.89***	-6.90***	0.08	-2.29	2.78***	-5.70***	0.09
Cu	Se	01.1990-12.2013	288	-2.58	3.89***	-6.90***	0.08	-3.03	4.64***	-5.40***	0.07
Cu	Co	01.1990-12.2013	288	-2.58	3.89***	-6.90***	0.08	-3.65**	1.41***	-6.78***	0.08
Fe	Dy	04.2001-12.2013	153	-1.64	4.44***	-5.80***	0.09	-3.47*	2.21***	-4.57***	0.08
Fe	Nd	01.2005-12.2013	108	-1.33	2.98***	-5.58***	0.11	-2.47	1.30***	-4.33***	0.08
Ni	Cu	01.1990-12.2013	288	-3.13	2.47***	-6.33***	0.05	-2.58	3.89***	-6.90***	0.08
Ni	Co	01.1990-12.2013	288	-3.13	2.47***	-6.33***	0.05	-3.65**	1.41***	-6.78***	0.08
Pb	Ag	01.1990-12.2013	288	-3.62**	3.89***	-5.26***	0.07	-2.39	4.36***	-5.14***	0.10
Pb	Cu	01.1990-12.2013	288	-3.62**	3.89***	-5.26***	0.07	-2.58	3.89***	-6.90***	0.08
Pb	Zn	01.1990-12.2013	288	-3.62**	3.89***	-5.26***	0.07	-3.45*	0.87***	-4.63***	0.06
Zn	In	01.1990-12.2013	288	-3.45*	0.87***	-4.63***	0.06	-3.06	1.81***	-4.96***	0.07
Zn	Ga	01.2004-12.2013	120	-2.00	0.42***	-3.86**	0.16	-2.45	0.42*	-3.90**	0.16
Ag	Cu	01.1990-12.2013	288	-2.39	4.36***	-5.14***	0.10	-2.58	3.89***	-6.90***	0.08
Ag	Ni	01.1990-12.2013	288	-2.39	4.36***	-5.14***	0.10	-3.13	2.47***	-6.33***	0.05
In	Ga	01.2004-12.2013	120	-2.17	1.93***	-3.75**	0.17	-2.45	0.42*	-3.90**	0.16
In	Se	01.1990-12.2013	288	-3.06	1.81***	-4.96***	0.07	-3.03	4.64***	-5.40***	0.07
In	Cu	01.1990-12.2013	288	-3.06	1.81***	-4.96***	0.07	-2.58	3.89***	-6.90***	0.08
Ga	Se	01.2004-12.2013	120	-2.45	0.42**	-3.90**	0.16	-2.31	0.55**	-4.14***	0.20
Ga	Cu	01.2004-12.2013	120	-2.45	0.42**	-3.90**	0.16	-2.60	1.51***	-4.46***	0.12
Ag	Ga	01.2004-12.2013	120	-1.83	3.00***	-3.99***	0.16	-2.45	0.42*	-3.90**	0.16
Ag	In	01.1990-12.2013	288	-2.39	4.36***	-5.14***	0.10	-3.06	1.81***	-4.96***	0.07
Li	Ni	01.1990-12.2013	288	-1.85	5.12***	-5.50***	0.24	-3.13	2.47***	-6.33***	0.05
Li	Co	01.1990-12.2013	288	-1.85	5.12***	-5.50***	0.24	-3.65**	1.41***	-6.78***	0.08
Mn	Li	01.1995-12.2013	228	-3.72**	2.22***	-5.09***	0.06	-2.03	4.52***	-4.83***	0.18
Mn	Ni	01.1995-12.2013	228	-3.72**	2.22***	-5.09***	0.06	-2.75	2.17***	-5.50***	0.07
Mn	Co	01.1995-12.2013	228	-3.72**	2.22	-5.09***	0.06	-2.95	1.24***	-5.75***	0.07
Cu	Nd	01.2005-12.2013	108	-3.00	0.70	-4.20***	0.11	-2.47	1.30***	-4.33***	0.08
Cu	Dy	04.2001-12.2013	153	-2.49	3.60	-5.26***	0.09	-3.47*	2.21***	-4.57***	0.08
Nd	Dy	01.2005-12.2013	108	-2.47	1.30	-4.33***	0.08	-2.43	1.64***	-3.65**	0.13

Table 15-4: Test statistics of the Breusch-Godfrey (BG) test for lag lengths chosen according to Bayesian information criterion (BIC) and the max lag lengths used to specify the VAR models. The null hypothesis of the BG-test states that the residuals are uncorrelated. For lag lengths that reject the null hypothesis, we increased the lag lengths until all serial autocorrelation issues are solved at a significant level of at least 10%.

* represents 10% significance level, ** 5% significance level and *** 1% significance level.

	Lag length based on BIC		Lag length upon increment	
Metal Pair	opt. Lag	χ^2	max. lag	χ^2
Cu-Mo	2	2.276***	12	1.239
Cu-Se	2	2.45***	12	1.139
Cu-Co	2	1.688***	5	1.363*
Fe-Dy	2	4.036***	29	1.508*
Fe-Nd	2	1.919***	4	1.366*
Ni-Cu	2	2.829***	27	1.383*
Ni-Co	2	1.693***	4	1.202
Ag-Cu	2	2.266***	19	1.32*
Ag-Ni	2	2.291***	8	1.311*
In-Ga	2	1.547**	3	1.353*
In-Se	3	2.065***	19	1.307*
In-Cu	3	2.012***	10	1.324*
Ga-Se	2	0.765	2	0.765
Ga-Cu	2	1.084	2	1.084
Ag-Ga	2	0.991	2	0.991
Ag-In	3	1.791***	5	1.332*
Li-Ni	2	2.499***	25	1.125
Li-Co	1	1.732***	2	1.168
Mn-Li	1	1.964***	3	1.247
Mn-Ni	2	2.814***	9	1.33*
Mn-Co	3	1.028	3	1.028
Cu-Nd	2	0.804	2	0.804
Cu-Dy	2	2.277***	12	1.266
Nd-Dy	3	3.73***	16	1.423*

Table 15-5 Results of the Granger-causality test of possible metal-pair combinations that are not tested in Chapter 9. Metal pairs that had sample amount of less than 60 as well as metal pairs, whose serial autocorrelation could not be solved even upon increasing the lag length of the bivariate VAR model up to a maximum of 30 lags, are not concluded since it is assumed that anything more than that would be overfitting the model and the results would be unreliable.

* represents 10% significance level, ** 5% significance level and *** 1% significance level.

	Ag	Al	Au	Cd	Co	Cr	Cu	Dy	Fe	Ga	In	Li	Mn	Mo	Nd	Ni	Pb	Se	Sn	Zn
Ag	-	2.5	-	-	-	23.4***	-	-	NA	-	-	-	-	7.8*	-	-	-	NA	NA	-
Al	0.1	NA	1.0	46.3***	0.8	14.2	18.8*	1.2	4.2	-	24.7***	1.3	6.3**	34.1***	1.1	25.3**	6.3	1.3	6.0**	15.0
Au	-	1.1	NA	3.1	1.6	22.7***	-	16.9	NA	2.1	5.5	88.1***	20.4***	5.7	1.1	11.2	-	NA	NA	-
Cd	-	33.2*	5.0	NA	-	-	-	-	NA	-	-	-	-	5.9	-	-	-	-	3.0	10.4
Co	-	12.0***	1.7	-	NA	30.7***	-	-	2.2	-	-	-	-	18.8***	-	-	2.6	-	8.4**	2.4
Cr	20.9**	21.9***	48.2***	44.8**	17.6**	NA	49.8***	3.0	NA	11.1*	19.0***	1.1	-	11.6	2.6	NA	49.8***	NA	NA	27.6**
Cu	-	19.8*	-	59.1***	-	117.9***	NA	-	NA	-	-	-	-	-	-	-	96.4***	-	32.9***	13.0
Dy	-	0.9	56.8***	-	-	0.1	-	-	-	-	-	-	-	0.1	-	-	1.4	-	27.0**	0.9
Fe	NA	4.0	NA	NA	2.3	NA	NA	-	NA	2.4	NA	NA	NA	0.2	-	6.4	NA	NA	NA	16.0
Ga	-	0.1	1.5	-	-	9.4	-	-	0.2	NA	-	-	-	2.9	-	-	9.2**	-	1.7	0.0
In	-	10.5	9.3*	-	-	1.7	-	-	NA	-	NA	-	-	17.9**	-	-	3.2	-	2.1	10.9*
Li	-	3.2	43.2***	-	-	5.1	-	-	NA	-	-	NA	-	32.3	-	-	8.6	-	11.8**	41.1
Mn	-	1.4	7.8	-	-	37.7	-	-	NA	-	-	-	NA	3.5	-	-	26.9***	-	5.3	7.3
Mo	0.7	31.0***	4.9	6.8*	3.9	17.3**	-	0.3	1.6	0.2	20.6***	116.9***	25.1***	NA	0.0	34.5***	16.5*	22.4***	1.7	21.4**
Nd	-	0.5	16.1***	-	-	0.8	-	-	-	-	-	-	-	0.2	NA	-	0.4	-	5.0	0.2
Ni	-	14.8	14.8**	-	-	NA	-	-	5.4	-	-	-	-	40.8***	-	NA	-	-	5.7	33.9***
Pb	-	20.9***	6.7	27.9	3.7	-	-	2.9	NA	0.4	16.2**	10.0	75.2***	29.6***	3.6	41.1**	NA	NA	78.4***	-
Se	NA	2.4	NA	-	-	NA	-	-	NA	-	-	-	-	1.7	-	-	NA	NA	66.5***	28.9***
Sn	NA	11.6***	NA	7.9***	2.8	NA	16.5	49.7***	NA	4.1	3.2	3.4	9.7**	17.8	3.7	11.2**	34.3***	49.7***	NA	16.2**
Zn	-	9.8	8.7	-	0.5	-	18.9*	1.6	17.2	-	-	20.8***	8.5*	20.3**	1.5	85.5***	-	25.7***	4.4	NA

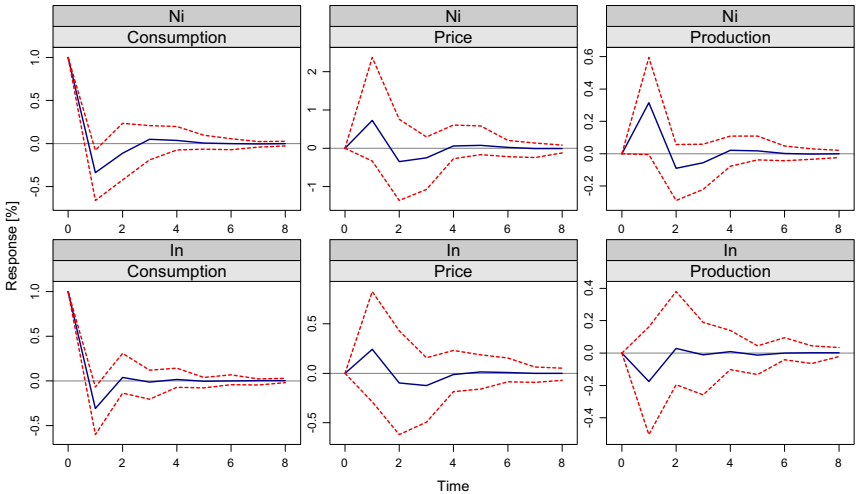

Figure 15-1: Responses of the change in log differences of price and production to a unit shock in the log differences of the consumption of nickel and indium. The dotted lines represent the 95% confidence intervals obtained by bootstrapping together with the impulse responses at 100 replications.

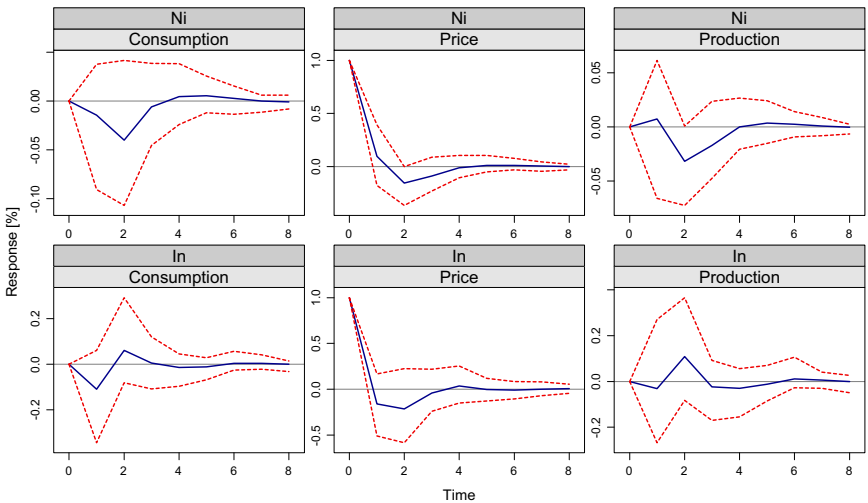

Figure 15-2: Responses of the change in log differences of consumption and production to a unit shock in the log differences of the price of nickel and indium. The dotted lines represent the 95% confidence intervals obtained by bootstrapping together with the impulse responses at 100 replications.

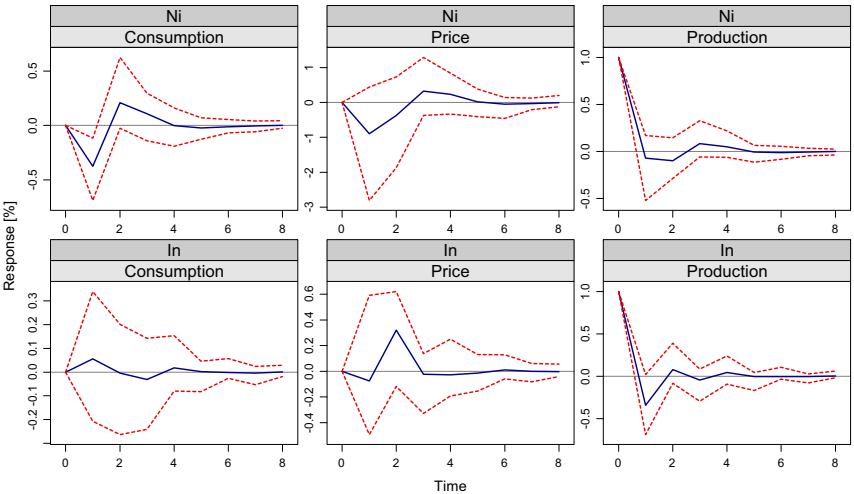

Figure 15-3: Responses of the change in log differences of price and consumption to a unit shock in the log differences of the production of nickel and indium. The dotted lines represent the 95% confidence intervals obtained by bootstrapping together with the impulse responses at 100 replications.

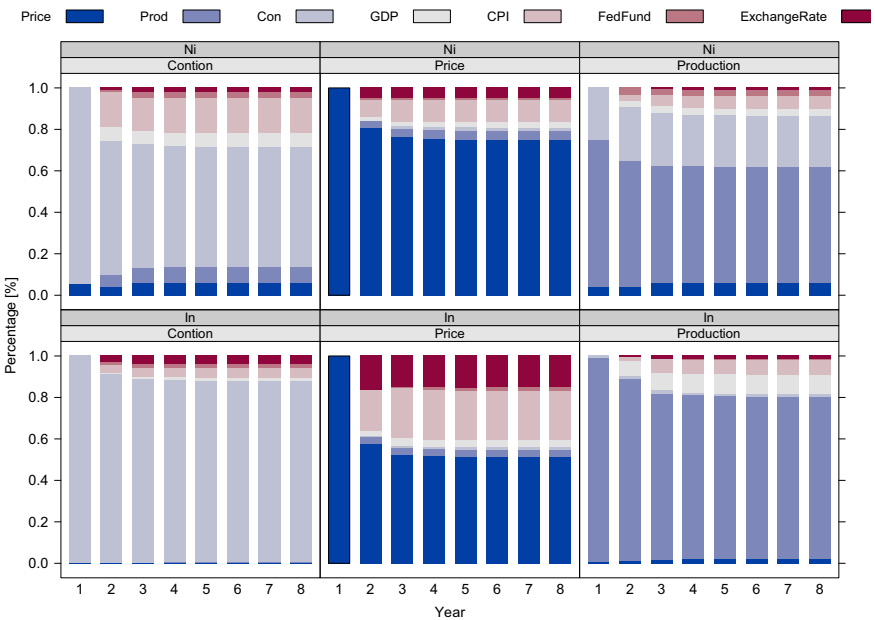

Figure 15-4: FEVD of the consumption, production and price of Indium (In) and Nickel (Ni). "Con" refers to consumption whereas "Prod" refers to production. The rest of the abbreviations refers to the macroeconomic variables as listed in Table 5.5.